

1 LATENCY, EXPRESSION AND SPLICING DURING INFECTION WITH HIV  
2 Scott Sherrill-Mix  
3 A DISSERTATION  
4 in  
5 Genomics and Computational Biology  
6 Presented to the Faculties of the University of Pennsylvania  
7 in  
8 Partial Fulfillment of the Requirements for the  
9 Degree of Doctor of Philosophy  
10 2015

11 Supervisor of Dissertation:

---

12 Frederic D. Bushman, Ph.D., Professor of Microbiology

13 Graduate Group Chairperson:

---

14 Li-San Wang, Ph.D., Associate Professor of Pathology and Laboratory Medicine

15 Dissertation Committee:

16 Nancy Zhang, Ph.D. Associate Professor of Statistics

17 Yoseph Barash, Ph.D., Assistant Professor of Genetics

18 Kristen Lynch, Ph.D., Professor of Biochemistry and Biophysics

19 Michael Malim, Ph.D., Professor of Infectious Diseases, King's College London

20 LATENCY, EXPRESSION AND SPLICING DURING INFECTION WITH HIV

21 © COPYRIGHT

22 2015

23 Scott A. Sherrill-Mix

24 This work is licensed under the

25 Creative Commons Attribution

26 NonCommercial-ShareAlike 3.0

27 License

28 To view a copy of this license, visit

29 <http://creativecommons.org/licenses/by-nc-sa/3.0/>

*Dedicated to William Maurer, Gayle Maurer & Michele Sherrill-Mix*

## ACKNOWLEDGEMENTS

32 I would like to thank

33 Rick Bushman

34 Christian Hoffmann wet lab

35 collaborators

36 Bushman lab Rithun Mukherjee, Karen Ocwieja, Nirav Malani, Troy Brady, Young Hwang,  
37 Brendan Kelly, Kyle Bittinger, Rebecca Custers-Allen, Serena Dollive, Frances Male, Jacque  
38 Young, Rohini Sinha, Sam Minot, Aubrey Bailey, Christopher Nobles, Stephanie Grunberg,  
39 Vesa Turkki, Anatoly Dryga, Eric Sherman, Greg Peterfreund, Yinghua Wu, Alice Laughlin,  
40 Sesh Sundararaman, Alexandra Bryson, Christel Chehoud, Erik Clarke, Arwa Abbas

41 My committee—Nancy Zhang, Yoseph Barash, Kristen Lynch and Michael Malim—have  
42 provided guidance and encouragement. Many faculty of GCB mentoring and teaching.  
43 Hannah Chervitz, Tiffany Barlow, Mali Skotheim, Caitlin Greig and Laurie Zimmerman  
44 for managing everything and helping manage the layers of bureaucracy. Funding from the  
45 HIV Immune Networks Team (HINT) consortium P01 AI090935 and NRSA computational  
46 genomics training grant T32 HG000046.

47 Ram Myers and Mike James for great previous mentoring.

48 Xiaofen and Otto

49 ...

## ABSTRACT

51 LATENCY, EXPRESSION AND SPLICING DURING INFECTION WITH HIV

52 Scott Sherrill-Mix

53 Frederic D. Bushman, Ph.D.

54 Over 35 million people are living with human immunodeficiency virus (HIV-1). The  
55 mechanisms causing integrated provirus to become latent, the diversity of spliced viral  
56 transcripts and the cellular response to infection are not fully characterized and hinder the  
57 eradication of HIV-1. We applied high-throughput sequencing to investigate the effects of  
58 host chromatin on proviral latency and variation of expression and splicing in both the host  
59 and virus during infection.

60 To evaluate the link between host chromatin and proviral latency, we compared genomic and  
61 epigenetic features to HIV-1 integration site data for latent and active provirus from five cell  
62 culture models. Latency was associated with chromosomal position within individual models.  
63 However, no shared mechanisms of latency were observed between cell culture models. These  
64 differences suggest that cell culture models may not completely reflect latency in patients.

65 We carried out two studies to explore mRNA populations during HIV infection. Single-  
66 molecule amplification and sequencing revealed that the clinical isolate HIV<sub>89.6</sub> produces at  
67 least 109 different spliced mRNAs. Viral message populations differed between cell types,  
68 between human donors and longitudinally during infection. We then sequenced mRNA  
69 from control and HIV<sub>89.6</sub>-infected primary human T cells. Over 17 percent of cellular genes  
70 showed altered activity associated with infection. These gene expression patterns differed  
71 from HIV infection in cell lines but paralleled infections in primary cells. Infection with  
72 HIV<sub>89.6</sub> increased intron retention in cellular genes and abundance of RNA from human  
73 endogenous retroviruses. We also quantified the frequency and location of chimeric HIV-host  
74 RNAs. These two studies together provided a detailed accounting of both HIV<sub>89.6</sub> and host

75 expression and alternative splicing.

76 A more cost-effective method of detecting viral load would aid patients with poor access to  
77 healthcare. We developed improved methods for assaying HIV-1 RNA using loop-mediated  
78 isothermal amplification based on primers targeting regions of the HIV-1 genome conserved  
79 across subtypes. Combined with lab-on-a-chip technology, these techniques allow quantitative  
80 measurements of viral load in a point-of-care device targeted to resource-limited settings.

81 This work disclosed novel HIV-host interactions and developed techniques and knowledge  
82 that will aid in the study and management of HIV-1 infection.

## TABLE OF CONTENTS

84	ABSTRACT .....	v
85	TABLE OF CONTENTS.....	vii
86	LIST OF TABLES .....	ix
87	LIST OF ILLUSTRATIONS .....	x
88	CHAPTER 1 : Introduction .....	1
89	1.1 The HIV epidemic .....	1
90	1.2 The HIV virus .....	4
91	1.3 HIV detection.....	10
92	1.4 Contributions .....	11
93	CHAPTER 2 : HIV latency and integration site placement in five cell-based models	12
94	2.1 Abstract .....	12
95	2.2 Background .....	13
96	2.3 Methods .....	15
97	2.4 Results.....	19
98	2.5 Conclusions .....	30
99	2.6 Availability of supporting data .....	32
100	2.7 Acknowledgements .....	32
101	CHAPTER 3 : Dynamic regulation of HIV-1 mRNA populations analyzed by single-molecule enrichment and long-read sequencing .....	33
103	3.1 Abstract .....	33
104	3.2 Introduction.....	34
105	3.3 Materials and methods.....	36
106	3.4 Results.....	43
107	3.5 Discussion .....	49
108	3.6 Acknowledgements .....	53
109	CHAPTER 4 : Gene activity in primary T cells infected with HIV <sub>89.6</sub> : intron retention and induction of distinctive genomic repeats .....	54
111	4.1 Abstract .....	54
112	4.2 Background .....	55
113	4.3 Methods .....	56
114	4.4 Results.....	60
115	4.5 Discussion .....	78
116	4.6 Conclusions .....	82
117	4.7 Availability of supporting data .....	83
118	4.8 Acknowledgements .....	83

119	CHAPTER 5 : A reverse transcription loop-mediated isothermal amplification assay	
120	optimized to detect multiple HIV subtypes .....	84
121	5.1 Abstract .....	84
122	5.2 Introduction .....	85
123	5.3 Methods .....	86
124	5.4 Results.....	88
125	5.5 Testing different primer designs .....	92
126	5.6 Discussion .....	96
127	5.7 Acknowledgments.....	98
128	CHAPTER 6 : Conclusions and future directions.....	99
129	6.1 Latency and integration location .....	99
130	6.2 HIV-1 alternative splicing.....	100
131	6.3 Host expression during HIV infection .....	103
132	6.4 LAMP PCR and lab-on-a-chip .....	104
133	APPENDICES .....	108
134	A.1 Generalized linear models of changes in use of mutually exclusive HIV-1 splice	
135	acceptors .....	108
136	A.2 Reproducible report of HIV integration sites and latency analysis .....	114
137	BIBLIOGRAPHY .....	146

## LIST OF TABLES

139	TABLE 2.1 : Integrations from <i>in vitro</i> models of latency .....	18
140	TABLE 2.2 : Genomic data available for comaprison to integration sites .....	20
141	TABLE 4.1 : Samples and RNA-Seq sequencing coverage .....	61
142	TABLE 4.2 : Data used for meta-analysis of expression changes in HIV .....	62

## LIST OF ILLUSTRATIONS

144	FIGURE 1.1 : The HIV replication cycle.....	4
145	FIGURE 1.2 : The HIV-1 genome .....	8
146	FIGURE 2.1 : Correlations of genomic features and latency .....	21
147	FIGURE 2.2 : Lasso regressions predicting latency .....	22
148	FIGURE 2.3 : Cellular expression and latency .....	24
149	FIGURE 2.4 : Strand orientation and latency .....	25
150	FIGURE 2.5 : Genes and latency .....	26
151	FIGURE 2.6 : Alphoid repeats and latency .....	27
152	FIGURE 2.7 : Acetylation and latency .....	29
153	FIGURE 2.8 : Shared expression status between near neighbors.....	29
154	FIGURE 3.1 : Mapping the splice donors and acceptors of HIV <sub>89.6</sub> .....	35
155	FIGURE 3.2 : Spliced transcripts produced from HIV <sub>89.6</sub> .....	42
156	FIGURE 3.3 : Novel transcripts utilizing acceptor A8c .....	47
157	FIGURE 3.4 : Temporal, cell type and donor variability in accumulation of HIV-1 messages.....	50
159	FIGURE 4.1 : Comparisons among studies quantifying cellular gene expression after HIV infection .....	63
160		
161	FIGURE 4.2 : Comparisons of the effect of HIV infection on gene expression to studies comparing subsets of immune cells .....	65
162		
163	FIGURE 4.3 : Changes in the abundance of intronic regions with HIV infection ...	67
164		
165	FIGURE 4.4 : Repeat categories enriched upon infection with HIV .....	69
166		
167	FIGURE 4.5 : Characteristics of LTR12C sequences associated with induction upon infection with HIV <sub>89.6</sub> .....	70
168		
169	FIGURE 4.6 : Estimating relative abundance of HIV <sub>89.6</sub> message size classes using RNA-Seq data .....	72
170		
171	FIGURE 4.7 : Transcription and splicing of the HIV <sub>89.6</sub> RNA .....	74
172		
173	FIGURE 4.8 : Chimeric RNA sequences containing both human and HIV sequences	78
174		
175		
176	FIGURE 5.1 : Amplification results for all RT-LAMP primer sets tested .....	90
177		
178	FIGURE 5.2 : Subtype-agnostic RT-LAMP primers design .....	91
179		
180	FIGURE 5.3 : Performance of the AceIN-26 primer set with different starting RNA concentrations .....	94
181		
182	FIGURE 5.4 : Replicate tests of the ACeIN-26 primer set over six HIV subtypes..	95
183		
184	FIGURE 6.1 : Ebola RT-LAMP primers design .....	107

## CHAPTER 1: Introduction

### 178 1.1 The HIV epidemic

179 In 1981, physicians began to notice a mysterious increase, often clustered in men who  
180 had sex with men or intravenous drug users, in the occurrences of Kaposi's sarcoma and  
181 pneumocystis pneumonia<sup>1–6</sup>.

182 Kaposi's sarcoma was, until 1981, a rare cancer in the US found largely in elderly men with  
183 Jewish or Mediterranean ancestry<sup>7</sup>. Kaposi's sarcoma had also been seen in immunocom-  
184 promised individuals<sup>8–10</sup> and there were suggestions that it was a virus-associated cancer<sup>11</sup>  
185 although the causative human herpesvirus would not be discovered for another decade<sup>12,13</sup>.

186 Pneumocystis pneumonia was known to be caused by infection of the alveoli with the yeast-  
187 like fungus *Pneumocystis jirovecii*<sup>14,15</sup>. Pneumocystis pneumonia was almost exclusively  
188 seen in patients with suppressed immune systems or immune disorders and rarely, if ever, in  
189 immunocompetent individuals<sup>15</sup>.

190 The mechanism for this spike of opportunistic infections was clarified when researchers found  
191 severe T cells depletion and decreases in cellular immunity in these patients<sup>4–6,16,17</sup>. This  
192 disease was eventually labeled acquired immunodeficiency syndrome (AIDS). However, the  
193 underlying cause remained unclear.

194 Potential transmissions by transfusion<sup>18–20</sup>, injection drug use<sup>4,17,21</sup>, maternal transmission<sup>22</sup>  
195 and both homosexual<sup>16,23</sup> and heterosexual<sup>17,24</sup> contact pointed towards an infectious agent.  
196 In 1983, a virus later named human immunodeficiency virus type 1 (HIV-1) was isolated  
197 from patient samples<sup>25–28</sup> and soon detected in most immunodeficient patients<sup>28–31</sup>.

198 Reports of AIDS and associated opportunistic infections in sub-Saharan Africa soon revealed  
199 widespread endemic infection<sup>32–35</sup> and a great diversity of viruses<sup>36–41</sup>. Retrospective studies  
200 suggested that the virus had been present, at least sporadically, in Europe and the USA  
201 for decades<sup>42,43</sup> and circulating for even longer in Africa<sup>33,44–48</sup>. Archived patient samples

202 containing HIV-1 genome fragments from as early as 1959 were found in what is now  
203 Kinshasa, in the Democratic Republic of Congo<sup>46</sup>. These samples showed extensive genome  
204 diversification already present in the 1960s, suggesting that HIV-1 had been circulating in  
205 humans for some time<sup>47,48</sup>. Phylogenetic analyses adding in contemporary HIV-1 type M  
206 sequences estimated a most recent common ancestor in the early 1900s<sup>48–53</sup>.

207 A virus similar to HIV causing AIDS in monkeys was soon discovered in macaques<sup>54,55</sup> and  
208 many other primates<sup>56</sup>. HIV-1 appeared most similar to a virus found in chimpanzees<sup>55,57</sup>  
209 and surveys of wild chimpanzees in Africa revealed a closely related simian immunodeficiency  
210 virus infecting chimpanzees in central Africa<sup>58–60</sup>.

211 The ancestor of HIV-1 was likely transmitted from a chimpanzee to a human, likely during  
212 harvest of chimpanzees for food<sup>61–66</sup>, in the forests of southeastern Cameroon. The virus  
213 was transported down the Sangha River<sup>67</sup> to the city of Kinshasha, where HIV-1 began its  
214 global spread<sup>38,48,53,68</sup>. A combination of social upheaval, increased mobility, urbanization  
215 and mass vaccination campaigns with unsterilized needles appear to have provided fuel for  
216 the growing epidemic<sup>53,69–71</sup>. A virus appears to have been carried from Africa to Haiti in  
217 the 1960s, perhaps by workers returning home from an exchange program<sup>35,68</sup>, and then  
218 into the US in the 1970s<sup>72</sup> before being detected in the US in 1981. In the past 34 years,  
219 HIV-1 has spread to over 78 million people and caused over 35 million deaths<sup>73</sup>.

220 In the early days of the epidemic, there were no tests to detect the virus, and no treatments.  
221 The presence of the virus was often revealed by the onset of AIDS. Opportunistic infections<sup>74</sup>  
222 and death usually followed soon after. The median survival time after diagnosis with AIDS  
223 was about 1 year<sup>75,76</sup>.

224 Isolation of the virus allowed the detection through assays of antibody response. Testing  
225 revealed that, from infection, patients had a median survival time of around a decade<sup>77–80</sup>.

226 In 1987, the successful trial of the reverse transcriptase inhibitor azidothymidine provided  
227 the first hope for treatment<sup>81–83</sup> but it soon became apparent that the fast mutation rate of

228 HIV<sup>84–90</sup> and strong selection by drug therapy could quickly create drug-resistant forms of  
229 virus in patients receiving single drug therapy<sup>91–100</sup>. Even with therapy, median survival  
230 time from AIDS diagnosis rose to only about 2 years<sup>76,82,101,102</sup>.

231 Additional antiretrovirals, again targeting reverse transcriptase, were developed<sup>103</sup>. Sequential  
232 or alternating administration of different antiretroviral drugs did not greatly improve  
233 prognosis<sup>104–108</sup>. Simultaneous treatment with two reverse transcriptase inhibitor offered  
234 modest benefits but viral escape was still common<sup>109–113</sup>.

235 Development of drugs targeting other stages of the HIV replication cycle allowed synergistic  
236 combinations of antiretroviral drugs<sup>114–119</sup>. The difficulty for HIV to evolve multiple drug  
237 resistant mutations<sup>120,121</sup> meant that therapy using simultaneous combinations of drugs  
238 finally began to offer patients more hope of long term survival<sup>122–126</sup>. With early triple  
239 therapy, median survival time rose to 20 years<sup>79,127</sup> and, with further development, now  
240 approaches the life expectancy of control populations<sup>128–131</sup>.

241 However although antiretrovirals effectively suppress HIV, there is currently no practicable  
242 cure<sup>132,133</sup>. If a patient, even a patient who had the virus suppressed to undetectable  
243 levels for years, stops treatment, then virus abundance quickly rebounds to pretreatment  
244 levels<sup>134–136</sup>.

245 Upon infection, latent HIV are quickly<sup>137,138</sup> established in resting CD4<sup>+</sup> T cells and  
246 macrophages. These latent provirus are long-lived and resistant to therapy and immune  
247 response<sup>139,140</sup>. Resting CD4<sup>+</sup> cells have half-lives of up to 40 months<sup>141,142</sup> meaning  
248 significant proportions of HIV will remain latent for decades yet can be stimulated at any  
249 time by activity in their host cell to reactivate and restart viral replication<sup>134–136,140,141,143,144</sup>.

250 Latently infected cells are one of the most significant barriers to curing HIV<sup>145</sup>. If the latent  
251 proviruses could be induced into activity and their host cells eliminated then the virus might  
252 be eradicated from its host<sup>146–149</sup>. Cell models of latency are used to study this problem in  
253 the lab<sup>150–152</sup>. In Chapter 2, we compare latent and active provirus among these cell models

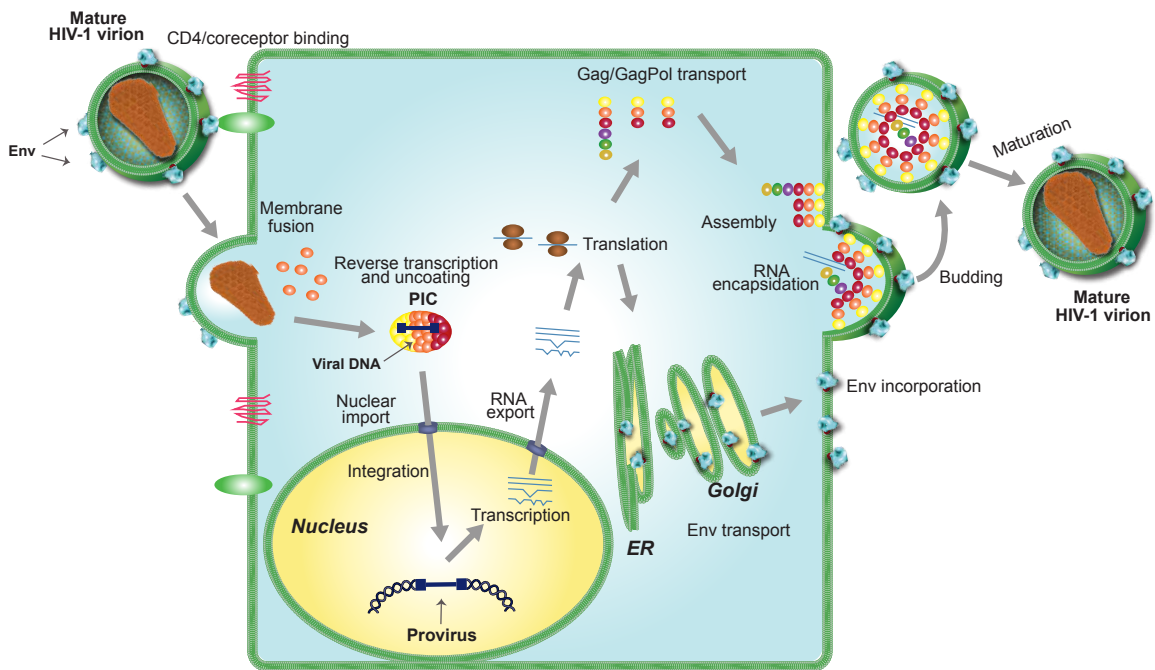


Figure 1.1: The HIV replication cycle

254 to see if latency relates to the chromosomal position of integration and whether models  
 255 share the same drivers of latency.

## 256 1.2 The HIV virus

257 HIV is an enveloped, single-strand positive-sense retrovirus (Figure 1.1). To replicate, the  
 258 virion gains access into a host cell through cellular receptors<sup>153–160</sup>. The viral RNA genome  
 259 is reverse transcribed to create a DNA intermediate that is integrated into a host cell  
 260 chromosome<sup>161–164</sup>. Host polymerase then transcribes viral messenger RNAs which are  
 261 translated in the cytoplasm. Full length RNA is packaged into budding particles along with  
 262 expressed viral proteins and the virion buds from the cell.

263 The HIV genome encodes genes for at least two polyproteins and seven proteins:

264 **Gag** (group specific antigens) is a myristoylated membrane protein which is anchored on  
 265 the virion surface and cleaved by viral protease after virion budding to produce matrix,  
 266 capsid, nucleocapsid and p6 protein along with two small spacer peptides SP1 and

267 SP2.

268 **MA** p17 (matrix) is a trimeric protein that supports the inside of the viral lipid bilayer  
269 to stabilize the virion<sup>165</sup>. It also aids in transport of the genome to the nucleus  
270 through a nuclear localization signal<sup>166</sup> and in nuclear import in non-dividing  
271 cells<sup>167</sup>.

272 **CA** p24 (capsid) proteins assemble to form a protective shell around the RNA genome  
273 of the virus. The viral capsid is composed of around 1500 copies of CA arranged  
274 into hexameric rings interspersed with 12 pentameric rings to form a fullerene  
275 cone<sup>168–171</sup>. CA binds cellular CPSF6<sup>172</sup>, cyclophilin A<sup>173,174</sup> and RanBP2<sup>175</sup>,  
276 perhaps to gain access to the nucleus<sup>175,176</sup> and to avoid premature uncoating  
277 and exposure of the viral genome to innate immune factors<sup>177</sup>.

278 **NC** p7 (nucleocapsid) recognizes the  $\psi$  packaging element of the viral genome<sup>178</sup>  
279 through two zinc-finger motifs and is packaged together with the RNA into  
280 virions<sup>179</sup>.

281 **p6** (protein 6 kda) is a small protein which appears to primarily recruit cellular  
282 proteins to allow virion budding from the cell membrane<sup>180–182</sup> and aid in the  
283 packaging of Vpr in to particles<sup>183</sup>.

284 **Pol** (polymerase) is cleaved by viral protease to produce reverse transcriptase, integrase  
285 and HIV protease. The Pol protein is generated when a ribosome translating *gag*  
286 meets a stem-loop in the HIV mRNA<sup>184</sup>, stutters and moves back a base, causing a  
287 -1 nucleotide frameshift when it continues translation<sup>185</sup>. Translational frameshifting  
288 happens in about  $\frac{1}{20}$  of translations<sup>186</sup>.

289 **RT** p51 (reverse transcriptase)<sup>187</sup> generates DNA from an RNA template<sup>161,162</sup>.  
290 Retrovirus package two copies of RNA in each virion<sup>188–190</sup>. If two different virus  
291 infect the same cell then interstrand transfer during the reverse transcription step

292 allows recombination between strains<sup>191–193</sup>. A lack of proofreading in the RT  
293 step leads to the high mutation rate of around  $2 \times 10^{-5}$  mutations per base per  
294 replication<sup>84–90</sup>.

295 **IN** p31 (integrase) is a dimeric enzyme which integrates the retroviral DNA into host  
296 chromatin<sup>164,194–197</sup>. Integrase removes two nucleotides from the 3' ends of  
297 the viral DNA and inserts the pair of viral ends into host DNA<sup>198</sup>.

298 **PR** (protease) is a dimeric aspartyl protease<sup>199</sup> that cleaves viral polyproteins Gag  
299 and Pol<sup>200,201</sup>.

300 **Env** gp160 is a trimeric transmembrane protein that mediates entry through fusion of  
301 viral and cellular membrane by binding its receptor CD4<sup>153–157</sup> and coreceptors  
302 CXCR4<sup>158</sup>, CCR3 or CCR5<sup>159,160</sup>. gp160 is cleaved into its active form, consisting of  
303 two subunits gp41 and gp120<sup>202</sup>, by cellular furin protease<sup>203</sup>. The envelope protein is  
304 highly glycosylated to form a mutable ‘glycan shield’ against host adaptive immune  
305 response<sup>204</sup>. There are about 14 Env proteins per virion<sup>205</sup>. Env sequence is highly  
306 variable within and between patients<sup>206,207</sup> due to positive selection from host immune  
307 recognition<sup>208–210</sup>.

308 **Tat** protein is a transactivator of expression from the HIV-1 long terminal repeat<sup>211–213</sup>.  
309 The virus does not replicate efficiently without this transactivation<sup>214</sup>. Tat may also  
310 regulate cellular expression such as downregulation of major histocompatibility complex  
311 type I expression<sup>215</sup>. Tat may suppress miRNA silencing pathway<sup>216–218</sup> but this  
312 remains controversial<sup>219</sup>.

313 **Rev** (regulator of expression of virion proteins) is a trans-activator protein that shuttles  
314 between the nucleus and cytoplasm<sup>220</sup> and causes the export of partially spliced and  
315 unspliced viral transcripts<sup>221–225</sup> from the nucleus through the recognition of a rev  
316 response element<sup>226,227</sup>.

317 **Nef** (negative factor) is a myristoylated membrane-associated protein<sup>228</sup> that is involved  
318 in multiple functions. Nef causes endocytosis of the viral entry receptors CD4<sup>229–233</sup>  
319 and CCR5<sup>234</sup> and major histocompatibility complex molecules<sup>235–238</sup>. Nef also in-  
320 duces T cell activation through interactions with signaling kinases and the T cell  
321 receptor<sup>239–243</sup>. In contrast, Nef in most other primate lentiviruses inhibits activation  
322 and inflammation<sup>244</sup> perhaps indicating that the gain of *vpu* in HIV-1 and its simian  
323 relatives allowed the loss of the immune inhibitory traits of *nef* and thus contributes  
324 to the increased pathogenecity of these viruses<sup>245,246</sup>.

325 **Vpr** (viral protein R) is a 15 kDa protein<sup>247,248</sup> with diverse functions. Vpr arrests the cell  
326 in the G2 phase of the cell cycle<sup>249–253</sup> and aids in transport of the viral genome to  
327 the nucleus<sup>166</sup>. Vpr also appears to trans-activate viral expression<sup>254,255</sup> and induce  
328 apoptosis<sup>256,257</sup> but these may be linked to conditions caused by cell cycle arrest. Vpr  
329 is incorporated into virions<sup>258,259</sup>.

330 **Vif** (virion infectivity factor) counteracts the cellular restriction factor APOBEC3G<sup>260</sup> by  
331 excluding APOBEC3G from incorporation into the virion<sup>261</sup> and causing APOBEC3G  
332 to be ubiquitinated and degraded<sup>262–264</sup>. APOBEC3G is otherwise packaged into  
333 virions<sup>265</sup> and deaminates the HIV genome during reverse transcription causing G-to-A  
334 hypermutation<sup>265–268</sup>.

335 **Vpu** Vpu (viral protein U)<sup>269,270</sup> is a small integral membrane protein which has two  
336 known functions; degradation of CD4 and downregulation of BST-2 from the cell  
337 membrane. Vpu causes cellular CD4 to be ubiquitinated and degraded<sup>271,272</sup> which  
338 prevents interactions between progeny virus and host cell CD4 receptor<sup>232,233,273,274</sup>  
339 and superinfection by other viruses<sup>230</sup> while also releasing Env proteins from CD4  
340 interactions in the endoplasmic reticulum<sup>275,276</sup>. Vpu also counteracts the cellular  
341 restriction factor BST-2, which would otherwise interfere with viral budding<sup>277,278</sup>.  
342 Vpu does not appear to be found in the virion<sup>279</sup>.

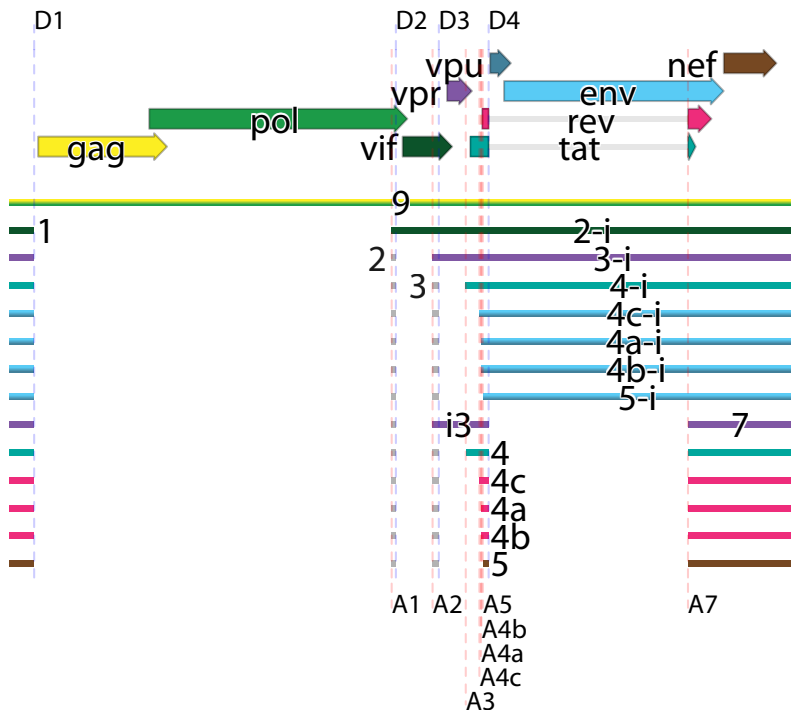


Figure 1.2: The HIV-1 genome. Arrows indicate open reading frames. Dashed lines show major splice acceptors (red) and donors (blue). Major spliceforms are shown as thin rectangles and colored according to their corresponding open reading frame.

343 A strong selective pressure for genome compactness<sup>280–282</sup> pushes HIV and other lentiviruses  
 344 to subvert host cell alternative splicing pathways to allow tighter packing of their genetic  
 345 information. Through weak splice sites<sup>283</sup> and overlapping reading frames (Figure 1.2), the  
 346 virus manages to produce regulated quantities of these nine proteins and polyproteins from  
 347 its single transcription start site and less than 10,000 base genome<sup>284</sup>.

348 In HIV, splicing occurs between at least four splice donors and eight splice acceptors<sup>284</sup>.  
 349 Two splice donors, D1 and D4, are relatively strong while the remaining donors and all  
 350 acceptors are fairly weak<sup>285</sup>. The weak acceptors seem balanced with Rev's nuclear export  
 351 activity. Several exonic splicing silencers<sup>286,287</sup> and exon splicing enhancers<sup>288,289</sup> and a  
 352 single intronic splicing silencer<sup>290</sup> in the viral genome interact with many human splicing  
 353 factors, including hnRNPs A1<sup>287,290</sup> H, F, 2H9, and A2<sup>291</sup> and SR proteins SRp40<sup>288,292</sup>,  
 354 SRp75<sup>292</sup>, ASF/SF2<sup>288</sup> and SC35<sup>291</sup>, to alter viral splicing<sup>284,293</sup>.

355 In Chapter 3, we investigate viral splicing and reveal unappreciated splice sites, novel proteins  
 356 and dynamic changes in viral splicing between human subjects, over time and between cell

357 types.

358 Inclusion and exclusion of a particular stretch of RNA into an mRNA is determined  
359 by a balance of RNA secondary structure<sup>291,294,295</sup>, chromatin structure<sup>296</sup>, nucleosome  
360 positioning<sup>297</sup>, histone marks<sup>298</sup>, previous splicings<sup>299</sup>, order of intron removal<sup>300,301</sup> and  
361 enhancers<sup>302</sup> and suppressors<sup>303</sup> that bind specific motifs<sup>304</sup>. Together these factors create  
362 a controllable splicing code<sup>305–307</sup>.

363 Alternative splicing may also play an unappreciated role in HIV-host interactions. Viral  
364 proteins interact with components of the cellular splicing complex<sup>308–310</sup>. These interactions  
365 have been reported to change splicing in viral<sup>309,311,312</sup> and cellular transcripts<sup>313,314</sup> and  
366 raise the possibility that the virus has evolved to alter host splicing. Although infection  
367 has been shown to cause genome-wide changes in the expression of cellular genes<sup>315–319</sup>,  
368 no genome-wide study of cellular alternative splicing during HIV infection has ever been  
369 reported.

370 Several viral proteins affect mRNA abundances. Rev causes export of unspliced viral mRNA  
371 that would otherwise be trapped in the nucleus<sup>320</sup> to be exported<sup>321,322</sup> and may also interact  
372 with splicing factors to alter viral splicing<sup>308</sup>. The HIV protein Tat is best known for its trans-  
373 activation of viral transcription<sup>211,323</sup> and triggering apoptosis in uninfected cells<sup>324,325</sup> but  
374 Tat also appears to independently affect alternative splicing of viral transcripts<sup>309,311,312,326</sup>.  
375 Viral protein Vpr is known to cause cell cycle arrest<sup>252</sup> with corresponding changes in ex-  
376 pression. Vpr also appears to alter alternative splicing of some cellular transcripts<sup>313,314</sup> and  
377 interact with the SMN complex<sup>310</sup>, which assembles spliceosomal snRNP<sup>327</sup>. Although all  
378 three of these proteins modify viral splicing, whether they also cause widespread alterations  
379 in cellular splicing is unknown.

380 In Chapter 4, we investigate splicing and expression during HIV infection and report  
381 global changes in intron retention and in the expression of endogenous retrovirus and  
382 retrotransposons.

383 **1.3 HIV detection**

384 Immunoassays are the current standard of care for the detection of HIV infection. These  
385 tests are based on the enzyme-linked immunosorbent assay (ELISA), using an enzyme linked  
386 to an antibody to produce a detectable signal only in the presence of antigen<sup>328–330</sup>.

387 The isolation of HIV<sup>25–28</sup> allowed the production of large quantities of virions that could  
388 be used as antigen. These virions were bound to a substrate, sera from patients added and  
389 any patients antibodies sensitive to HIV allowed to bind. Any unbound antibodies were  
390 washed away. Then a peroxidase enzyme-labeled antibody targeted to human antibody was  
391 added, allowed to bind and the unbound antibodies again washed away. Any HIV-targeted  
392 patient antibodies would bind the antigen and be bound in turn by the peroxidase-labeled  
393 antibody so that the peroxidase would change the color of media<sup>30,31,331</sup>. These tests had a  
394 large false positive rate and the standard procedure was to perform multiple ELISA tests  
395 follow by a Western blot test before informing patients<sup>332,333</sup> but false positives were still  
396 prevalent<sup>334</sup>. More conservative criteria and cleaner lab procedures reduced false positives<sup>335</sup>.  
397 Four generations of development<sup>336</sup> have resulted in more sensitive and specific detection of  
398 patient antibodies along with earlier detection using antibodies directly able to detect the  
399 HIV capsid protein<sup>337,338</sup>.

400 Rapid immunoassays with less specificity but able to provide results in 30 minutes have  
401 been developed to allow point-of-care testing. Immediate results reduce patient stress and  
402 reduces the number of patients lost to follow up prior to delivery of results<sup>339–341</sup>. Rapid  
403 tests detecting HIV in oral fluids have been developed and obviate the need for a blood  
404 draw<sup>342–344</sup> and allow self testing at home<sup>345,346</sup>.

405 Immunoassays provide robust and affordable point-of-care detection of HIV but no viable  
406 point-of-care assays for viral load exist<sup>347</sup>. Existing laboratory-based tests are relatively  
407 expensive and require specialized equipment making access difficult in resource-limited  
408 settings<sup>348,349</sup>. Without viral load measures, CD4<sup>+</sup> T cell counts or clinical presentation

409 are used to infer the emergence of viral drug resistance. These criteria are not specific nor  
410 sensitive enough without viral load measures so many patients are unnecessarily switched to  
411 second line therapy<sup>350,351</sup> or switched too late leading to accumulations of drug resistant  
412 mutations<sup>352</sup>. Medecins Sans Frontieres describe point-of-care viral load tests as “desperately  
413 needed”<sup>347</sup>. In Chapter 5, we design loop-mediated isothermal amplification methods that  
414 can be used with microfluidics to create a point-of-care assay viral load in resource-limited  
415 settings.

416 **1.4 Contributions**

417 Much of this work was performed as part of a large collaboration. It would not tell a  
418 complete story in isolation. Therefore, I have preserved the chapters in published form and  
419 detailed my contribution to each project at the start of the chapter.

420

## CHAPTER 2: HIV latency and integration site placement in five cell-based models

421

This chapter was originally published as:

S Sherrill-Mix, MK Lewinski, M Famiglietti, A Bosque, N Malani, KE Ocwieja, CC Berry, D Looney, L Shan et al. 2013. HIV latency and integration site placement in five cell-based models. *Retrovirology*, 10:90. doi: 10.1186/1742-4690-10-90

422

I led the computational analysis, with assistance from CC Berry and N Malani. MK Lewinski, D Looney and J Guatelli analyzed integration sites using IonTorrent sequencing. M Famiglietti, A Bosque and V Planelles prepared DNA from latent and activated T cells using the Central Memory CD4 + model. L Shan, RF Siliciano, MJ Pace, LM Agosto, KE Ocwieja and U O'Doherty contributed data and suggestions. FD Bushman and I planned the overall study. I produced the figures. FD Bushman and I wrote the paper.

Additional files are available at [http://www.retrovirology.com/  
content/10/1/90/additional](http://www.retrovirology.com/content/10/1/90/additional)

423

### 2.1 Abstract

424

Background: HIV infection can be treated effectively with antiretroviral agents, but the persistence of a latent reservoir of integrated proviruses prevents eradication of HIV from infected individuals. The chromosomal environment of integrated proviruses has been proposed to influence HIV latency, but the determinants of transcriptional repression have not been fully clarified, and it is unclear whether the same molecular mechanisms drive latency in different cell culture models.

425

Results: Here we compare data from five different *in vitro* models of latency based on primary human T cells or a T cell line. Cells were infected *in vitro* and separated into

432 fractions containing proviruses that were either expressed or silent/inducible, and integration  
433 site populations sequenced from each. We compared the locations of 6,252 expressed  
434 proviruses to those of 6,184 silent/inducible proviruses with respect to 140 forms of genomic  
435 annotation, many analyzed over chromosomal intervals of multiple lengths. A regularized  
436 logistic regression model linking proviral expression status to genomic features revealed no  
437 predictors of latency that performed better than chance, though several genomic features  
438 were significantly associated with proviral expression in individual models. Proviruses in the  
439 same chromosomal region did tend to share the same expressed or silent/inducible status if  
440 they were from the same cell culture model, but not if they were from different models.

441 Conclusions: The silent/inducible phenotype appears to be associated with chromosomal  
442 position, but the molecular basis is not fully clarified and may differ among *in vitro* models  
443 of latency.

## 444 2.2 Background

445 Highly active antiretroviral therapy (HAART) can suppress HIV-1 replication in infected pa-  
446 tients, but the ability of HIV to persist as an inducible reservoir of latent proviruses<sup>134,140,143</sup>  
447 obstructs eradication of the virus and functional cure<sup>145</sup>. These latent proviruses are long  
448 lived<sup>141,142</sup> and relatively invisible to the immune system<sup>139,140</sup>. The potential for even a  
449 single virus to restart infection despite successful antiviral therapy means that it may be  
450 necessary to eliminate all latent proviruses to eradicate HIV from an infected person.

451 After integration, a positive feedback loop of Tat transactivation appears to partition  
452 proviral gene activity into either of two stable states<sup>354–356</sup>—abundant Tat driving high  
453 proviral expression or little Tat leading to quiescent latency. Similar to the positional effect  
454 variegation observed in fruit fly chromosomal rearrangements<sup>357,358</sup>, studies on cell clones  
455 with single integrations show that differing integration sites can have large differences in  
456 proviral expression<sup>359–361</sup>. These data suggest that integration site location, along with the  
457 cellular environment<sup>361–364</sup>, influences the balance between latency and proviral expression.

458 Associations between latency and genomic features have also been reported in collections of  
459 integration sites from cell culture models although the consistency of these effects across  
460 model systems and their relationships to latency in patients remains uncertain. Lewinski  
461 et al.<sup>150</sup> reported that proviruses integrated in gene deserts, alphoid repeats and highly  
462 expressed genes are more likely to have low expression. Shan et al.<sup>151</sup> reported an association  
463 between latency and integration in the same transcriptional orientation as host genes. Pace  
464 et al.<sup>152</sup> found that silent and expressed provirus integration sites differed in the abundance  
465 and expression levels of nearby genes, GC content, CpG islands and alphoid repeats. In  
466 model systems with defined integration sites, Lenasi et al.<sup>365</sup> reported decreased and Han  
467 et al.<sup>366</sup> reported increased viral transcription when the provirus is downstream of a highly  
468 expressed host gene.

469 Cell-based models of latency are important for many aspects of HIV research, including  
470 screening small molecules that can reverse latency and potentially allow eradication<sup>367,368</sup>.  
471 Location-driven differences in expression are preserved even after demethylation and histone  
472 deacetylase treatment<sup>359</sup>, which suggests that integration location has the potential to  
473 confound “shock and kill” anti-latency treatments<sup>369,370</sup>. A greater understanding of the  
474 effects of integration site location on latency could thus affect antiretroviral development.

475 To search for features of integration site associated with latency, we generated a set of  
476 inducible and expressed integration sites using a primary central memory CD4<sup>+</sup> T cell model  
477 of latency<sup>371,372</sup>, collected four previously reported integration site datasets and modeled  
478 the effects of genomic features near the integration site on the expression status of these  
479 proviruses. Although some genomic features associated with latency in individual models,  
480 no feature was consistently associated with proviral expression across all five cell culture  
481 models. However, closely neighboring proviruses within the same cellular model shared the  
482 same latency status much more often than expected by chance suggesting that chromosomal  
483 position of integration affects latency but that the mechanism remains unclear or differs  
484 between cell culture models. Thus these data help inform the design of experiments in HIV

485 eradication research.

486 **2.3 Methods**

487 **2.3.1 Integration sites**

488 Naive CD4<sup>+</sup> T cells were purified by negative selection from peripheral blood mononuclear  
489 cells. The cells were activated with anti-CD3 and anti-CD28 (+TGF-beta, anti-IL-12, and  
490 anti-IL-4) to generate “non-polarized” cells (the in vitro equivalent of central memory T  
491 cells). Five days after isolation, cells were infected with an NL4-3-based virus with GFP in  
492 place of Nef and the LAI envelope (X4) provided in trans at a concentration of 500 ng of  
493 p24 as measured by ELISA per million cells. Based on previous experience with this model,  
494 this amount of p24 should produce an MOI of approximately 0.15. Cells were cultured  
495 in the presence of IL-2. Two days post-infection, cells were sorted for GFP+; this active  
496 population expresses GFP even when treated with flavopiridol, although for this study they  
497 were not treated. The inducible population was the set of GFP negative cells from the initial  
498 sort that, 9 days post-infection, were activated with anti-CD3 and anti-CD28 and sorted for  
499 GFP production.

500 Genomic DNA from the inducible and expressed populations was digested with MseI, ligated  
501 to an adapter, and amplified by ligation-mediated PCR essentially as in Wu et al.<sup>373</sup> and  
502 Mitchell et al.<sup>374</sup> except that the nested PCR primers included sequence for the Ion Torrent  
503 P1 adapter and adapter A sequence with a 5 base barcode sequence specific to the inducible  
504 or expressed conditions. Amplicons were sequenced using an Ion Torrent Personal Genome  
505 Machine (PGM) according to manufacturer’s instructions using an Ion 316 chip and the Ion  
506 PGM 200 Sequencing kit (Life Technologies). The sequence reads were sorted into samples  
507 by barcode. All reads were required to match the expected 5' sequence with a Levenshtein  
508 edit distance less than 3 from the expected barcode, 5' primer and HIV long terminal repeat  
509 (LTR). The 5' primer and HIV sequence, along with the 3' primer if present, were trimmed  
510 from the read. Sequences with less than 24 bases remaining or containing any eight base

511 window with an average quality less than 15 were discarded. Duplicate reads and reads  
512 forming an exact substring of a longer read were removed.

513 **2.3.2 Analysis**

514 All statistical analysis was performed in R 2.15.2<sup>375</sup>. The analyses are described in a  
515 reproducible report (Appendix A.2). The annotated integration site data necessary to  
516 perform the analyses and the compilable code to generate this reproducible report are  
517 provided as supplemental information<sup>353</sup>. The new Central Memory CD4<sup>+</sup> data set was  
518 analyzed as in Berry et al.<sup>376</sup>. The integration patterns appeared similar to previously  
519 reported HIV integration site datasets<sup>377</sup>.

520 **2.3.3 Previously published data**

521 We collected integration sites from three previously reported studies (Table 2.1), for a total  
522 of four expressed versus silent/inducible pairs of samples. These studies used primary CD4<sup>+</sup>  
523 T cells or Jurkat cells infected with HIV or HIV-derived constructs as cell culture models of  
524 latency. Flow cytometry allowed cells expressing viral encoded proteins to be sorted from  
525 non-expressing cells. In two of the studies, these non-expressing populations were stimulated  
526 to ensure that the provirus could be aroused from latency. Specific differences in protocol  
527 between the study sets are summarized below.

528 **Jurkat** Lewinski et al.<sup>150</sup> infected Jurkat cells with a VSV-G pseudotyped, GFP-expressing  
529 pEV731 HIV construct (LTR-Tat-IRES-GFP)<sup>359</sup> at an MOI of 0.1. The cells were  
530 sorted into GFP+ and GFP- two to four days after infection. GFP+ cells were sorted  
531 again two weeks after infection and cells that were again GFP+ were collected for  
532 integration site sequencing. GFP- cells were sorted for GFP negativity twice more  
533 then stimulated with TNF $\alpha$ . Cells that were GFP+ after stimulation were collected  
534 for integration site sequencing. DNA was digested with MseI or a combination of NheI,  
535 SpeI and XbaI, ligated to adapters for nested PCR, amplified and sequenced by Sanger  
536 capillary electrophoresis.

537 **Bcl-2 transduced CD4<sup>+</sup>** Shan et al.<sup>151</sup> transduced CD4<sup>+</sup> T cells with Bcl-2, costimulated  
538 with bound anti-CD3 and soluble anti-CD28 antibodies, interleukin-2 and T cell growth  
539 factor and then infected with X4-pseudotyped GFP-expressing NL4-3- $\delta$ 6-drEGFP  
540 construct<sup>378</sup> at an MOI of less than 0.1. DNA was extracted, digested with PstI and  
541 circularized<sup>379</sup>. HIV-human junctions were amplified by reverse PCR and sequenced  
542 using Sanger capillary electrophoresis.

543 **Active CD4<sup>+</sup> & Resting CD4<sup>+</sup>** Pace et al.<sup>152</sup> spinoculated CD4<sup>+</sup> T cells with HIV  
544 NL4-3 at an MOI of 0.1. After 96 hours, the cells were stained for intracellular Gag  
545 CD25, CD69 and HLA-DR and sorted into four subpopulations based on activation  
546 state and Gag expression; activated Gag-, activated Gag+, resting Gag- and resting  
547 Gag+. The ability of the viruses to reactivate was not tested although previous studies  
548 have shown that the majority are likely inducible<sup>380</sup>. Genomic DNA was extracted and  
549 digested with restriction enzymes MseI and Tsp509 and ligated to adapters. Proviral  
550 LTR-host genome junctions were sequenced by 454 pyrosequencing after nested PCR.

551 All datasets were processed using the hiReadsProcessor R package<sup>381</sup>. Adaptor trimmed  
552 reads were aligned to UCSC freeze hg19 using BLAT<sup>382</sup>. Genomic alignments were scored  
553 and required to start within the first three bases of a read with 98% identity. Alignments for  
554 a given read with a BLAT score less than the maximum score for that read were discarded.  
555 Reads giving rise to multiple best scoring genomic alignments were excluded, while reads  
556 with a single best hit were dereplicated and converged if within 5bp of each other. The  
557 Bcl-2 transduced CD4<sup>+</sup> sample was sequenced from U3 in the 5' HIV LTR while the other  
558 samples were sequenced from U5 in the 3' LTR. To account for the 5 base duplication of  
559 host DNA caused by HIV integration, the chromosomal coordinates of the Bcl-2 transduced  
560 CD4<sup>+</sup> sample were adjusted by  $\pm 4$  bases.

561 To allow for alignment difficulties in the analysis of genomic repeats, reads with multiple  
562 best scoring alignments, along with the single best hit reads used above, were included in  
563 the repeat analyses. If any best scoring alignment for a read fell within a repeat, then that

Title	Cell type	Virus	Time of harvest after infection	Sequencing	Generation of expressed vs. silent/inducible	Citation	Silent/inducible unique sites	Expressed unique sites
Jurkat	Jurkat cells	HIV vector pEV731 (LTR-Tat-IRES-GFP)	2 weeks	Sanger	TNF $\alpha$ , GFP expression	Lewinski et al. <sup>150</sup>	463 inducible	643
Bcl-2 transduced CD4 $^{+}$	Primary CD4 $^{+}$ T cells (Bcl-2 transduced)	HIV NL4-3- $\delta$ 6-drEGFP (inactivated <i>gag</i> , <i>vif</i> , <i>vpr</i> , <i>vpu</i> , <i>nef</i> and <i>env</i> replaced by GFP)	3 days + 3-4 weeks + 3 days	Sanger	anti-CD3, anti-CD28 antibodies, GFP expression	Shan et al. <sup>151</sup>	446 inducible	273
Active CD4 $^{+}$	Primary active CD4 $^{+}$ T cells	HIV NL4-3	3 days	454	high vs. low Gag	Pace et al. <sup>152</sup>	1604 silent	1274
Resting CD4 $^{+}$	Primary resting CD4 $^{+}$ T cells	HIV NL4-3	3 days	454	high vs. low Gag	Pace et al. <sup>152</sup>	1942 silent	784
Central Memory CD4 $^{+}$	Primary central memory CD4 $^{+}$ T cells	HIV NL4-3 $\Delta$ Nef GFP	2 days/9 days	Ion-Torrent	anti-CD3, anti-CD28 antibodies, GFP expression	This paper	1729 inducible	3278

Table 2.1: HIV-1 integration datasets from *in vitro* models of latency where the proviruses were determined to be silent/inducible or expressed

564 read was considered to map to that repeat.

### 565 2.3.4 Genomic features

566 A total of 140 whole genome features for CD4 $^{+}$  T-cells were gathered from data sources  
 567 indicated in Table 2.2. For features encoded as peaks or hotspots, the log of the distance of  
 568 each integration site to the nearest border was used for modeling. Integration sites from  
 569 HIV 89.6 infection in primary CD4 $^{+}$  T cells<sup>383</sup> were used to count nearby integrations and  
 570 determine a  $\pm$ 20bp position weight matrix for integration targets. Illumina RNA-Seq from  
 571 active CD4 $^{+}$  cells (Chapter 4) was used to estimate raw cellular expression and fragments  
 572 per kilobase of transcript per million mapped reads for genes as calculated by Cufflinks<sup>384</sup>.  
 573 For sequence-based data like RNA-Seq and ChIP-Seq, the number of reads aligned within  
 574 a  $\pm$  50, 500, 5,000 50,000 and 500,000 bp windows of each integration site were counted  
 575 and log transformed. In addition, chromatin state classifications derived from a hidden

576 Markov model based on histone marks and a few binding factors<sup>385</sup> were included as binary  
577 variables. All data from previous genomic freezes were converted to hg19 using liftover<sup>386</sup>.

## 578 2.4 Results

579 The combination of integration site data newly reported here (set named “Central Memory  
580 CD4<sup>+</sup>”) with previously published data (sets named “Jurkat”, “Bcl-2 transduced CD4<sup>+</sup>”,  
581 “Active CD4<sup>+</sup>”, and “Resting CD4<sup>+</sup>”) provides a collection of 12,436 integration sites (Table  
582 2.1) where the expression status of the provirus—silent/inducible or expressed—is known.  
583 In three of the datasets, Jurkat, Central Memory CD4<sup>+</sup> and Bcl-2 transduced CD4<sup>+</sup>, the  
584 proviruses were sorted based on inducibility. In the Resting CD4<sup>+</sup> and Active CD4<sup>+</sup> datasets,  
585 cells were sorted only based on proviral expression. Previous studies have shown that most  
586 silent proviruses in this model system are inducible<sup>380</sup>.

### 587 2.4.1 Global model

588 If a genomic feature and latency are monotonically related then we should be able to detect  
589 this relationship using Spearman rank correlation. In addition if a feature has a consistent  
590 effect across models we should see a consistent pattern in the direction of correlation. A  
591 simple first look for correlation between genomic features (Table 2.2) and latency status  
592 yielded inconsistent results among the five samples with no variables having a significant  
593 Spearman rank correlation across all, or even four out of five, of the samples (Figure 2.1).  
594 This suggests that there is not a consistent simple monotonic relationship between the  
595 genomic variable and latency, or that any such correlations are modest and not detectable  
596 across all studies given the available statistical power. We return to some of the stronger  
597 trends below.

598 To investigate whether a combination of variables may affect latency, we fit a lasso-regularized  
599 logistic regression, as implemented in the R package glmnet<sup>395</sup>, to predict latency using  
600 the genomic variables. The relationship between silent/inducible status and each genomic  
601 variable was allowed to vary between models by including the interaction of genomic features

<b>Group</b>	<b>Type</b>	<b>Source</b>	<b>Number</b>	<b>Types</b>
T cell expression	RNA-Seq	Chapter 4	1	RNA
Jurkat expression	RNA-Seq	Encode <sup>387</sup>	1	wgEncodeHudsonalphaRnaSeq
Integration sites	Locations	Berry et al. <sup>383</sup>	1	sites
DNase sensitivity	DNA-Seq/peaks	Encode <sup>387</sup>	1	wgEncodeOpenChromDnase
Methylation	DNA-Seq	388	1	Methyl
CpG	Locations	UCSC <sup>389</sup>	1	cpgIslandExt
Sequence-based	Continuous	—	4	% GC, HIV PWM score, distance to centrosome, chromosomal position
Repeats	Locations	UCSC <sup>389</sup>	16	DNA, LINE, Low_complexity, LTR, Other, RC, RNA, rRNA, Satellite, scRNA, Simple_repeat, SINE, snRNA, srpRNA, tRNA, alphoid
Histone features	ChIP-Seq/Peaks	Wang et al. <sup>390</sup>	18	H2AK5ac, H2AK9ac, H2BK120ac, H2BK12ac, H2BK20ac, H2BK5ac, H3K14ac, H3K18ac, H3K23ac, H3K27ac, H3K36ac, H3K4ac, H3K9ac, H4K12ac, H4K16ac, H4K5ac, H4K8ac, H4K91ac
Histone features	ChIP-Seq/Peaks	Barski et al. <sup>391</sup>	23	CTCF, H2AZ, H2BK5me1, H3K27me1, H3K27me2, H3K27me3, H3K36me1, H3K36me3, H3K4me1, H3K4me2, H3K4me3, H3K79me1, H3K79me2, H3K79me3, H3K9me1, H3K9me2, H3K9me3, H3R2me1, H3R2me2, H4K20me1, H4K20me3, H4R3me2, PolII
Chromatin state	Binary	Ernst and Kellis <sup>385</sup>	51	state <sub>1</sub> ,state <sub>2</sub> ,...,state <sub>51</sub>
HATs and HDACs	ChIP-Seq	Wang et al. <sup>392</sup>	11	Resting-HDAC1, Resting-HDAC2, Resting-HDAC3, Resting-HDAC6, Resting-p300, Resting-CBP, Resting-MOF, Resting-PCAF, Resting-Tip60, Active-HDAC6, Active-Tip60
Nucleosome	ChIP-Seq	Schones et al. <sup>393</sup>	2	Resting-Nucleosomes, Active Nucleosomes
UCSC genes	Locations	Hsu et al. <sup>394</sup>	4	in gene, in gene (same strand), gene count, distance to nearest gene, in exon, in intron

Table 2.2: Genomic data available for comparison to HIV integration sites

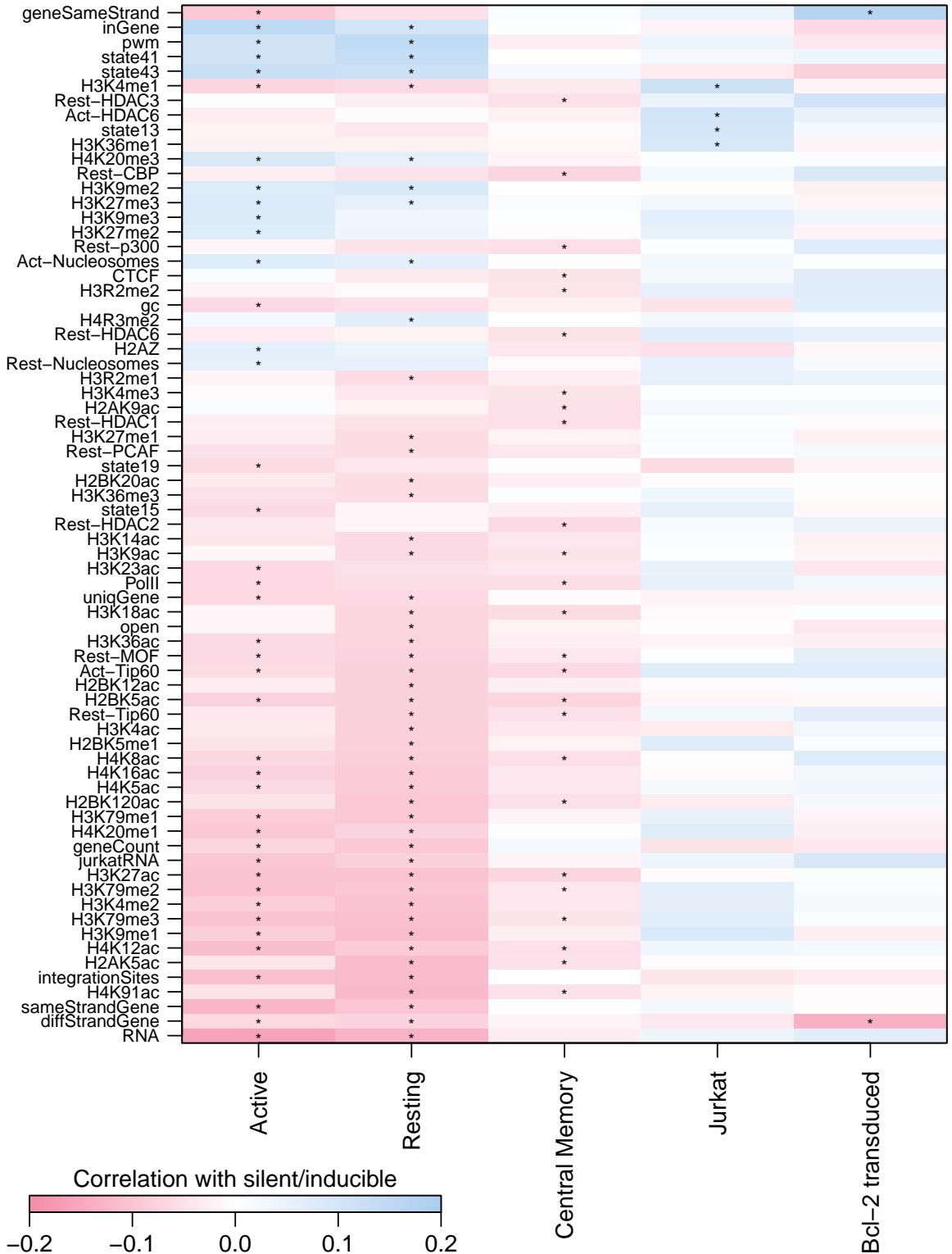


Figure 2.1: Spearman rank correlation between proviral expression status and genomic features. Only genomic features with at least one correlation with latency with a false discovery rate  $q$ -value  $< 0.01$  (marked by asterisks) are shown.

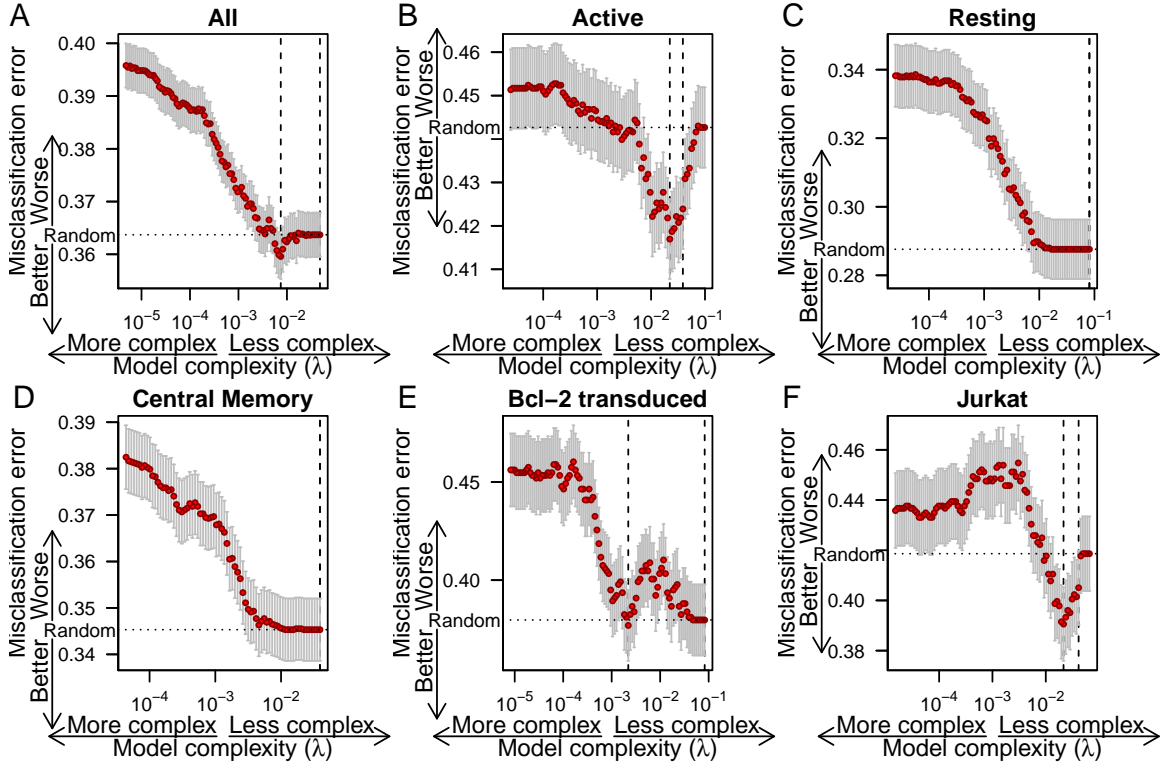


Figure 2.2: Misclassification error from cross validation for lasso regressions of silent/inducible status on genomic features as a function of  $\lambda$ , the regularization coefficient for the lasso regression, for all cell culture models combined and each individual cell culture model. The number of variables included and size of coefficients in the model increases to the left. Whiskers show the standard error of mean misclassification error. Dashed vertical lines indicate the minimum misclassification error and the simplest model within one standard error. Dotted horizontal line indicates the misclassification error expected from random guessing.

602 with dummy variables indicating cellular model. The  $\lambda$  smoothing parameter of the lasso  
 603 regression was optimized by finding the  $\lambda$  with lowest classification error in 480-fold cross  
 604 validation and finding the simplest model with misclassification error within one standard  
 605 error.

606 The proportion of silent/inducible sites varied between the samples. To avoid the model  
 607 overfitting on this source of variation, an indicator variable for each sample was included in  
 608 the base model. The base model with no genomic variables was selected as the best model by  
 609 cross validation (Figure 2.2A). This suggest that there is not a consistent linear relationship  
 610 between an additive combination of genomic variables and latency across all models.

611 When each dataset was fit individually with leave-one-out cross validation, improvements in  
612 cross-validated misclassification error were only observed in the Active CD4<sup>+</sup> (5.8% decrease  
613 in misclassification error, standard error: 2.1) and Jurkat (6.7% decrease in misclassification  
614 error, standard error: 3.5) samples (Figure 2.2B-F). There was no overlap in variables  
615 selected for the Active CD4<sup>+</sup> and Jurkat samples.

616 Finding little global association between latency and genomic features, we investigated  
617 whether predictors of latency reported previously by single studies were consistently associ-  
618 ated with latency across studies.

#### 619 **2.4.2 Cellular transcription**

620 Model systems with defined integration sites show upstream transcription can interfere with  
621 viral transcription<sup>396</sup> and that cellular transcription in the same orientation may interfere  
622 with viral transcription<sup>365</sup> or increase viral transcription<sup>366</sup> and in opposite orientations  
623 may decrease transcription<sup>366</sup>. In integration site studies, integration outside genes appears  
624 to increase latency<sup>150</sup> but high transcription of nearby host cell genes may cause increased  
625 latency<sup>150,151</sup>. In addition, Tat or other viral proteins may affect cellular transcription<sup>319,397</sup>.

626 To look at transcription and latency, we ran a logistic regression of silent/inducible status  
627 on a quartic function of RNA expression, as determined by RNA-Seq reads within 5,000  
628 bases in Jurkat cells for the Jurkat sample or CD4<sup>+</sup> T cells for the remaining samples,  
629 interacted with indicator variables encoding cell culture model. There appears to be little  
630 agreement between samples (Figure 2.3). The Resting CD4<sup>+</sup> and Active CD4<sup>+</sup> datasets  
631 show an enrichment in silent proviruses in regions with low gene expression. The other three  
632 studies show the opposite or no relationship for low expression regions. The two samples  
633 showing increased silence in areas of low expression (Resting CD4<sup>+</sup> and Active CD4<sup>+</sup>) are  
634 from a study that did not check whether inactive viruses could be activated. One possible  
635 explanation is that regions with low gene transcription may harbor proviruses that are not  
636 easily activated, though some other discrepancy between *in vitro* systems could also explain

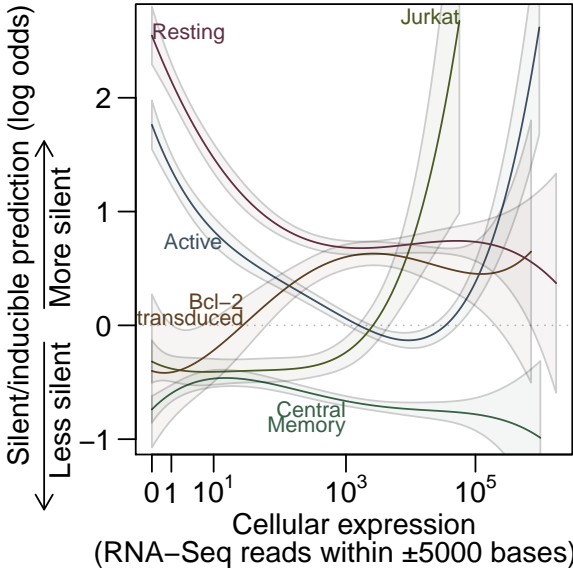


Figure 2.3: Predictions from a logistic regression of silent/inducible status on cellular RNA expression. High y-axis values are predicted to be silent/inducible. Dashed line shows where equal odds of silent/inducible and expressed are predicted. Solid lines show predictions from the regression for each sample and shaded regions indicate one standard error from the modeled predictions.

the difference. Both the Jurkat and Active CD4<sup>+</sup> samples appear to increase in latency with increasing expression while the remaining three studies did not show a strong trend.

#### 2.4.3 Orientation bias

Shan et al.<sup>151</sup> reported that inducible proviruses were oriented in the same strand as the host cell genes into which they had integrated more often than chance. This orientation bias was still reproduced after our reprocessing of the Bcl-2 transduced CD4<sup>+</sup> sample from Shan et al.<sup>151</sup>. However, the proportion of provirus oriented in the same strand as host genes did not differ significantly from 50% in the other samples (Figure 2.4). Perhaps orientation bias and transcriptional interference are especially sensitive to parameters of the model system.

#### 2.4.4 Gene deserts

Lewinski et al.<sup>150</sup> reported increased latency in gene deserts. In the collected data, integration outside known genes was associated with latency (Fisher's exact test,  $p < 10^{-6}$ ). This seemed to largely be driven by the Active CD4<sup>+</sup> and Resting CD4<sup>+</sup> samples with significant association found individually in only those two samples (both  $p < 10^{-8}$ ) and no significant association observed in the other three samples (Figure 2.5A). Looking only at integration sites outside genes, silent sites in the Resting CD4<sup>+</sup> sample had a mean distance to the

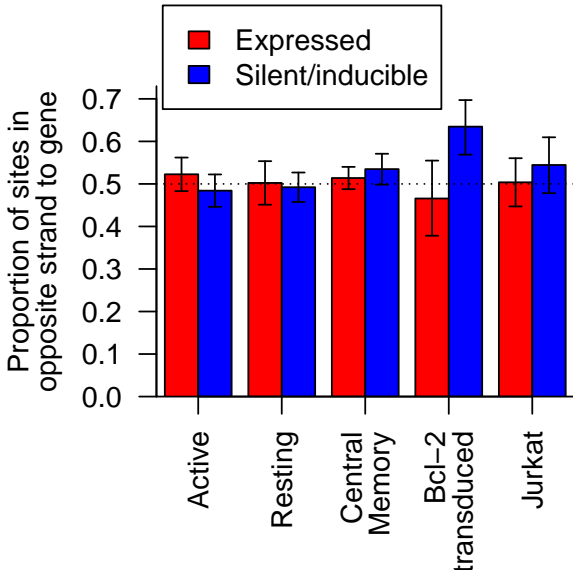


Figure 2.4: The proportion of provirus integrated in the opposite strand compared to cellular genes in silent/inducible (blue) and expressed (red) samples. Error bars show the 95% Clopper-Pearson binomial confidence interval.

653 nearest gene 2.5 times greater than that of expressed sites (95% CI: 2.2–6.2 $\times$ ,  $p < 10^{-6}$ ,  
 654 Welch two sample t-test on log transformed distance) (Figure 2.5B). The Active CD4 $^{+}$   
 655 sample had a small difference that did not survive Bonferroni correction.

656 Lewinski et al.<sup>150</sup> also reported decreased latency near CpG islands and reasoned this was  
 657 tied to the increased latency in gene deserts. In the Resting CD4 $^{+}$  sample, silent sites were  
 658 on average further from CpG islands than expressed sites (Bonferroni corrected Welch's two  
 659 sample T test,  $p = 0.006$ ), but there was no significant relationship between silent/inducible  
 660 status and log distance to CpG island after Bonferroni correction if the integration site's  
 661 location inside or outside of a gene was accounted for first (analysis of deviance).

#### 662 2.4.5 Alphoid repeats

663 Alphoid repeats are repetitive DNA sequences found largely in the heterochromatin of  
 664 centromeres<sup>398</sup>. Integration near heterochromatic alphoid repeats has been reported to  
 665 associate with latency<sup>150,152,360</sup>. Looking only at uniquely mapping sites, there was no  
 666 statistically significant association between latency and location inside an alphoid repeat in  
 667 pooled or individual samples (Fisher's exact test).

668 Since alphoid repeats are both problematic to assemble in genomes and difficult to map

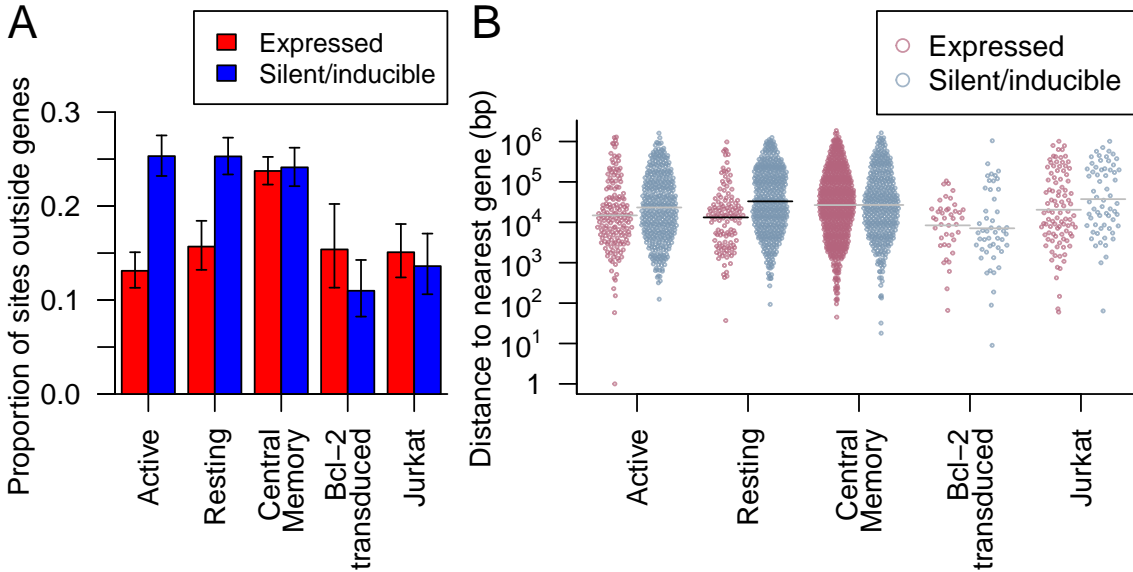


Figure 2.5: (A) The proportion of provirus integrated outside genes in silent/inducible (blue) and expressed (red) samples. Error bars show the 95% Clopper-Pearson binomial confidence interval. (B) The nearest distance to any gene for integration sites (points) outside genes in the five samples. Points are spread in proportion to kernel density estimates. Horizontal lines indicate sample means where there was a significant difference in means between silent/inducible and expressed provirus (black) or no significant difference (grey).

669 onto, we reasoned that some alphoid hits might be lost or miscounted in the filtering  
 670 procedures of the standard workup. To counteract this, we treated each sequence read as an  
 671 independent observation of a proviral integration and included sequence reads with more  
 672 than one best scoring alignment. For multiply aligned reads, we considered the read to have  
 673 been inside an alphoid repeat if any of its best scoring alignments fell within a repeat. We  
 674 found 74 reads with potential alphoid mappings. Integration inside alphoid repeats was  
 675 significantly associated with the expression status of a provirus in the Resting CD4<sup>+</sup>, Jurkat  
 676 and Central Memory CD4<sup>+</sup> datasets (Bonferroni corrected Fisher's exact test, all  $p < 0.05$ )  
 677 and approached significance in the Active CD4<sup>+</sup> dataset ( $p = 0.053$ ) (Figure 2.6). The Bcl-2  
 678 transduced CD4<sup>+</sup> data did not contain any integration sites in alphoid repeats, probably due  
 679 to 1) the relatively low number of integration sites in the dataset and 2) to the requirement  
 680 for cleavage at two Pst1 restriction sites, which are not found in the consensus sequence of  
 681 alphoid repeats<sup>399</sup>. Of the 1340 repeat types in the RepeatMasker database<sup>399</sup>, only alphoid  
 682 repeats achieved a significant association with proviral expression in more than two datasets.

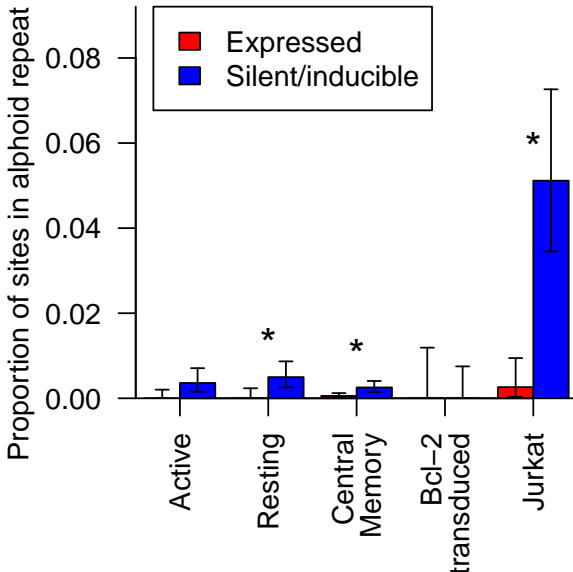


Figure 2.6: The proportion of integration sites with matches in alphoid repeats in silent/inducible (blue) and expressed (red) cells in five samples. Error bars show the 95% Clopper-Pearson binomial confidence interval. Asterisks indicate significant associations between integrations within an alphoid repeat and proviral expression status (Bonferroni corrected Fisher's exact test  $p < 0.05$ ).

#### 683 2.4.6 Acetylation

684 Histone marks or chromatin remodeling, especially involving the key “Nuc-1” histone near  
 685 the transcription start site in the viral LTR, appear to affect viral expression<sup>361,400,401</sup>.  
 686 Based on this effect, histone deacetylase inhibitors have been developed as potential HIV  
 687 treatments and show some promise in disrupting latency<sup>370</sup>. In these genome-wide datasets,  
 688 we do not have information on the state of individual LTR nucleosomes. However, repressive  
 689 chromatin does seem to spread to nearby locations if not blocked by insulators<sup>357,358</sup> and  
 690 the state of neighboring chromatin could affect proviral transcription independently of  
 691 provirus-associated histones.

692 We found that the number of ChIP-seq reads near an integration site from several histone  
 693 acetylation marks (Figure 2.1) were associated with efficient expression in the Active CD4<sup>+</sup>,  
 694 Resting CD4<sup>+</sup> and Central Memory CD4<sup>+</sup> samples. H4K12ac had the strongest association  
 695 (Bonferroni corrected Fisher's method combination of Spearman's  $\rho$ ,  $p < 10^{-25}$ ) with  
 696 silence/latency (Figure 2.7A).

697 Although the appearance of several significantly associated acetylation marks might suggest  
 698 acetylation exerts a considerable effect on the expression of a provirus, there are strong

699 correlations among these marks, so their effects may not be independent. To account for  
700 the correlations between these variables, we performed a principal component analysis  
701 (PCA) to convert the correlated acetylation marks into a series of uncorrelated principal  
702 components that capture much of the variance within a few components. Here, the first  
703 principal component explained 59% of the variance and the first ten components 84%.  
704 Several of these principal components again displayed significant associations with latency  
705 in the Active CD4<sup>+</sup>, Resting CD4<sup>+</sup> and Central Memory CD4<sup>+</sup> samples but no significant  
706 correlations in the Bcl-2 transduced CD4<sup>+</sup> or Jurkat samples (Figure 2.7B). A logistic  
707 regression of expression status on the first ten principal components and sample did not  
708 reduce misclassification error from a base model including only sample in 480-fold cross  
709 validation (base model misclassification error: 36.4%, PCA model: 36.5%). This suggests  
710 that acetylation of neighboring chromatin does not exert strong effects on latency in all  
711 samples.

#### 712 2.4.7 Clustering

713 We reasoned that if there was a strong relationship between latency and chromosomal  
714 position, then integration sites that are near one another on the same chromosome should  
715 share the same expression status more often than expected by chance. To test this, we  
716 compared how often pairs of proviruses shared the same expression status in relation to  
717 the distance between the two sites (Figure 2.8). Pairs of sites with little distance between  
718 integration locations did share the same expression status more often than expected by  
719 chance (e.g. neighbors closer than 100bp, Fisher exact test  $p = 0.0002$ ). Breaking out the  
720 data to separate between sample and within sample pairings showed that this matching was  
721 limited to neighbors within the same experimental model (Figure 2.8), emphasizing that  
722 chromosomal environment does appear to influence latency, but the factors involved differ  
723 among experimental models of latency.

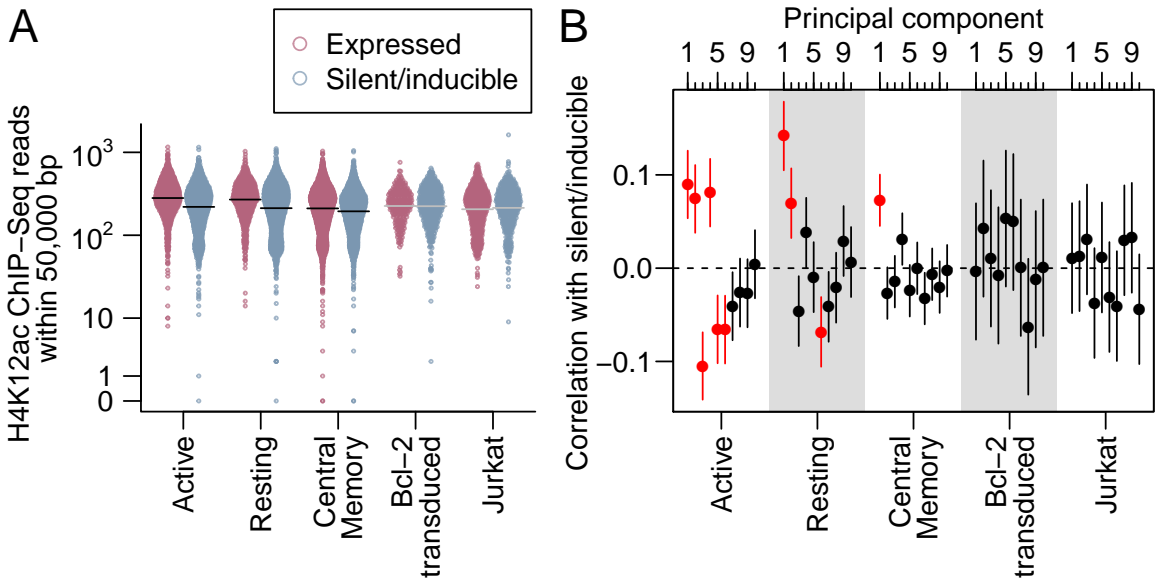


Figure 2.7: (A) The number of ChIP-seq reads for H4K12ac, the histone mark with the lowest Fisher's method  $p$ -value for correlation with latency, within 50,000 bases across the five samples. Integration sites (points) are spread in proportion to kernel density estimates. Horizontal lines indicate sample means where there was a significant difference (black) in means between silent/inducible and expressed provirus or no significant difference (grey). (B) The correlation (points) and its 95% confidence interval (vertical lines) between principal components of acetylation and silent/inducible status for each of the five samples. Red indicates correlations with a Bonferroni-corrected  $p$ -value  $< 0.05$ .

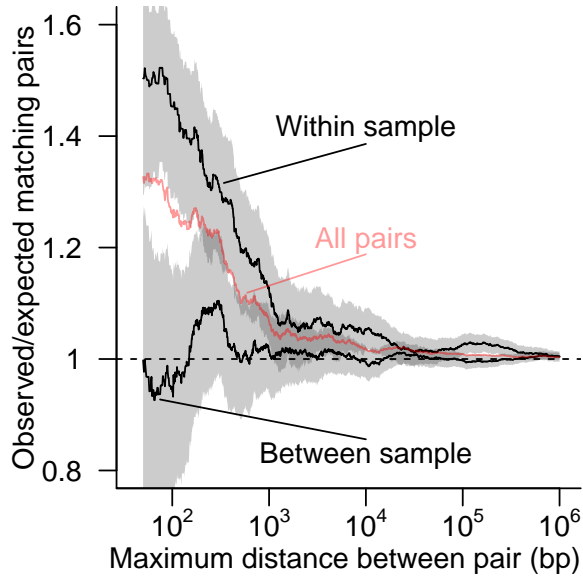


Figure 2.8: The ratio of the number of pairs of proviruses with matching expression status to the number of matches expected by random pairings given the frequency of silent/inducible proviruses. All possible pairs of proviruses integrated within a given distance of each other on the same chromosome (red line) were separated into two sets; one with both proviruses from within the same cell culture model and one with proviruses paired between two different cell culture models (black lines). The shaded region shows the 95% Clopper-Pearson binomial confidence interval for within and between sample pairings. The dashed horizontal line shows the ratio of 1 expected if there is no association between the expression status of neighboring proviruses.

## 724 2.5 Conclusions

725 Here we compared the latency status of HIV-1 proviruses in five model systems with the  
726 genomic features surrounding their integration sites. Surprisingly, no relationships between  
727 genomic features near the integration location and latency achieved significance in all models.  
728 Proviruses from the same cellular model integrated in nearby positions did share the same  
729 latency status much more often than predicted by chance, indicating the existence of local  
730 features influencing latency, but these were not consistent among models. This suggests that  
731 whatever features are affecting latency are highly local and model-specific, and that we may  
732 not have access to all relevant chromosomal features e.g. <sup>402–405</sup>.

733 In addition to differences in experimental conditions, methodological issues have the potential  
734 to obscure patterns. Examples include multiply infected cells, inactivated viruses and  
735 inaccurate assessment of HIV gene activity—each of these are discussed below.

736 A latent provirus integrated into the same cell as an expressed provirus will be erroneously  
737 sorted as expressed, potentially confounding analysis. A low multiplicity of infection (MOI)  
738 will help to avoid this problem, but there is still the potential for a significant proportion of  
739 the cells studied to contain multiple integrations. This problem arises because although cells  
740 with multiple integrations form a small proportion of total cells, most of the total are cells  
741 lacking an integrated provirus and thus are excluded by experimental design. For example,  
742 assuming integrations are Poisson distributed with an MOI of 0.1 (1 integration per 10 cells),  
743 90.5% of cells will not contain a provirus, 9% of cells will contain one proviral integration  
744 and 0.5% of cells will contain multiple integrations. The cells without an integration are  
745 not amplified by HIV-targeted PCR leaving only 9.5% of the total cells. Of these cells  
746 actually under study, 4.9% will contain multiple integrations. Thus the signal from expressed  
747 proviruses may be muted by the presence of latent proviruses in the expressed population.

748 The replication cycle of HIV is error prone, and a significant proportion of virions contain  
749 mutated genomes<sup>87</sup>. In studies that do not check for inducibility, mutant proviruses

750 integrated in regions of the genome otherwise favorable to proviral expression can be sorted  
751 into the latent pool due to mutational inactivation. This problem of inactivated provirus  
752 is worse when latent provirus are rare and exacerbated further when looking at latency in  
753 the cells of HIV patients due to selective enrichment of inactivated proviruses incapable  
754 of spreading infection<sup>140</sup>. Here, the effects of mutation are minimized in the datasets that  
755 required inducible viral expression (Jurkat, Bcl-2 transduced CD4<sup>+</sup>, Central Memory CD4<sup>+</sup>)  
756 but may be a confounder in the two datasets that were sorted based on lack of viral expression  
757 only (Active CD4<sup>+</sup>, Resting CD4<sup>+</sup>).

758 Inaccurate staining or leaky markers may also result in misclassification of proviruses. False  
759 positives and false negatives will result in incorrectly sorted latent and expressed integrations.  
760 For example, if 5% of cells not containing Gag are labeled as Gag+ and there are an equal  
761 amount of latent and expressed integration sites, then 4.8% of integrations labeled expressed  
762 will actually be latent. If a category is rare, false staining has even greater potential to cause  
763 error. For example, if only 5% of sites are latent and a Gag stain has a false negative rate  
764 of 5%, then we would expect 48.7% of sites classified as latent to actually be mislabeled  
765 expressed integrations.

766 Attempts to induce latent proviruses in patients have so far focused on using histone  
767 deacetylase inhibitors, raising interest in associations with histone acetylation in these data.  
768 An important caveat in results from these genome-wide data is that histone modification  
769 near the integrated provirus may not be representative of modification within the provirus  
770 at the key “Nuc-1” nucleosome of the transcription start site<sup>401</sup>, though local correlations in  
771 chromatin states are well established from studies of position effect variegation<sup>357,358</sup>. We  
772 found that some histone acetylation marks were significantly associated with viral expression  
773 in some but not all samples (Figures 2.1, 2.7). This lack of association may be due to a  
774 lack of power in these studies, but the confidence intervals suggest that any correlations  
775 between acetylations and latency are unlikely to be strong. These weak correlations raise  
776 the possibility that there are populations of latent proviruses that are not associated with

777 acetylation and may not be inducible by histone deacetylase inhibitors.

778 This study highlights that the choice of model system can have a large effect on measurements  
779 of latency. Further studies are needed to determine which *in vitro* models best reflect latency  
780 *in vivo*. Different cell models may report genuinely different mechanisms of latency. While we  
781 did see some relationship between histone acetylation and latency, paralleling a recent clinical  
782 trial of SAHA<sup>370</sup>, associations with histone acetylation did not explain a large fraction of  
783 the difference between latent and expresssed proviruses in any of the five models. One  
784 possible explanation is that there may be multiple mechanisms that maintain proviruses in a  
785 latent state. To be successful, shock-and-kill treatments must induce and destroy all latent  
786 proviruses to eliminate HIV from an infected individual, raising the question of whether  
787 multiple simultaneous inducing treatments will be necessary.

788 **2.6 Availability of supporting data**

789 Sequence reads from the Central Memory CD4<sup>+</sup> sample reported here, the Resting CD4<sup>+</sup>  
790 and Active CD4<sup>+</sup> data reported by Pace et al.<sup>152</sup>, the Bcl-2 transduced CD4<sup>+</sup> data reported  
791 by Shan et al.<sup>151</sup> and reprocessed data originally reported by Lewinski et al.<sup>150</sup> are available  
792 at the Sequence Read Archive under accession number SRP028573.

793 **2.7 Acknowledgements**

794 We would like to thank Werner Witke for assistance with IonTorrent sequencing. This  
795 work was supported in part by NIH grants R01 AI 052845-11 to FDB, R21AI 096993 and  
796 K02AI078766 to UO'D, 5T32HG000046 to SS-M, AI087508 to VP and R01AI038201 to  
797 JG, the Penn Genome Frontiers Institute, the University of Pennsylvania Center for AIDS  
798 Research (CFAR) P30 AI 045008 and the University of California, San Diego, CFAR P30  
799 AI036214.

800      **CHAPTER 3: Dynamic regulation of HIV-1 mRNA populations**  
801      **analyzed by single-molecule enrichment and long-read**  
802      **sequencing**

This chapter was originally published as:

KE Ocwieja, S Sherrill-Mix, R Mukherjee, R Custers-  
Allen, P David, M Brown, S Wang, DR Link, J Olson  
et al. 2012. Dynamic regulation of HIV-1 mRNA popu-  
lations analyzed by single-molecule enrichment and long-  
read sequencing. *Nucleic Acids Res*, 40:10345–10355. doi:  
10.1093/nar/gks753

803      FD Bushman, K Travers, DR Link, E Schadt, KE Ocwieja and R Mukher-  
jee conceived and designed the experiment. KE Ocwieja and R Custers-  
Allen carried out sample preparation and experimental validation. P  
David and J Olson performed single-molecule amplification. K Travers  
and S Wang performed sequencing. KE Ocwieja, M Brown and I analyzed  
the data. KE Ocwieja and I produced the figures. KE Ocwieja, FD  
Bushman and I wrote the manuscript.

Supplementary data are available at [http://nar.oxfordjournals.org/  
content/40/20/10345/suppl/DC1](http://nar.oxfordjournals.org/content/40/20/10345/suppl/DC1)

804      **3.1 Abstract**

805      Alternative RNA splicing greatly expands the repertoire of proteins encoded by genomes.  
806      Next-generation sequencing (NGS) is attractive for studying alternative splicing because  
807      of the efficiency and low cost per base, but short reads typical of NGS only report mRNA  
808      fragments containing one or few splice junctions. Here, we used single-molecule amplification  
809      and long-read sequencing to study the HIV-1 provirus, which is only 9700 bp in length, but  
810      encodes nine major proteins via alternative splicing. Our data showed that the clinical isolate  
811      HIV<sub>89.6</sub> produces at least 109 different spliced RNAs, including a previously unappreciated  
812      ~1 kb class of messages, two of which encode new proteins. HIV-1 message populations

813 differed between cell types, longitudinally during infection, and among T cells from different  
814 human donors. These findings open a new window on a little studied aspect of HIV-1  
815 replication, suggest therapeutic opportunities and provide advanced tools for the study of  
816 alternative splicing.

### 817 3.2 Introduction

818 Alternative splicing greatly expands the information content of genomes by producing  
819 multiple mRNAs from individual transcription units. Approximately 95% of human genes  
820 with multiple exons encode RNA transcripts that are alternatively spliced, and mutations  
821 that affect alternative splicing are associated with diseases ranging from cystic fibrosis to  
822 chronic lymphoproliferative leukemia<sup>407–411</sup>. Work to decipher an RNA ‘splicing code’ has  
823 revealed that multiple interactions between trans-acting factors and RNA elements determine  
824 splicing patterns, though regulation is little understood for most genes<sup>305</sup>.

825 The integrated HIV-1 provirus is ~9700 bp in length and has a single transcription start  
826 site, but according to the published literature yields at least 47 different mRNAs encoding  
827 9 proteins or polyproteins, making HIV an attractive model for studies of alternative  
828 splicing<sup>412</sup>. HIV mRNAs fall into three classes: the unspliced RNA genome, which encodes  
829 Gag/Gag-Pol; partially spliced transcripts, ~4 kb in length, encoding Vif, Vpr, a one-exon  
830 version of Tat, and Env/Vpu; and completely spliced mRNAs of roughly 2 kb encoding  
831 Tat, Rev and Nef (Figure 3.1A). Additional rare ‘cryptic’ splice donors (5’ splice sites) and  
832 acceptors (3’ splice sites) contribute even more mRNAs<sup>413–418</sup>. A complex array of positive  
833 and negative cis-acting elements surrounding each splice site regulates the relative abundance  
834 of the HIV-1 mRNAs, and disrupting the balance of message ratios impairs viral replication  
835 in several models<sup>284,419–425</sup>. Studies have suggested strain-specific splicing patterns may  
836 exist<sup>412,426,427</sup>. However, detailed studies of complete message populations have not been  
837 reported for clinical isolates of HIV-1.

838 Several groups have demonstrated tissue- and differentiation-specific splicing of cellular

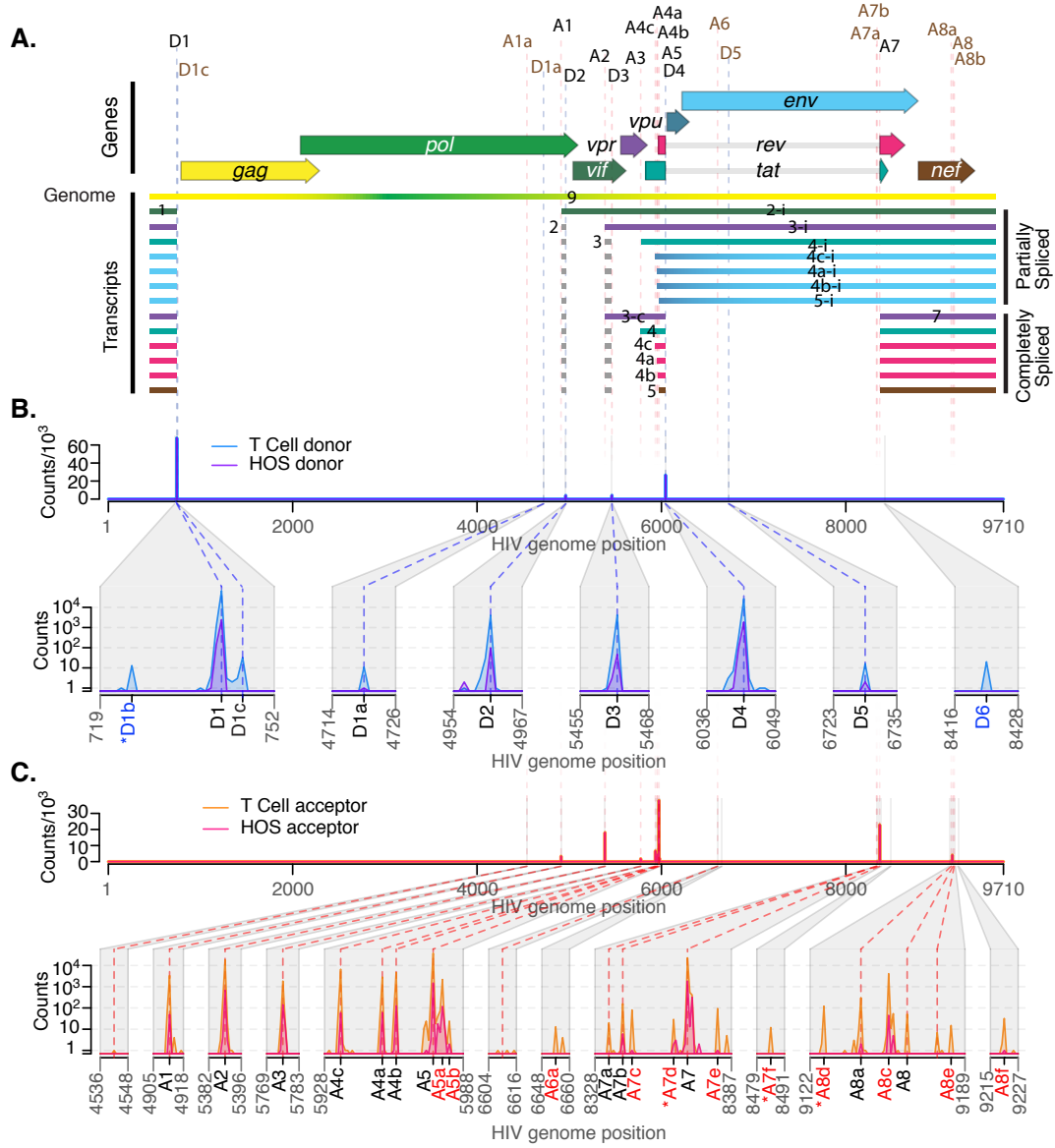


Figure 3.1: Mapping the splice donors and acceptors of HIV<sub>89.6</sub>. PacBio sequence reads of HIV<sub>89.6</sub> cDNA from infected HOS-CD4-CCR5 (HOS) and CD4<sup>+</sup> T cells were aligned to the HIV<sub>89.6</sub> genome shown in (A). Exons of the conserved HIV-1 transcripts are colored according to the encoded gene. Conserved (black) and published cryptic (brown) splice donors ('D') and acceptors ('A') are shown. Gaps in HIV-1 sequence alignments with at least one end located at a published or verified splice donor or acceptor were defined as introns. For each base of the HIV<sub>89.6</sub> genome, the number of sequence reads in which that base occurred at the 5'-end (B) or 3'-end (C) of an intron is plotted for each cell type. Putative splice donors and acceptors were defined as loci that were found in at least 10 reads at the 5'- and 3'-ends of introns in sequence alignments from T-cell infections. Regions containing splice sites are enlarged for clarity. Asterisks indicate putative splice sites that are adjacent to dinucleotides other than the consensus GT and AG.

839 genes<sup>408,428,429</sup>. Importantly for HIV, these include changes during T-cell activation<sup>430,431</sup>,  
840 raising the question of how cell-specific splicing affects HIV replication. While most studies  
841 of HIV-1 splicing have been conducted in cell lines using lab-adapted viral strains, limited  
842 works in PBMCs from infected patients, monocytes and macrophages have suggested that  
843 differences may indeed exist in relevant cell types<sup>414,426,432,433</sup>. Moreover, human splicing  
844 patterns differ between individuals, but such polymorphisms have not been investigated in  
845 the context of HIV infection<sup>434,435</sup>.

846 Here, we use deep sequencing to comprehensively characterize the transcriptome of an early  
847 passage clinical isolate, HIV<sub>89.6</sub><sup>436</sup>, in primary CD4<sup>+</sup> T cells from seven human donors  
848 and in the human osteosarcoma (HOS) cell line. Many deep sequencing techniques provide  
849 short reads, which rarely query more than a single exon-exon junction. To distinguish  
850 the full structure of HIV-1 mRNAs, which can contain several splice junctions, we used  
851 Pacific Biosciences (PacBio) sequencing technology, which yields read lengths up to 10 kb<sup>437</sup>.  
852 We used RainDance Technologies single-molecule PCR enrichment to preserve ratios of  
853 RNAs during preparation of sequencing templates. We identified previously published and  
854 novel HIV-1 transcripts and determined that HIV<sub>89.6</sub> encodes a minimum of 109 different  
855 splice forms. These included a new size class of transcripts, some of which contain novel  
856 open reading frames (ORFs) that encode new proteins. We also found significant variation  
857 between cell types, over time during infection of HOS cells and among individuals. These  
858 data reveal unanticipated complexity and dynamics in HIV-1 message populations, begin  
859 to clarify a little studied dimension of HIV-1 replication and suggest possible targets for  
860 therapeutic interventions.

861 **3.3 Materials and methods**

862 **3.3.1 Cell culture and viral infections**

863 HIV<sub>89.6</sub> was generated by transfection and subsequent expansion in SupT1 cells. Primary  
864 T cells were isolated by the University of Pennsylvania Center for AIDS Research Im-

865 munology core and confirmed to be homozygous for the wild-type CCR5 allele as shown  
866 in Supplementary Table S1 and described in Supplementary Methods. HOS-CD4-CCR5  
867 cells<sup>438,439</sup> were obtained through the AIDS Research and Reference Reagent Program,  
868 Division of AIDS, NIAID, NIH from Dr Nathaniel Landau. Single round infections in T  
869 cells and HOS-CD4-CCR5 cells were performed using standard methods (see Supplementary  
870 Methods).

871 **3.3.2 RNA and reverse transcription**

872 Total cellular RNA was purified using the Illustra RNA kit (GE Life Sciences, Fairfield, CT,  
873 USA) from  $5 \times 10^6$  cells per infection. Viral cDNA was made using a reverse transcription  
874 primer complementary to a sequence in U3 (RTprime, Supplementary Table S2). We used  
875 Superscript III reverse transcriptase (Invitrogen) in the presence of RNaseOUT (Invitrogen)  
876 to conduct first-strand cDNA synthesis from equal amounts of total cellular RNA from each  
877 HOS-CD4-CCR5 time point (15.2  $\mu$ g) and from each T-cell infection (3  $\mu$ g) according to the  
878 manufacturer's instructions for gene-specific priming of long cDNAs, and then treated with  
879 RNaseH (Invitrogen). We checked for full reverse transcription of the longest (unspliced)  
880 viral cDNAs by PCR using primers that bind in the first major intron of HIV<sub>89.6</sub> (keo003,  
881 keo004, Supplementary Table S2, data not shown).

882 **3.3.3 Bulk RT-PCR and cloning**

883 Transcripts were amplified from cellular RNA using the Onestep RT-PCR kit (Qiagen)  
884 with primer pairs keo056/keo057 and keo058/keo059 (Supplementary Table S2) with the  
885 following amplification: 5 cycles of 30 s at 94°C, 12 s at 56°C, 40 s at 72°C; then 30 cycles  
886 of 30 s at 94°C, 14 s at 56°C, 40 s at 72°C; and finally 10 min at 72°C. For verification of  
887 dynamic changes, primers F1.2 and R1.2 were used with 35 cycles of 30 s at 94°C, 30 s at  
888 56°C and 45 s at 72°C followed by 10 min at 72°C. Products were resolved on agarose gels  
889 (Nusieve 3:1, Lonza for verification of dynamic changes, Invitrogen for cloning) stained with  
890 ethidium-bromide (Sigma) for visualization, or SYBR Safe DNA gel stain (Invitrogen) for

891 cloning (keo056/keo057 amplified material). DNA was purified using Qiaquick gel extraction  
892 kit (Qiagen) and cloned using the TOPO TA cloning kit (Invitrogen). Plasmid DNA was  
893 prepared using Qiaprep Spin Miniprep kit (Qiagen). Inserts were identified and verified  
894 using Sanger sequencing. The cDNAs for *tat*<sup>8c</sup>, *tat* (1 and 2 exon), *ref*, *rev* and *nef*, and the  
895 transcript with exon structure 1-5-8c were cloned into the expression vector pIRES2-AcGFP1  
896 (Clonetech) as described in Supplementary Methods.

### 897 **3.3.4 Assays of protein activity and HIV replication**

898 Activity and HIV replication assays were performed as described in Supplementary Methods.  
899 Tat activity expressed from each cDNA was measured in TZM-bl cells<sup>204</sup> (gift of Dr Robert  
900 W. Doms). Rev activity was assayed in HEK-293T cells co-transfected with pCMVGagPol-  
901 RRE-R, a reporter plasmid from which Gag and Pol are expressed in a Rev-dependent  
902 manner (gift of David Rekosh)<sup>440</sup>. Intracellular and released supernatant p24 was measured  
903 from cells transfected with expression constructs and infected with HIV<sub>89.6</sub>.

### 904 **3.3.5 Western blotting**

905 HEK-293T cells were transfected with expression constructs and treated with MG132 (EMD  
906 Chemicals) to inhibit the proteasome or DMSO (Supplementary Methods). Proteins were  
907 detected by immunoblotting using a mouse antibody that recognizes the carboxy terminus  
908 of HIV-1 Nef diluted 1:1000 in 5% milk (gift of Dr James Hoxie)<sup>441</sup>. Horseradish peroxidase  
909 (HRP)-conjugated secondary rabbit-anti-mouse antibody (p0260, DAKO) was used for  
910 detection with SuperSignal West Pico Chemiluminescent Substrate (Thermo Scientific).  
911 Beta-tubulin was used as a loading control, detected by the HRP-conjugated antibody  
912 (ab21058, Abcam).

### 913 **3.3.6 Single-molecule amplification**

914 Amplification was performed by RainDance Technologies using a protocol similar to that  
915 previously reported (detailed description in Supplementary Methods)<sup>442</sup>. Amplification

916 was carried out in droplets to suppress competition between amplicons. PCR droplets  
917 were generated on the RDT 1000 (RainDance Technologies) using the manufacturer's  
918 recommended protocol. The custom primer libraries for this study contained 18 (HOS-CD4-  
919 CCR5 cells) or 20 (primary T cells) PCR primer pairs designed to amplify different HIV  
920 RNA isoforms (Supplementary Table S2).

921 **3.3.7 Single-molecule sequencing**

922 DNA amplification products from the RainDance PCR droplets were converted to SMRTbell  
923 templates using the PacBio RS DNA Template Preparation Kit. Sequencing was performed by  
924 Pacific Biosciences using the PacBio SMRT sequencing technology as described<sup>437</sup>. Sequence  
925 information was acquired during real time as the immobilized DNA polymerase translocated  
926 along the template molecule. Prior to sequence acquisition, hairpin adapters were ligated to  
927 each DNA template end so that DNA polymerase could traverse DNA molecules multiple  
928 times during rolling circle replication (SMRTbell template sequencing<sup>443</sup>), allowing error  
929 control by calculating the consensus ('circular consensus sequence' or CCS). For raw reads,  
930 the average length was 2860 nt, and 10% were > 5000 nt. After condensing into consensus  
931 reads, the mean read length was 249.5 nt, due to the use of a shorter Pacific Biosciences  
932 sequencing protocol to accommodate the small size of many amplicons. Consensus reads of  
933 1% were > 1100 nt. Sequencing data were collected in 45-min movies.

934 **3.3.8 Data analysis**

935 Raw reads were processed to produce CCSs. Raw reads were also retained to help in primer  
936 identification and to avoid biasing against long reads. Reads were aligned against the human  
937 genome using Blat<sup>382</sup>. Misprimed reads matching the RT primer, reads with a CCS length  
938 shorter than 40 nt or raw length shorter than 100 nt and reads matching the human genome  
939 were discarded. Filtered reads were aligned against the HIV<sub>89.6</sub> reference genome. Potential  
940 novel donors and acceptors were found by filtering putative splice junctions in the Blat  
941 hits for a perfect sequence match 20 bases up- and downstream of the junction, ignoring

942 homopolymer errors, and requiring that one end of the junction be a known splice site. Local  
943 maximums within a 5-nt span with > 9 such junctions were called as novel splice sites.

944 Filter-passed reads were aligned against all expected fragments based on primers and known  
945 and novel junctions. Primers were identified in CCS reads by an edit distance  $\leq 1$  from  
946 the primer in the start or end of the read, in raw reads by an edit distance  $\leq 5$  from a  
947 concatenation of the primer, hairpin adapter and the reverse complement of the primer, and  
948 in both types of reads by a Blat hit spanning an entire expected fragment.

949 Gaps in Blat hits were ignored if  $\leq 10$  bases long or in regions of likely poor read quality  
950  $\leq 20$  bases long where an inferred insertion of unmatched bases in the read occurred at the  
951 same location as skipped bases in the reference. Any Blat hits with a gap  $> 10$  nt remaining  
952 in the query read were discarded. If HIV sequence was repeated in a given read (likely due  
953 to PacBio circular sequencing), the alignments were collapsed into the union of the coverage.  
954 Gaps in the HIV sequence found in uninterrupted query sequence were called as tentative  
955 introns. Splice junctions were assigned to conserved or previously identified (published  
956 or in this work) splice sites and reads appearing to contain donors or acceptors further  
957 than 5 nt away from these sites were discarded. Reads with Blat hits outside the expected  
958 primer range were discarded from that primer grouping. The assigned primer pair, observed  
959 junctions and exonic sequence were used to assign each read to a given spliceform (specific  
960 transcript structure) or set of possible spliceforms. Partial sequences that did not extend  
961 through both primers were assigned to specific transcripts if the read contained enough  
962 information to rule out all other spliceforms or if all other possible spliceforms contained  
963 rare (< 1% usage) donors or acceptors (Supplementary Table S3). Otherwise, the read was  
964 called indeterminate.

965 To calculate the ratios of transcripts within the partially spliced class, we counted the  
966 number of reads for each assigned spliceform amplified by primer pair 1.3 and divided by the  
967 total number of assigned partially spliced reads amplified with these primers (Supplementary  
968 Figure S1 and Supplementary Table S2). Assigned sequences amplified with primer pairs

969 1.4 and 4.1 (full-length cDNAs, T cells only) were used to calculate ratios of transcripts  
970 within each of the two completely splice classes ( $\sim 2$  and  $\sim 1$  kb). To compare ratios of  $\sim 2$   
971 kb transcripts calculated within reads from primer pairs 1.4 and 4.1, we normalized ratios  
972 from pair 4.1 to the *nef* 2 transcript (containing exons 1, 5 and 7). Due to size biases  
973 inherent in the approach, we did not compare across size classes, and unspliced transcripts  
974 were not included in ratio analysis. For all ratio analysis, transcripts including cryptic or  
975 novel junctions were counted only if they appeared in at least five reads, otherwise they  
976 were excluded from the analysis and from the count of total assigned reads.

977 To estimate the minimum total number of transcripts present, partial sequence reads were  
978 included. Each exon-exon junction occurring in at least five reads and not previously assigned  
979 to a particular transcript (Figure 3.2) was counted as evidence of an additional transcript  
980 (47 additional junctions were detected, see Supplementary Table S4). If two such junctions  
981 could conceivably occur in a single mRNA, we counted only one unless we could verify from  
982 sequence reads that they were amplified from separate cDNAs, resulting in 31 additional  
983 transcripts. The minimum transcript number calculated by a greedy algorithm treating  
984 introns as events in a scheduling problem agreed with the above calculation.

985 Several groups have demonstrated tissue- and differentiation-specific splicing of cellular  
986 genes<sup>408,428,429</sup>. Importantly for HIV, these include changes during T-cell activation<sup>430,431</sup>,  
987 raising the question of how cell-specific splicing affects HIV replication. While most studies  
988 of HIV-1 splicing have been conducted in cell lines using lab-adapted viral strains, limited  
989 works in PBMCs from infected patients, monocytes and macrophages have suggested that  
990 differences may indeed exist in relevant cell types<sup>414,426,432,433</sup>. Moreover, human splicing  
991 patterns differ between individuals, but such polymorphisms have not been investigated in  
992 the context of HIV infection<sup>434,435</sup>.

993 For studies of transcript dynamics, reads from primer pairs 1.2, 1.3 and 1.4 containing  
994 junctions between D1 or any donor and each of five mutually exclusive acceptors, A3, A4c,  
995 A4a, A4b, A5 and A5a, were collected and their ratios calculated.

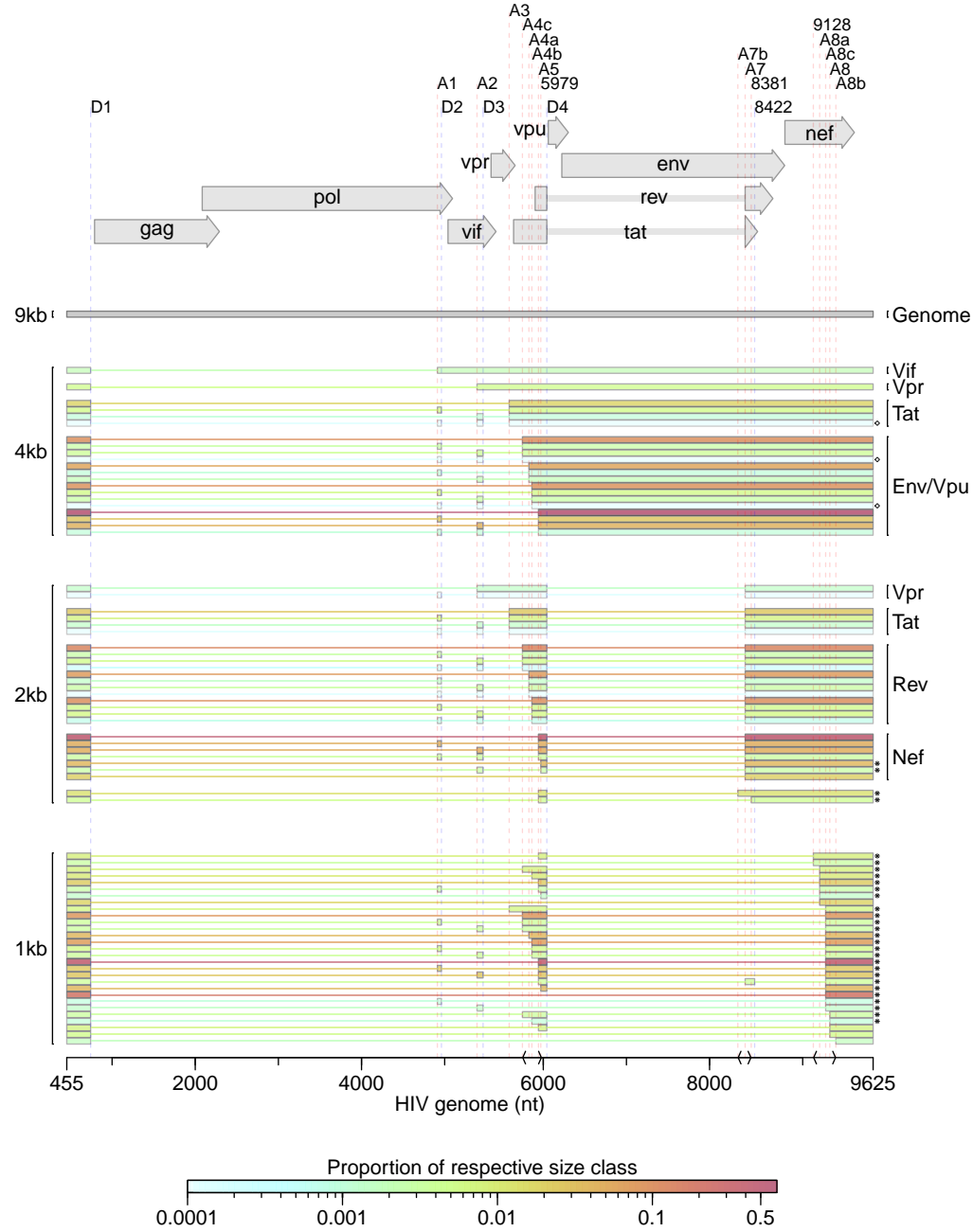


Figure 3.2: HIV<sub>89.6</sub> transcripts in T cells for which the full message structure was determined are shown arranged by size class. Thick bars correspond to exons and thin lines to excised introns. For the well-conserved transcripts, encoded proteins are indicated. The relative abundance of each transcript within its size class is indicated by color. Asterisks denote transcripts that have not been reported previously to our knowledge. Of the 47 conserved HIV-1 transcripts, three were detected in fewer than five reads (indicated with ◊) and two messages were not detected and are not shown (one encoding Vpr and one encoding Env/Vpu). Depicted non-conserved transcripts (using novel or cryptic splice sites) were each detected in at least five independent sequence reads across samples from at least two different human T-cell donors.

996 **3.3.9 Statistical analysis**

997 Statistical modeling was performed using generalized linear modeling as described in Supple-  
998 mentary Report S2. All analyses were performed in R 2.14.0 (R Development Core)<sup>375</sup>.

999 **3.3.10 Data access**

1000 Sequence data is available in the SRA database with the following accession numbers:  
1001 SRP014319.

1002 **3.4 Results**

1003 **3.4.1 Sequencing HIV-1 transcripts produced in primary T cells and HOS cells**

1004 In order to characterize HIV-1 transcript populations, we prepared viral cDNA from primary  
1005 CD4<sup>+</sup> T cells of seven different healthy human donors infected in vitro with HIV<sub>89.6</sub>, an early  
1006 passage dual-tropic clade-B clinical isolate (Supplementary Figure S1, human donor data  
1007 in Supplementary Table S1)<sup>436</sup>. We also studied HIV messages produced in infected HOS  
1008 cells engineered to express CD4 and CCR5 (HOS-CD4-CCR5) because these cells support  
1009 efficient HIV replication and engineered variants are widely used in HIV research. HOS  
1010 cells were harvested at 18, 24 and 48 hours post infection (hpi) to investigate longitudinal  
1011 changes during infection, and for comparison to 48 h infected T cells.

1012 To preserve the relative proportions of template molecules while amplifying the cDNA, we  
1013 used RainDance Technologies' single-molecule micro-droplet based PCR<sup>442</sup>. Droplet libraries  
1014 containing multiple overlapping primer pairs were designed to query all message forms and  
1015 allow later calculation of relative abundance (Supplementary Table S2 and Supplementary  
1016 Figure S1). Each primer was unique so that sequences could be assigned to a specific  
1017 primer pair, which helped reconstruct the origin of sequence reads and deduce message  
1018 structures. Amplified DNA products were sequenced using Single Molecule Real-Time  
1019 (SMRT) technology from Pacific Biosciences<sup>437,443</sup>. We obtained 847 492 filtered reads of  
1020 amplified HIV-1 transcripts in primary CD4<sup>+</sup> T cells and 89 350 in HOS cells. The longest

1021 sequenced continuous stretch of HIV-1 cDNA was 2629 bp.

1022 **3.4.2 Splice donors and acceptors**

1023 We aligned PacBio reads containing HIV sequences to the HIV<sub>89.6</sub> genome and identified  
1024 candidate introns as recurring gaps in our sequences. Using this approach, we observed  
1025 splicing at each of the widely conserved major splice donors and acceptors and several  
1026 published cryptic sites (Figure 3.1A, hereafter referred to by their identifications shown in  
1027 this figure, ‘D’ for donors, ‘A’ for acceptors).

1028 In addition, we identified 13 putative novel splice sites: 2 donors and 11 acceptors (Figure  
1029 3.1 and Supplementary Table S3). In order to be selected as a bona fide splice site and  
1030 remove artifacts possibly created by recombination during sample preparation, we required  
1031 that the new acceptor or donor was observed spliced to previously reported splice donors or  
1032 acceptors in > 10 sequence reads in CD4<sup>+</sup> T cells. The most frequently used novel splice site  
1033 was an acceptor that we have termed A8c because it lies near A8, A8a and A8b (discussed  
1034 in detail below). Additional novel sites are further discussed in Supplementary Report S1.

1035 Most of the new splice sites adhered to consensus sequences for the standard spliceosome  
1036 (Supplementary Table S3). However, there appeared to be one splice donor upstream of  
1037 D1 with a cytidine in place of the usual uracil 2 nt downstream of the splice site. Similar  
1038 ‘GC donors’ appear in 1% of known splice junctions in humans<sup>444</sup>. Of the novel splice  
1039 acceptors, three were preceded by dinucleotides other than the consensus AG. Alternative  
1040 dinucleotides are used infrequently as splice acceptors<sup>445–448</sup>; however, it is possible that our  
1041 deep sequencing method allowed us to observe rare events.

1042 **3.4.3 Structures of spliced HIV<sub>89.6</sub> RNAs**

1043 To quantify the populations of HIV-1 transcripts, we aligned all reads to the collection of  
1044 47 well-established spliced HIV-1 transcripts and detected 45 of them (Figure 3.2). We  
1045 additionally aligned reads to the HIV<sub>89.6</sub> genome allowing all possible combinations of splice

1046 junctions—canonical, cryptic or novel—determined from the sequencing data (Figure 3.1),  
1047 yielding an additional 32 complete transcripts, 19 of which were novel. The data also provide  
1048 evidence for more novel splice junctions but in incomplete sequences, implying the existence  
1049 of additional new transcripts (Supplementary Table S4 and Supplementary Report S1). The  
1050 full data set taken together provides evidence for least 109 different HIV<sub>89.6</sub> transcripts in  
1051 primary T cells.

1052 Amplification primers that isolated the two main classes of spliced messages allowed us to  
1053 determine the ratios of mRNAs in each (Figure 3.2 and Supplementary Table S5). Within  
1054 the partially spliced class of transcripts, *env/vpu*, *tat* (1-exon), *vpr* and *vif* messages existed  
1055 in an average ratio of 96:4:< 1:< 1 in CD4<sup>+</sup> T cells. The ratio of *nef:rev:tat:vpr* within  
1056 the ~2 kb transcript class was 64:33:3:< 1. Consistent with previous reports, the most  
1057 abundant transcript in each class contained the splice junction from D1 to A5 (D1^A5)—an  
1058 *env/vpu* transcript contributing 64% of the partially spliced class, and a completely spliced  
1059 *nef* transcript contributing 47% of ~2 kb messages (Figure 3.2)<sup>412,449</sup>. The relatively  
1060 low abundance of transcripts encoding Tat suggests that Tat sufficiently stimulates HIV  
1061 transcription elongation at low concentrations, or that the *tat* transcripts must be efficiently  
1062 translated. Due to biases inherent in the reverse transcription step, we could only compare  
1063 transcripts within each size class, and we note that our methods have not been validated  
1064 for empirical quantification. However, the ratios were roughly confirmed using overlapping  
1065 sequence reads obtained with alternate primer pairs and by end point RT-PCR analysis of  
1066 HIV-1 RNAs (data not shown).

1067 Exons 2 and 3 are non-coding exons whose inclusion in transcripts other than *vif* and *vpr*  
1068 has no known function. We found that they were included in other messages infrequently,  
1069 each in ~7–8% of transcripts in the ~2 kb completely spliced class of transcripts and 5%  
1070 of partially spliced transcripts accumulating in T cells. This is consistent with previous  
1071 measurements in the partially spliced class but much lower than has been estimated for  
1072 completely spliced transcripts in HeLa cells, suggesting cell-type-specific splicing patterns

1073 may influence inclusion of these exons<sup>412</sup>.

1074 **3.4.4 A novel ~1 kb class of completely spliced transcripts**

1075 Primers placed near the 5'- and 3'-ends of the HIV<sub>89.6</sub> genome amplified a second class of  
1076 completely spliced transcripts ~1 kb in length. In place of A7, these transcripts use a set of  
1077 little studied splice acceptors located ~800 bp downstream within the 3'-TR. Two groups  
1078 have previously observed splicing from D1 to acceptors A8, A8a and A8b in this region,  
1079 yielding messages of this size class in patient samples; however, none of these could be  
1080 translated to a protein of significant length<sup>414,418</sup>. We determined the complete structure of  
1081 29 members of the 1-kb class (Figure 3.2 and Supplementary Table S5). The most abundant  
1082 messages observed in this class use the novel acceptor A8c to define their terminal exon. For  
1083 HIV89.6, acceptor A8c was used nearly as frequently as A7, which gives us the 2-kb class  
1084 of transcripts (Supplementary Table S3), and this was supported by end point RT-PCR  
1085 analysis (data not shown).

1086 Acceptor A8c is not well conserved in HIV-1/SIVcpz (14%), although it is conserved in clade  
1087 G viruses (> 95%) and most HIV-2/SIVsmm genomes (86%)<sup>450</sup>. This is due to the poor  
1088 conservation of an adenine at the wobble base position of the 123rd codon (proline) of the  
1089 Nef reading frame, which creates the AG dinucleotide generally required at splice acceptors.  
1090 Since any base at this position would code for proline, there does not seem to be strong  
1091 selection for a splice acceptor here. However, A8c is displaced from nearby well-conserved  
1092 (> 90%) cryptic acceptors A8a and A8b by multiples of 3 bp (12 and 21 bp, respectively),  
1093 so splicing to any of these three acceptors would create similar ORFs. All HIVs and SIVs  
1094 maintain at least one of these three acceptors, suggesting possible function<sup>450</sup>. We confirmed  
1095 that the 1 kb transcripts using A8a, A8b and A8c were present in infected HOS and T cells  
1096 by end point RT-PCR using additional primer pairs and by Sanger sequencing of cloned  
1097 transcripts (Figure 3.3A and B; data not shown).

1098 The 1-kb transcript containing exons 1, 4 and 8c (1-4-8c, where exon 8c begins at A8c

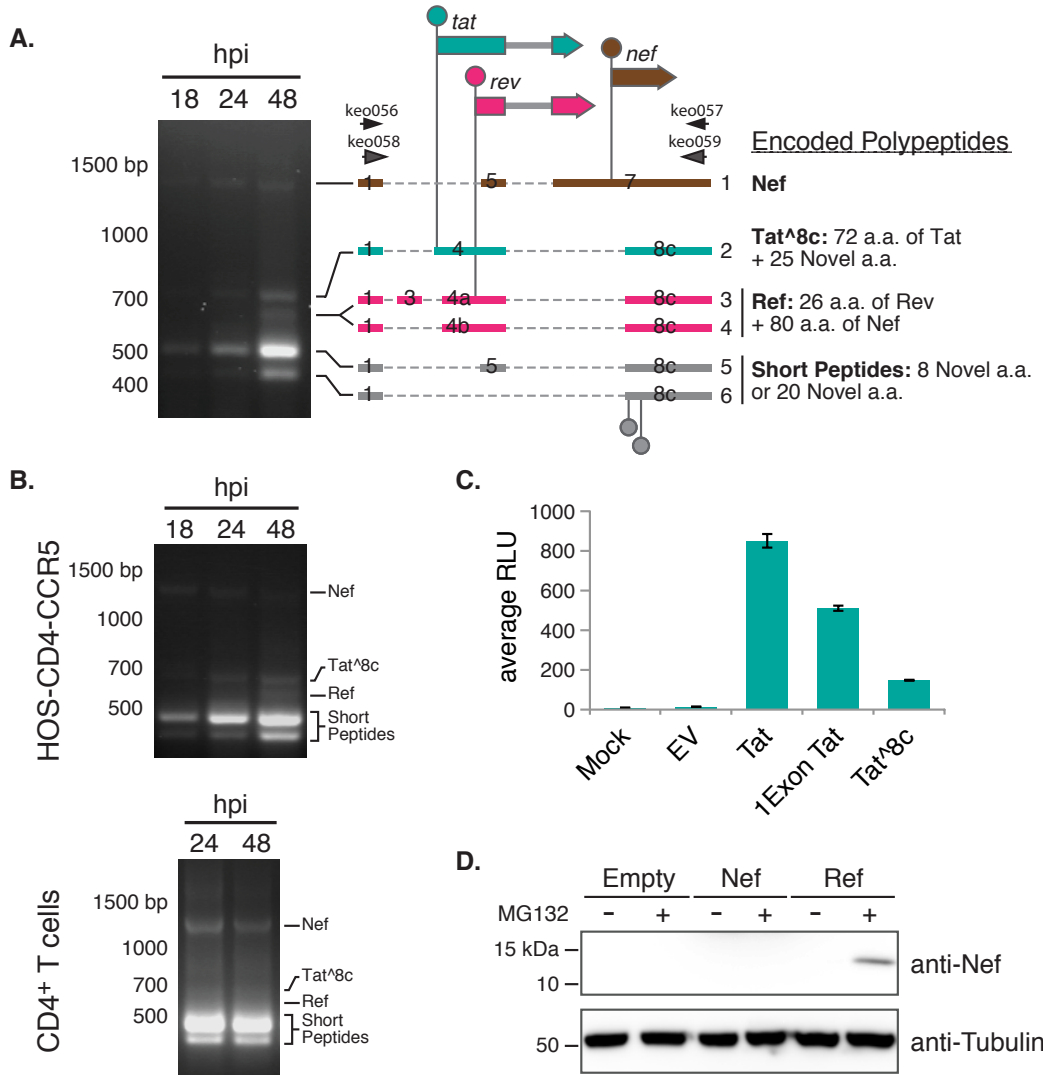


Figure 3.3: HIV<sub>89.6</sub> transcripts were amplified by RT-PCR using RNA from infected HOS-CD4-CCR5 cells with primers keo056 and keo057. Major bands detected after gel electrophoresis were cloned from the 48 hpi sample and message structures determined by Sanger sequencing. Thick bars represent exons and dashed lines excised introns. Genes are shown above (not to scale) with start codons indicated by circles. Messages 1, 2, 4 and 5 were cloned into expression plasmids for activity assays. (B) Confirmation of presence of the ~1 kb message RNAs in HOS-CD4-CCR5 and primary CD4<sup>+</sup> T cells (human donor 1, harvested 24 and 48 hpi). An independent primer pair (keo058 and keo059) was used to amplify transcripts by RT-PCR. (C) Tat activity was measured in Tzm-bl cells as Tat-dependent luciferase production after transient transfection with expression plasmids. (D) Western blot showing expression of protein of the predicted size for Ref (12.5 kb) in cells transfected with the Ref expression construct and treated with proteasome inhibitor MG132, detected by an antibody recognizing the carboxy-terminus of Nef. Expression plasmid encoding Nef was included to control for possible expression of partial Nef peptides or breakdown products from the Nef ORF.

1099 and extends to the poly-adenylation site) encodes the first exon of Tat followed by 25  
1100 novel amino acids (termed Tat<sup>8c</sup>). Tat<sup>8c</sup> showed activity when overexpressed in cells  
1101 containing a Tat reporter construct (Figure 3.3C, nucleotide and amino acid sequences in  
1102 Supplementary Table S6). Transcripts with exon structures 1-4a/b/c-8c encode a novel  
1103 fusion of the amino-terminal 26 amino acids of Rev and the carboxy-terminal 80 amino acids  
1104 of Nef, hereafter referred to as Ref. We did not detect Rev activity on overexpression of  
1105 the *ref* transcript, and Ref did not appear to interfere with the normal function of Rev or  
1106 with HIV replication (Supplementary Figure S2). Ref was detectable by western blot using  
1107 antibodies targeting the C terminus of Nef after inhibition of the proteasome, suggesting  
1108 that the fusion is expressed but not stable (Figure 3.3D). Thus, Ref has the potential to  
1109 encode a new epitope potentially relevant in immune detection of HIV. The transcripts with  
1110 exon structures 1-5-8c and 1-8c encode at most a short peptide, and so are candidates for  
1111 acting as regulatory RNAs.

### 1112 **3.4.5 Temporal dynamics of transcript populations**

1113 To assess longitudinal variation, we investigated HIV<sub>89.6</sub> transcript populations during the  
1114 course of a single round of infection in HOS-CD4-CCR5 cells. A sensitive method for  
1115 comparison among conditions involves quantifying utilization of six mutually exclusive splice  
1116 acceptors A3, A4c, A4a, A4b, A5 and a novel acceptor just downstream of A5 termed  
1117 A5a. Splicing at these acceptors determines the relative levels of messages encoding Tat  
1118 and Env/Vpu in the partially spliced class and messages encoding Tat, Rev and Nef in the  
1119 completely spliced class.

1120 We observed longitudinal changes in the levels of these messages in HOS cells over 12–  
1121 48 h that were statistically significant ( $p < 10^{-10}$ ; generalized linear model described in  
1122 Supplementary Report S2). This pattern was especially evident in junctions involving donor 1  
1123 spliced to each of these acceptors (Figure 3.4A). Most dramatically, transcripts with splicing  
1124 junctions between D1 and A3 (tat messages) increased with time ( $p < 10^{-10}$ ), while D1<sup>8c</sup>A4b  
1125 junctions (used in *env/vpu* or *rev* messages) were used reciprocally less ( $p < 10^{-10}$ ). Such

1126 kinetic changes affecting specific transcripts both with and without the Rev-response element  
1127 cannot be explained by the accumulation of Rev, and they may reflect differential transcript  
1128 stability or HIV-induced alterations to the host splicing machinery. Temporal changes in  
1129 HOS cells were confirmed using end point RT-PCR and analysis after electrophoresis on  
1130 ethidium-stained gels (Figure 3.4B).

### 1131 **3.4.6 Cell-type-specific splicing patterns**

1132 We also compared splicing between T cells and HOS cells and found significant cell type  
1133 differences ( $p < 10^{-10}$ ). For example, while transcripts with D1^A5 junctions were dominant  
1134 in both cell types, messages using the D1^A4c splice junction (encoding Env/Vpu or Rev)  
1135 made up the bulk of the remaining transcripts in T cells but were a minor species in  
1136 HOS-CD4-CCR5 cells. Likewise, Tat messages (using A3), which were quite abundant in  
1137 HOS cells at all time points, contributed relatively little to populations of transcripts in  
1138 primary T cells harvested at 48 hpi (Figure 3.4A). We also used end point PCR and analysis  
1139 on ethidium-bromide-stained gels to confirm that the relative ratios of transcripts containing  
1140 junctions to A3, A4a, A4b and A4c were different in HOS and T cells (Figure 3.4B).

### 1141 **3.4.7 Human variation in HIV-1 splicing**

1142 Quantitative comparisons also revealed modest differences in splicing between primary CD4<sup>+</sup>  
1143 T cells isolated from different human donors that were statistically significant ( $p < 10^{-10}$ )  
1144 under a generalized linear model (Figure 3.4A). The magnitudes of predicted differences  
1145 were small, all < 33% and most < 10%.

## 1146 **3.5 Discussion**

1147 Use of single-molecule enrichment and long-read single-molecule sequencing has made possible  
1148 the most complete study to date of the composition of HIV-1 message populations, revealing  
1149 several new layers of regulation. Studies of the low-passage HIV89.6 isolate in a relevant cell  
1150 type showed numerous differences from studies of lab-adapted HIV strains in transformed

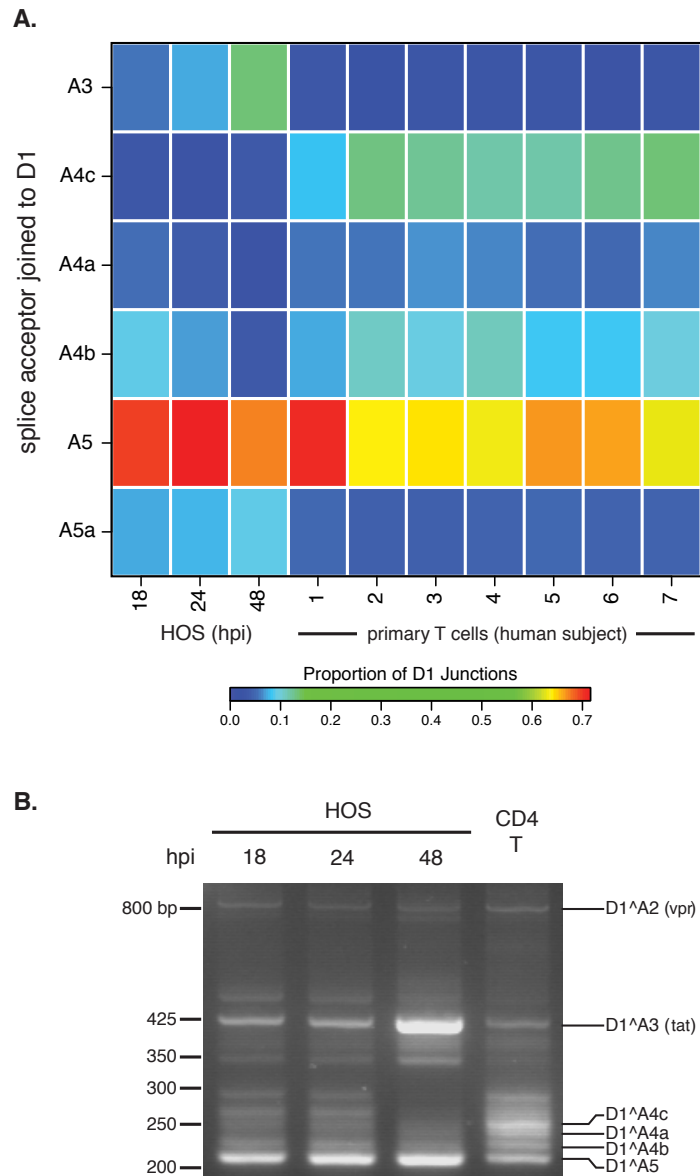


Figure 3.4: Temporal, cell type and donor variability in accumulation of HIV-1 messages. (A) In order to highlight changes in ratios of HIV-1 transcripts accumulating over time during infection and between HOS-CD4-CCR5 cells and primary T cells, we used PacBio read counts to calculate proportions of transcripts with splicing from the first major splice donor, D1, to each of the mutually exclusive acceptors: A3, A4c, A4a, A4c, A5 and the novel putative acceptor A5a. The heat map shows average data for T cell and HOS cell samples in columns with the color tiles indicating the proportion of D1 splicing to each of the mutually exclusive acceptors (rows), according to the color scale shown. (B) Reverse transcription and bulk PCR amplification of HIV<sub>89.6</sub> transcripts from HOS cells and primary T cells from one human subject (subject 3) resolved by agarose gel electrophoresis and stained with ethidium bromide verified temporal and cell type changes shown in (A).

1151 cell lines, highlighting the importance of studying the most relevant models. These data  
1152 also illustrate the limitations of gel-based assays for studying HIV-1 message population.  
1153 Multiple different combinations of HIV-1 exons yield mRNAs of similar sizes that are easily  
1154 confused in typical assays using gel electrophoresis. Thus, in many settings the more detailed  
1155 information provided by single-molecule amplification and single-molecule DNA sequencing  
1156 is more useful.

1157 Using these methods, we have detected significant variations between HIV message pop-  
1158 ulations generated in T cells from different human donors. The differences were modest  
1159 compared to those observed between cell types or time points, perhaps not surprisingly  
1160 since any human polymorphisms strongly affecting mRNA processing might interfere with  
1161 normal gene expression. However, because tight calibration of message levels is important to  
1162 HIV-1, the observed differences in message ratios might affect HIV-1 acquisition or disease  
1163 progression. The variation in observed transcripts could also be affected by different kinetics  
1164 of infection in T cells from the different donors. In either case, these data suggest that human  
1165 polymorphisms may exist that affect HIV-1 message populations in infected individuals,  
1166 providing a new candidate mechanism connecting human genetic variation with measures of  
1167 HIV disease.

1168 Sequences from the 89.6 viral strain revealed a class of small (~1 kb) completely spliced  
1169 transcripts, most contributed by splicing to a new poorly conserved acceptor A8c. These  
1170 encoded two new proteins, one of which had Tat activity, and we showed that another, a  
1171 Rev-Nef fusion termed Ref, could be detected in cells. HIV<sub>89.6</sub> is a particularly cytotoxic virus  
1172 isolated from the CSF of a patient, and it forms unusually large syncitia in macrophages<sup>436</sup>.  
1173 The abundance of 1-kb transcripts produced by this virus provides a possible explanation  
1174 for its unique properties. In addition to the novel acceptor A8c, we have also identified 3  
1175 putative novel splice donors and 11 putative novel acceptors, which require further studied  
1176 to clarify possible functions.

1177 The wealth of new messages found here in HIV<sub>89.6</sub> and in other HIV-1 isolates suggests there

may be ongoing evolution of novel splice sites and new ORFs. Because splice acceptors in HIV-1 are weak<sup>284</sup>, mutations creating sequences that even slightly resemble the 3' splice site consensus may be occasionally recruited as novel acceptors, creating new mRNAs. In fact, new splice signals may evolve with relative ease—it has been estimated that reasonable matches to the consensus for splice donors, acceptors and branch-point sites occur within random sequence every 290, 490 and 24 bp, respectively<sup>451</sup>, though sequence substitutions in HIV are usually also constrained by overlapping viral coding regions. We and others have observed appearance of novel exons within the major HIV-1 introns<sup>413,415,416</sup>. Such long stretches of RNA relatively devoid of competing splice sites may be particularly poised to evolve new signals. On the other hand, most of the putative novel splice acceptors we observed clustered near previously identified acceptors in HIV-1, suggesting that conserved cis-acting splicing signals may recruit factors that act promiscuously on new nearby sequences. Clusters of splice sites might also provide redundancies that protect vital messages, as suggested previously<sup>452,453</sup>. Frequent evolution of new splice sites may allow viruses to test out new combinations of exons, potentially yielding new RNAs and proteins, like those reported here. However, such novelty must compete with immune constraints—unstable novel polypeptides like Ref can be targeted to the proteasome and presented on MHC molecules as new epitopes for immune recognition.

HIV has likely evolved to produce calibrated message populations in T cells which seem to be altered with relative ease, as in infection in HOS cells, suggesting that therapeutic disruption of correct splicing may be feasible. A few studies have begun to explore small molecule therapy to disrupt HIV-1 splicing<sup>419,423</sup>. Several factors could be responsible for the differences we observed between HOS and T cells, including hnRNP A/B and H, SC35, SF2/ASF and SRp40<sup>288,454</sup>. Inhibition of SF2/ASF has already been shown to abrogate HIV-1 replication in vitro<sup>419</sup>. Thus the lability seen here for function of these factors suggests they may be attractive antiretroviral targets.

1204    **3.6 Acknowledgements**

1205    We would like to thank the University of Pennsylvania Center for AIDS Research (CFAR) for  
1206    preparation of viral stocks and isolation of primary CD4<sup>+</sup> T cells; James A. Hoxie, Ronald  
1207    G. Collman, Jianxin You, Robert W. Doms, Paul Bates, David Rekosh and members of the  
1208    Bushman laboratory for reagents, helpful discussion and technical expertise.

1209      **CHAPTER 4: Gene activity in primary T cells infected with HIV<sub>89.6</sub>:**  
1210                  **intron retention and induction of distinctive genomic**  
1211                  **repeats**

This chapter is under review as:

S Sherrill-Mix, K Ocieja and F Bushman. Under Review.  
Gene activity in primary T cells infected with HIV89.6: in-  
tron retention and induction of distinctive genomic repeats.  
*Retrovirology*

KE Ocieja performed the infections and sequencing. I analyzed the data.

KE Ocieja, FD Bushman and I planned the overall study. I produced  
the figures. FD Bushman and I wrote the paper.

1213      **4.1 Abstract**

1214      Background: HIV infection has been reported to alter cellular gene activity, but published  
1215      studies have commonly assayed transformed cell lines and lab-adapted HIV strains, yielding  
1216      inconsistent results. Here we carried out a deep RNA-Seq analysis of primary human T cells  
1217      infected with the low passage HIV isolate HIV<sub>89.6</sub>.

1218      Results: Seventeen percent of cellular genes showed altered activity 48 hours after infection.  
1219      In a meta-analysis including four other studies, our data differed from studies of transcription  
1220      after HIV infection of cell lines but showed more parallels with infections of primary cells.  
1221      We found a global trend toward retention of introns after infection, suggestive of a novel  
1222      cellular response to infection. HIV<sub>89.6</sub> infection was also associated with activation of human  
1223      endogenous retroviruses (HERVs) and several retrotransposons, of interest as possible novel  
1224      antigens that could serve as vaccine targets. The most highly activated group of HERVs  
1225      was a subset of the ERV-9, a group not reported previously to be induced by HIV. Analysis  
1226      showed that activation was associated with a particular variant of an ERV-9 long terminal  
1227      repeat that contains an indel near the U3-R border. These data also allowed quantification of  
1228      >70 splice forms of the HIV<sub>89.6</sub> RNA and specified the main types of chimeric HIV<sub>89.6</sub>-host

1229 RNAs. Comparison to 147,281 integration site sequences from the same infected cells allowed  
1230 quantification of authentic versus artifactual chimeric reads (0.1% of the total), showing  
1231 that 5' read-in, splicing out of HIV<sub>89.6</sub> from the D4 donor and 3' read-through were the most  
1232 common HIV<sub>89.6</sub>-host cell chimeric RNA forms.

1233 Conclusions: Analysis of RNA abundance after infection of primary T cells with the low  
1234 passage HIV<sub>89.6</sub> isolate disclosed multiple novel features of HIV-host interactions, notably  
1235 intron retention and induction of transcription of distinctive retrotransposons and endogenous  
1236 retroviruses.

## 1237 4.2 Background

1238 HIV replication requires integration of a cDNA copy of the viral RNA genome into cellular  
1239 chromosomes, followed by transcription and splicing to yield viral mRNA. Alternative  
1240 splicing allows the small 9.1 kb HIV genome to generate at least 108 mRNA transcripts  
1241 encoding at least 9 proteins and polyproteins<sup>284,406,412,417,456,457</sup>. During replication, HIV  
1242 also reprograms cellular transcription and splicing. For example, the virus-encoded Vpr  
1243 protein arrests the cell cycle<sup>249,251,252,254</sup> and the viral Tat protein binds to P-TEFb and  
1244 alters transcript at the HIV promoter and some cellular promoters<sup>458–463</sup>.

1245 Multiple studies suggest that cells detect HIV infection and respond by inducing inter-  
1246 feron-regulated, apoptotic and stress response pathways<sup>319,464–471</sup>. Several studies have also  
1247 suggested that HIV infection disrupts normal cellular splicing pathways<sup>433,471</sup>. However,  
1248 results have varied with many experimental parameters, including target cell type, HIV  
1249 isolate and the duration of infection. Many of the published studies focused on infections  
1250 with lab-adapted HIV strains in transformed cell lines<sup>317,319,464,471–473</sup>, and so results may  
1251 not be fully reflective of infections in patients.

1252 In this study, we sought to generate data more resembling HIV replication in patients  
1253 by analyzing transcriptional responses after infection of primary T cells with HIV<sub>89.6</sub>, a  
1254 low passage patient isolate<sup>436</sup>. This represents a continuation of a long term effort to

understand HIV-host cell interactions at the transcriptional level that began with analysis of transcription by HIV<sub>89.6</sub> in primary T cells using Pacific Biosciences long read single molecule sequencing<sup>406</sup>. Our strategy here was to analyze a single time after infection in depth, analyzing over 1 billion sequence reads from HIV<sub>89.6</sub> infected and uninfected host cells. These data were then combined with 147,281 unique integration site sequences from the same infections and the Pacific Biosciences data on HIV<sub>89.6</sub> transcription to 1) elucidate effects of HIV infection on host cell mRNA abundances and splicing, 2) characterize viral message structure in detail and 3) probe the nature of the chimeras formed between host cell and viral RNAs.

### 4.3 Methods

#### 4.3.1 Cell culture and viral infections

HIV<sub>89.6</sub> stocks were generated by the University of Pennsylvania Center for Aids Research. 293T cells were transfected with a plasmid encoding an HIV<sub>89.6</sub> provirus, and harvested virus was passaged in SupT1 cells once. Viral stocks were quantified by measuring p24 antigen content. Primary CD4<sup>+</sup> T cells were isolated by the University of Pennsylvania Center for AIDS research Immunology Core from apheresis product from a single healthy male donor (ND365) using the RosetteSep Human CD4<sup>+</sup> T Cell Enrichment Cocktail (StemCell Technologies).

T cells were stimulated for 3 days at  $0.5 \times 10^6$  cells per milliliter in R10 media (RPMI 1640 with GlutaMAX (Invitrogen) supplemented with 10% FBS (Sigma-Aldrich) with 100 units U/mL recombinant IL2 (Novartis) + 5 $\mu$ g/mL PHA-L (Sigma-Aldrich)). Cells were infected in triplicate and mock infections were performed in duplicate. For each infection,  $6.6 \times 10^6$  cells were mixed with 1.32  $\mu$ g HIV<sub>89.6</sub> in a total volume of 2.25 mL. Infection mixtures were split into three wells of a 6 well plate for spinoculation at 1200 g for 2 hr at 37°C. Cells were incubated an additional 2 hr at 37°C. Cells were then pooled into flasks and volume was increased to a total of 12 mL. Spreading infection was allowed to proceed 48 hr at 37°C,

1281 after which cells were harvested.  $1 \times 10^6$  cells were harvested for flow cytometry, and  $6 \times 10^6$   
1282 cells were pelleted following two washes in PBS for nucleic acid extraction. Genomic DNA  
1283 and total RNA were isolated from  $6 \times 10^6$  T cells per infection using the AllPrep DNA/RNA  
1284 Mini Kit (Qiagen) with Qiashredder columns (Qiagen) for homogenization according to the  
1285 manufacturer's instructions. DNA was eluted in 140  $\mu\text{L}$  elution buffer. RNA samples were  
1286 treated with DNase prior to elution in 40  $\mu\text{L}$  water.

1287 **4.3.2 Analysis of HIV<sub>89.6</sub> integration sites in primary T cells**

1288 Integration site sequences were determined for DNA fractions from the above infections  
1289 after ligation mediated PCR<sup>383</sup>. A total of 147,281 unique integration site sequences were  
1290 determined. An analysis of integration site distributions for these samples was reported in  
1291 Berry et al.<sup>383</sup>.

1292 **4.3.3 mRNA sequencing**

1293 Messenger RNA was isolated and amplified from purified total cellular RNA (3  $\mu\text{L}$  or  
1294 approximately 9  $\mu\text{g}$  from each uninfected sample, 25  $\mu\text{L}$  or approximately 3  $\mu\text{g}$  from each  
1295 infected sample) using the Illumina TruSeq RNA sample preparation kit according to  
1296 manufacturer's protocol. SuperScript III (Invitrogen) was used for reverse transcription.  
1297 Each sample was tagged with a separate barcode and sequenced on an Illumina HiSeq 2000  
1298 using 100-bp paired-end chemistry.

1299 **4.3.4 Flow cytometry**

1300 To assess percent infected cells,  $1 \times 10^6$  cells per infection were stained for flow cytometry.  
1301 All staining incubations were at room temperature. Cells were first washed in PBS and  
1302 then twice in FACS wash buffer (PBS, 2.5% FBS, 2 mM EDTA). Cells were fixed and  
1303 permeabilized with CytoFix/CytoPerm (BD) for 20 minutes and washed with Perm-Wash  
1304 Buffer (BD) before staining with anti-HIV-Gag-PE (Beckman Coulter) for 60 min. Finally  
1305 cells were washed in FACS wash buffer and resuspended in 3% PFA. Samples were run

1306 on a LSRII (BD) and analyzed with FlowJo 8.8.6 (Treestar). Cells were gated as follows:  
1307 lymphocytes (SSC-A by FSC-A), then singlets (FSC-A by FSC-H), then by Gag expression  
1308 (FSC-A by Gag).

1309 **4.3.5 Analysis**

1310 Reads were aligned to the human genome using a combination of BLAT<sup>382</sup> and Bowtie<sup>474</sup>  
1311 through the Rum pipeline<sup>475</sup>. Estimates of fragments per kilobase of transcript per million  
1312 mapped reads and changes in expression for cellular genes were calculated by Cufflinks<sup>384</sup>.  
1313 Reads found to contain sequence similar to the HIV genome using a suffix tree algorithm were  
1314 aligned against the HIV<sub>89.6</sub> genome using BLAT<sup>382</sup>. All statistical analyses were performed  
1315 in R 3.1.2<sup>375</sup>. RNA-Seq reads from Chang et al.<sup>319</sup> were downloaded from the Sequence  
1316 Read Archive (SRP013224) and aligned using the Rum pipeline.

1317 Gene lists were obtained from the supplementary materials of four other studies of differential  
1318 gene expression during HIV infection<sup>319,469,473,476</sup>. We called genes differentially expressed  
1319 in Li et al.<sup>476</sup> if they had a reported  $p < 0.01$  or in Lefebvre et al.<sup>473</sup>, Chang et al.<sup>319</sup>  
1320 and Imbeault et al.<sup>469</sup> if they had an adjusted  $p < 0.05$ . We called genes as differentially  
1321 expressed in our own study if the adjusted  $p < 0.01$ . For the comparison of differentially  
1322 expressed genes regardless of direction in figure 4.1 (below the diagonal), it was unclear  
1323 exactly how many genes were studied in each study so we assumed a background of the  
1324 14,192 genes (the number of genes which could be tested for significance in our data).

1325 We obtained transcriptional profiles comparing immune cell subsets from the Molecular  
1326 Signatures Database<sup>477</sup>. MSigDB set names from the MSigDB used in Figure 4.2A were  
1327 GSE10325 LUPUS CD4 TCELL VS LUPUS BCELL, GSE10325 CD4 TCELL VS MYELOID,  
1328 GSE10325 CD4 TCELL VS BCELL, GSE10325 LUPUS CD4 TCELL VS LUPUS MYELOID,  
1329 GSE3982 MEMORY CD4 TCELL VS TH1, GSE22886 CD4 TCELL VS BCELL NAIVE,  
1330 GSE11057 CD4 CENT MEM VS PBMC, GSE11057 CD4 EFF MEM VS PBMC, GSE3982  
1331 MEMORY CD4 TCELL VS TH2 and GSE11057 PBMC VS MEM CD4 TCELL and in

1332 Figure 4.2B were GSE36476 CTRL VS TSST ACT 72H MEMORY CD4 TCELL OLD,  
1333 GSE10325 CD4 TCELL VS LUPUS CD4 TCELL, GSE22886 NAIVE CD4 TCELL VS 12H  
1334 ACT TH1, GSE3982 CENT MEMORY CD4 TCELL VS TH1, GSE17974 CTRL VS ACT  
1335 IL4 AND ANTI IL12 48H CD4 TCELL, GSE24634 IL4 VS CTRL TREATED NAIVE CD4  
1336 TCELL DAY5, GSE24634 NAIVE CD4 TCELL VS DAY10 IL4 CONV TREG, GSE1460  
1337 CD4 THYMOCYTE VS THYMIC STROMAL CELL and GSE1460 INTRATHYMIC T  
1338 PROGENITOR VS NAIVE CD4 TCELL ADULT BLOOD.

1339 We downloaded the RepeatMasker track from the UCSC genome browser<sup>478</sup> and used the  
1340 SAMtools library<sup>479</sup> to assign reads to the repeat regions. HERV-K age estimates were  
1341 obtained from the supplementary materials of Subramanian et al.<sup>480</sup>.

1342 We used a Bayesian estimate of the ratio of expression in uninfected and HIV infected  
1343 samples to account for sampling effort and differing expression in genomic regions. We  
1344 modeled the observed counts as a binomial distribution with a flat beta prior ( $\alpha = 1, \beta = 1$ )  
1345 separately for uninfected and infected samples. We then Monte Carlo sampled the two  
1346 posterior distribution to estimate the posterior distribution of the ratio. For introns, the  
1347 number of binomial successes was set to the number of reads mapped to the intron and the  
1348 number of trials was the total number of reads observed in the genes overlapping that intron.  
1349 For repeat regions, the number of binomial successes was set to the number of reads mapped  
1350 to that region and the number of trials was the total number of reads mapped to the human  
1351 genome.

1352 To estimate determinants of LTR12C expression, we fit a logistic regression for which  
1353 LTR12C increased in expression with HIV<sub>89.6</sub> infection (95% Bayesian credible interval  
1354 >1) on to characteristics of the LTR12C regions. We extracted all the LTR12C regions  
1355 from the human genome and determined the U3-R boundary using a ends free alignment of  
1356 the previously reported U3-R border<sup>481–485</sup> against the sequences. Regions less than 1,000  
1357 bases long were discarded. Previous studies disagreed about the location of the LTR12C  
1358 transcription start site and it appears that transcription may start in several places<sup>482,483</sup>.

1359 We took the 5' most site that had agreement between studies (transcription starting with  
1360 TGGCAACCC). We split the sequences into short, medium and long length classes based  
1361 on an indel about 70 bases upstream from the transcription start site. For each length class,  
1362 we generated a consensus sequence and counted the Levenshtein edit distance between the  
1363 consensuses and each corresponding sequence. We also counted the number of NFY motifs  
1364 (CCAAT or ATTGG), MZF1 motifs (GTGGGG) and GATA2 motifs (GATA or TATC)  
1365 in the entire U3 region or checked in any of the three motifs was present in the 150 bases  
1366 upstream of the TSS. A final regression model was selected using stepwise regression with  
1367 an AIC cutoff of 5. For display, the LTR12C sequences were aligned with MUSCLE<sup>486</sup>.

1368 The abundance of the HIV RNA size classes was estimated as described in Additional File  
1369 5. These estimates were then multiplied by the within size class proportions estimated by  
1370 Ocwieja et al.<sup>406</sup> using PacBio sequencing of HIV<sub>89.6</sub> to yield proportions over 78 measured  
1371 HIV<sub>89.6</sub> RNAs.

## 1372 4.4 Results

### 1373 4.4.1 Infections studied

1374 HIV<sub>89.6</sub>, a clade B primary clinical isolate<sup>436</sup>, was used to infect primary CD4<sup>+</sup> T cells from  
1375 a single human donor in three replicate infections. For comparison, two additional replicates  
1376 from the same donor were mock infected. Samples were harvested after 48 hours of infection,  
1377 which allowed for widespread infection in the primary T cell cultures, though some cells may  
1378 be infected secondarily by viruses produced in the first round. Thus cultures probably were  
1379 not tightly synchronized but did have extensive representation of infected primary T cells.  
1380 From these samples, we obtained 1,161,705,678 101-bp reads from primary CD4<sup>+</sup> T cells  
1381 from a single donor; 1,021,207,853 were mapped to the human genome and 24,783,844 to  
1382 the HIV<sub>89.6</sub> provirus (Table 4.1). Below we first discuss the influence of infection on cellular  
1383 gene activity and RNA splicing, then analyze HIV RNAs and lastly analyze chimeras formed  
1384 between HIV and cellular RNAs.

Sample	Infection rate (%)	Reads	Human reads	HIV reads	% HIV	% HIV in infected
Uninfected-1	—	232,450,106	212,391,460	—	—	—
Uninfected-2	—	235,048,212	203,760,783	—	—	—
Infected-1	37.5	234,378,088	199,871,662	10,219,315	4.86	13.0
Infected-2	26	226,078,422	198,436,507	7,322,556	3.56	13.7
Infected-3	21	233,750,850	205,747,441	7,241,973	3.40	16.2

Table 4.1: Samples used in this study, their infection rates and sequencing depth.

1385 **4.4.2 Changes in gene activity in primary T cells upon infection with HIV<sub>89.6</sub>**

1386 Changes in host cell gene expression have been reported during HIV infection<sup>317–319,464–471,473</sup>  
 1387 and differences in expression have been observed associated with the stage<sup>476</sup> and progres-  
 1388 sion<sup>487</sup> of disease. Here we observed significant changes in gene expression (false discovery  
 1389 rate corrected  $q < 0.01$ ) in 3,142 genes, 17.1% of expressed cellular genes (Additional file 1).  
 1390 The genes with most extreme increases, all  $>6\times$  fold higher, during HIV infection included  
 1391 IFI44L, RSAD2, HMOX1, MX1, USP18, IGJ, OAS1, CMPK2, DDX60, IFI44, IFI6, IFNG  
 1392 and CCL3. All of these have been reported to be involved in innate immunity<sup>488</sup> or are  
 1393 interferon inducible<sup>489</sup>, highlighting a strong innate immune response in the cells studied.  
 1394 Genes with the largest decreases, all  $>3\times$  fold lower, were GNG4, GPA33, IL6R, CCR8,  
 1395 RORC, AFF2 and CCR2.

1396 Many gene ontology categories were significantly enriched for differentially expressed genes  
 1397 (Additional file 2). Notably upregulated with infection were genes involved in apoptosis,  
 1398 immune responses and cytokine production (all  $q < 10^{-4}$ ) and down-regulated were genes  
 1399 involved in viral gene expression, nonsense-mediated decay and translation elongation and  
 1400 termination (all  $q < 10^{-19}$ ). These changes suggest that the cells responded to HIV infection  
 1401 with the induction of inflammatory, interferon regulated and apoptotic responses, patterns  
 1402 posited from several previous studies<sup>319,464–470,472,473,490</sup>. Several genes were activated that  
 1403 were characteristic of other hematopoietic lineages, e.g. hemoglobin  $\beta$ , CD8, CD20 and  
 1404 CD117, while several CD4 $^+$  T cell specific genes, e.g. CD4 and CD3, were downregulated,  
 1405 potentially consistent with de-differentiation of infected and bystander cells. We return to

Cell type	HIV type	Differentially expressed genes (Up/Down)	Study
Primary CD4 <sup>+</sup> T	HIV <sub>89.6</sub>	3393 (1756/1637)	This study
Primary CD4 <sup>+</sup> T	NL4-3 BAL-IRES-HSA	228 (182/46)	Imbeault et al. <sup>469</sup>
Lymph node biopsies	Acute infection	448 (383/65)	Li et al. <sup>476</sup>
SupT1	HIV <sub>LAI</sub>	4997 (2666/2331)	Chang et al. <sup>319</sup>
SupT1	NL4-3Δenv-eGFP/VSV-G	579 (212/367)	Lefebvre et al. <sup>473</sup>

Table 4.2: Data from this study and four others used for meta-analysis of human gene expression changes during HIV infection

1406 this point in the discussion.

1407 **4.4.3 Comparison of transcriptional profiles from HIV<sub>89.6</sub> infection of primary**  
 1408 **T cells to data on HIV infection in other cell types**

1409 We sought to identify the transcriptional responses that were most conserved upon HIV  
 1410 infection and so collected and analyzed data from four other studies of transcription in  
 1411 HIV-infected cells (Table 4.2). These included two studies of infection of the SupT1 cell  
 1412 line<sup>319,473</sup>, a study of primary CD4<sup>+</sup> T cells<sup>469</sup> and a study of lymphatic tissue in acutely  
 1413 viremic patients<sup>476</sup>. Genes were scored as increased or decreased in activity after infection,  
 1414 and the amount of agreement was compared among the different studies.

1415 No gene was called as differentially expressed in all five studies. Eight genes were differentially  
 1416 expressed in the same direction in 4 out of 5 studies; AQP3 and EPHX2 were down-regulated  
 1417 with HIV infection and CD70, EGR1, FOS, ISG20, RGS16 and SAMD9L were up-regulated.  
 1418 A full listing is provided in Additional file 4. Several of the up-regulated genes are known to  
 1419 be interferon inducible, again emphasizing the role of innate immune pathways.

1420 For each pair of studies, we compared whether they agreed on the identities of differentially  
 1421 expressed genes and whether they agreed on the direction of change (Figure 4.1). The  
 1422 estimated alterations in gene activity showed notable differences in the responses to infection  
 1423 in primary cells versus the SupT1 cell line. The two SupT1 studies were significantly similar  
 1424 ( $p < 10^{-15}$ ) to each other but were not significantly associated (Lefebvre et al.<sup>473</sup>,  $p = 0.2$ )  
 1425 or were negatively associated (Chang et al.<sup>319</sup>,  $p = 10^{-7}$ ) with data from lymphatic tissue

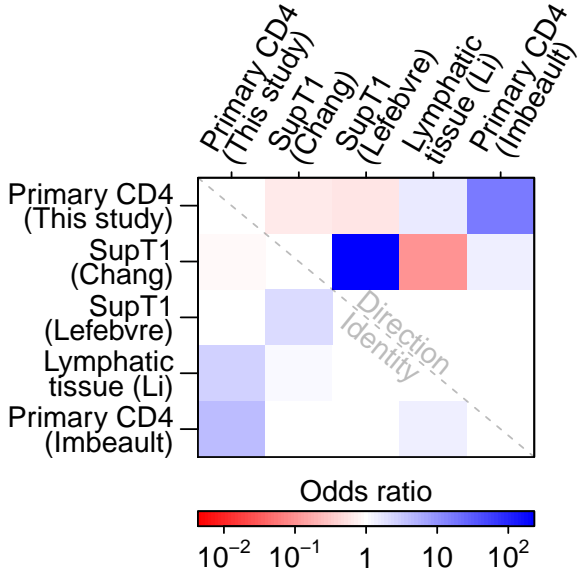


Figure 4.1: Comparisons among studies quantifying cellular gene expression after HIV infection. For each pair of studies, the association between up- and down-regulation calls was measured for genes identified by both studies as differentially expressed (above the diagonal). As another comparison, we also measured the agreement between studies for which genes were called differentially expressed regardless of direction (below the diagonal). The color scale shows the conservative (i.e. closest to 1) boundary of the confidence interval of the odds ratio with blue indicating a positive association and red a negative association between studies. For confidence intervals overlapping 1, the value was set to 1. Therefore all colored squares indicate significant associations.

in acute HIV patients. The primary T cell study reported here was significantly associated with the second study in primary cells ( $p < 10^{-15}$ ) and with a study of lymphatic tissue from patients acutely infected with HIV ( $p = 0.003$ ). Our primary T cell data was negatively associated with the SupT1 studies (both  $p < 10^{-3}$ ). This documents significant differences in responses to HIV infection between infected primary cells and SupT1 cells and suggests that results of infections in primary cells more closely align with actual acute HIV infections in patients. SupT1 cells might be expected to respond to infection differently than primary cells since they have several nonsynonymous mutations in innate immunity genes<sup>491</sup>, have blocks in immune signaling pathways<sup>492</sup> and fail to activate many interferon stimulated genes during HIV infection<sup>470</sup>.

#### 4.4.4 Comparison of the HIV infected cell transcriptional profiles to additional experimental T cell profiles

To investigate the transcriptional changes in more depth, we compared the results of the five studies of HIV infection to transcriptional profiles comparing immune cell subsets available at the Molecular Signatures Database (MSigDB)<sup>477</sup>. The MSigDB reports genes that are

1441 increased or decreased in relative expression for each of 185 pairs of transcriptional profiles  
1442 involving CD4<sup>+</sup> T cells. We compared the lists of affected genes in each pair to genes altered  
1443 in activity by HIV infection. Those pairs of studies with the most significant associations  
1444 with HIV<sub>89.6</sub> data are show in Figure 4.2A. For comparison, the associations with the four  
1445 other HIV transcriptional profiling studies mentioned above are shown as well.

1446 The most significant associations for our data showed gene expression in HIV<sub>89.6</sub>-infected  
1447 cells moving away from typical T cell expression patterns and towards patterns more similar  
1448 to B cells, myeloid cells and bulk peripheral blood mononuclear cells (all Fisher's  $p < 10^{-15}$ )  
1449 (Figure 4.2A). These changes were also seen, although to a lesser extent, in the Imbeault  
1450 et al.<sup>493</sup> study which also used primary CD4<sup>+</sup> T cells.

1451 For comparison, we also extracted those profiles most strongly associated with the transcrip-  
1452 tional data on lymphatic tissue of HIV patients<sup>476</sup>. The profiles showed patterns similar to  
1453 strongly stimulated T cells, autoimmune disease and to the Th1 T cell subset (all  $p < 0.01$ )  
1454 (Figure 4.2B). Our data in primary CD4<sup>+</sup> T cells paralleled the changes seen in lymphatic  
1455 tissue. These transcriptional changes again highlights the strong immune response generated  
1456 by HIV infection in primary cells.

#### 1457 4.4.5 Intron retention

1458 Cells respond to infection by shutting down macromolecular synthesis at multiple levels<sup>494–498</sup>,  
1459 so we investigated whether cells also showed perturbations in splicing efficiency after infection.  
1460 As a probe, we created a database of cellular genomic regions annotated exclusively as exons  
1461 or introns in all spliceforms in the UCSC gene database<sup>394</sup> and quantified expression in  
1462 these regions in infected and uninfected cells. We found a significant increase in intronic  
1463 sequences relative to exonic sequence (Wilcoxon  $p < 10^{-15}$ ) (Figure 4.3A). This increase  
1464 in intronic sequence was reproducible between replicates in our study (Kendall's  $\tau=0.42$ ,  
1465  $p < 10^{-15}$ ) (Figure 4.3B). We reanalyzed RNA-Seq data from Chang et al.<sup>319</sup> and also  
1466 documented intron retention which correlated with the changes seen in our data (Kendall's

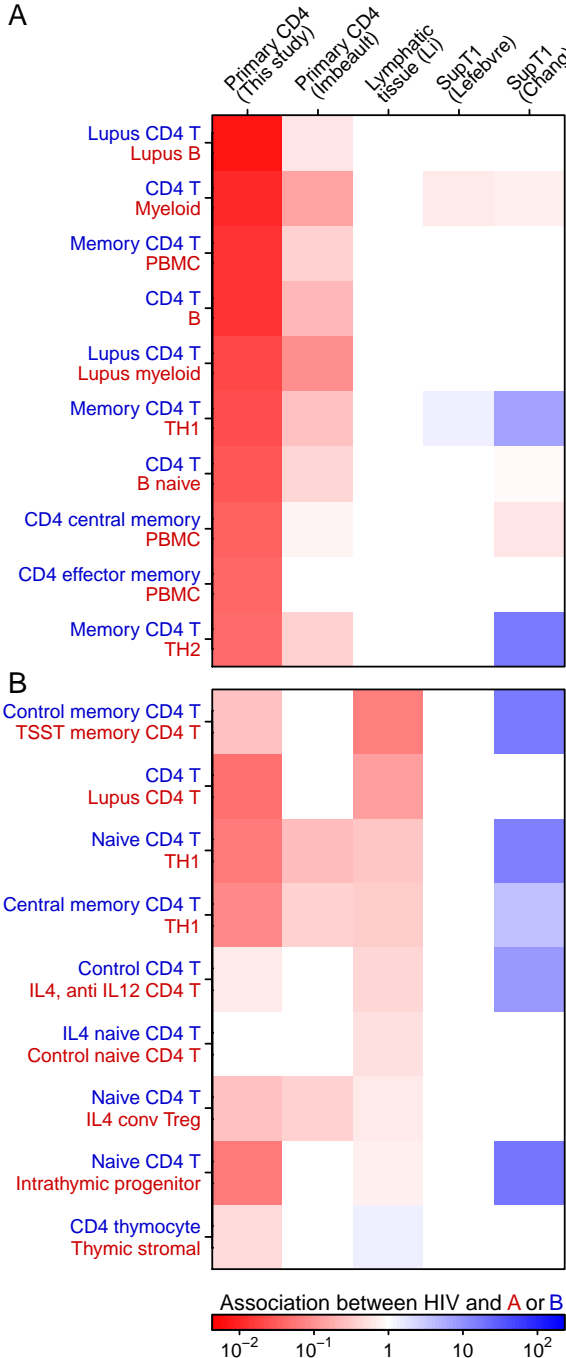


Figure 4.2: Comparisons of the effect of HIV infection on gene expression to studies comparing subsets of immune cells. The MSigDB database was used to extract 185 sets of differentially expressed genes from pairs of transcriptional profiling studies of immune cell subsets involving CD4<sup>+</sup> T cells. For each pair of studies, we used Fisher's exact test to measure the association between up- and down-regulation calls for genes identified as differentially expressed in both our HIV study and the comparator immune subsets. A) The transcriptional profiles with strongest associations with changes observed in our study of HIV<sub>89.6</sub> infection of primary T cells. Blue indicates a positive association between changes seen in HIV infected cells and the first immune subset (text colored blue) while red indicates a positive association with the second immune subset (text colored red). The color scale shows the conservative (i.e. closest to 1) boundary of the confidence interval of the odds ratio. For confidence intervals overlapping 1, the value was set to 1. Therefore all colored squares indicate significant associations. B) As in A, but showing the transcriptional profiles most strongly associated with changes observed in lymph node biopsies from acutely infected patients<sup>476</sup>.

1467  $\tau=0.12$ ,  $p < 10^{-15}$ ) (Figure 4.3C).

1468 A possible artifactual explanation for enrichment of intronic sequences could involve greater  
1469 DNA contamination in the infected cells samples. That is, if the relative amount of DNA  
1470 differed between treatments, the amount of apparent intronic sequences could also differ  
1471 due to sequencing of contaminating DNA. To examine whether DNA contamination was  
1472 abundant in our samples, we compiled a collection of 27 large gene desert regions, defined  
1473 here as 1) regions outside the centrosome and first and last cytoband, 2) containing less than  
1474 1% unknown sequence, 3) containing no genes annotated in UCSC genes<sup>394</sup>, 4) containing  
1475 no repeats annotated in the repeatMasker database<sup>399</sup> and 5) spanning more than 100  
1476 kb. No reads were mapped to these 41 Mb of gene deserts in any sample, arguing against  
1477 explanations based on DNA contamination. Thus these data indicate that intron retention  
1478 was increased in these cell populations upon HIV infection, revealing a previously undisclosed  
1479 aspect of the host cell transcriptional response to infection.

1480 Previous studies have reported changes in the expression and localization of splicing factors  
1481 with HIV infection<sup>433,499,500</sup>. In our data, HIV<sub>89.6</sub> infection significantly altered the expression  
1482 of genes involved in RNA splicing ( $p = 2 \times 10^{-7}$ ) and nonsense-mediated decay ( $p < 10^{-15}$ ).  
1483 Genes related to nonsense-mediated decay genes showed a strong pattern of lowered RNA  
1484 abundance, with 71 out of 118 annotated genes significantly lower in expression after infection.  
1485 These patterns suggest potential mechanisms for the intron retention observed here.

#### 1486 4.4.6 Induction of transcription from HERVs and LINEs by HIV<sub>89.6</sub> infection

1487 HIV infection has been reported to induce expression of certain HERVs, particularly HERV-  
1488 K<sup>501–503</sup>, and LINE and Alu transposable elements<sup>504</sup>, providing candidate markers of  
1489 infection and possible vaccine targets. Thus we analyzed our data in primary T cells infected  
1490 with HIV<sub>89.6</sub> to investigate the expression of HERVs, LINEs and other repeated sequences.  
1491 Figure 4.4A shows a comparison of the association between changes in expression with  
1492 HIV<sub>89.6</sub> infection and the various genomic repeat types over varying levels of differential

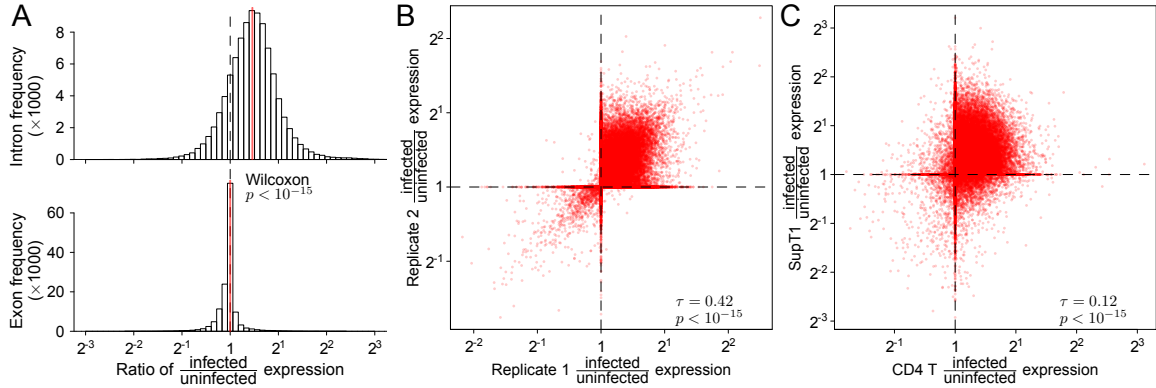


Figure 4.3: Changes in the abundance of intronic regions with HIV infection. Expression of intronic and exonic regions was quantified as the proportion of reads mapping within the intron/exon out of the total reads mapping to the transcription units overlapping that intron/exon. A) Comparison of the ratios of expression between infected and uninfected replicates in exclusively intronic or exonic regions of transcription units. B) Reproducibility of intron retention between replicates. Each point quantifies the change in expression with HIV infection for a specific intronic region. The x-axis shows changes in gene activity accompanying infection for one set of replicates (Infected-1 and Infected-2 vs. Uninfected-1) and the y-axis shows the same data for different replicates (Infected-3 vs. Uninfected-2). C) Reproducibility of intron retention between studies. The plot is arranged as in B but with all data from our study combined on the x-axis and corresponding data from Chang et al.<sup>319</sup> on the y-axis.

1493 expression. At high levels of expression, ERV-9 (odds ratio at  $4\times$  expression: 152, 95%  
 1494 CI: 82.5–259) and its long terminal repeat LTR12C (odds ratio at  $4\times$  expression: 144, 95%  
 1495 CI: 98.2–207) are the only repeats highly associated with upregulation during HIV infection.  
 1496 Looking at genomic repeats with any significant increase, the expression of many recently  
 1497 acquired genomic repeats, including L1HS, LTR5\_Hs (a human specific LTR of HERV-K),  
 1498 AluYa5, AluYg6 and SVA\_D and SVA\_F, were associated with HIV<sub>89.6</sub> infection (Figure  
 1499 4.4B).

1500 We saw a relationship between the age of genomic repeats and its likelihood of being induced  
 1501 by HIV<sub>89.6</sub> infection. The most highly enriched repeats were associated with relatively  
 1502 recent hominid-specific repeat classes as annotated by the RepeatMasker database (repeat  
 1503 classes with  $p < 10^{-50}$  odds ratio: 31.6, 95% CI: 8.88–112). In HERV-K (HML-2), the  
 1504 most recently active endogenous retrovirus in the human genome<sup>480,505,506</sup>, we saw that  
 1505 integrations unique to the human genome<sup>480</sup> were more likely to be differentially expressed

1506 than older HERV-Ks (odds ratio: 5.38, 95% CI: 1.93–16.0).

1507 Previous RNA-Seq studies of cellular expression during HIV infection in transformed cell  
1508 lines did not report increases in HERV mRNA<sup>319,473</sup>. To investigate this difference, we  
1509 downloaded and analyzed the RNA-Seq data from Chang et al.<sup>319</sup>, which quantified gene  
1510 activity in transformed SupT1 cells infected with a lab-adapted strain of HIV. We found a  
1511 much higher level of HERV expression in their data in both HIV infected cells and uninfected  
1512 controls than in primary cells (Figure 4.4C). We suspect that in SupT1 cells, as with many  
1513 cancerous cells<sup>507–511</sup>, the baseline expression of transposons and endogenous retroviruses is  
1514 higher than in primary cells, masking further induction by HIV infection.

1515 We observed heterogeneous expression among ERV-9/LTR12C sequences and so investigated  
1516 the primary sequence determinants. We observed that ERV-9/LTR12C has three variants of  
1517 differing length in the U3 region just upstream of the transcription start site (Figure 4.5A),  
1518 an important region for transcription initiation<sup>482</sup>. The U3 region of LTR12C also contains  
1519 multiple motifs for transcription factors NFY, GATA2 and MZF1<sup>485</sup>. To clarify factors  
1520 affecting expression levels, we counted the number of motifs matching these transcription  
1521 factors, assigned each LTR12C to one of the length classes, counted the number of mutations  
1522 away from the consensus for that length class and checked for integration in a transcription  
1523 unit. We then carried out a regression analysis to test the effects of these variables on  
1524 LTR12C differential expression. We found that HIV<sub>89.6</sub> induced transcription was more  
1525 likely with the fewer mutations away from consensus, the number of locations matching the  
1526 NFY transcription factor binding motif (CCAAT) and LTRs containing the short length  
1527 variant of the 3' U3 region. The presence of a MZF1 motif near the transcription start site  
1528 decreased transcription (Figure 4.5B).

#### 1529 4.4.7 HIV mRNA synthesis and splicing

1530 Over 24 million Illumina reads mapped to HIV<sub>89.6</sub>, yielding an average coverage of over  
1531 240,000-fold. Reads mapping to HIV<sub>89.6</sub> comprised between 3.4–4.8% of mapped reads in

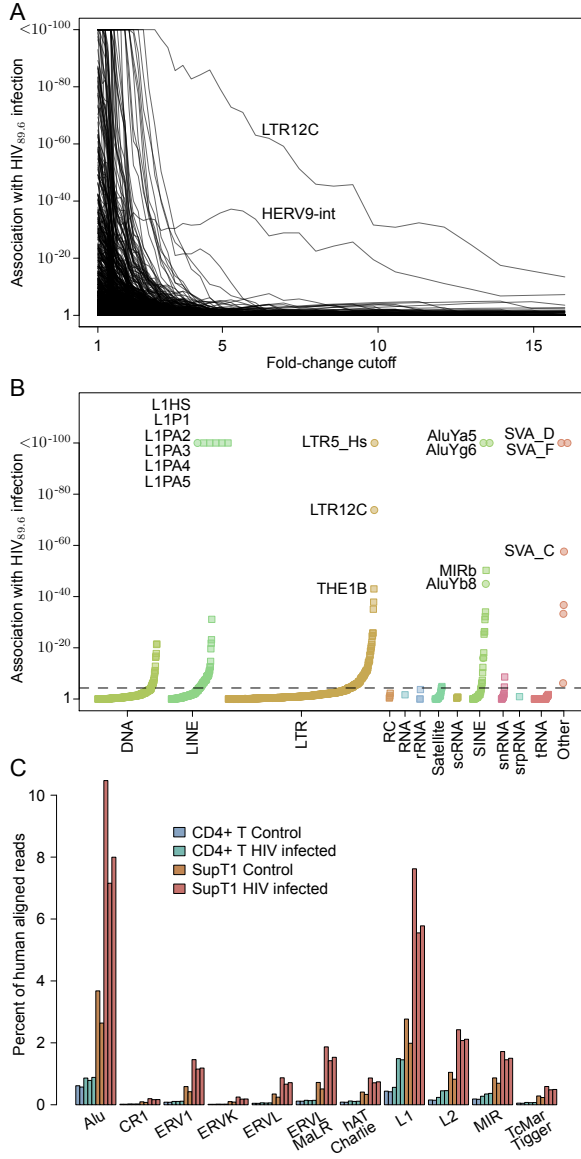


Figure 4.4: Repeat categories enriched upon infection with HIV. A) The association of repeat regions differentially expressed after HIV<sub>89.6</sub> infection of primary T cells observed for varying thresholds of differential expression. The threshold used to call a gene differentially expressed based on the Bayesian posterior median was varied and Fisher's exact test was used to assess whether any genomic repeats had a significant association with this differential expression. Note that only ERV-9 (annotated as HERV9-int in the RepeatMasker database) and its corresponding long terminal repeat LTR12C were significantly associated with large changes in expression. B) Enrichment of repeat categories in regions differentially expressed (Bayesian 95% credible interval >1) between HIV-infected and control CD4<sup>+</sup> T cells. The repeated sequences are ordered on the x-axis by the extent of induction within each class, the y-axis shows the p-value for upregulation after infection. The dashed line indicates a Bonferroni corrected  $p$  value of 0.05. (C) The proportion of human mapped reads that align within classes of genomic repeats for data from primary CD4<sup>+</sup> T cells from this study and SupT1 cells from Chang et al.<sup>319</sup>. A single read mapping multiple times to a given category was only counted once.

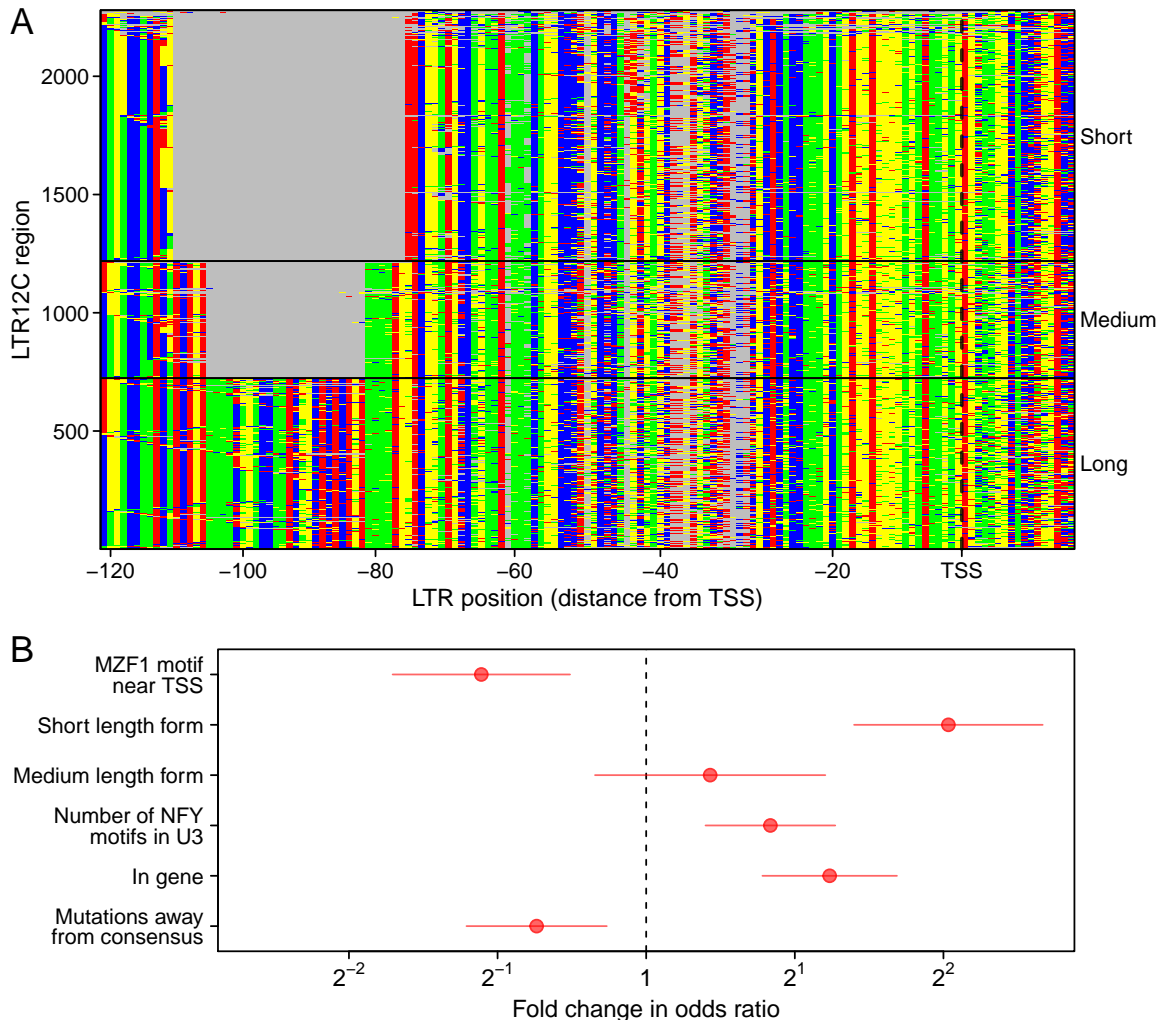


Figure 4.5: Characteristics of LTR12C sequences associated with induction upon infection of primary T cells with HIV<sub>89.6</sub>. A) An alignment of the 3' end of the U3 region of repeats annotated as ERV-9 LTR12C. Each row is a LTR sequence and each column a base in that sequence colored by nucleotide identity. Three distinct classes are visible with a short, medium and long form. Mutations away from the consensus can also be seen. B) The coefficients (points) and  $\pm 1.96$  standard errors (horizontal lines) of a logistic regression comparing differential expression of LTR12C to the presence of MZF1 and NFY motifs, short/medium/long length alternate forms of the U3-R region, mutations away from the consensus for each length form and integration inside a transcription unit. The coefficient shown for mutations away from consensus is for a 10 mutation difference and the coefficient shown for NFY motifs is for a change of 5 additional motifs. All other coefficients are for binary values.

1532 the infected samples (Table 4.1). Assuming HIV-infected cells contain the same amount of  
1533 mRNA as uninfected cells and adjusting for rates of infection ranging between 21–37.5%  
1534 (Table 4.1), we estimate that HIV transcripts comprise between 13.0–16.2% of the total  
1535 polyadenylated mRNA nucleotides in infected cells 48 hours after initial infection. This  
1536 parallels previous estimates of around 10%<sup>512</sup> at 48 hours postinfection, 38% at 24 hours<sup>319</sup>  
1537 or 30% after 72 hours<sup>464</sup>.

1538 Over 47,257 single reads spanned previously reported HIV splice junctions, allowing a  
1539 quantitative assessment of donor and acceptor utilization (Figure 4.7A). As expected from  
1540 previous studies<sup>406,412</sup>, the most abundant junctions were D1-A5 and D4-A7. We confirmed  
1541 the use of unusual splice acceptors A8c and A5a, previously reported in HIV<sub>89.6</sub><sup>406</sup>. In  
1542 our data, we also see a higher abundance of D1-A1 and D1-A2 splice junctions than might  
1543 be expected<sup>406,412</sup>, although previous studies reported proportional abundance within size  
1544 classes, making comparisons between size classes uncertain.

1545 A 3' bias is apparent in our sequencing data (Additional file 5). This could be due to the  
1546 poly-A capture step of the protocol where any break in the RNA would result in distal  
1547 5' sequences being lost<sup>513</sup>. We used sequence reads from the large unspliced HIV intron  
1548 1 to measure this bias using a regression of the log of the number of fragments with a  
1549 5'-most end starting at a given position against the distance of that position from the  
1550 viral polyadenylation site, yielding an estimated probability of breakage of 0.021% per base  
1551 (Additional file 5). Given this rate of termination, there is only a 14% chance of reaching  
1552 the 5' end of the 9171 nt unspliced HIV genome  $((1 - 0.00021)^{9171})$ .

1553 Ocwieja et al.<sup>406</sup> determined the relative abundance of HIV<sub>89.6</sub> of similarly sized transcripts  
1554 using PacBio single molecule sequencing, but were not able to estimate the relative abundance  
1555 of all transcripts due to a sequencing bias favoring shorter transcripts. For this reason,  
1556 relative abundances could only be specified within message size classes (i.e. the 4 kb, 2 kb  
1557 and unexpectedly a 1 kb size class as well) and the overall quantitative abundances were  
1558 unknown. The RNA-Seq data reported here are unable to determine complete transcript

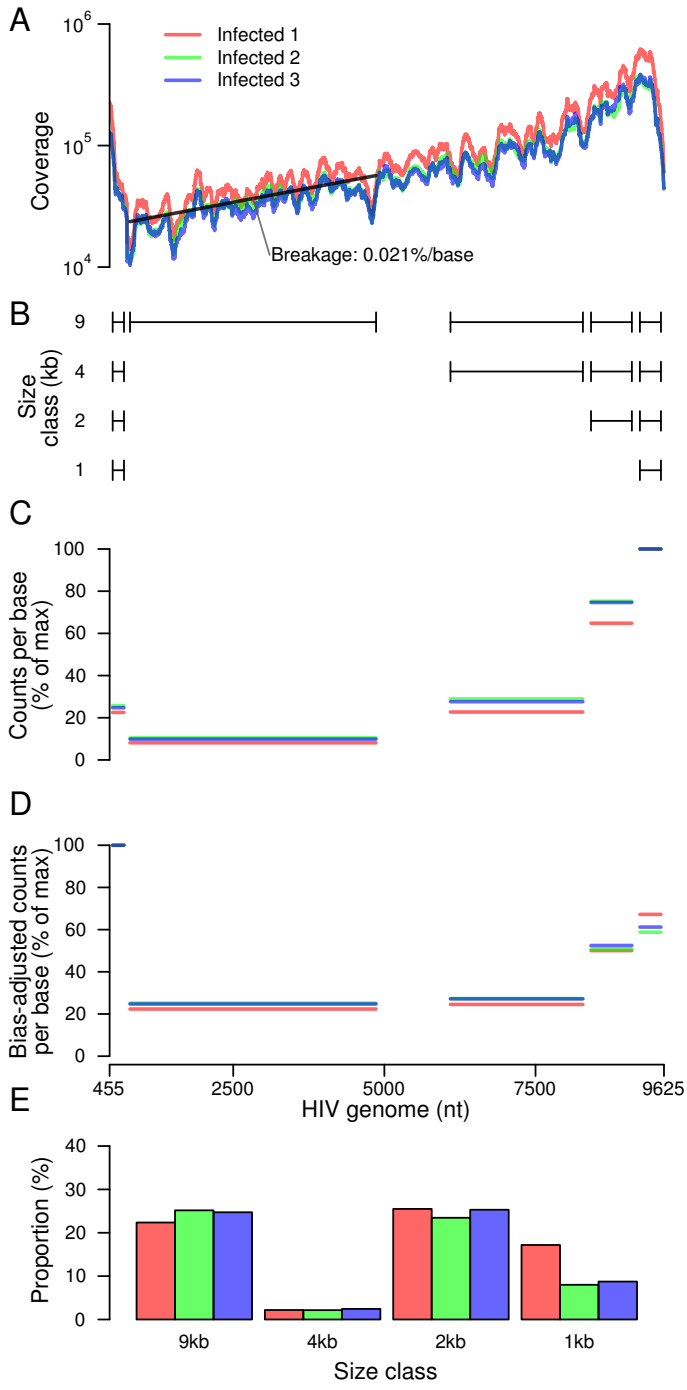


Figure 4.6: Estimating relative abundance of HIV<sub>89.6</sub> message size classes using RNA-Seq data.

A) RNA-Seq coverage of the HIV<sub>89.6</sub> genome for the replicates in this study. Each replicate is indicated by a different color. The HIV genome is shown on the x-axis and the number of reads that aligned to each position is shown on the y-axis. Black line indicates the 0.021% coverage decrease per base distance from the 3' end of the mRNA estimated from a least squares fit on the read counts in the first intron.

B) Diagram of the segments of the HIV<sub>89.6</sub> RNA present in each of 9 kb, 4 kb, 2 kb and 1 kb size class.

C) The proportion of reads mapped to each of the segments of the HIV<sub>89.6</sub> genome shown in B adjusted by the length of the segment. Each replicate is shown by a different color.

D) Corrected representation of RNA segments from the different size classes. Because cDNA synthesis was primed from the polyA tail, more 3' sequences are recovered preferentially. Using the bias estimate from A, we adjusted each genome segment by the inverse of the bias predicted based on its distance from the 3' end of the mRNA. Corrected proportions for the indicated RNA segments are shown colored by replicate.

E) The proportion of each size class was inferred using the estimates in D by calculating the difference between segments. Replicates are indicated by color.

abundance because the short read length does not allow reconstruction of multiply spliced messages but do permit estimation of size class abundances after correcting for 3' bias (Additional file 5). Thus the PacBio data reported by Ocwieja et al.<sup>406</sup> and the Illumina data reported here can be combined together to determine complete relative abundance of all HIV<sub>89.6</sub> transcripts (Figure 4.7B).

The most abundant HIV mRNAs were the unspliced HIV genome (37.6%), a transcript encoding Nef (D1-A5-D4-A7: 15.5%), two 1 kb size class transcripts (D1-A5-D4-A8c: 10.6%, D1-A8c: 4.9%) and two Rev-encoding transcripts (D1-A4c-D4-A7: 4.2%, D1-A4b-D4-A7: 3.1%). The function of this large amount of 1 kb transcript is unknown. These two 1 kb transcripts do not appear to encode significant open reading frames although other 1 kb transcripts can encode a Rev-Nef fusion<sup>406</sup>.

Using these abundances, we can estimate the number of HIV<sub>89.6</sub> genomes in these primary T cells 48 hours after infection. To determine the proportion of the mRNA nucleotides from viral transcripts, we multiplied the estimated abundances by their transcript lengths. Unspliced genome transcripts appear to form 79% of the mRNA nucleotides from HIV<sub>89.6</sub> transcripts. Assuming T cells contain at least 0.1 pg of mRNA then an infected cell should contain at least 0.011 pg of unspliced HIV transcript ( $0.1\text{pg} \times 0.14 \frac{\text{HIV mRNA nt}}{\text{cell mRNA nt}} \times 0.79 \frac{\text{unspliced mRNA nt}}{\text{HIV mRNA nt}}$ ) or, assuming 9171 bases of RNA weigh about  $5 \times 10^{-6}$  pg, at least 2200 HIV genomes at 48 hour post infection. This estimate roughly agrees with previous estimates of HIV production per cell<sup>512,514,515</sup>.

#### 4.4.8 Human-HIV chimeric reads

The suggestion that HIV integration may disrupt cellular cancer-associated genes and thereby promote cell proliferation<sup>516–519</sup> has focused attention on the range of novel message types formed when HIV integrates within transcription units<sup>353,410,520–522</sup>. Chimeric reads containing HIV and cellular sequence are also of clinical interest due to the potential of lentiviral vectors to trigger oncogenesis in gene therapy patients through insertional

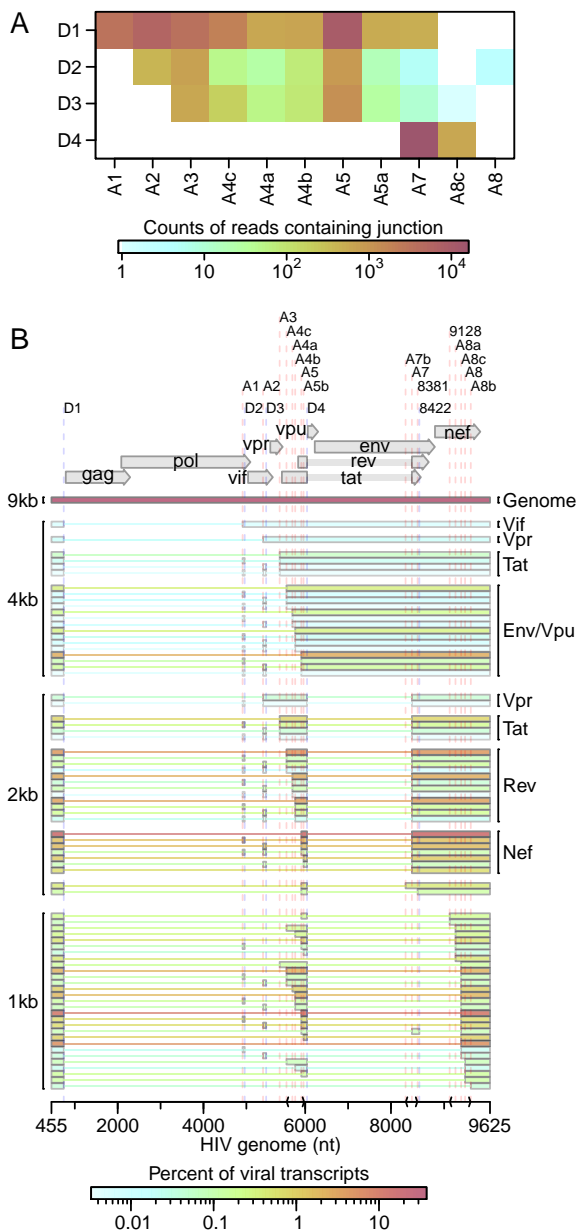


Figure 4.7: Transcription and splicing of the HIV<sub>89.6</sub> RNA. A) Junctions between HIV splice donors and acceptors observed in the RNA-Seq data. Acceptors are shown as the columns and donors as the rows with the coloring indicating the frequency of each pairing. B) The relative abundance of all HIV<sub>89.6</sub> transcripts as determined by a combination of PacBio sequencing<sup>406</sup> and Illumina sequencing. Message structures were generated by targeted long read single molecule sequencing, which allowed association of multiple splice junctions in single sequence reads. The Illumina short read sequencing allowed normalization of message abundances between size classes. The inferred HIV message population is shown colored by relative abundance.

1585 mutagenesis<sup>523–526</sup>.

1586 In our data, 80,045 reads contained sequences matching to both HIV and human genomic  
1587 DNA, but a considerable complication arises because chimeras can be formed artifactually  
1588 during the preparation of libraries for sequence analysis<sup>527–534</sup>. Many of the chimeric  
1589 sequences in our data contained junctions between the HIV and human sequence where the  
1590 ends of the human and HIV sequence were similar and potentially complementary (Figure  
1591 4.8A). This raises the concern that some of these chimeras could be products of in vitro  
1592 recombinations during the reverse transcription, amplification and sequencing processes.  
1593 Template switching between sequences with shared similarity is a well established property  
1594 of retroviral reverse transcriptase enzymes used in RNA-Seq library preparation<sup>535–537</sup>.  
1595 Priming off incomplete transcripts during DNA synthesis is another potential source of  
1596 chimeric transcripts<sup>527,528,538,539</sup>. Failing to account for chimeras can hinder interpretation  
1597 of deep sequencing data<sup>529–534</sup>.

1598 Also consistent with artificial chimera formation, 7,354 reads (9.2% of chimeric messages)  
1599 contained HIV sequences joined to human mitochondrial sequences, yet HIV proviruses have  
1600 not previously been found integrated in mitochondrial DNA<sup>410</sup>. To probe this further, we  
1601 used ligation-mediated PCR to recover integration site junctions from the same infected cell  
1602 populations analyzed by RNA seq, yielding 147,281 unique integration sites (Figure 4.8B)<sup>383</sup>.  
1603 No integrations in mitochondrial DNA were detected. We conclude that chimeric HIV-  
1604 mitochondrial sequence reads in the RNA-seq data represent artifacts of library construction  
1605 and so used these chimeras as an assay to evaluate subsequent data filtering steps. We  
1606 reasoned that reads without sequence similarity at junctions between human and HIV  
1607 mapping were less likely to be artifacts caused by template switching. Filtering to only reads  
1608 where no overlap and no unknown intervening sequence was present between human and HIV  
1609 portions left 2181 junctions and reduced the proportion of reads containing mitochondrial  
1610 DNA to 2.4%. Of the remaining HIV-human chimeric reads, the HIV portion of 605 sequences  
1611 bordered the 3' or 5' end of HIV or an HIV splice donor or acceptor. Filtering to these

1612 more likely authentic junctions left only 2 (0.3%) chimeric reads containing mitochondrial  
1613 sequence. This decrease in likely mitochondrial artifacts suggests that the filtering was  
1614 effective. The high rate of mitochondrial chimeras in the unfiltered sequences raises the  
1615 concern that artifacts may easily distort results in studies using similar amplification and  
1616 sequencing techniques.

1617 Chimeric messages composed of HIV and cellular RNA sequences can be formed by cellular  
1618 gene transcription reading into the integrated provirus, by HIV transcription reading out  
1619 through the viral polyadenylation site or by splicing between human and viral splice sites.  
1620 In our filtered data, the predominant forms appear to be derived from reading through the  
1621 HIV polyadenylation signal into the surrounding DNA (78%), splicing out of the viral D4  
1622 splice donor to join to human slice acceptors (17%) and reading into the HIV 5' LTR from  
1623 human sequence (4.0%) (Figure 4.8C). No splice site other than D4 had more than two  
1624 chimeric reads observed.

1625 The filtered chimeric reads had many traits consistent with biological chimera formation.  
1626 The reads containing HIV D4 joined to human sequences had the characteristics expected of  
1627 splicing—72.1% of the chimeric junctions mapped to known human acceptors and 96.1%  
1628 mapped to a location immediately preceded by the AG consensus of human mRNA acceptors.  
1629 The reads containing the 5' or 3' LTR border were almost exclusively (93%) found in  
1630 transcription units, with odds of being in a gene 2.3-fold (95% CI: 1.6–3.2×) higher than  
1631 integration sites from the same sample. The 5' or 3' chimeras were also more likely to be  
1632 located in an exon than integration sites even after excluding any integration or chimera not  
1633 located in a transcription unit (odds ratio: 2.1×, 95% CI: 1.6–2.6×).

1634 We next compared whether the human and viral segments of chimeric reads agreed or  
1635 disagreed in orientation (i.e. strand transcribed) for reads with the human portion mapped  
1636 within annotated transcription units. The sequencing technique used here does not preserve  
1637 strand information, but we can check whether the strand of a sequence read agrees or  
1638 disagrees with the annotated gene strand and compare this to the observed strand of the

1639 HIV portion of the read. We found a strong association between the orientation of the  
1640 human and HIV portions of chimeric reads within 3' and 5' chimeras (odds ratio: 6.2 $\times$ ,  
1641 95% CI: 3.9–10.2 $\times$ ). This highly significant enrichment of HIV and human genes in the  
1642 same orientation (Fisher's exact test  $p < 10^{-15}$ ) might indicate that antisense HIV RNA  
1643 is rapidly degraded by a response to double-stranded RNA or that polymerases oriented  
1644 in opposing directions interfere with one another during elongation. Chimeras involving  
1645 HIV splice donor D4 were even more highly enriched for matching orientations (odds ratio:  
1646 52.5 $\times$ , 95% CI: 12.1–307 $\times$ ) suggesting that pairing with human splice acceptors may add  
1647 an additional constraint on the orientation of D4 chimeric reads.

1648 Based on these data, we can propose a lower bound on the relative abundance of chimeras. If  
1649 we assume that our filtering removed nearly all artifacts so that we have few false positives,  
1650 then our estimate should be lower than the true proportion of chimeras. In our data, only  
1651  $\frac{604}{12,689,879} = 0.0048\%$  of reads containing sequence mapping to HIV also contained identifiable  
1652 chimeric junctions. However, this is an underestimate because in an HIV-derived mRNA, any  
1653 fragment of the sequence will be mappable to HIV, while for a chimeric sequence only a read  
1654 spanning the HIV-human junction will allow identification of a chimera. If we assume that  
1655 25 bases of sequence are necessary to map to human or HIV sequence, then, with the 100-bp  
1656 reads used here, only read fragments starting between 75- and 25-bp downstream of the  
1657 chimeric junction will be identifiable. If we assume the average chimeric mRNA sequences is  
1658 at least 2 kb long, then a read from a chimeric sequence has at most a  $\frac{50}{2000} = 2.5\%$  chance  
1659 of containing a mappable junction. Thus, a lower bound for the proportion of HIV mRNA  
1660 that also contain human-derived sequences is 0.2% ( $\frac{0.0048\%}{2.5\%}$ ). Looking only at splicing from  
1661 HIV donor D4, we saw 16,843 reads containing a junction from D4 to an HIV acceptor and  
1662 104 reads from D4 to human sequence. Thus, in our data, 0.6% of D4 splice products form  
1663 junctions with human acceptors instead of HIV acceptors.

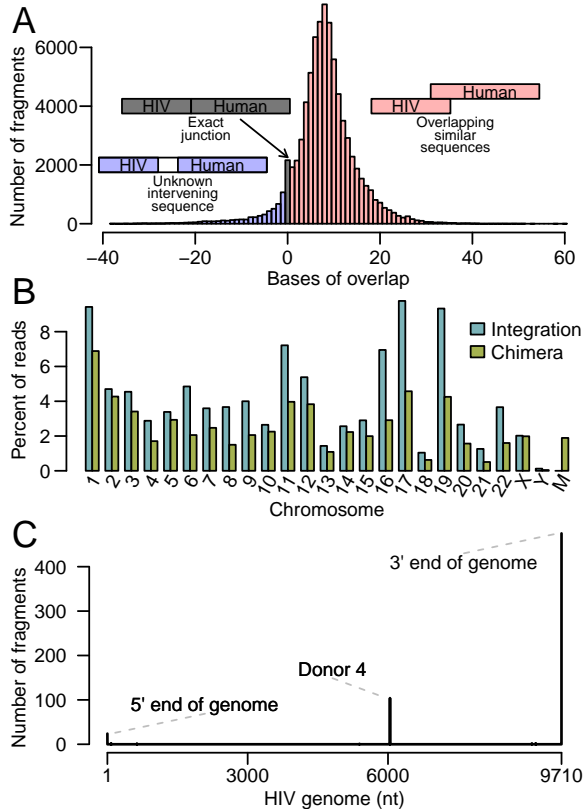


Figure 4.8: Analysis of chimeric RNA sequences containing both human and HIV sequences. A) The length of overlapping sequence (regions of complementarity potentially favoring chimera formation) matching both human and HIV at inferred chimeric junctions. The x-axis shows the length of the overlap and the y-axis shows the frequency of chimeric junctions with the indicated extent of overlap. B) Chromosomal distribution of uniquely mapping HIV integration sites from the same infections of primary T cells and comparison to uniquely mapping human sequences in chimeric reads observed in RNA-Seq. Note that the mitochondrial genome, denoted as M, has no authentic integration sites but does have extensive matches to chimeric junctions found in the RNA-Seq data. C) Counts of the location in the HIV genome of the HIV-human junctions in filtered chimeric reads.

## 1664 4.5 Discussion

1665 Here we used RNA-Seq to analyze mRNA accumulation and splicing in primary T cells  
 1666 infected with the low passage isolate HIV<sub>89.6</sub>. We did not carry out dense time series  
 1667 analysis, compare different human cell donors or compare different perturbations of the  
 1668 infections—instead, we focused on generating a dense data set at a single time point. We  
 1669 analyzed replicate infected cell and control samples to allow discrimination of within-condition  
 1670 versus between-condition variation and assessed differences using a series of bioinformatic  
 1671 approaches. Many previous studies have used microarray technology or RNA-Seq to study  
 1672 gene activity in HIV-infected cells<sup>317,319,464–473</sup>, usually analyzing infections of transformed  
 1673 cell lines or laboratory adapted strains of HIV-1. Here we present what is to our knowledge  
 1674 the deepest RNA-Seq data set reported for infection in primary T cells using a low passage  
 1675 HIV isolate (HIV<sub>89.6</sub>). This data set was paired with a set of 147,281 unique integration  
 1676 site sequences extracted from the same infections, which were critical to our ability to

1677 quality control chimeric reads. An advantage of studies using cell lines and laboratory  
1678 adapted strains is that often a high percent of cell infection can be achieved, whereas in  
1679 this study we achieved only ~30% infection. However, we report distinctive features of the  
1680 transcriptional response not seen in studies of HIV infections in cell lines. Novel in this  
1681 study are 1) identification of intron retention as a consequence of HIV infection, 2) the  
1682 finding of activation of ERV-9/LTR12C after HIV infection, 3) generation of a quantitative  
1683 account of the structures and abundances of over 70 HIV<sub>89.6</sub> messages and 4) clarification of  
1684 the predominant types of HIV-host transcriptional chimeras. These findings are discussed  
1685 below.

1686 Broad changes in host cell mRNA abundances were evident after infection, with over 17% of  
1687 expressed genes changing significantly in activity. Changes included expected response to  
1688 viral infection, apoptosis and T cell activation. Although it is not possible here to separate  
1689 the response of infected and bystander cells, this study highlights the drastic changes in  
1690 cellular expression caused by HIV-1 infection. In a meta-analysis including four previously  
1691 published studies, no gene was detected as differentially expressed in all five studies and  
1692 only a handful of genes appeared in four out of five studies. Further analysis showed that  
1693 expression changes appear to be cell type specific, raising concerns that studies using cell  
1694 lines may not fully reflect host cell responses in *in vivo* infections.

1695 Unexpectedly, intronic sequences were more common in the RNA-Seq data from cells after  
1696 HIV<sub>89.6</sub> infection than in mock infected cells. The mechanism is unclear. It is possible  
1697 that the splicing machinery is reduced in activity after 48 hours of infection, perhaps as a  
1698 part of the antiviral response of infected and bystander cells. HIV infection does appear to  
1699 alter expression and localization of some splicing factors<sup>433,500</sup>. In addition, we saw a large  
1700 reduction in the abundance of mRNA from nonsense-mediated decay related genes, perhaps  
1701 indicating that RNA surveillance is loosened thus allowing more unspliced or aberrantly  
1702 spliced transcripts. Alternatively, fully spliced mRNAs might be more rapidly degraded after  
1703 infection, possibly by interferon-mediated induction of RNaseL<sup>540</sup>. A speculative possibility

1704 is that HIV<sub>89.6</sub> encodes a factor that alters cellular splicing or promotes mRNA degradation  
1705 to optimize splicing and translation of viral messages.

1706 Infection resulted in increased expression of specific cellular repeated sequences. HERVs, in  
1707 particular HERV-K, have previously been observed to show increased RNA accumulation with  
1708 HIV infection<sup>501–503,541</sup> and possibly represent vaccine targets because of their production of  
1709 distinctive proteins<sup>507,541–545</sup>. Here, though we saw modest increases in HERV-K expression,  
1710 ERV-9 had the greatest change in expression (33 LTR12C and 14 ERV-9 annotated regions  
1711 with greater than 4× change in expression). Previous RNA-Seq studies of HIV infection in  
1712 cell lines did not report increases in HERV expression<sup>319,473</sup> but this difference is likely due  
1713 to a much higher baseline expression of HERVs in transformed cell lines. We also observed  
1714 increases in LINE and Alu element transcription, as has been reported previously<sup>504</sup>, and  
1715 expression changes in ERV-9/LTR12C expression associated with transcription factor motifs  
1716 and U3 variants.

1717 Many of the repeated sequence elements that were induced by HIV<sub>89.6</sub> infection are relatively  
1718 recently integrated in the human genome. The reason for this pattern is unclear. It may  
1719 be that older elements have accumulated more mutations, resulting in an inactivation of  
1720 transcriptional signals. Alternatively, perhaps the elements that are induced have been  
1721 recruited for transcriptional control of cellular functions, so that their transcriptional activity  
1722 is preserved evolutionarily<sup>484,546,547</sup>.

1723 Comparison of results of sequencing HIV<sub>89.6</sub> messages using long-read single molecule  
1724 sequencing (Pacific Biosciences) and dense short read sequencing (Illumina data reported  
1725 here) allowed a full quantitative accounting of more than 70 HIV<sub>89.6</sub> splice forms. The full  
1726 length unspliced HIV RNA comprised 37.6% of all messages, corresponding to about 2000  
1727 genomes per cell. Notably abundant messages included those encoding Nef (D1-A5-D4-A7:  
1728 15.5%) and two Rev-encoding transcripts (D1-A4c-D4-A7: 4.2%, D1-A4b-D4-A7: 3.1%).  
1729 The full set of messages is summarized in Figure 4.7B. Our previous analysis revealed an  
1730 unusually prominent 1 kb size class. HIV<sub>89.6</sub> encodes a rare splice acceptor (A8c) within Nef

1731 responsible for formation of the short messages. Our data indicated that two members of the  
1732 1-kb size class, D1-A5-D4-A8c and D1-A8c, accounted for 10.6% and 4.9% of all messages.  
1733 The 1 kb size class as a whole accounted for fully 20% of messages. Most HIV/SIV variants  
1734 appear to encode an acceptor near this position, suggesting a potential unknown function  
1735 for these short spliced forms<sup>406,414,418</sup>.

1736 After filtering, we detected a sizeable number of apparently authentic chimeras containing  
1737 both HIV and cellular sequences, allowing comparison to examples of host-cell modification  
1738 by integration. Mechanisms of insertional activation have been studied intensively in animal  
1739 models of transformation and in adverse events in human gene therapy. One of the most  
1740 common mechanisms involves insertion of a retroviral enhancer near a cellular promoter,  
1741 so that the rate of initiation is increased and normal cellular messages are increased in  
1742 abundance. However, another common mechanism involves formation of chimeric messages  
1743 involving both cellular and viral/vector sequences. In HIV infection, examples of insertion  
1744 in the Bach2 and MKL2 genes have been associated with long term persistence of particular  
1745 cell clones<sup>516–519</sup>. In these cells, proviruses were integrated within the cellular transcription  
1746 unit, and the transcriptional direction of the integrated provirus was the same as that of  
1747 Bach2 or MKL2. This would allow formation of a fusion of the 5' HIV sequences with 3'  
1748 Bach2 sequences, potentially involving the most common events seen here (either 3' read out  
1749 or splicing from HIV D4 to a cellular exon). However, a closely studied example of clonal  
1750 expansion in a successful lentiviral vector gene therapy for beta-thalassemia was associated  
1751 with expansion of a cell clone harboring an integrated vector within the transcription unit  
1752 of HMGA2. In this case the message spliced into the vector and terminated, removing  
1753 a negative regulatory sequence normally present in the 3' end HMGA2 message<sup>523</sup>. A  
1754 targeted study in vitro of chimeric message formation by lentiviral vectors showed examples  
1755 of multiple types of read-in and -out and splice-in and -out<sup>525</sup>, which may have been more  
1756 frequent and more varied than for HIV<sup>89.6</sup> proviruses studied here. The lack of splicing or  
1757 reading into HIV in this study may be a reflection of the high rate HIV transcription in  
1758 these infected cells—because HIV was so highly expressed, there would be more opportunities

1759 for polymerase to splice out of or read through the HIV genome than to read or splice in.  
1760 The vast majority of HIV proviruses in expanded clones in well-suppressed patients now  
1761 appear to be defective<sup>519</sup>—going forward, it will be of interest to investigate whether these  
1762 HIV proviruses are damaged in ways that promote formation of chimeric transcripts.

1763 Lastly, we note that several features of the transcriptional response to HIV<sub>89.6</sub> infection were  
1764 suggestive of de-differentiation away from T cell specific expression patterns. The increase  
1765 in expression of cellular HERVs and LINEs is characteristic of cells in early development.  
1766 Specific HERVs and transposons, including ERV-9/LTR12C and HERV-K, have been  
1767 implicated in regulating gene activity early in development<sup>484,546,548–551</sup>. Several genes  
1768 related to other hematopoietic cell types showed elevated RNA abundance after HIV<sub>89.6</sub>  
1769 infection. These data are of interest given the finding that patients undergoing long term  
1770 ART can contain long lived T cell clones that may contribute to the latent reservoir<sup>519,552–555</sup>.  
1771 Possibly the transcriptional responses seen in infected primary T cells here are reflective  
1772 of processes leading to formation of the long-lived latently-infected cells with stem-like  
1773 properties.

#### 1774 4.6 Conclusions

1775 Infections of primary T cells with a low passage HIV isolate show several distinctive features  
1776 compared with previously published data using T cell lines and/or lab-adapted HIV strains.  
1777 We found strong changes in expression in genes related to immune response and apoptosis  
1778 similar to studies of HIV infection in patient samples and primary cells but different from  
1779 studies performed in SupT1 cell lines. Notable changes after infection included intron  
1780 retention and activation of recently integrated retrotransposons and endogenous retroviruses,  
1781 in particular LTR12C/ERV-9. We also present complete absolute estimation of over 70  
1782 messages from HIV<sub>89.6</sub> and specify the major virus-host chimeras as read out from the 3'  
1783 end of the provirus and splicing from viral splice donor 4 to cellular acceptors.

1784 **4.7 Availability of supporting data**

1785 RNA-Seq reads from this study are available at the Sequence Read Archive under accession  
1786 number SRP055981. The integration site data is available at the Sequence Read Archive  
1787 under accession number SRP057555.

1788 **4.8 Acknowledgements**

1789 We would like to thank the University of Pennsylvania Center for AIDS Research (P30  
1790 AI045008) for preparation of viral stocks and isolation of primary CD4<sup>+</sup> T cells; Ronald  
1791 G. Collman and members of the Bushman laboratory for reagents, helpful discussion and  
1792 technical expertise. This work was funded by NIH grant R01 AI052845, the HIV Immune  
1793 Networks Team (HINT) consortium P01 AI090935 and NRSA computational genomics  
1794 training grant T32 HG000046.

1795  
1796  
1797

## CHAPTER 5: A reverse transcription loop-mediated isothermal amplification assay optimized to detect multiple HIV subtypes

This chapter was originally published as:

KE Ocwieja\*, S Sherrill-Mix\*, C Liu, J Song, H Bau and FD Bushman. 2015. A reverse transcription loop-mediated isothermal amplification assay optimized to detect multiple HIV subtypes. *PLoS One*, 10:e0117852. doi: 10.1371/journal.pone.0117852

1798

KE Ocwieja and I were joint first authors. KE Ocwieja, C Liu, H Bau, FD Bushman and I conceived the experiments. KE Ocwieja and I designed the assay. KE Ocwieja, C Liu and J Song performed the experiments. KE Ocwieja, J Song and I analyzed the data. I produced the figures. KE Ocwieja, C Liu, H Bau, FD Bushman and I wrote the paper.

Supporting information are available at <http://journals.plos.org/plosone/article?id=10.1371/journal.pone.0117852#sec011>

1799

### 5.1 Abstract

Diagnostic methods for detecting and quantifying HIV RNA have been improving, but efficient methods for point-of-care analysis are still needed, particularly for applications in resource-limited settings. Detection based on reverse-transcription loop-mediated isothermal amplification (RT-LAMP) is particularly useful for this, because when combined with fluorescence-based DNA detection, RT-LAMP can be implemented with minimal equipment and expense. Assays have been developed to detect HIV RNA with RT-LAMP, but existing methods detect only a limited subset of HIV subtypes. Here we report a bioinformatic study to develop optimized primers, followed by empirical testing of 44 new primer designs. One primer set (ACeIN-26), targeting the HIV integrase coding region, consistently detected subtypes A, B, C, D, and G. The assay was sensitive to at least 5000 copies per reaction for

1810 subtypes A, B, C, D, and G, with Z-factors of above 0.69 (detection of the minor subtype F  
1811 was found to be unreliable). There are already rapid and efficient assays available for detecting  
1812 HIV infection in a binary yes/no format, but the rapid RT-LAMP assay described here has  
1813 additional uses, including 1) tracking response to medication by comparing longitudinal  
1814 values for a subject, 2) detecting of infection in neonates unimpeded by the presence of  
1815 maternal antibody, and 3) detecting infection prior to seroconversion.

## 1816 **5.2 Introduction**

1817 Despite the introduction of efficient antiretroviral therapy, HIV infection and AIDS continue  
1818 to cause a worldwide health crisis<sup>557</sup>. Methods for detecting HIV infection have improved  
1819 greatly with time<sup>558</sup>—today rapid assays are available that can detect HIV infection in a  
1820 yes-no format using a home test kit that detects antibodies in saliva. Viral load assays that  
1821 quantify viral RNA with quick turn-around time are widely available in the developed world.  
1822 However, quantitative viral load assays are not commonly available with actionable time  
1823 scales in much of the developing world. This motivates the development of new rapid and  
1824 quantitative assays that can be used at the point of care with minimal infrastructure<sup>559,560</sup>.

1825 One simple and quantitative detection method involves reverse transcription-based loop  
1826 mediated isothermal amplification (RT-LAMP)<sup>561</sup>. In this method, a DNA copy of the viral  
1827 RNA is generated by reverse transcriptase, and then isothermal amplification is carried out to  
1828 increase the amount of total DNA. Primer binding sites are chosen so that a series of strand  
1829 displacement steps allow continuous synthesis of DNA without requiring thermocycling.  
1830 Reaction products can be detected by adding an intercalating dye to reaction mixtures  
1831 that fluoresces only when bound to DNA, allowing quantification of product formation by  
1832 measurement of fluorescence intensity. Such assays can potentially be packaged in simple  
1833 self-contained devices and read out with no technology beyond a cell phone.

1834 RT-LAMP assays for HIV-1 have been developed previously and reported to show high  
1835 sensitivity and specificity for subtype B, the most common HIV strain in the developed

world<sup>560,562,563</sup>. Another recent study reported RT-LAMP primer set optimized for the detection of HIV variants circulating in China<sup>564</sup>, and another on confirmatory RT-LAMP for group M viruses<sup>565</sup>. Assays have also been developed for HIV-2<sup>566</sup>. A complication arises in using available RT-LAMP assays due to the variation of HIV genomic sequences among the HIV subtypes<sup>567,568</sup>, so that an RT-LAMP assay optimized for one viral subtype may not detect viral RNA of another subtype<sup>569</sup>. Tests presented below show that many RT-LAMP assays are efficient for detecting subtype B, for which they were designed, but often performed poorly on other subtypes. Subtype C infects the greatest number of people worldwide, including in Sub-Saharan Africa, where such RT-LAMP assays would be most valuable, motivating optimization for subtype C. Several additional non-B subtypes are also responsible for significant burdens of disease world-wide<sup>570</sup>.

Here we present the development of an RT-LAMP assay capable of detecting HIV-1 subtypes A, B, C, D, and G. We first carried out a bioinformatic analysis to identify regions conserved in all the HIV subtypes. We then tested 44 different combinations of RT-LAMP primers targeting this region in over 700 individual assays, allowing identification of a primer set (ACeIN-26) that was suitable for detecting these subtypes. We propose that the optimized RT-LAMP assay may be useful for quantifying HIV RNA copy numbers in point-of-care applications in the developing world, where multiple different subtypes may be encountered.

### 5.3 Methods

#### 5.3.1 Viral strains used in this study

Viral strains tested included HIV-1 92/UG/029 (Uganda) (subtype A, NIH AIDS Reagent program reagent number 1650), HIV-1 THRO (subtype B, plasmid derived, University of Pennsylvania CFAR)<sup>571</sup>, CH269 (subtype C, plasmid derived, University of Pennsylvania CFAR)<sup>571</sup>, UG0242 (subtype D, University of Pennsylvania CFAR), 93BRO20 (subtype F, University of Pennsylvania CFAR), HIV-1 G3 (subtype G, NIH AIDS Reagent program reagent number 3187)<sup>572</sup>.

1862 Viral stocks were prepared by transfection and infection. Culture supernatants were cleared  
1863 of cellular debris by centrifugation at 1500g for 10 min. The supernatant containing virus  
1864 was then treated with 100 U DNase (Roche) per 450 uL virus for 15 min at 30°C. RNA was  
1865 isolated using the QiaAmp Viral RNA mini kit (Qiagen GmbH, Hilden, Germany). RNA  
1866 was eluted in 80 uL of the provided elution buffer and stored at -80°C.

1867 Concentration of viral RNA copies was calculated from p24 capsid antigen capture assay  
1868 results provided by the University of Pennsylvania CFAR or the NIH AIDS-reagent program.  
1869 In calculating viral RNA copy numbers, we assumed that all p24 was incorporated in virions,  
1870 all RNA was recovered completely from stocks, 2 genomes were present per virion, 2000 p24  
1871 molecules per viral particle, and the molecular weight of HIV-1 p24 was 25.6 kDa.

1872 **5.3.2 Assays**

1873 RT-LAMP reaction mixtures (15  $\mu$ L) contained 0.2  $\mu$ M each of primers F3 and B3 (if a  
1874 primer set used multiple B3 primers, mixture contained 0.2  $\mu$ M of each); 1.6  $\mu$ M each of FIP  
1875 and BIP primers (if a primer set had multiple FIP primes, reaction mixture contained 0.8  
1876  $\mu$ M of each FIP primer); and 0.8  $\mu$ M each of LoopF and LoopB primers; 7.5  $\mu$ L OptiGene  
1877 Isothermal Mastermix ISO-100nd (Optigene, UK), ROX reference dye (0.15  $\mu$ L from a 50X  
1878 stock), EvaGreen dye (0.4  $\mu$ L from a 20X stock; Biotium, Hayward, CA); HIV RNA in 4.7  
1879  $\mu$ L; AMV reverse transcriptase (10U/ $\mu$ L) 0.1  $\mu$ L and water to 15  $\mu$ L In most cases where  
1880 two primer sets were combined, the total primer concentration within the reaction was  
1881 doubled such that the above individual primer molarities were maintained. For the mixture  
1882 ACeIN-26+F-IN (S2 Table, line 46), the total primer concentration was not doubled—the  
1883 F-IN primer set comprised 25% of the total primer concentration, and the ACeIN-26 primer  
1884 set comprised 75% of the total primer concentration with the ratios of primers listed above  
1885 preserved. This mixture was combined 1:1 with the ACe-PR primer set (S2 Table, line 47)  
1886 such that total primer concentration in the final mixture was doubled.

1887 Amplification was measured using the 7500-Fast Real Time PCR system from Applied

1888 Biosystems with the following settings: 1 minute at 62°C; 60 cycles of 30 seconds at 62°C  
1889 and 30 seconds at 63°C. Data was collected every minute. Product structure was assessed  
1890 using dissociation curves which showed denaturation at 83°C. Products from selected  
1891 amplification reactions were analyzed by agarose gel electrophoresis and showed a ladder of  
1892 low molecular weight products (data not shown).

1893 Product synthesis was quantified as the cycle of threshold for 10% amplification. Z-factors<sup>573</sup>  
1894 were calculated from tests of 24 replicates using the ACeIN26 primer set in assays with viral  
1895 RNA of each subtype. No detection after 60 min was given a value of 61 min in the Z-factor  
1896 calculation.

## 1897 5.4 Results

### 1898 5.4.1 Testing published RT-LAMP primer sets against multiple HIV subtypes

1899 We first assessed the performance of existing RT-LAMP assays on RNA samples from  
1900 multiple HIV subtypes. We obtained viral stocks from HIV subtypes A, B, C, D, F, and  
1901 G, estimated the numbers of virions per ml, and extracted RNA. RNAs were mixed with  
1902 RT-LAMP reagents which included the six RT-LAMP primers, designated F3, B3, FIP, BIP,  
1903 LF and LB<sup>561</sup>. Reactions also contained reverse transcriptase, DNA polymerase, nucleotides  
1904 and the intercalating fluorescent EvaGreen dye, which yields a fluorescent signal upon DNA  
1905 binding. DNA synthesis was quantified as the increase in fluorescence intensity over time,  
1906 which yielded a typical curve describing exponential growth with saturation (examples are  
1907 shown below). Results are expressed as threshold times ( $T_t$ ) for achieving 10% of maximum  
1908 fluorescence intensity at the HIV RNA template copy number tested.

1909 In initial tests, published primer sets targeting the HIV-1 subtype B coding regions for  
1910 capsid (CA), protease (PR), and reverse transcriptase (RT) (named B-CA, B-PR and B-RT)  
1911 were assayed in reactions with RNAs from four of the subtypes. Results with each primer set  
1912 tested are shown in Figure 5.1 in heat map format, where each tile summarizes the results of  
1913 tests of 5000 RNA copies. Primers and their groupings into sets are summarized in S1 and

1914 S2 Tables, average assay results are in S3 Table, and raw assay data is in S4 Table. Assays  
1915 (Figure 5.1, top) with the B-CA, B-PR and B-RT primer sets detected subtypes B and D  
1916 at 5000 RNA copies with threshold times less than 20 min. However, assays with B-CA  
1917 and B-RT detected subtypes C and F with threshold times > 50 min, indicating inefficient  
1918 amplification and the potential for poor separation between signal and noise. B-PR did  
1919 not detect subtype C at all. In an effort to improve the breadth of detection, we first tried  
1920 mixing the B-PR primers, which detected clade F (albeit with limited efficiency) with the  
1921 B-CA and B-RT primers (Figure 5.1 and S3 and S4 Tables). In neither case did this provide  
1922 coverage of all four clades tested. We thus did not test these primer sets on RNAs from the  
1923 remaining subtypes and instead sought to develop primer sets targeting different regions of  
1924 the HIV genome.

1925 **5.4.2 Primer design strategy**

1926 To design primers that detected multiple HIV subtypes efficiently, we analyzed alignments  
1927 of HIV genomes (downloaded from the Los Alamos National Laboratory site<sup>567</sup>) for regions  
1928 with similarity across most viruses, revealing that a segment of the pol gene encoding  
1929 IN was particularly conserved (Figure 5.2A). A total of six primers are required for each  
1930 RT-LAMP assay<sup>561</sup>. We used the EIKEN primer design tool to identify an initial primer set  
1931 targeting this region. In further analysis, positions in the alignments were identified within  
1932 primer landing sites that commonly contained multiple different bases. Primer positions  
1933 were manually adjusted to avoid these bases when possible, and when necessary mixtures  
1934 were formulated containing each of these commonly occurring bases (S1 and S2 Tables).  
1935 An extensive series of variants targeting the IN coding region was tested empirically in  
1936 assays containing RNAs from multiple subtypes (5000 RNA copies per reaction, over 700  
1937 total assays; S3 and S4 Tables). Based on initial results, primers were further modified by  
1938 adjusting the primer position or addition of locked nucleic acids as described below.

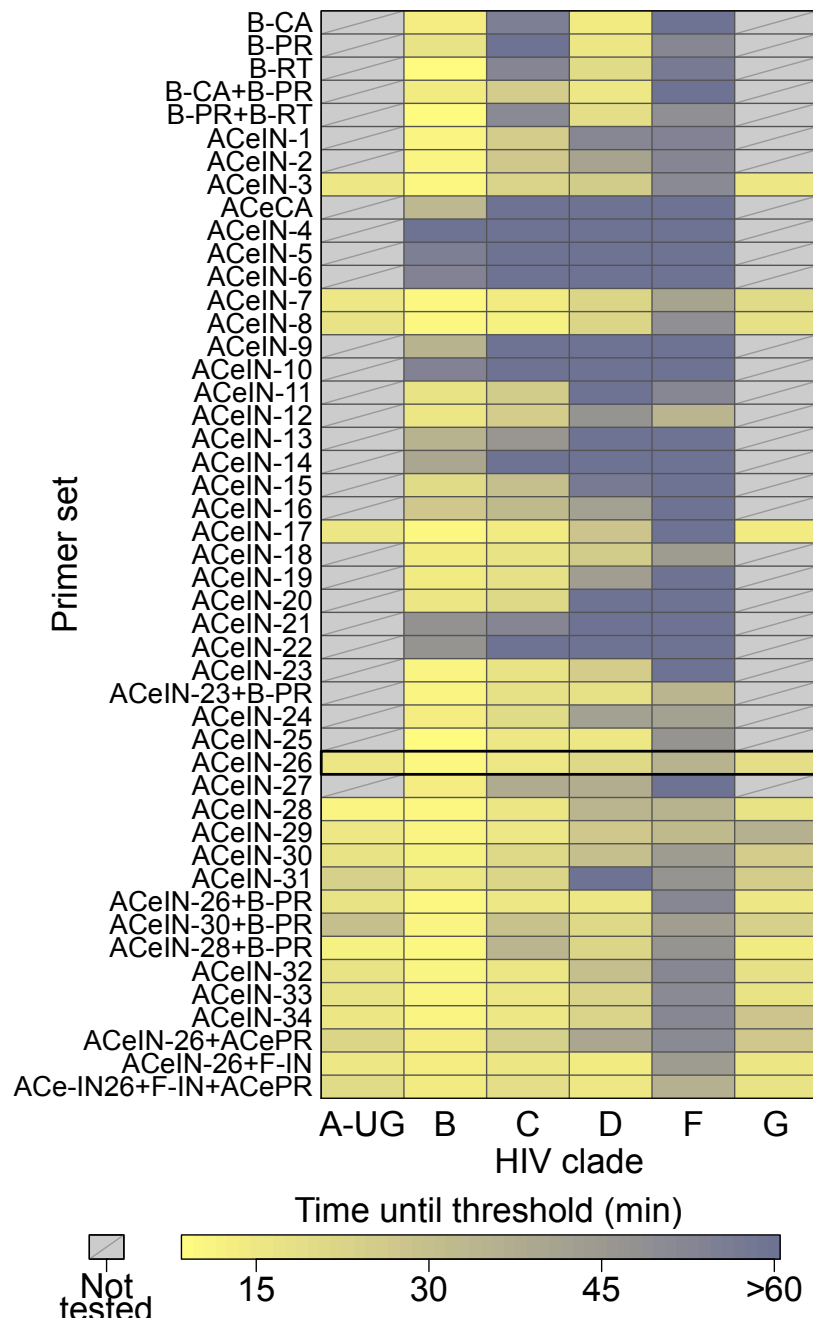


Figure 5.1: Summary of amplification results for all the RT-LAMP primer sets tested in this study. The data is shown as a heat map, with more intense yellow coloring indicating shorter amplification times (key at bottom). Primer sets tested are named along the left of the figure. Primer sequences, and their organization into LAMP primer sets, are catalogued in S1 and S2 Tables. The raw data and averaged data are collected in S3 and S4 Tables. ACeIN-26 primer set (highlighted) had one of the best performances across the subtypes and a relatively simple primer design.

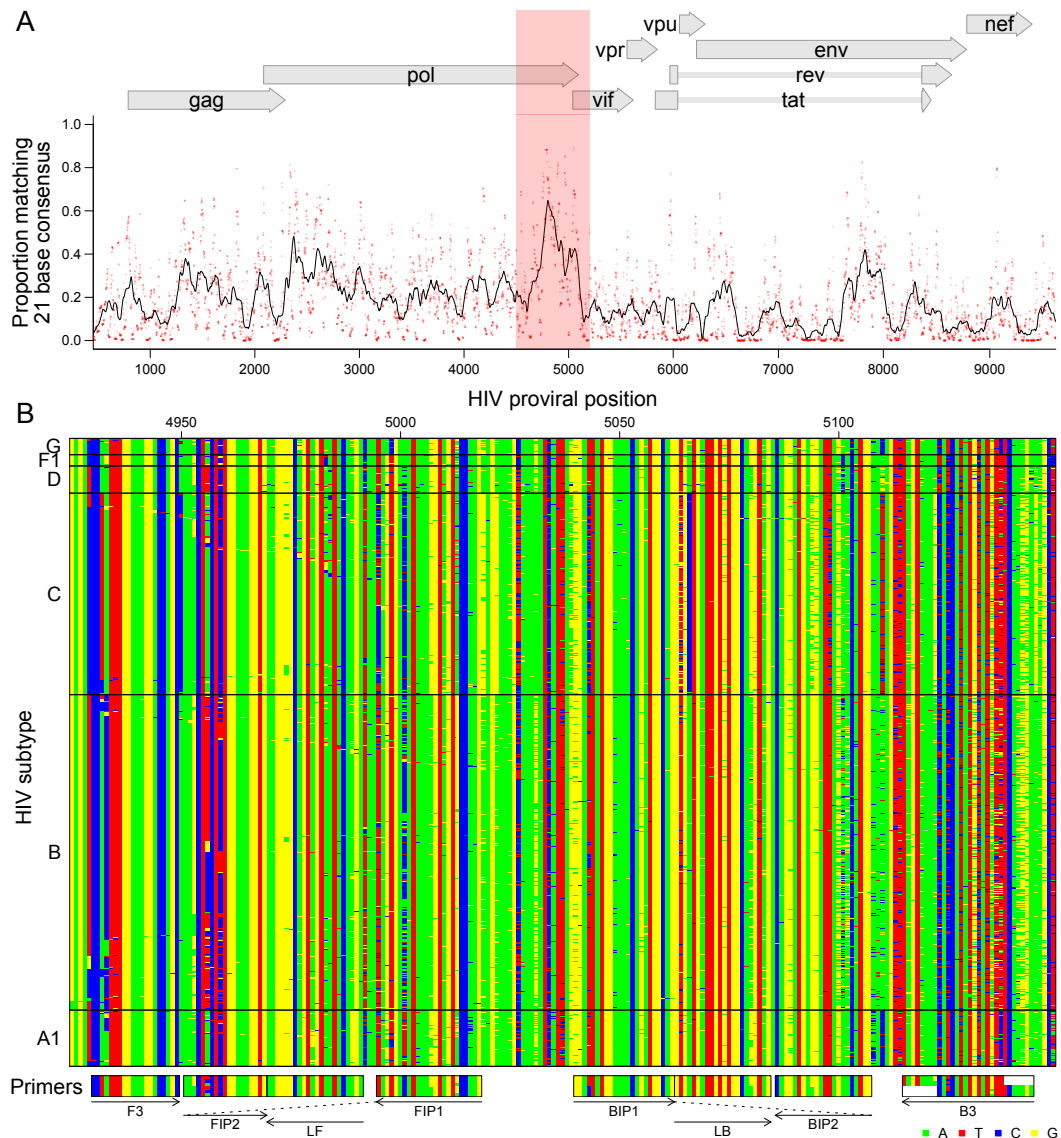


Figure 5.2: Bioinformatic analysis to design subtype-agnostic RT-LAMP primers. A) Conservation of sequence in HIV. HIV genomes ( $n = 1340$ ) from the Los Alamos National Laboratory collection were aligned and conservation calculated. The x-axis shows the coordinate on the HIV genome, the y-axis shows the proportion of sequences matching the consensus for each 21 base segment of the genome (red points). The black line shows a 101 base sliding average over these proportions. The vertical red shading shows the region targeted for LAMP primer design that was used as input into the EIKEN primer design tool. Numbering is relative to the HIV<sub>89.6</sub> sequence. B) Aligned genomes, showing the locations of the ACeIN-26 primers. Sequences are shown with DNA bases color-coded as shown at the lower right. Each row indicates an HIV sequence and each column a base in that sequence. Horizontal lines separate the HIV subtypes (labeled at left). Arrows indicate the strand targeted by each primer. Primers targeting the negative strand of the virus are shown as reverse compliments for ease of viewing.

1939    **5.5 Testing different primer designs**

1940    Our first design, ACeIN-1 (“ACe” for “All Clade” and “IN” for “integrase”), targeted the  
1941    HIV IN coding region and contained multiple bases at selected sites to broaden detection  
1942    (Figure 5.1). ACeIN-2 and-3 have primers (B3) with slightly different landing sites. Tests  
1943    showed that the mixture of primers allowed amplification with a shorter threshold time than  
1944    did either alone (Figure 5.1).

1945    We also tried to design a new primer set to the CA coding region (Figure 5.1, ACeCA)  
1946    but found that the set only amplified clade B, and not efficiently. Thus this design was  
1947    abandoned.

1948    ACeIN-3 through-6 were altered by inserting a polyT sequence between the two different  
1949    sections of FIP and BIP in various combinations, a modification introduced with the goal of  
1950    improving primer folding, but these designs performed quite poorly (Figure 5.1).

1951    Because the FIP primer appeared to bind the region with most variability among clades, we  
1952    tried variations that bound to several nearby regions. These were tried with and without  
1953    the polyT containing BIP and FIP primers in various combinations (Figure 5.1, ACeIN-7  
1954    through-22). We also tried mixing all of the variations of FIP together (ACeIN-23; S2 Table).  
1955    The ACeIN-23 primer set was tried as a mixture with the B-PR set to try to capture clade  
1956    F, yielding a relatively effective primer set (Figure 5.1, ACeIN-23+B-PR).

1957    In an effort to increase affinity, an additional G/C pair was added to F3 and tested with  
1958    various other IN primers (Figure 5.1, ACeIN-24 through-31). Testing showed improvement,  
1959    with ACeIN-26 showing particularly robust amplification.

1960    In a second effort to increase primer affinities, we substituted locked nucleic acids (LNAs) for  
1961    selected bases that were particularly highly conserved among subtypes (Figure 5.1, ACeIN-30,  
1962    -31, -32, -33, and-34). Some improvement was shown over the non-LNA containing bases.  
1963    However, the ACeIN-26 primer set was as effective as or better than any LNA containing

1964 primer sets.

1965 In further tests, the ACeIN-26, -28 and-30 primers were tested combined with the ACePR  
1966 primer set (a slightly modified version of the B-PR primer set, S2 Table, row 2, designed  
1967 to accommodate a wider selection of HIV-1 subtypes) but no improvement was seen and  
1968 efficiency may even have fallen for some subtypes. We also designed a primer set that  
1969 matched exactly to the targeted sequences found in the problematic subtype F, and mixed  
1970 this set with the ACeIN-26 primers. However, no improvement was seen (Figure 5.1, mixtures  
1971 with F-IN set). Mixing the ACeIN-26 primers with both the ACePR and F-specific primers  
1972 did yield effective primer sets (Figure 5.1, ACeIN26+F-IN and ACeIN26+F-IN+ACePR).  
1973 However, amplification efficiency was not greatly improved over the ACeIN-26 primer set, so  
1974 we proceeded with the simpler ACeIN-26 primer set (Figure 5.2B) in further studies.

1975 **5.5.1 Performance of the optimized RT-LAMP assay**

1976 The ACeIN-26 RT-LAMP primer set was next tested to determine the minimum concentration  
1977 of RNA detectable under the reaction conditions studied (Figure 5.3). RNA template amounts  
1978 were titrated and time to detection quantified. Tests showed detection after less than 20  
1979 min of incubation for 50 copies of subtypes A or B, detection after less than 30 min for 5000  
1980 copies for C, D, and G, and detection after less than 20 min for 50,000 copies for F.

1981 For clinical implementation the reliability of an assay is critical. This is commonly sum-  
1982 marized as a Z-factor<sup>573</sup>, which takes into account both the separation in means between  
1983 positive and negative samples and the variance in measurement of each. An assay with  
1984 a Z-factor above 0.5 is judged to be an excellent assay. Z-factors for detection of each of  
1985 the subtypes at 5000 RNA copies per reaction were > 0.50 for subtypes A, B, C, D, and  
1986 G, respectively (Figure 5.4, n = 24 replicates per test). Detection of subtype F at 5000  
1987 copies per reaction was sporadic, showing a much lower Z-factor. Therefore our ACeIN-26  
1988 RT-LAMP primer set appears well suited to detect 5000 copies of subtypes A, B, C, D and  
1989 G.

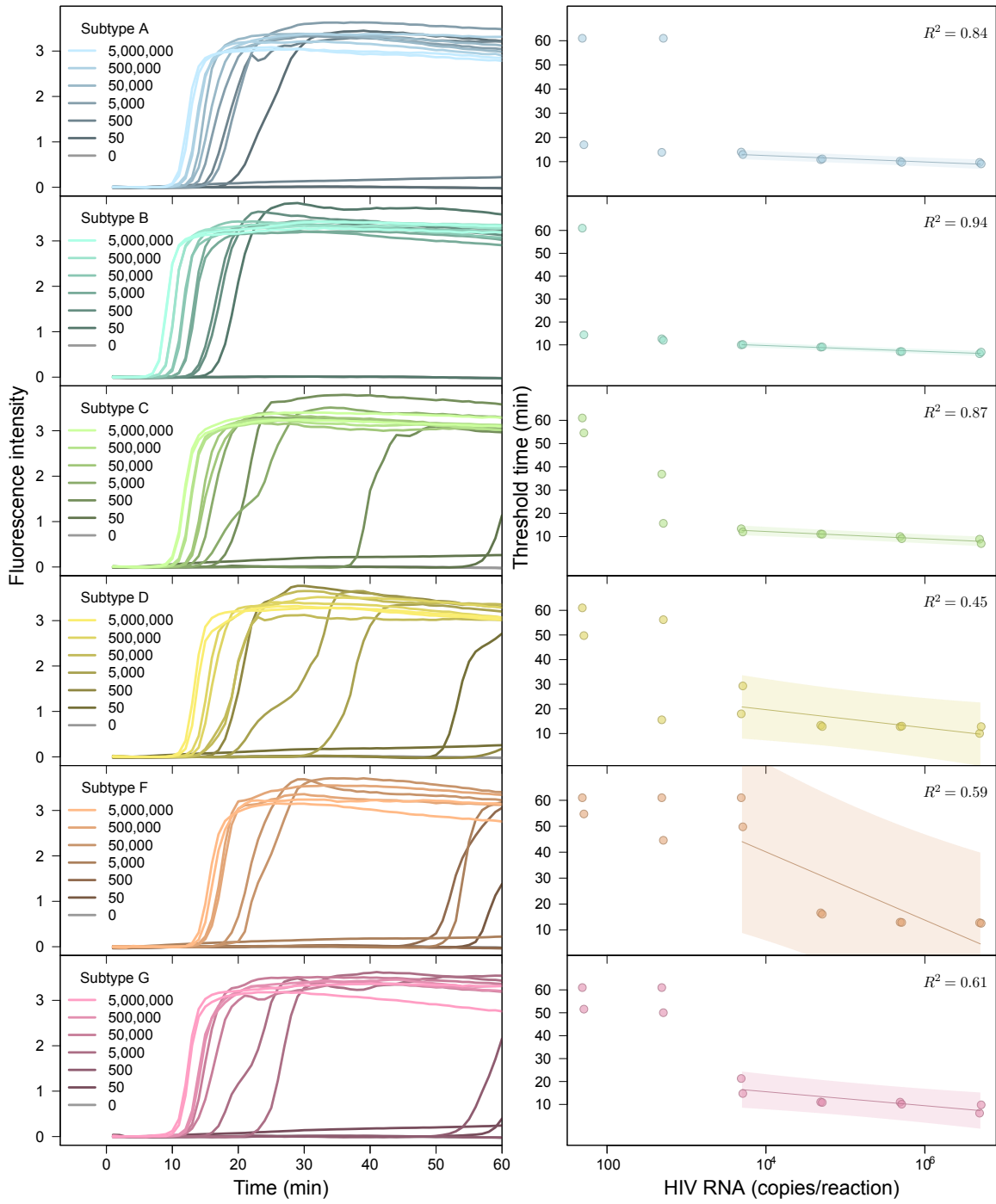


Figure 5.3: Performance of the AceIN-26 primer set with different starting RNA concentrations. Tests of each subtype are shown as rows. In each lettered panel, the left shows the raw accumulation of fluorescence signal (y-axis) as a function of time (x-axis); the right panel shows the threshold time (y-axis) as a function of log RNA copy number (x-axis) added to the reaction. In the right hand panels, values were dithered where two points overlapped to allow visualization of both.

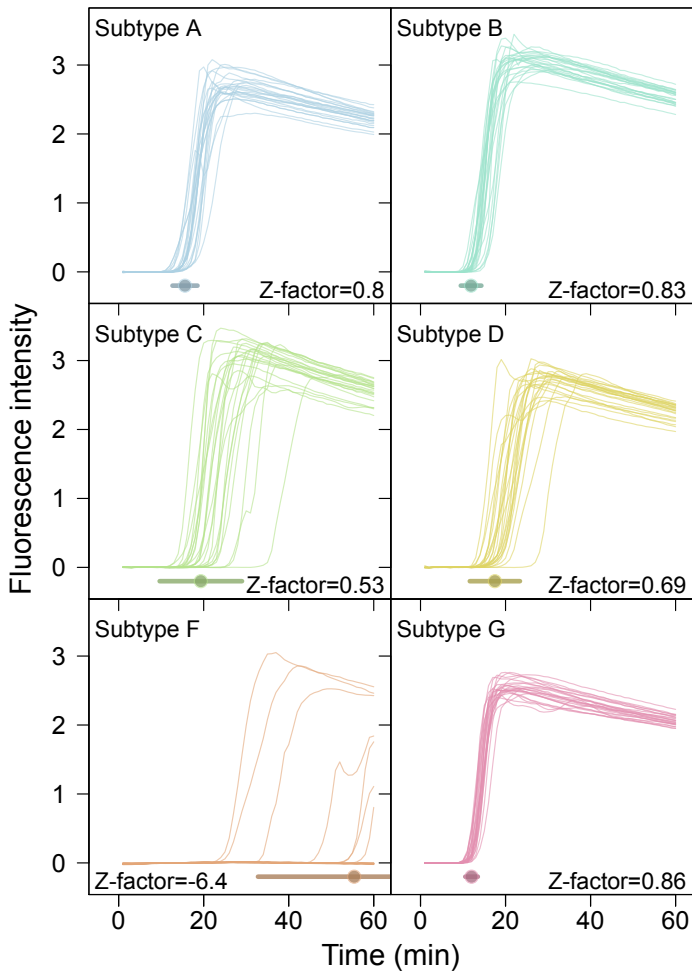


Figure 5.4: Examples of time course assays, displaying replicate tests of RT-LAMP primer set ACeIN-26 tested over six HIV subtypes, used in Z-factor calculations. A total of 5000 RNA copies were tested in each 15  $\mu$ L reaction. Time is shown on the x-axis, Fluorescence intensity on the y-axis. Replicates are distinguished using an arbitrary color code. Z-factor values and standard deviations are shown on each panel.

1990 **5.6 Discussion**

1991 Here we present an RT-LAMP assay optimized to identify multiple HIV subtypes. Infections  
1992 with subtype B predominate in most parts of the developed world, but elsewhere other  
1993 subtypes are more common<sup>570</sup>. Thus nucleic acid-based assays for use in the developing  
1994 world need to query HIV subtypes more broadly. Previously reported RT-LAMP assays,  
1995 while effective at detecting subtype B, commonly showed poor ability to detect at least some  
1996 of the HIV subtypes, including C, which is common in the developing world (Figure 5.1).  
1997 Here we first carried out an initial bioinformatic survey to identify regions conserved across  
1998 all HIV subtypes that could serve as binding sites for RT-LAMP primers. We then tested  
1999 primer sets targeting these regions empirically for efficiency. Testing 44 different primer  
2000 sets revealed that assays containing ACeIN-26 were effective in detecting 5000 copies of  
2001 RNA from subtypes A, B, C, D, and G within 30 minutes of incubation. For these five  
2002 subtypes, the times of incubation to reach the threshold times were not too different, which  
2003 simplifies interpretation when the subtype in the sample is unknown. Regardless of the  
2004 efficiency, these assays can be applied to longitudinal studies of changes in viral load within  
2005 an individual. We propose that RT-LAMP assays based on the ACeIN-26 primer set can be  
2006 useful world-wide for assaying HIV-1 viral loads in infected patients.  
2007 There are several limitations to our study. Subtypes A, B, C, D, and G were detected  
2008 efficiently and showed Z-factors above 0.5, but subtype F was detected reliably only with  
2009 higher template amounts, probably due to more extensive mismatches with the ACeIN-26  
2010 primer set. Subtype F is estimated, however, to comprise only 0.59% of all infections  
2011 globally<sup>570</sup>, though it is common in some regions. For many of the common circulating  
2012 recombinant forms, such as AE and BC, the target site for ACeIN-26 is from a subtype  
2013 known to be efficiently detected, though in some cases the efficiency of detection is not easy  
2014 to predict and will need to be tested. We did not test subtypes beyond A, B, C, D, F and  
2015 G, and we did not attempt to assess multiple different variants within each subtype. Thus,  
2016 while we do know that our RT-LAMP assays are more widely applicable than many of those

2017 reported previously, we do not know whether they are able to detect all strains efficiently. In  
2018 addition, although we carried out more than 700 assays in this study, there remain multiple  
2019 parameters that could be optimized further, such as primer concentrations, salt type and  
2020 concentration, temperature, and divalent metal concentrations, so there are likely further  
2021 opportunities for improvement. Also, possible effects of RNA quality on assay performance  
2022 were not tested rigorously.

2023 A particularly important parameter for further optimization is primer sequence. Several  
2024 groups have recently published primer sets optimized for broad detection of different HIV  
2025 lineages<sup>564,565</sup>, offering opportunities for creating sophisticated primer blends with increased  
2026 breadth of detection. However, in developing such mixtures, it will be important to monitor  
2027 for possible complicating interactions of primers with each other. As an example of ongoing  
2028 development of mixtures, we found that addition of another primer to the ACeIN-26 set  
2029 that was matched to a common subtype C lineage allowed improved detection of subtype C  
2030 variants (S1 Report). In order to improve detection of subtype F, which was suboptimal with  
2031 ACeIN-26, additional primer sets could be mixed to specifically target subtype F, though  
2032 the ones we tried so far did not work well. It will be useful to explore the performance of  
2033 broader primer mixtures in future work.

2034 Today rapid assays are available that can report infection efficiently, for example by detecting  
2035 anti-HIV antibodies in oral samples—however, the nucleic acid-based method presented here  
2036 has additional potential uses. We envision combining the RT-LAMP assay with simple  
2037 point-of-care devices for purifying blood plasma<sup>559</sup> and quantitative analysis of accumulation  
2038 of fluorescent signals<sup>574</sup>. In one implementation of the technology, cell phones could be used  
2039 to capture and analyze results, thereby minimizing equipment costs. Point-of-care devices are  
2040 available facilitating the concentration of viral RNA from blood plasma or saliva<sup>574</sup> to allow  
2041 the detection of the 1000 RNA copy threshold that the WHO defines as virological treatment  
2042 failure (World Health Organization, Consolidated ARV guidelines, June 2013). Together,  
2043 these methods will allow assessment of parameters beyond just the presence/absence of

2044 infection. Quantitative RT-LAMP assays should allow tracking of responses to medication,  
2045 detection in neonates (where immunological tests are confounded by presence of maternal  
2046 antibody), and early detection before seroconversion.

2047 **5.7 Acknowledgments**

2048 We are grateful to members of the Bushman and Bau laboratory for help and suggestions.

## CHAPTER 6: Conclusions and future directions

2050 In this dissertation, we described studies characterizing HIV-1 latency, expression and  
2051 alternative splicing and host cell response to infection. We then developed point-of-care  
2052 methods for the detection of infection and quantification of viral load. These projects suggest  
2053 many avenues for continuing research.

### 2054 6.1 Latency and integration location

2055 In Chapter 2, we showed that the chromosomal location of integration affects proviral latency  
2056 but the mechanisms appear to differ between cell culture models. Similarly a recent study  
2057 of nine cell culture models found that no single model reliably predicted the performance of  
2058 activating compounds in *ex vivo* tests of latently infected cells from HIV patients<sup>575</sup>. This  
2059 suggests that either some cell culture models do not accurately reflect latency in patients or  
2060 that there are diverse subsets of cells with differing mechanisms of latency within patients.

2061 Cell culture models are currently used to screen potentially therapeutic compounds<sup>148,575</sup>. If  
2062 some cell culture models are not representative of *in vivo* conditions then potential treatments  
2063 may be discarded or marked for development erroneously. Further comparisons between  
2064 additional cell culture models and additional replicates of existing models might allow  
2065 discrimination between batch/lab effects and reveal patterns between models. Comparison  
2066 with cells extracted from patients or infected lab animals might offer a gold standard  
2067 comparison although it is difficult to obtain large amounts of cells and difficult to distinguish  
2068 defective provirus from latent provirus in such populations.

2069 Various treatments are now being considered for the reactivation of latent provirus<sup>575</sup>. To  
2070 further understand the mechanisms of these treatments, it would be informative to compare  
2071 the features of latent provirus induced by a given treatment to latent viable provirus  
2072 remaining uninduced. Repeated cell sorting and integration site sequencing might provide  
2073 insight on mechanism. For example, one could first sort out cells with active provirus, then

2074 treat with the potential latency modulator and sort out cells with newly active provirus and  
2075 then treat with a strong inducer or alternative stimuli and sort out cell with newly activated  
2076 provirus. This would give subsets of cells where latent proviruses had been activated by  
2077 treatment and cells with provirus which were not activated by treatment but still inducible.  
2078 Synergies between treatments could be assessed and the location of integration sites could  
2079 be determined and used to locate patterns of genomic features correlated with induction for  
2080 each treatment.

2081 Current efforts at “shock and kill” therapy, inducing latent virus to activate and then  
2082 eliminating infected cells, focus on histone deacetylase inhibitors. If there are diverse  
2083 mechanisms of latency within patients then much of the latent reservoir may remain  
2084 unactivated by single-target therapies. Clinical trials with histone deacetylase inhibitors  
2085 have shown some small increases in viral RNA but little decrease in the latent reservoir of  
2086 HIV<sup>370,576–578</sup>. It appears that the majority of viable latent provirus from patient cells are  
2087 not reactivated by current therapies<sup>579</sup>. These results are particularly worrisome because a  
2088 functional cure for HIV will likely require a greater than 10,000-fold reduction of the latent  
2089 reservoir<sup>580</sup>.

2090 In Chapter 2, we used publicly available genomic data. Perhaps there is some chromosomal  
2091 feature with a strong association with latency but the data is not currently available or  
2092 varies greatly between cell populations. More varieties of annotations are rapidly becoming  
2093 available<sup>581–585</sup>. Decreasing sequencing costs<sup>586–588</sup> may also make it feasible to measure  
2094 more epigenetic features in the exact cell population of interest. Repeating analyses similar  
2095 to Chapter 2, perhaps by simply rerunning the reproducible report in Appendix A.2 with  
2096 new data, would allow any new features to be monitored for correlations with latency.

## 2097 **6.2 HIV-1 alternative splicing**

2098 In Chapters 3 and 4, we showed that HIV RNA spliceforms are more diverse than previously  
2099 appreciated and estimated the abundances of viral spliceforms. We also showed that splicing

2100 at some splice sites vary between host subjects, between cell types and over the course of  
2101 infection. Further characterization of viral splicing would be beneficial to the study and  
2102 treatment of HIV-1 especially as there were some technical limitations to our research that  
2103 might be improved upon using current techniques.

2104 We studied HIV splicing using droplet PCR<sup>442</sup> and a set of customized primer in Chapter  
2105 3 and bulk sequencing of cellular mRNA in Chapter 4. Sequencing biases and difficulties  
2106 determining full length transcripts from short reads hindered characterization of HIV  
2107 sequencing. One alternative to these techniques is the targeted capture and enrichment<sup>589,590</sup>  
2108 of HIV-specific sequences. Using probes targeted to conserved regions of HIV, similar to  
2109 finding conserved regions for primers as in Chapter 5, would allow for enrichment of viral  
2110 reads without the biases induced by primer-based PCR while still allowing for efficient use  
2111 of sequencing effort.

2112 The research in Chapter 3 was also limited by a short read bias in the PacBio sequencing.  
2113 PacBio sequencing has improved<sup>591</sup> and additional long read sequencers have been devel-  
2114 oped<sup>592–594</sup>. In addition, Illumina MiSeq sequencers can now produce 25 million paired 300  
2115 bp reads in a single run<sup>595,596</sup> and better spliceform estimation methods are being devel-  
2116 oped<sup>597,598</sup>. These improved sequencing techniques might allow for more straightforward  
2117 analysis of new samples and verification of our previous results.

2118 RNA transcribed antisense to the canonically expressed strand of HIV have been ob-  
2119 served<sup>473,599–604</sup>. These transcripts may be translated to proteins<sup>605,606</sup> that trigger immune  
2120 response in infected individuals<sup>604,605,607</sup>. Our sequencing techniques were designed only for  
2121 the HIV positive strand (Chapter 3) or did not preserve strand information (Chapter 4).  
2122 Strand-specific sequencing<sup>608,609</sup> of multiple HIV strains under varying cellular conditions  
2123 would clarify the identity of these transcripts.

2124 Cryptic polypeptides encoding epitopes recognized through major histocompatibility complex  
2125 type I also appear to be generated from alternative reading frames in the sense strand of

2126 the virus<sup>610,611</sup>. Ribosome profiling<sup>612–614</sup> of infected cells might reveal whether transcripts  
2127 generated through alternative splicing or antisense expression are likely to be translated.  
2128 These cryptic transcripts could offer new opportunities in vaccine design<sup>604,607,615,616</sup> but  
2129 first their abundance, identity and conservation across strains of HIV must be ascertained.

2130 We observed that splicing varies over the course of infection, between human subjects and  
2131 between cell types. Further sampling could reveal additional patterns in these splicing  
2132 changes.

2133 Long-lived reservoir of HIV infected cells exist in both macrophages<sup>617,618</sup> and resting  
2134 central memory CD4 T cells<sup>139,140,143,619,620</sup>. It may be difficult to obtain enough viral  
2135 RNA from resting CD4 cells<sup>619</sup> but macrophages provide an interesting target. Splicing  
2136 changes due to differing abundances of splice factors have been reported in macrophages<sup>433</sup>.  
2137 Characterization of splicing in these important reservoirs might aid in the understanding of  
2138 latency.

2139 We quantified the splicing of a single clinical isolate and showed unexpected diversity. Most  
2140 previous studies of HIV splicing have been performed with lab-adapted strains<sup>412</sup>. Additional  
2141 studies could determine if the high number of transcripts seen here is an anomaly and whether  
2142 additional cryptic splice sites and novel proteins or epitopes exist. In addition, an important  
2143 subset of HIV are the founder viruses transmitted between hosts<sup>621,622</sup>. These viruses are  
2144 not well studied and perhaps their splicing and gene expression differ from the rest of the  
2145 viral swarm of infected patients. Comparisons to splicing in other retroviral taxa might  
2146 highlight evolution and adaptation in this viral lineage.

2147 Disruption of RNA processing can drastically reduce viral replication<sup>288,623–626</sup>. Inhibi-  
2148 tion of cellular splicing factors reduces viral reproduction in many genome-wide siRNA  
2149 screens<sup>420,422,627</sup> and several members of the spliceosome interact with viral proteins in  
2150 affinity pulldowns<sup>310</sup>. Small molecules that inhibit cellular SR splicing proteins and disrupt  
2151 viral splicing show promise as antiretroviral therapies<sup>419,628–630</sup>. Characterization of splicing

2152 in cells treated with splicing inhibitors could reveal potential escape pathways and optimal  
2153 combinations of drug therapies.

2154 **6.3 Host expression during HIV infection**

2155 In Chapter 4, we saw many changes in host expression and splicing in HIV infected cells  
2156 including intron retention and strong changes in apoptotic and innate immunity genes.  
2157 We focused on generating a dense data set at a single time point and subject to allow  
2158 discrimination of within-condition versus between-condition variation. Further sampling  
2159 using more human subjects and time points, improved sequencing techniques, alternative  
2160 culturing and extraction and more viral strains would clarify and extend these patterns.

2161 In our primary cell infections, only about 25% of cells were infected with HIV. This makes  
2162 it difficult to distinguish between the responses of bystander and infected cells. In addition,  
2163 changes in expression due to cellular response to infection are confounded with changes  
2164 due to hijacking of cellular controls by the virus. For example, bystander cell death has  
2165 been suggested as a major driver of HIV pathogenesis<sup>631,632</sup> but our data do not make it  
2166 clear whether bystander or infected cells are undergoing apoptosis. Cell pull-down with a  
2167 labelled HIV strain<sup>493</sup> or an anti-Env antibody<sup>633</sup> or flow cytometry with a labelled antibody  
2168 targeting HIV antigen<sup>152,634</sup> might allow the separation of bystander and infected cells.

2169 Additionally, abortive infections can drive cell death<sup>632,635</sup> so our populations might be a  
2170 mix of three responses; cells responding to a progressive infection, cells responding to an  
2171 aborted infection and cells responding to neighbor cell infections. A useful control might be  
2172 to infect cells with integrase-deficient virions to guarantee that all infections are aborted.  
2173 This would provide a good measure of innate immune response and the effect of abortive  
2174 infections undiluted by productive HIV infection and help to deconvolute the patterns seen  
2175 in mixed populations.

2176 HIV infection appeared to increase the abundance of intronic sequences. We observed a  
2177 significant decrease of nonsense-mediated decay-related genes so perhaps these transcripts

2178 escape degradation due to decreased cellular RNA surveillance. Alternatively, HIV Vpr  
2179 protein has been reported to disrupt nuclear integrity and allow mixing of nuclear and  
2180 cytoplasmic components<sup>253</sup>. These sequences might represent incompletely spliced mRNA  
2181 that escaped into the cytoplasm before processing. Infection with a Vpr-deficient HIV virus  
2182 and separate isolation of RNA from nuclear and cytoplasmic compartments<sup>636–638</sup> would  
2183 test these hypotheses.

2184 We saw that chimeric sequences were almost entirely derived from read-in or -out from  
2185 viral long terminal repeats or splicing from the viral splice donor D4 to human acceptors.  
2186 With this knowledge, we could use targeted amplification of these three sites, analogous to  
2187 integration site sequencing<sup>383,410,520</sup>, on cellular cDNA to get a much deeper and cleaner  
2188 sampling of chimera formation. Comparison of these data to deeply sequenced integration  
2189 site data from the same samples might reveal associations between integration location and  
2190 chimera formation.

2191 MicroRNA are small RNAs that block translation through base pairing with comple-  
2192 mentary mRNA<sup>639–641</sup>. Viral derived microRNA, perhaps in part from Dicer processing  
2193 of the structured trans-activation response element of HIV<sup>601,642–644</sup>, may suppress HIV  
2194 expression<sup>217,645,646</sup> and inhibit apoptosis<sup>644</sup> but the presence of such microRNA is controver-  
2195 sial<sup>219,647</sup>. HIV may suppress silencing by microRNA<sup>216–218</sup> but this is also controversial<sup>219</sup>.  
2196 Cellular microRNA may have antiviral effects<sup>648,649</sup> or be exploited by HIV to enhance  
2197 replication<sup>650–654</sup> or promote latency<sup>655,656</sup> but there seems to be disagreement on which  
2198 microRNA are involved among different studies<sup>657</sup>. High-throughput genome-wide assays of  
2199 small RNA<sup>473,490</sup> from primary cells infected with patient isolates would help clarify these  
2200 debates.

## 2201 **6.4 LAMP PCR and lab-on-a-chip**

2202 In Chapter 5, we report a loop-mediated isothermal amplification system using primers  
2203 optimized to detect most subtypes of HIV-1. An alternative to a single broadly targeted

2204 primer set would be to design separate primer sets targeted specifically to each subtype so  
2205 that a positive amplification would then be able to discriminate viral subtype. Different viral  
2206 subtypes can have different rates of disease progression<sup>658–661</sup>, transmission dynamics<sup>662–664</sup>  
2207 and response to treatment<sup>665–667</sup>. Simple low-cost devices with multiple reactions chambers  
2208 could be used to both identify viral subtype, estimate viral load<sup>668,669</sup> and allow more  
2209 informed treatment decisions.

2210 A LAMP chip with subtype-specific primers would also allow the detection of intersubtype  
2211 superinfections. Superinfection of a single individual with multiple distinct strains of HIV is  
2212 common in high risk individuals<sup>554,670–673</sup> and the general population<sup>674</sup>. Superinfection with  
2213 a phenotypically different strain of HIV can lead to disease progression<sup>675–680</sup> or drug resis-  
2214 tance<sup>681</sup>. Superinfection also allows recombination between divergent strains<sup>670,676,677,679,682</sup>  
2215 and this rapid exchange of genetic information can lead to more fit recombinant strains and  
2216 worsen the global epidemic<sup>58,62,677,683,684</sup>. LAMP detection of superinfection could allow  
2217 early intervention and suppression in superinfected individuals.

2218 The techniques described in Chapter 5 also allow for rapid development of detection assays  
2219 for novel pathogens. For example, in a recent outbreak in West Africa, Zaire ebolavirus  
2220 has infected over 26,000 confirmed, probable and suspected cases and caused over 11,000  
2221 reported deaths<sup>685–687</sup>. Early detection and quarantine are essential to the control of this  
2222 epidemic<sup>688</sup>. Amplification of Ebolavirus nucleic acid through polymerase chain reaction is  
2223 the best diagnostic test currently available but the necessary resources are often not available  
2224 in these resource-poor regions<sup>689,690</sup>. Antigen-based tests are quicker and available at the  
2225 point-of-care but are not as accurate or sensitive as polymerase chain reaction tests and are  
2226 still in limited supply<sup>690</sup>. Loop-mediated isothermal amplification offers the potential for  
2227 rapid, sensitive and efficient detection of Ebolavirus RNA but available LAMP primers<sup>691</sup> do  
2228 not match the current outbreak strain. Using sequences from the recent outbreak<sup>685,692</sup> and  
2229 the methods described in Chapter 5, we designed primers to match all known Zaire ebolavirus  
2230 (Figure 6.1). These primer combined with simple lab-on-a-chip devices for purifying blood

2231 plasma<sup>559</sup> and imaging fluorescent signals<sup>574,668</sup> could allow rapid point-of-care detection of  
2232 Ebolavirus.

2233 **6.4.1 Conclusions**

2234 These studies contribute to the study and treatment of HIV-1 by revealing aspects of latency,  
2235 expression and host response. They highlight the importance of primary cell models and  
2236 the effects that host cell can have on viral processes. With rapidly increasing sequencing  
2237 throughput, studies like those presented here offer the opportunity for a deeper and broader  
2238 understanding of HIV-1 biology and host response and further development of diagnostics  
2239 and therapeutics.

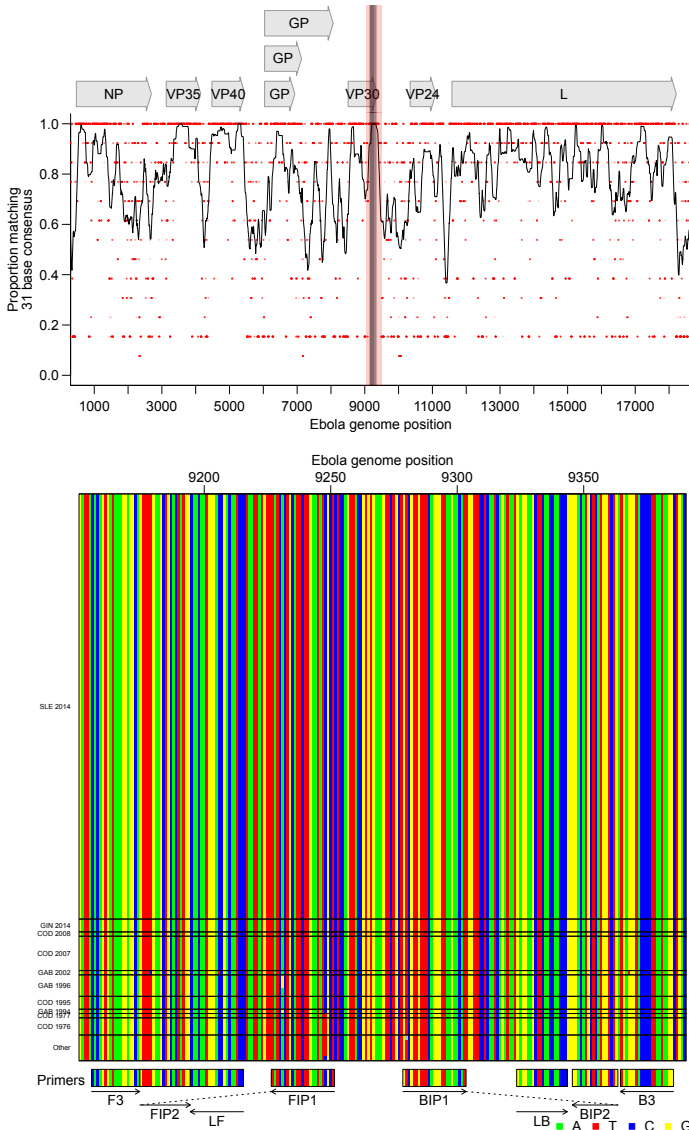


Figure 6.1: Bioinformatic analysis to design Ebolavirus RT-LAMP primers. A) Conservation of sequence in Ebolavirus. Ebolavirus genomes ( $n = 131$ ) from Genbank and sequences from the recent Zaire Ebolavirus outbreak<sup>685</sup> were aligned and conservation calculated. The x-axis shows the coordinate on the Ebola genome, the y-axis shows the proportion of sequences matching the consensus for each 21 base segment of the genome (red points). The black line shows a 101 base sliding average over these proportions. The vertical red shading shows the region targeted for LAMP primer design that was used as input into the EIKEN primer design tool and grey shading indicates the area covered by the optimized primer set. Numbering is relative to the Ebola Mayinga sequence. B) Aligned genomes, showing the locations of the LAMP primers. Sequences in the grey-shaded region in A are shown, with DNA bases color-coded as shown at the lower right. Each row indicates an Ebolavirus sequence and each column a base in that sequence. Horizontal lines separate Ebolavirus outbreaks (SLE: Seirra Leone, GIN: Guinea, COD: DR Congo, GAB: Gabon). Arrows indicate the strand targeted by each primer. Primers targeting the negative strand of the virus are shown as reverse compliments for ease of viewing.

## APPENDIX A.1 : Generalized linear models of changes in use of mutually exclusive HIV-1 splice acceptors

Reads splicing from D1 to one of five mutually exclusive acceptors, D3, D4c, D4a, D4b, D5, and D5a, in three primers, 1.2, 1.3 and 1.4, were collected. Since these data are based on counts, we modeled them as Poisson distributed with an extra variance term allowing for additional variance using a quasi-Poisson generalized linear model with log link. We accounted for differences in sequencing effort by including the total number of D1 to mutually exclusive acceptors reads in each primer-sample as an offset. Differences in the read counts a) over time,b) between human donor and c) cell type were analyzed separately. A term was included for each acceptor and its interaction with the variable of interest. The models included primer and replicate terms and their individual interactions with acceptor to account for any confounding factors.

### A.1.1 HOS vs T Cells

R command:

```
glm(count~offset(log(total)) + acceptor:primer + acceptor:  
    isHos  
    + acceptor, data = mutEx[mutEx$time == 48,],  
    family = 'quasipoisson')
```

Difference between HOS and T cells may be confounded by run differences between early sequencing and later sequencing. Verification by agarose gel (Figure 3.4b) suggest that these differences are likely biological.

Variable	Df	Deviance	Resid. Df	Resid. Dev	F	Pr(>F)
NULL	395	138 330				
acceptor	5	133 985	390	4345	9004	$<2.2 \times 10^{-16}$
acceptor:primer	12	751	378	3594	21.03	$<2.2 \times 10^{-16}$
acceptor:isHos	6	2466	372	1127	138.1	$<2.2 \times 10^{-16}$

So after accounting for primer-acceptor bias, the difference between HOS and T cells is significant.

The interesting terms in the model are:

Variable	Estimate	Std. Error	t value	Pr(> t )
acceptorA3:isHosTRUE	1.4717	0.065 86	22.35	$<2.2 \times 10^{-16}$
acceptorA4a:isHosTRUE	-0.9449	0.1246	-7.583	$2.73 \times 10^{-13}$
acceptorA4b:isHosTRUE	-0.9285	0.1059	-8.767	$<2.2 \times 10^{-16}$
acceptorA4c:isHosTRUE	-1.228	0.1066	-11.51	$<2.2 \times 10^{-16}$
acceptorA5:isHosTRUE	0.090 82	0.026 08	3.483	0.000 555
acceptorA5a:isHosTRUE	0.6308	0.079 40	7.945	$2.33 \times 10^{-14}$

So it appears A3 is up; A4c, A4a and A4b are down; A5 is up a little and A5a up in HOS.

### A.1.2 HOS Over Time

R command:

```
glm(value~offset(log(total)) + acceptor + acceptor:primer
+ acceptor:time, data=mutEx[mutEx$isHos ,],
family = 'quasipoisson')
```

Looking only within HOS, we see a significant linear effect of time:

Variable	Df	Deviance	Resid. Df	Resid. Dev	F	Pr(>F)
NULL	53	17962				
acceptor	5	17710	48	252.2	6698	$<2.2 \times 10^{-16}$
acceptor:primer	12	18.0	36	234.2	2.834	0.01018
acceptor:time	6	217.8	30	16.4	68.65	$3.57 \times 10^{-16}$

We are assuming that a particular acceptor will have the same change in all three primers here.

The interesting terms are:

Variable	Estimate	Std. Error	t value	Pr(> t )
acceptorA3:time	0.02477	0.001778	13.93	$1.22 \times 10^{-14}$
acceptorA4a:time	-0.01621	0.002812	-5.765	$2.69 \times 10^{-6}$
acceptorA4b:time	-0.02526	0.002271	-11.12	$3.62 \times 10^{-12}$
acceptorA4c:time	0.015867	0.003050	5.202	$1.32 \times 10^{-5}$
acceptorA5:time	-0.001918	0.0006313	-3.038	0.0049
acceptorA5a:time	0.004919	0.001969	2.499	0.0182

So A3, A4c and A5a increase over time and A4a, A4b and A5 decrease over time. All of these coefficients are with a log link and linear and so multiplicative. That means that for example A3 will increase 2.5%/hour ( $\exp(.0247)$ ) or equivalently 81% ( $1.025^{24}$ ) over 24hours.

### A.1.3 Between Human Comparison

R command:

```
glm(value~offset(log(total)) + acceptor + acceptor:run
+ acceptor:primer + acceptor:subject ,
data=mutEx[!mutEx$ishos,], family = 'quasipoisson')
```

In humans, we added a term to account for any potential run bias between the three replicates. Subject refers to the seven human blood donors from which T cells were collected:

Variable	Df	Deviance	Resid. Df	Resid. Dev	F	Pr(>F)
NULL	377	128 430				
acceptor	5	126 446	372	1985	19 598	$<2.2 \times 10^{-16}$
acceptor:run	12	136	360	1849	8.792	$1.77 \times 10^{-14}$
acceptor:primer	12	850	348	998	54.91	$<2.2 \times 10^{-16}$
acceptor:subject	36	597	312	401	12.86	$<2.2 \times 10^{-16}$

So after accounting for any run and primer bias, subject ID has a statistically significant effect on our observed counts. If we compare everything to subject 7, the interesting terms are:

Variable	Estimate	Std. Error	t value	Pr(> t )
acceptorA3:subject6	-0.001 399	0.072 86	-0.019	0.9847
acceptorA4a:subject6	-0.112 90	0.049 44	-2.284	0.023 07
acceptorA4b:subject6	-0.054 33	0.040 38	-1.345	0.1795
acceptorA4c:subject6	0.028 29	0.033 60	0.842	0.4005
acceptorA5:subject6	0.016 83	0.016 00	1.051	0.2939
acceptorA5a:subject6	-0.030 85	0.060 92	-0.506	0.6129
acceptorA3:subject5	-0.077 67	0.074 23	-1.046	0.2962
acceptorA4a:subject5	-0.1144	0.049 82	-2.296	0.0223
acceptorA4b:subject5	-0.0684	0.040 90	-1.672	0.0956
acceptorA4c:subject5	-0.085 85	0.034 75	-2.471	0.0140
acceptorA5:subject5	0.038 88	0.016 16	2.406	0.0167
acceptorA5a:subject5	0.078 77	0.060 38	1.304	0.1930
acceptorA3:subject4	-0.1849	0.095 78	-1.931	0.0544
acceptorA4a:subject4	0.071 86	0.057 91	1.241	0.2156
acceptorA4b:subject4	0.126 20	0.047 14	2.677	0.0078
acceptorA4c:subject4	-0.100 21	0.043 03	-2.329	0.0205
acceptorA5:subject4	-0.001 16	0.019 69	-0.059	0.9531
acceptorA5a:subject4	0.023 46	0.073 53	0.319	0.7499
acceptorA3:subject3	-0.003 51	0.086 65	-0.041	0.9677
acceptorA4a:subject3	0.071 07	0.055 64	1.277	0.2024
acceptorA4b:subject3	0.006 46	0.046 99	0.138	0.8907
acceptorA4c:subject3	-0.063 34	0.040 76	-1.554	0.1212
acceptorA5:subject3	0.010 52	0.018 87	0.557	0.5776
acceptorA5a:subject3	-0.070 95	0.072 85	-0.974	0.3309
acceptorA3:subject2	-0.2329	0.091 76	-2.539	0.0116
acceptorA4a:subject2	0.024 05	0.056 43	0.426	0.6702
acceptorA4b:subject2	0.1107	0.045 35	2.441	0.0152
acceptorA4c:subject2	0.021 76	0.039 52	0.551	0.5823
acceptorA5:subject2	-0.003 760	0.018 69	-0.201	0.8407
acceptorA5a:subject2	-0.1608	0.073 51	-2.187	0.0295
acceptorA3:subject1	0.095 36	0.065 56	1.454	0.1468
acceptorA4a:subject1	0.029 32	0.044 31	0.662	0.5087
acceptorA4b:subject1	-0.2144	0.038 43	-5.578	$5.28 \times 10^{-8}$
acceptorA4c:subject1	-0.3974	0.033 85	-11.74	$<2.2 \times 10^{-16}$
acceptorA5:subject1	0.091 44	0.014 70	6.221	$1.58 \times 10^{-9}$
acceptorA5a:subject1	0.027 47	0.055 94	0.491	0.6238

So there were small but significant effects between subjects especially between subject 1 and subjects 2–7. A potential confounder is that T cells were collected from apheresis product in

subject 1 and from whole blood in subjects 2–7 although why this would affect later assays is unknown.

## APPENDIX A.2 : Reproducible report of HIV integration sites and latency analysis

### A.2.1 Supplementary data

Additional File 2 is a gzipped csv file that includes a row for each uniquely mapped provirus and its surrounding genomic annotations. The csv file should have 12436 rows (excluding header) with 6252 expressed and 6184 latent proviruses.

```
integrationData <- read.csv("AdditionalFile2.csv.gz",
  stringsAsFactors = FALSE)

nrow(integrationData)

## [1] 12436

table(integrationData$isLatent)

##
##  FALSE   TRUE
##  6252   6184
```

### A.2.2 Lasso regression

The lasso regressions take a while to run so I've turned down the number of cross validations here (set `eval=FALSE` below to completely skip this step). Leave one out and 480-fold cross validation were used in the paper but processing may take a few days without parallel processing. Lasso regression requires the R `glmnet` package.

```

notFitColumns <- c("id", "chr", "pos", "strand", "sample", "isLatent")

samples <- unique(as.character(integrationData$sample))

sampleMatrix <- do.call(cbind, lapply(samples, function(x)
  integrationData$sample ==
  x))

colnames(sampleMatrix) <- gsub(" ", "_", samples)

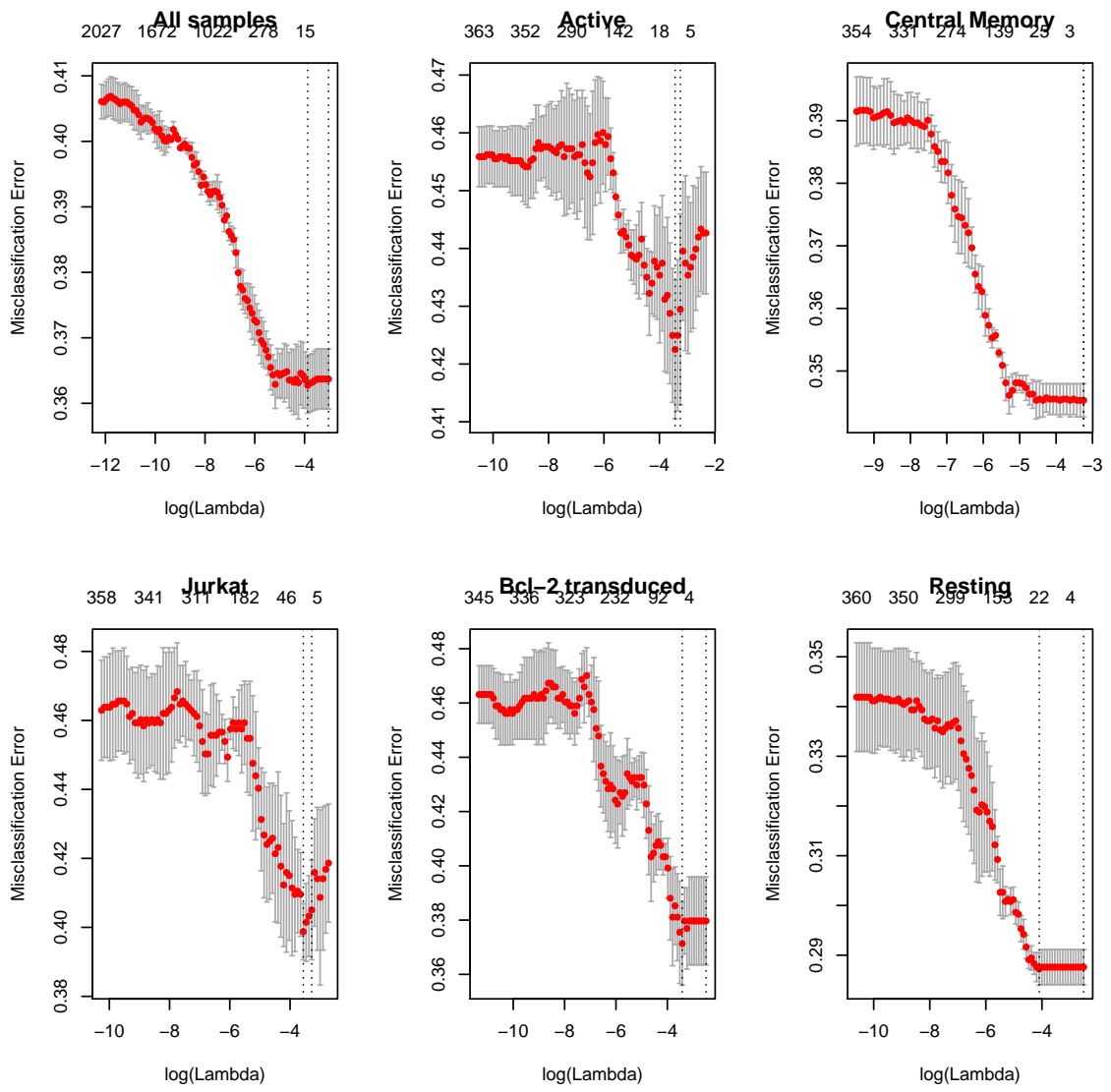
interact <- function(predMatrix, columns, addNames = NULL) {
  out <- do.call(cbind, lapply(1:ncol(columns), function(x)
    predMatrix *
    columns[, x]))
  if (!is.null(addNames)) {
    if (length(addNames) != ncol(columns)) {
      stop(simpleError("Names not same length as columns"))
    }
    colnames(out) <- sprintf("%s_%s", rep(addNames, each =
      ncol(predMatrix)),
      rep(colnames(predMatrix), length(addNames)))
  }
  return(out)
}

fitData <- as.matrix(integrationData[, !colnames(
  integrationData) %in%]

```

```
notFitColumns])  
  
fitData2 <- as.matrix(cbind(interact(fitData, sampleMatrix,  
colnames(sampleMatrix)),  
fitData, sampleMatrix))
```

```
library(glmnet)  
  
penalties <- rep(1, ncol(fitData2))  
  
penalties[ncol(fitData2) - (ncol(sampleMatrix):1) + 1] <- 0  
  
lassoFit <- cv.glmnet(fitData2, integrationData$isLatent,  
family = "binomial",  
type.measure = "class", nfolds = 3, penalty.factor =  
penalties)  
  
seperateFits <- lapply(samples, function(x) cv.glmnet(fitData[  
integrationData$sample ==  
x, ], integrationData$isLatent[integrationData$sample ==  
x], family = "binomial", type.measure = "class", nfolds =  
3))  
  
names(seperateFits) <- samples
```



### A.2.3 Correlation

We looked for correlation between the genomic variables and expression status of the proviruses.

```
corMat <- apply(fitData, 2, function(x) sapply(samples,
  function(y) {
    selector <- integrationData$sample == y
```

```

    if (sd(x[selector]) == 0)
      return(0)

    isLatent <- integrationData[selector, "isLatent"]
    cor(as.numeric(isLatent), x[selector], method = "spearman"
    ")
  }))

quantile(cormat, seq(0, 1, 0.1))

##          0%           10%          20%          30%
## -0.185223020 -0.081555830 -0.048938130 -0.030895834
##          40%           50%          60%          70%
## -0.018053321 -0.005613895  0.003580982  0.017822483
##          80%           90%         100%
##  0.036694554  0.062003356  0.170642314

```

If we looked for genomic variables consistently correlated or anti-correlated with proviral expression status with an FDR q-value less than 0.01, no variable was significantly correlated in more than 3 samples.

```

pMat <- apply(fitData, 2, function(x) sapply(samples, function
(y) {
  selector <- integrationData$sample == y
  if (sd(x[selector]) == 0)
    return(NA)
  isLatent <- integrationData[selector, "isLatent"]
  cor.test(as.numeric(isLatent), x[selector], method =
  "spearman",

```

```

exact = FALSE)$p.value
}))

adjustPMat <- pMat

adjustPMat[, ] <- p.adjust(pMat, "fdr")

downPMat <- upPMat <- adjustPMat

downPMat[corMat > 0] <- 1

upPMat[corMat < 0] <- 1

table(apply(upPMat < 0.01 & !is.na(upPMat), 2, sum))

##
##      0     1     2     3
## 298   27   38   10

table(apply(downPMat < 0.01 & !is.na(downPMat), 2, sum))

##
##      0     1     2     3
## 216   36   63   58

```

#### A.2.4 RNA expression

We fit a logistic regression to a polynomial of log RNA-Seq reads within 5000 bases from Jurkat cells for the Jurkat sample and T cells for the rest.

```

rna <- ifelse(integrationData$sample == "Jurkat",
               integrationData$log_jurkatRNA,

```

```

integrationData$rna_5000)

rna2 <- rna^2

rna3 <- rna^3 # 

rna4 <- rna^4

glmData <- data.frame(isLatent = integrationData$isLatent ,
sample = integrationData$sample ,
rna, rna2, rna3, rna4)

glmMod <- glm(isLatent ~ sample * rna + sample * rna2 + sample
*
rna3 + sample * rna4, data = glmData, family = "binomial")

summary(glmMod)

## 

## Call:
## glm(formula = isLatent ~ sample * rna + sample * rna2 +
## sample *
##     rna3 + sample * rna4, family = "binomial", data =
## glmData)

## 

## Deviance Residuals:
##      Min        1Q    Median        3Q       Max
## -2.2899   -0.9864   -0.8676    1.0960    1.6007

## 

## Coefficients:
##                                         Estimate Std. Error z value
##
```

```

## (Intercept)           1.7623655  0.2138859  8.240
## sampleBcl-2 transduced -2.1625912  0.7061524 -3.062
## sampleCentral Memory      -2.5010063  0.2437685 -10.260
## sampleJurkat            -2.0800202  0.2836871 -7.332
## sampleResting             0.7840481  0.3312247  2.367
## rna                      -0.6567268  0.2344422 -2.801
## rna2                     0.1387703  0.0770589  1.801
## rna3                     -0.0167219  0.0094076 -1.777
## rna4                     0.0007572  0.0003845  1.969
## sampleBcl-2 transduced:rna 0.5750186  0.6366537  0.903
## sampleCentral Memory:rna   0.9067758  0.2750955  3.296
## sampleJurkat:rna          0.5294036  0.3867163  1.369
## sampleResting:rna          0.0366276  0.3436248  0.107
## sampleBcl-2 transduced:rna2 -0.0369353  0.1878816 -0.197
## sampleCentral Memory:rna2   -0.2106715  0.0915492 -2.301
## sampleJurkat:rna2          -0.0766215  0.1641153 -0.467
## sampleResting:rna2          -0.0760450  0.1086998 -0.700
## sampleBcl-2 transduced:rna3 0.0032503  0.0213743  0.152
## sampleCentral Memory:rna3   0.0237064  0.0112661  2.104
## sampleJurkat:rna3          0.0042183  0.0263910  0.160
## sampleResting:rna3          0.0153132  0.0128711  1.190
## sampleBcl-2 transduced:rna4 -0.0002532  0.0008267 -0.306
## sampleCentral Memory:rna4   -0.0009877  0.0004627 -2.135
## sampleJurkat:rna4           0.0001725  0.0014215  0.121
## sampleResting:rna4          -0.0008049  0.0005119 -1.572
## Pr(>|z|)
## (Intercept) < 2e-16 ***

```

```

## sampleBcl-2 transduced          0.00219  **
## sampleCentral Memory           < 2e-16 ***
## sampleJurkat                  2.27e-13 ***
## sampleResting                 0.01793 *
## rna                          0.00509  **
## rna2                         0.07173 .
## rna3                         0.07549 .
## rna4                         0.04891 *
## sampleBcl-2 transduced:rna    0.36643
## sampleCentral Memory:rna      0.00098  ***
## sampleJurkat:rna              0.17101
## sampleResting:rna             0.91511
## sampleBcl-2 transduced:rna2   0.84415
## sampleCentral Memory:rna2     0.02138 *
## sampleJurkat:rna2            0.64059
## sampleResting:rna2           0.48419
## sampleBcl-2 transduced:rna3   0.87913
## sampleCentral Memory:rna3     0.03536 *
## sampleJurkat:rna3            0.87301
## sampleResting:rna3           0.23415
## sampleBcl-2 transduced:rna4   0.75939
## sampleCentral Memory:rna4     0.03280 *
## sampleJurkat:rna4            0.90339
## sampleResting:rna4           0.11585
## ---
## Signif. codes:
## 0  '***' 0.001 '**' 0.01 '*' 0.05 '.' 0.1 ' ' 1

```

```

## 
## (Dispersion parameter for binomial family taken to be 1)

## 
##      Null deviance: 17240    on 12435    degrees of freedom
## Residual deviance: 15874    on 12411    degrees of freedom
## AIC: 15924

## 
## Number of Fisher Scoring iterations: 4

```

### A.2.5 Strand orientation

We used a Fisher's exact test to check if silent/inducible proviruses were enriched when integrated in the same strand orientation as cellular genes.

```

selector <- integrationData$inGene == 1

strandTable <- with(integrationData[selector, ], table(ifelse(
  isLatent,
  "Silent/Inducible", "Active"), ifelse(inGeneSameStrand ==
  1, "Same", "Diff"), sample))

apply(strandTable, 3, fisher.test)

## $Active

## 
##      Fisher's Exact Test for Count Data

## 
## data: array(newX[, i], d.call, dn.call)
## p-value = 0.06061
## alternative hypothesis: true odds ratio is not equal to 1

```

```
## 95 percent confidence interval:  
## 0.7219466 1.0081995  
  
## sample estimates:  
  
## odds ratio  
## 0.8532127  
  
##  
  
##  
  
## $`Bcl-2 transduced`  
  
##  
  
## Fisher's Exact Test for Count Data  
  
##  
  
## data: array(newX[, i], d.call, dn.call)  
## p-value = 2.177e-05  
  
## alternative hypothesis: true odds ratio is not equal to 1  
  
## 95 percent confidence interval:  
## 1.446896 2.872562  
  
## sample estimates:  
  
## odds ratio  
## 2.036148  
  
##  
  
##  
  
## $`Central Memory`  
  
##  
  
## Fisher's Exact Test for Count Data  
  
##  
  
## data: array(newX[, i], d.call, dn.call)  
## p-value = 0.2907
```

```
## alternative hypothesis: true odds ratio is not equal to 1
## 95 percent confidence interval:
## 0.9386167 1.2320238
## sample estimates:
## odds ratio
## 1.07529
##
##
## $Jurkat
##
## Fisher's Exact Test for Count Data
##
## data: array(newX[, i], d.call, dn.call)
## p-value = 0.1674
## alternative hypothesis: true odds ratio is not equal to 1
## 95 percent confidence interval:
## 0.9207548 1.5699893
## sample estimates:
## odds ratio
## 1.202007
##
##
## $Resting
##
## Fisher's Exact Test for Count Data
##
## data: array(newX[, i], d.call, dn.call)
```

```

## p-value = 0.5732
## alternative hypothesis: true odds ratio is not equal to 1
## 95 percent confidence interval:
## 0.7825231 1.1405158
## sample estimates:
## odds ratio
## 0.9447415

```

### A.2.6 Acetylation

To reduce correlation between acetylation marks, we generated the first ten principal components of the acetylation data and ran a logistic regression against them. We compared the cross validated performance of this regression with a base model only including which dataset the integration site came from. The cross-validation here has been reduced for efficiency but 480-fold cross-validation was used in the paper.

```

acetyl <- integrationData[, !grepl("logDist", colnames(
  integrationData)) &
  grepl("ac", colnames(integrationData))]

acetylPCA <- princomp(acetyl)

cumsum(acetylPCA$sdev[1:10]^2/sum(acetylPCA$sdev^2))

##      Comp.1      Comp.2      Comp.3      Comp.4      Comp.5      Comp.6
## 0.5947268 0.6786611 0.7267433 0.7610502 0.7833616 0.7964470
##      Comp.7      Comp.8      Comp.9      Comp.10
## 0.8093295 0.8215027 0.8299358 0.8372584

cv.glm <- function(model, K = nrow(thisData), subsets = NULL)
{

```

```

modelCall <- model$call

thisData <- eval(modelCall$data)

n <- nrow(thisData)

if (is.null(subsets))

  subsets <- split(1:n, sample(rep(1:K, length.out = n)))

  )

preds <- lapply(subsets, function(outGroup) {

  subsetData <- thisData[-outGroup, , drop = FALSE]

  predData <- thisData[outGroup, , drop = FALSE]

  thisModel <- modelCall

  thisModel$data <- subsetData

  return(predict(eval(thisModel), predData))

})

pred <- unlist(preds)[order(unlist(subsets))]

subsetId <- rep(1:K, sapply(subsets, length))[order(unlist
  (subsets))]

return(data.frame(pred, subsetId))
}

inData <- data.frame(isLatent = integrationData$isLatent ,
  sample = as.factor(integrationData$sample),
  acetylPCA$score[, 1:10])

modelPreds <- cv.glm(glm(isLatent ~ sample + Comp.1 + Comp.2 +
  Comp.3 + Comp.4 + Comp.5 + Comp.6 + Comp.7 + Comp.8 + Comp
  .9 +
  Comp.10, family = "binomial", data = inData), K = 5)

```

```

basePreds <- cv.glm(glm(isLatent ~ sample, family = "binomial
",
data = inData), subsets = split(1:nrow(inData),
modelPreds$subsetId),
K = 5)

modelCorrect <- sum((modelPreds$pred > 0) ==
integrationData$isLatent)
baseCorrect <- sum((basePreds$pred > 0) ==
integrationData$isLatent)

prop.test(c(baseCorrect, modelCorrect), rep(nrow(
integrationData),
2))

##
##      2-sample test for equality of proportions with
##      continuity correction
##
## data: c(baseCorrect, modelCorrect) out of rep(nrow(
## integrationData), 2)
## X-squared = 0.00017372, df = 1, p-value = 0.9895
## alternative hypothesis: two.sided
## 95 percent confidence interval:
## -0.01187726 0.01219890
## sample estimates:
## prop 1     prop 2
## 0.6362978 0.6361370

```

### A.2.7 Gene deserts

We used Fisher's exact test to look for an association between integration outside a gene and proviral expression status.

```
geneTable <- table(integrationData$isLatent ,  
                    integrationData$inGene ,  
                    integrationData$sample)  
  
apply(geneTable , 3 , fisher.test)  
  
## $Active  
##  
##      Fisher's Exact Test for Count Data  
##  
## data: array(newX[, i] , d.call , dn.call)  
## p-value < 2.2e-16  
## alternative hypothesis: true odds ratio is not equal to 1  
## 95 percent confidence interval:  
##  0.3629548 0.5446204  
## sample estimates:  
## odds ratio  
##  0.4452621  
##  
##  
## $`Bcl-2 transduced`  
##  
##      Fisher's Exact Test for Count Data  
##  
## data: array(newX[, i] , d.call , dn.call)
```

```
## p-value = 0.1052
## alternative hypothesis: true odds ratio is not equal to 1
## 95 percent confidence interval:
## 0.9203418 2.3478599
## sample estimates:
## odds ratio
## 1.472224
##
##
## $`Central Memory`
##
## Fisher's Exact Test for Count Data
##
## data: array(newX[, i], d.call, dn.call)
## p-value = 0.7803
## alternative hypothesis: true odds ratio is not equal to 1
## 95 percent confidence interval:
## 0.8525329 1.1253952
## sample estimates:
## odds ratio
## 0.9791165
##
##
## $Jurkat
##
## Fisher's Exact Test for Count Data
##
```

```

## data: array(newX[, i], d.call, dn.call)
## p-value = 0.5443
## alternative hypothesis: true odds ratio is not equal to 1
## 95 percent confidence interval:
## 0.7909269 1.6167285
## sample estimates:
## odds ratio
## 1.127836
##
##
## $Resting
##
## Fisher's Exact Test for Count Data
##
## data: array(newX[, i], d.call, dn.call)
## p-value = 3.071e-08
## alternative hypothesis: true odds ratio is not equal to 1
## 95 percent confidence interval:
## 0.4384828 0.6864112
## sample estimates:
## odds ratio
## 0.5500205

```

We used a two-sample t-test to investigate whether there was a significant difference in distance to the nearest gene between expressed and silent/inducible proviruses integrated outside genes.

```

geneDistData <- integrationData[!integrationData$inGene , c(
  "isLatent",
  "logDist_nearest", "sample")]

by(geneDistData, geneDistData$sample, function(x) t.test(
  logDist_nearest ~
  isLatent, data = x))

## geneDistData$sample: Active

##
##      Welch Two Sample t-test
##
## data: logDist_nearest by isLatent
## t = -2.4539, df = 287.73, p-value = 0.01472
## alternative hypothesis: true difference in means is not
## equal to 0
## 95 percent confidence interval:
## -0.80738340 -0.08867607
## sample estimates:
## mean in group FALSE mean in group TRUE
## 9.608737 10.056767
##
## -----
## geneDistData$sample: Bcl-2 transduced
##
##      Welch Two Sample t-test
##
## data: logDist_nearest by isLatent
## t = 0.40978, df = 86.2, p-value = 0.683

```

```

## alternative hypothesis: true difference in means is not
## equal to 0

## 95 percent confidence interval:
## -0.6309351 0.9586004

## sample estimates:

## mean in group FALSE mean in group TRUE
## 9.036872 8.873039

## -----
## geneDistData$sample: Central Memory

## Welch Two Sample t-test

## data: logDist_nearest by isLatent
## t = -0.07188, df = 861.61, p-value = 0.9427

## alternative hypothesis: true difference in means is not
## equal to 0

## 95 percent confidence interval:
## -0.2371374 0.2203819

## sample estimates:

## mean in group FALSE mean in group TRUE
## 10.19225 10.20063

## -----
## geneDistData$sample: Jurkat

## Welch Two Sample t-test

```

```

## 

## data: logDist_nearest by isLatent
## t = -1.8217, df = 139.56, p-value = 0.07064
## alternative hypothesis: true difference in means is not
## equal to 0
## 95 percent confidence interval:
## -1.26342086 0.05167979
## sample estimates:
## mean in group FALSE mean in group TRUE
## 9.925782 10.531652
##
## -----
## geneDistData$sample: Resting
##
## Welch Two Sample t-test
##
## data: logDist_nearest by isLatent
## t = -5.1275, df = 193.49, p-value = 7.096e-07
## alternative hypothesis: true difference in means is not
## equal to 0
## 95 percent confidence interval:
## -1.2687917 -0.5638568
## sample estimates:
## mean in group FALSE mean in group TRUE
## 9.489931 10.406255

```

To check for a relationship between silent/inducible status and distance to CpG islands, we

used a two sample t-test on the logged distance and saw a significant difference between silent/inducible and expressed proviruses (before accounting for a correlation between being near CpG islands and in genes)

```
t.test(integrationData$logDist_cpg ~ integrationData$isLatent)

##
##      Welch Two Sample t-test
##
## data: integrationData$logDist_cpg by
##       integrationData$isLatent
## t = -2.0233, df = 12381, p-value = 0.04306
## alternative hypothesis: true difference in means is not
## equal to 0
## 95 percent confidence interval:
## -0.105657514 -0.001675563
## sample estimates:
## mean in group FALSE   mean in group TRUE
##                 10.16362             10.21728

sapply(unique(integrationData$sample), function(x) with(
  integrationData[integrationData$sample ==
    x, ], p.adjust(t.test(logDist_cpg ~ isLatent)$p.value,
    method = "bonferroni",
    n = 5)))

##          Active     Central Memory           Jurkat
##          0.512040457     1.000000000     1.000000000
## Bcl-2 transduced           Resting
##          1.000000000     0.005866539
```

Many CpG islands are found near genes. To account for this relationship, we used an ANOVA test including whether the integration site was inside a gene prior to including CpG islands. After including integration inside genes, CpG islands were not significantly associated with silent/inducible status of the proviruses with all samples grouped or individually after Bonferroni correction for multiple comparisons.

```

anova(with(integrationData, glm(isLatent ~ I(logDist_nearest
==

0) + logDist_cpg, family = "binomial")), test = "Chisq")

## Analysis of Deviance Table

##
## Model: binomial, link: logit

##
## Response: isLatent

##
## Terms added sequentially (first to last)

##
##                                     Df Deviance Resid. Df Resid. Dev
## NULL                               12435      17240
## I(logDist_nearest == 0)    1     26.2682    12434      17213
## logDist_cpg                      1      1.1328    12433      17212
##                                     Pr(>Chi)
## NULL
## I(logDist_nearest == 0) 2.971e-07 ***
## logDist_cpg                  0.2872
## ---
## Signif. codes:

```

```

## 0 '***' 0.001 '**' 0.01 '*' 0.05 '.' 0.1 ' ' 1

sapply(unique(integrationData$sample), function(x) {
  p.adjust(anova(with(integrationData[integrationData$sample
  ==

x, ], glm(isLatent ~ I(logDist_nearest == 0) +
logDist_cpg,
family = "binomial")), test = "Chisq")["logDist_cpg",
"Pr(>Chi)"], method = "bonferroni", n = 5)
})

##          Active      Central Memory           Jurkat
## 1.0000000 1.0000000
## Bcl-2 transduced             Resting
## 1.0000000 0.2007788

```

### A.2.8 Alphoid repeats

When analyzing repetitive elements, we treated each read as an independent observation and included reads with multiple alignments to the genome. Additional File 3 is a gzipped csv file containing a row for each read with multiple alignments and one row for each dereplicated integration site with a single alignment with the count variable indicating the number of reads dereplicated to that integration site. There should be 26,190 rows (excluding header) with 14,494 rows of expressed provirus and 11,696 rows of silent/inducible provirus.

```

repeats <- read.csv("AdditionalFile3.csv.gz", check.names =
FALSE,
stringsAsFactors = FALSE)

nrow(repeats)

```

To analyze whether there was an association between proviral expression status and integration within alphoid repeats, we used Fisher's exact test with a Bonferroni correction for five samples. For comparison, we looked at the association between proviral expression and the other repeats in the RepeatMasker database. We did not Bonferroni correct for the multiple repeat types so that the repeats could be compared with the analysis of alphoid repeats (for which we had an a priori hypothesis for an association with latency).

```
dummyX <- rep(c(TRUE, FALSE), 2)

dummyY <- rep(c(TRUE, FALSE), each = 2)

repeatData <- repeats[, !colnames(repeats) %in%
  notRepeatColumns]

repeatData <- repeatData[, apply(repeatData, 2, sum) > 0]

testRepeats <- function(x, repeats) {
  sapply(samples, function(thisSample, repeats) {
    selector <- repeats$sample == thisSample
    repLatent <- rep(repeats$isLatent[selector],
      repeats$count[selector])
    repRepeat <- rep(x[selector], repeats$count[selector])
```

```

fisher.test(table(c(dummyX, repLatent), c(dummyY,
repRepeat)) -
1)p.value
}, repeats)
}

repeatPs <- apply(repeatData, 2, testRepeats, repeats[, notRepeatColumns])

table(apply(repeatPs * 5 < 0.05, 2, sum))

##
##    0     1     2     3
## 611   76   15     1

which(apply(repeatPs * 5 < 0.05, 2, sum) >= 3)

## ALR/Alpha
##          178

p.adjust(repeatPs[, "ALR/Alpha"], "bonferroni")

##          Active   Central Memory        Jurkat
## 5.026890e-02 3.940207e-03 1.027189e-08
## Bcl-2 transduced           Resting
## 1.000000e+00 2.424896e-02

```

### A.2.9 Neighbors

We looked at all pairs of viruses on the same chromosome separated by no more than a given distance, e.g. 100 bases, either with all samples pooled or split between within sample

pairs or between sample pairs.

```
allNeighbors <- data.frame(id1 = 0, id2 = 0)[0, ]  
  
ids <- 1:nrow(integrationData)  
  
for (chr in unique(integrationData$chr)) {  
  chrSelector <- integrationData$chr == chr  
  neighborPairs <- data.frame(id1 = rep(ids[chrSelector],  
    sum(chrSelector)),  
    id2 = rep(ids[chrSelector], each = sum(chrSelector)))  
  neighborPairs <- neighborPairs[neighborPairs$id1 <  
    neighborPairs$id2,  
    ]  
  allNeighbors <- rbind(allNeighbors, neighborPairs)  
}  
  
allNeighbors$dist <- abs(integrationData$pos[allNeighbors$id1]  
-  
  integrationData$pos[allNeighbors$id2])  
  
allNeighbors$latent1 <- integrationData$isLatent [  
  allNeighbors$id1]  
  
allNeighbors$latent2 <- integrationData$isLatent [  
  allNeighbors$id2]  
  
allNeighbors$sample1 <- integrationData$sample [  
  allNeighbors$id1]  
  
allNeighbors$sample2 <- integrationData$sample [  
  allNeighbors$id2]
```

The expected number of matching pairs was calculated as  $\sum_{j \in \text{samples}} n_{j,d}(\theta_{j,d}\theta_{\neg j,d} + (1 - \theta_{j,d})(1 - \theta_{\neg j,d}))$  for between sample,  $\sum_{j \in \text{samples}} n_{j,d}(\theta_{j,d}^2 + (1 - \theta_{j,d})^2)$  for within sample and  $n_d(\theta_d^2 + (1 - \theta_d)^2)$  for all pairs, where  $n_{j,d}$  is the number of pairs of proviruses separated by no more than  $d$  base pairs where the first provirus is from sample  $j$ ,  $\theta_{j,d}$  is the proportion of silent/inducible proviruses in sample  $j$  appearing in at least one pair of proviruses separated by less than  $d$  base pairs and  $\neg j$  means all samples except sample  $j$ .

```

dists <- unique(round(10^seq(1, 6, 1)))

pairings <- do.call(rbind, lapply(dists, function(x,
  allNeighbors) {
  inSelector <- allNeighbors$dist <= x &
  allNeighbors$sample1 ==
  allNeighbors$sample2
  outSelector <- allNeighbors$dist <= x &
  allNeighbors$sample1 != allNeighbors$sample2
  allSelector <- allNeighbors$dist <= x
  out <- data.frame(dist = x, observedIn = sum(allNeighbors[
    inSelector,
    "latent1"] == allNeighbors[inSelector, "latent2"]),
    observedOut = sum(allNeighbors[outSelector,
    "latent1"] == allNeighbors[outSelector, "latent2"]),
    observedAll = sum(allNeighbors[allSelector, "latent1"])
    ==
    allNeighbors[allSelector, "latent2"]), totalIn =
  
```

```

        sum(inSelector) ,

totalOut = sum(outSelector), totalAll = sum(
    allSelector))

out$expectedIn <- sum(with(allNeighbors[inSelector, ],
    sapply(samples,
        function(x) {

            inLatent <- c(latent1[sample1 == x], latent2[
                sample2 ==
                x])[!duplicated(c(id1[sample1 == x], id2[
                    sample2 ==
                    x]))]

            if (length(inLatent) == 0) return(0)
            return(sum(sample1 == x) * (mean(inLatent)^2 +
                mean(!inLatent)^2))
        })))
}

out$expectedOut <- sum(with(allNeighbors[outSelector, ],
    sapply(samples, function(x) {

        inLatent <- c(latent1[sample1 == x], latent2[
            sample2 ==
            x])[!duplicated(c(id1[sample1 == x], id2[
                sample2 ==
                x]))]

        outLatent <- c(latent1[sample1 != x], latent2[
            sample2 !=
            x])[!duplicated(c(id1[sample1 != x], id2[
                sample2 !=
                x]))]
    })))
}

```

```

    if (length(inLatent) == 0) return(0)

    return(sum(sample1 == x) * (mean(inLatent) * mean(
        outLatent) +
        mean(!inLatent) * mean(!outLatent)))
    }))

out$expectedAll <- sum(with(allNeighbors[allSelector, ],
{
    allLatent <- c(latent1, latent2)[!duplicated(c(id1
        ,
        id2))]

    return(length(latent1) * (mean(allLatent)^2 + mean
        (!allLatent)^2))
})
return(out)
}, allNeighbors))

rownames(pairings) <- pairings$dist

```

To look for more matches than expected by random pairing between neighboring proviruses, we used a one sample Z-test of proportion to compare the observed number of matching pairs with the expected proportion of pairs.

```

combinations <- c(All = "All", `Between sample` = "Out", `
    Within sample` = "In")

lapply(combinations, function(x, pairing) {
    vars <- sprintf(c("observed%s", "expected%s", "total%s"),
        x)
    expectedProb <- pairing[, vars[2]]/pairing[, vars[3]]

```

```

prop.test(pairing[, vars[1]], pairing[, vars[3]], p =
  expectedProb)
}, pairings["100", ])

## $All

##
##      1-sample proportions test with continuity correction
##

## data:  pairing[, vars[1]] out of pairing[, vars[3]], null
## probability expectedProb

## X-squared = 13.002, df = 1, p-value = 0.0003111
## alternative hypothesis: true p is not equal to 0.5000141
## 95 percent confidence interval:
##  0.5586837 0.6962353
## sample estimates:
##   p
## 0.63
##
##
## $`Between sample`

##
##      1-sample proportions test with continuity correction
##

## data:  pairing[, vars[1]] out of pairing[, vars[3]], null
## probability expectedProb

## X-squared = 0.21919, df = 1, p-value = 0.6397
## alternative hypothesis: true p is not equal to 0.4836763
## 95 percent confidence interval:

```

```

##  0.3570532 0.5572662

## sample estimates:

##          p
## 0.4554455

##
## 

## $`Within sample`


##      1-sample proportions test with continuity correction

## 

## data: pairing[, vars[1]] out of pairing[, vars[3]], null
## probability expectedProb
## X-squared = 24.446, df = 1, p-value = 7.644e-07
## alternative hypothesis: true p is not equal to 0.5561437
## 95 percent confidence interval:
##  0.7140170 0.8776751
## sample estimates:
##          p
## 0.8080808

```

### A.2.10 Compiling this document

This document was generated using R's Sweave function (<http://en.wikipedia.org/wiki/Sweave>). If you would like to regenerate this document, download Additional Files 2, 3 and 4 from Sherrill-Mix et al.<sup>353</sup> and make sure the files are all in the same directory and named AdditionalFile2.csv.gz, AdditionalFile3.csv.gz and AdditionalFile4.Rnw. Then compile by going to that directory and using the commands:

R CMD Sweave AdditionalFile4.Rnw

pdflatex AdditionalFile4.tex

Note that you will need R and L<sup>A</sup>T<sub>E</sub>X (and the R package glmnet if you would like to rerun the lasso regressions) installed.

## BIBLIOGRAPHY

- [1] MS Gottlieb, HM Schanker, PT Fan, A Saxon, JD Weisman and I Pozalski. 1981. Pneumocystis pneumonia—Los Angeles. *MMWR Morb Mortal Wkly Rep*, 30:250–252
- [2] A Friedman-Kien, L Laubenstein, M Marmor, K Hymes, J Green, A Ragaz, J Gottlieb, F Muggia, R Demopoulos and M Weintraub. 1981. Kaposi's sarcoma and Pneumocystis pneumonia among homosexual men—New York City and California. *MMWR Morb Mortal Wkly Rep*, 30:305–308
- [3] KB Hymes, T Cheung, JB Greene, NS Prose, A Marcus, H Ballard, DC William and LJ Laubenstein. 1981. Kaposi's sarcoma in homosexual men—a report of eight cases. *Lancet*, 2:598–600. doi: 10.1016/S0140-6736(81)92740-9
- [4] H Masur, MA Michelis, JB Greene, I Onorato, RA Stouwe, RS Holzman, G Wormser, L Brettman, M Lange et al. 1981. An outbreak of community-acquired Pneumocystis carinii pneumonia: initial manifestation of cellular immune dysfunction. *N Engl J Med*, 305:1431–1438. doi: 10.1056/NEJM198112103052402
- [5] FP Siegal, C Lopez, GS Hammer, AE Brown, SJ Kornfeld, J Gold, J Hassett, SZ Hirschman, C Cunningham-Rundles and BR Adelsberg. 1981. Severe acquired immunodeficiency in male homosexuals, manifested by chronic perianal ulcerative herpes simplex lesion. *N Engl J Med*, 305:1439–1444. doi: 10.1056/NEJM198112103052403
- [6] MS Gottlieb, R Schroff, HM Schanker, JD Weisman, PT Fan, RA Wolf and A Saxon. 1981. Pneumocystis carinii pneumonia and mucosal candidiasis in previously healthy homosexual men: evidence of a new acquired cellular immunodeficiency. *N Engl J Med*, 305:1425–1431. doi: 10.1056/NEJM198112103052401
- [7] Y Laor and RA Schwartz. 1979. Epidemiologic aspects of American Kaposi's sarcoma. *J Surg Oncol*, 12:299–303. doi: 10.1002/jso.2930120403
- [8] MB Klein, FA Pereira and I Kantor. 1974. Kaposi Sarcoma complicating systemic lupus erythematosus treated with immunosuppression. *Arch Dermatol*, 110:602–604. doi: 10.1001/archderm.1974.01630100058014
- [9] BD Myers, E Kessler, J Levi, A Pick, JB Rosenfeld and P Tikvah. 1974. Kaposi sarcoma in kidney transplant recipients. *Arch Intern Med*, 133:307–311. doi: 10.1001/archinte.1974.00320140145017
- [10] SB Kapadia and JR Krause. 1977. Kaposi's sarcoma after long-term alkylating agent therapy for multiple myeloma. *South Med J*, 70:1011–1013
- [11] B Safai and RA Good. 1981. Kaposi's sarcoma: a review and recent developments. *CA Cancer J Clin*, 31:2–12. doi: 10.3322/canclin.31.1.2

- [12] Y Chang, E Cesarman, MS Pessin, F Lee, J Culpepper, DM Knowles and PS Moore. 1994. Identification of herpesvirus-like DNA sequences in AIDS-associated Kaposi's sarcoma. *Science*, 266:1865–1869. doi: 10.1126/science.7997879
- [13] F Sitas, H Carrara, V Beral, R Newton, G Reeves, D Bull, U Jentsch, R Pacella-Norman, D Bourboulia et al. 1999. Antibodies against human herpesvirus 8 in black South African patients with cancer. *N Engl J Med*, 340:1863–1871. doi: 10.1056/NEJM199906173402403
- [14] BA Burke and RA Good. 1973. Pneumocystis carinii infection. *Medicine (Baltimore)*, 52:23–51
- [15] WT Hughes. 1977. Pneumocystis carinii pneumonia. *N Engl J Med*, 297:1381–1383. doi: 10.1056/NEJM197712222972505
- [16] J Gerstoft, A Malchow-Møller, I Bygbjerg, E Dickmeiss, C Enk, P Halberg, S Haahr, M Jacobsen, K Jensen et al. 1982. Severe acquired immunodeficiency in European homosexual men. *Br Med J (Clin Res Ed)*, 285:17–19
- [17] H Masur, MA Michelis, GP Wormser, S Lewin, J Gold, ML Tapper, J Giron, CW Lerner, D Armstrong et al. 1982. Opportunistic infection in previously healthy women. Initial manifestations of a community-acquired cellular immunodeficiency. *Ann Intern Med*, 97:533–539
- [18] A Ammann, M Cowan, D Wara, H Goldman, H Perkins, R Lanzerotti, J Gullett, A Duff, S Dritz and J Chin. 1982. Possible transfusion-associated acquired immune deficiency syndrome (AIDS) — California. *MMWR Morb Mortal Wkly Rep*, 31:652–654
- [19] N Ehrenkranz, J Rubini, R Gunn, C Horsburgh, T Collins, U Hasiba, W Hathaway, W Doig, R Hopkins and J Elliott. 1982. Pneumocystis carinii pneumonia among persons with hemophilia A. *MMWR Morb Mortal Wkly Rep*, 31:365–367
- [20] MC Poon, A Landay, J Alexander, W Birch, M Eyster, H Al-Mondhiry, J Ballard, E Witte, C Hayes et al. 1982. Update on acquired immune deficiency syndrome (AIDS) among patients with hemophilia A. *MMWR Morb Mortal Wkly Rep*, 31:644–6, 652
- [21] JB Greene, GS Sidhu, S Lewin, JF Levine, H Masur, MS Simberkoff, P Nicholas, RC Good, SB Zolla-Pazner et al. 1982. Mycobacterium avium-intracellulare: a cause of disseminated life-threatening infection in homosexuals and drug abusers. *Ann Intern Med*, 97:539–546
- [22] R O'Reilly, D Kirkpatrick, CB Small, R Klein, H Keltz, G Friedland, K Bromberg, S Fikrig, H Mendez et al. 1982. Unexplained immunodeficiency and opportunistic infections in infants—New York, New Jersey, California. *MMWR Morb Mortal Wkly Rep*, 31:665–667
- [23] S Fannin, M Gottlieb, J Weisman, E Rogolsky, T Prendergast, J Chin, A Friedman-

- Kien, L Laubenstein, S Friedman and R Rothenberg. 1982. A cluster of Kaposi's sarcoma and Pneumocystis carinii pneumonia among homosexual male residents of Los Angeles and Orange Counties, California. *MMWR Morb Mortal Wkly Rep*, 31: 305–307
- [24] C Harris, CB Small, G Friedland, R Klein, B Moll, E Emeson, I Spigland, N Steigbigel, R Reiss et al. 1983. Immunodeficiency among female sexual partners of males with acquired immune deficiency syndrome (AIDS) — New York. *MMWR Morb Mortal Wkly Rep*, 31:697–698
  - [25] F Barré-Sinoussi, JC Chermann, F Rey, MT Nugeyre, S Chamaret, J Gruest, C Dauguet, C Axler-Blin, F Vézinet-Brun et al. 1983. Isolation of a T-lymphotropic retrovirus from a patient at risk for acquired immune deficiency syndrome (AIDS). *Science*, 220: 868–871
  - [26] RC Gallo, PS Sarin, EP Gelmann, M Robert-Guroff, E Richardson, VS Kalyanaraman, D Mann, GD Sidhu, RE Stahl et al. 1983. Isolation of human T-cell leukemia virus in acquired immune deficiency syndrome (AIDS). *Science*, 220:865–867. doi: 10.1126/science.6601823
  - [27] M Popovic, MG Sarngadharan, E Read and RC Gallo. 1984. Detection, isolation, and continuous production of cytopathic retroviruses (HTLV-III) from patients with AIDS and pre-AIDS. *Science*, 224:497–500. doi: 10.1126/science.6200935
  - [28] JA Levy, AD Hoffman, SM Kramer, JA Landis, JM Shimabukuro and LS Oshiro. 1984. Isolation of lymphocytopathic retroviruses from San Francisco patients with AIDS. *Science*, 225:840–842. doi: 10.1126/science.6206563
  - [29] RC Gallo, SZ Salahuddin, M Popovic, GM Shearer, M Kaplan, BF Haynes, TJ Parker, R Redfield, J Oleske and B Safai. 1984. Frequent detection and isolation of cytopathic retroviruses (HTLV-III) from patients with AIDS and at risk for AIDS. *Science*, 224: 500–503. doi: 10.1126/science.6200936
  - [30] MG Sarngadharan, M Popovic, L Bruch, J Schüpbach and RC Gallo. 1984. Antibodies reactive with human T-lymphotropic retroviruses (HTLV-III) in the serum of patients with AIDS. *Science*, 224:506–508. doi: 10.1126/science.6324345
  - [31] B Safai, MG Sarngadharan, JE Groopman, K Arnett, M Popovic, A Sliski, J Schüpbach and RC Gallo. 1984. Seroepidemiological studies of human T-lymphotropic retrovirus type III in acquired immunodeficiency syndrome. *Lancet*, 1:1438–1440. doi: 10.1016/S0140-6736(84)91933-0
  - [32] N Clumeck, F Mascart-Lemone, J de Maubeuge, D Brenez and L Marcelis. 1983. Acquired immune deficiency syndrome in Black Africans. *Lancet*, 1:642. doi: 10.1016/S0140-6736(83)91808-1
  - [33] N Clumeck, J Sonnet, H Taelman, S Cran and P Henrivaux. 1984. Acquired immune

- deficiency syndrome in Belgium and its relation to Central Africa. *Ann N Y Acad Sci*, 437:264–269. doi: 10.1111/j.1749-6632.1984.tb37144.x
- [34] P Van de Perre, D Rouvroy, P Lepage, J Bogaerts, P Kestelyn, J Kayihigi, AC Hekker, JP Butzler and N Clumeck. 1984. Acquired immunodeficiency syndrome in Rwanda. *Lancet*, 2:62–65. doi: 10.1016/S0140-6736(84)90240-X
- [35] P Piot, TC Quinn, H Taelman, FM Feinsod, KB Minlangu, O Wobin, N Mbendi, P Mazebo, K Ndangi and W Stevens. 1984. Acquired immunodeficiency syndrome in a heterosexual population in Zaire. *Lancet*, 2:65–69. doi: 10.1016/S0140-6736(84)90241-1
- [36] JN Nkengasong, W Janssens, L Heyndrickx, K Fransen, PM Ndumbe, J Motte, A Leonaers, M Ngolle, J Ayuk and P Piot. 1994. Genotypic subtypes of HIV-1 in Cameroon. *AIDS*, 8:1405–1412
- [37] J Louwagie, W Janssens, J Mascola, L Heyndrickx, P Hegerich, G van der Groen, FE McCutchan and DS Burke. 1995. Genetic diversity of the envelope glycoprotein from human immunodeficiency virus type 1 isolates of African origin. *J Virol*, 69: 263–271
- [38] N Vidal, M Peeters, C Mulanga-Kabeya, N Nzilambi, D Robertson, W Ilunga, H Sema, K Tshimanga, B Bongo and E Delaporte. 2000. Unprecedented degree of human immunodeficiency virus type 1 (HIV-1) group M genetic diversity in the Democratic Republic of Congo suggests that the HIV-1 pandemic originated in Central Africa. *J Virol*, 74:10498–10507. doi: 10.1128/JVI.74.22.10498-10507.2000
- [39] A Rambaut, DL Robertson, OG Pybus, M Peeters and EC Holmes. 2001. Human immunodeficiency virus. Phylogeny and the origin of HIV-1. *Nature*, 410:1047–1048. doi: 10.1038/35074179
- [40] C Yang, B Dash, SL Hanna, HS Frances, N Nzilambi, RC Colebunders, M St Louis, TC Quinn, TM Folks and RB Lal. 2001. Predominance of HIV type 1 subtype G among commercial sex workers from Kinshasa, Democratic Republic of Congo. *AIDS Res Hum Retroviruses*, 17:361–365. doi: 10.1089/08892220150503726
- [41] ML Kalish, KE Robbins, D Pieniazek, A Schaefer, N Nzilambi, TC Quinn, ME St Louis, AS Youngpairoj, J Phillips et al. 2004. Recombinant viruses and early global HIV-1 epidemic. *Emerg Infect Dis*, 10:1227–1234. doi: 10.3201/eid1007.030904
- [42] SS Frøland, P Jenum, CF Lindboe, KW Webring, PJ Linnestad and T Böhmer. 1988. HIV-1 infection in Norwegian family before 1970. *Lancet*, 1:1344–1345. doi: 10.1016/S0140-6736(88)92164-2
- [43] RF Garry, MH Witte, AA Gottlieb, M Elvin-Lewis, MS Gottlieb, CL Witte, SS Alexander, WR Cole and W Drake, Jr. 1988. Documentation of an AIDS virus infection in the United States in 1968. *JAMA*, 260:2085–2087. doi: 10.1001/jama.1988.03410140097031

- [44] IC Bygbjerg. 1983. AIDS in a Danish surgeon (Zaire, 1976). *Lancet*, 1:925. doi: 10.1016/S0140-6736(83)91348-X
- [45] J Vandepitte, R Verwilghen and P Zachee. 1983. AIDS and cryptococcosis (Zaire, 1977). *Lancet*, 1:925–926. doi: 10.1016/S0140-6736(83)91349-1
- [46] AJ Nahmias, J Weiss, X Yao, F Lee, R Kodsi, M Schanfield, T Matthews, D Bolognesi, D Durack and A Motulsky. 1986. Evidence for human infection with an HTLV III/LAV-like virus in Central Africa, 1959. *Lancet*, 1:1279–1280. doi: 10.1016/S0140-6736(86)91422-4
- [47] T Zhu, BT Korber, AJ Nahmias, E Hooper, PM Sharp and DD Ho. 1998. An African HIV-1 sequence from 1959 and implications for the origin of the epidemic. *Nature*, 391:594–597. doi: 10.1038/35400
- [48] M Worobey, M Gemmel, DE Teuwen, T Haselkorn, K Kunstman, M Bunce, JJ Muyembe, JMM Kabongo, RM Kalengayi et al. 2008. Direct evidence of extensive diversity of HIV-1 in Kinshasa by 1960. *Nature*, 455:661–664. doi: 10.1038/nature07390
- [49] B Korber, M Muldoon, J Theiler, F Gao, R Gupta, A Lapedes, BH Hahn, S Wolinsky and T Bhattacharya. 2000. Timing the ancestor of the HIV-1 pandemic strains. *Science*, 288:1789–1796. doi: 10.1126/science.288.5472.1789
- [50] M Salemi, K Strimmer, WW Hall, M Duffy, E Delaporte, S Mboup, M Peeters and AM Vandamme. 2001. Dating the common ancestor of SIVcpz and HIV-1 group M and the origin of HIV-1 subtypes using a new method to uncover clock-like molecular evolution. *FASEB J*, 15:276–278. doi: 10.1096/fj.00-0449fje
- [51] PM Sharp, E Bailes, RR Chaudhuri, CM Rodenburg, MO Santiago and BH Hahn. 2001. The origins of acquired immune deficiency syndrome viruses: where and when? *Philos Trans R Soc Lond B Biol Sci*, 356:867–876. doi: 10.1098/rstb.2001.0863
- [52] K Yusim, M Peeters, OG Pybus, T Bhattacharya, E Delaporte, C Mulanga, M Muldoon, J Theiler and B Korber. 2001. Using human immunodeficiency virus type 1 sequences to infer historical features of the acquired immune deficiency syndrome epidemic and human immunodeficiency virus evolution. *Philos Trans R Soc Lond B Biol Sci*, 356: 855–866. doi: 10.1098/rstb.2001.0859
- [53] NR Faria, A Rambaut, MA Suchard, G Baele, T Bedford, MJ Ward, AJ Tatem, JD Sousa, N Arinaminpathy et al. 2014. The early spread and epidemic ignition of HIV-1 in human populations. *Science*, 346:56–61. doi: 10.1126/science.1256739
- [54] MD Daniel, NL Letvin, NW King, M Kannagi, PK Sehgal, RD Hunt, PJ Kanki, M Essex and RC Desrosiers. 1985. Isolation of T-cell tropic HTLV-III-like retrovirus from macaques. *Science*, 228:1201–1204. doi: 10.1126/science.3159089
- [55] M Peeters, C Honoré, T Huet, L Bedjabaga, S Ossari, P Bussi, RW Cooper and

- E Delaporte. 1989. Isolation and partial characterization of an HIV-related virus occurring naturally in chimpanzees in Gabon. *AIDS*, 3:625–630
- [56] M Peeters, V Courgnaud and B Abela. 2001. Genetic diversity of lentiviruses in non-human primates. *AIDS Rev*, 3:3–10
- [57] T Huet, R Cheynier, A Meyerhans, G Roelants and S Wain-Hobson. 1990. Genetic organization of a chimpanzee lentivirus related to HIV-1. *Nature*, 345:356–359. doi: 10.1038/345356a0
- [58] F Gao, E Bailes, DL Robertson, Y Chen, CM Rodenburg, SF Michael, LB Cummins, LO Arthur, M Peeters et al. 1999. Origin of HIV-1 in the chimpanzee Pan troglodytes troglodytes. *Nature*, 397:436–441. doi: 10.1038/17130
- [59] BF Keele, F Van Heuverswyn, Y Li, E Bailes, J Takehisa, ML Santiago, F Bibollet-Ruche, Y Chen, LV Wain et al. 2006. Chimpanzee reservoirs of pandemic and nonpandemic HIV-1. *Science*, 313:523–526. doi: 10.1126/science.1126531
- [60] F Van Heuverswyn, Y Li, E Bailes, C Neel, B Lafay, BF Keele, KS Shaw, J Takehisa, MH Kraus et al. 2007. Genetic diversity and phylogeographic clustering of SIVcpzPtt in wild chimpanzees in Cameroon. *Virology*, 368:155–171. doi: 10.1016/j.virol.2007.06.018
- [61] E Bowen-Jones and S Pendry. 1999. The threat to primates and other mammals from the bushmeat trade in Africa, and how this threat could be diminished. *Oryx*, 33: 233–246. doi: 10.1046/j.1365-3008.1999.00066.x
- [62] BH Hahn, GM Shaw, KM De Cock and PM Sharp. 2000. AIDS as a zoonosis: scientific and public health implications. *Science*, 287:607–614. doi: 10.1126/science.287.5453.607
- [63] M Peeters, V Courgnaud, B Abela, P Auzel, X Pourrut, F Bibollet-Ruche, S Loul, F Liegeois, C Butel et al. 2002. Risk to human health from a plethora of simian immunodeficiency viruses in primate bushmeat. *Emerg Infect Dis*, 8:451–457. doi: 10.3201/eid0805.010522
- [64] ND Wolfe, TA Prosser, JK Carr, U Tamoufe, E Mpoudi-Ngole, JN Torimiro, M LeBreton, FE McCutchan, DL Birx and DS Burke. 2004. Exposure to nonhuman primates in rural Cameroon. *Emerg Infect Dis*, 10:2094–2099. doi: 10.3201/eid1012.040062
- [65] ND Wolfe, W Heneine, JK Carr, AD Garcia, V Shanmugam, U Tamoufe, JN Torimiro, AT Prosser, M Lebreton et al. 2005. Emergence of unique primate T-lymphotropic viruses among central African bushmeat hunters. *Proc Natl Acad Sci U S A*, 102: 7994–7999. doi: 10.1073/pnas.0501734102
- [66] ML Kalish, ND Wolfe, CB Ndongmo, J McNicholl, KE Robbins, M Aidoo, PN Fonjungo, G Alemnji, C Zeh et al. 2005. Central African hunters exposed to simian immunodeficiency virus. *Emerg Infect Dis*, 11:1928–1930. doi: 10.3201/eid1112.050394

- [67] PM Sharp and BH Hahn. 2008. AIDS: prehistory of HIV-1. *Nature*, 455:605–606. doi: 10.1038/455605a
- [68] D Vangroenweghe. 2001. The earliest cases of human immunodeficiency virus type 1 group M in Congo-Kinshasa, Rwanda and Burundi and the origin of acquired immune deficiency syndrome. *Philos Trans R Soc Lond B Biol Sci*, 356:923–925. doi: 10.1098/rstb.2001.0876
- [69] A Chitnis, D Rawls and J Moore. 2000. Origin of HIV type 1 in colonial French Equatorial Africa? *AIDS Res Hum Retroviruses*, 16:5–8. doi: 10.1089/088922200309548
- [70] JD de Sousa, V Müller, P Lemey and AM Vandamme. 2010. High GUD incidence in the early 20 century created a particularly permissive time window for the origin and initial spread of epidemic HIV strains. *PLoS One*, 5:e9936. doi: 10.1371/journal.pone.0009936
- [71] JD de Sousa, C Alvarez, AM Vandamme and V Müller. 2012. Enhanced heterosexual transmission hypothesis for the origin of pandemic HIV-1. *Viruses*, 4:1950–1983. doi: 10.3390/v4101950
- [72] MTP Gilbert, A Rambaut, G Wlasiuk, TJ Spira, AE Pitchenik and M Worobey. 2007. The emergence of HIV/AIDS in the Americas and beyond. *Proc Natl Acad Sci U S A*, 104:18566–18570. doi: 10.1073/pnas.0705329104
- [73] UNAIDS Communications and Global Advocacy. 2014. Fact sheet 2014. URL <http://www.unaids.org/en/resources/campaigns/2014/2014gapreport/factsheet>
- [74] RD Moore and RE Chaisson. 1996. Natural history of opportunistic disease in an HIV-infected urban clinical cohort. *Ann Intern Med*, 124:633–642. doi: 10.7326/0003-4819-124-7-199604010-00003
- [75] R Rothenberg, M Woelfel, R Stoneburner, J Milberg, R Parker and B Truman. 1987. Survival with the acquired immunodeficiency syndrome. Experience with 5833 cases in New York City. *N Engl J Med*, 317:1297–1302. doi: 10.1056/NEJM198711193172101
- [76] S Vella, M Giuliano, P Pezzotti, MG Agresti, C Tomino, M Floridia, D Greco, M Moroni, G Visco and F Milazzo. 1992. Survival of zidovudine-treated patients with AIDS compared with that of contemporary untreated patients. *JAMA*, 267:1232–1236. doi: 10.1001/jama.1992.03480090080031
- [77] KJ Lui, DN Lawrence, WM Morgan, TA Peterman, HW Havercos and DJ Bregman. 1986. A model-based approach for estimating the mean incubation period of transfusion-associated acquired immunodeficiency syndrome. *Proc Natl Acad Sci U S A*, 83: 3051–3055
- [78] MM Deschamps, DW Fitzgerald, JW Pape and W Johnson, Jr. 2000. HIV infection in Haiti: natural history and disease progression. *AIDS*, 14:2515–2521

- [79] KM Harrison, R Song and X Zhang. 2010. Life expectancy after HIV diagnosis based on national HIV surveillance data from 25 states, United States. *J Acquir Immune Defic Syndr*, 53:124–130. doi: 10.1097/QAI.0b013e3181b563e7
- [80] Collaborative Group on AIDS Incubation and HIV Survival. 2000. Time from HIV-1 seroconversion to AIDS and death before widespread use of highly-active antiretroviral therapy: a collaborative re-analysis. *Lancet*, 355:1131–1137. doi: 10.1016/S0140-6736(00)02061-4
- [81] MA Fischl, DD Richman, MH Grieco, MS Gottlieb, PA Volberding, OL Laskin, JM Leedom, JE Groopman, D Mildvan and RT Schooley. 1987. The efficacy of azidothymidine (AZT) in the treatment of patients with AIDS and AIDS-related complex. A double-blind, placebo-controlled trial. *N Engl J Med*, 317:185–191. doi: 10.1056/NEJM198707233170401
- [82] MA Fischl, DD Richman, DM Causey, MH Grieco, Y Bryson, D Mildvan, OL Laskin, JE Groopman, PA Volberding and RT Schooley. 1989. Prolonged zidovudine therapy in patients with AIDS and advanced AIDS-related complex. *JAMA*, 262:2405–2410. doi: 10.1001/jama.1989.03430170067030
- [83] PA Volberding, SW Lagakos, MA Koch, C Pettinelli, MW Myers, DK Booth, H Balfour, Jr, RC Reichman, JA Bartlett et al. 1990. Zidovudine in asymptomatic human immunodeficiency virus infection. A controlled trial in persons with fewer than 500 CD4-positive cells per cubic millimeter. *N Engl J Med*, 322:941–949. doi: 10.1056/NEJM199004053221401
- [84] BH Hahn, GM Shaw, ME Taylor, RR Redfield, PD Markham, SZ Salahuddin, F Wong-Staal, RC Gallo, ES Parks and WP Parks. 1986. Genetic variation in HTLV-III/LAV over time in patients with AIDS or at risk for AIDS. *Science*, 232:1548–1553. doi: 10.1126/science.3012778
- [85] BD Preston, BJ Poiesz and LA Loeb. 1988. Fidelity of HIV-1 reverse transcriptase. *Science*, 242:1168–1171. doi: 10.1126/science.2460924
- [86] JD Roberts, K Bebenek and TA Kunkel. 1988. The accuracy of reverse transcriptase from HIV-1. *Science*, 242:1171–1173. doi: 10.1126/science.2460925
- [87] LM Mansky and HM Temin. 1995. Lower in vivo mutation rate of human immunodeficiency virus type 1 than that predicted from the fidelity of purified reverse transcriptase. *J Virol*, 69:5087–5094
- [88] LM Mansky. 1996. The mutation rate of human immunodeficiency virus type 1 is influenced by the vpr gene. *Virology*, 222:391–400. doi: 10.1006/viro.1996.0436
- [89] ME Abram, AL Ferris, W Shao, WG Alvord and SH Hughes. 2010. Nature, position, and frequency of mutations made in a single cycle of HIV-1 replication. *J Virol*, 84: 9864–9878. doi: 10.1128/JVI.00915-10

- [90] V Achuthan, BJ Keith, BA Connolly and JJ DeStefano. 2014. Human immunodeficiency virus reverse transcriptase displays dramatically higher fidelity under physiological magnesium conditions in vitro. *J Virol*, 88:8514–8527. doi: 10.1128/JVI.00752-14
- [91] BA Larder, G Darby and DD Richman. 1989. HIV with reduced sensitivity to zidovudine (AZT) isolated during prolonged therapy. *Science*, 243:1731–1734. doi: 10.1126/science.2467383
- [92] BA Larder and SD Kemp. 1989. Multiple mutations in HIV-1 reverse transcriptase confer high-level resistance to zidovudine (AZT). *Science*, 246:1155–1158. doi: 10.1126/science.2479983
- [93] S Land, G Terloar, D McPhee, C Birch, R Doherty, D Cooper and I Gust. 1990. Decreased in vitro susceptibility to zidovudine of HIV isolates obtained from patients with AIDS. *J Infect Dis*, 161:326–329. doi: 10.1093/infdis/161.2.326
- [94] CA Boucher, M Tersmette, JM Lange, P Kellam, RE de Goede, JW Mulder, G Darby, J Goudsmit and BA Larder. 1990. Zidovudine sensitivity of human immunodeficiency viruses from high-risk, symptom-free individuals during therapy. *Lancet*, 336:585–590. doi: 10.1016/0140-6736(90)93391-2
- [95] DD Richman, JM Grimes and SW Lagakos. 1990. Effect of stage of disease and drug dose on zidovudine susceptibilities of isolates of human immunodeficiency virus. *J Acquir Immune Defic Syndr*, 3:743–746
- [96] DD Richman, JC Guatelli, J Grimes, A Tsiatis and T Gingeras. 1991. Detection of mutations associated with zidovudine resistance in human immunodeficiency virus by use of the polymerase chain reaction. *J Infect Dis*, 164:1075–1081. doi: 10.1093/infdis/164.6.1075
- [97] JE Fitzgibbon, RM Howell, CA Haberzettl, SJ Sperber, DJ Gocke and DT Dubin. 1992. Human immunodeficiency virus type 1 pol gene mutations which cause decreased susceptibility to 2',3'-dideoxycytidine. *Antimicrob Agents Chemother*, 36:153–157. doi: 10.1128/AAC.36.1.153
- [98] DD Richman, D Havlir, J Corbeil, D Looney, C Ignacio, SA Spector, J Sullivan, S Cheeseman, K Barringer and D Pauletti. 1994. Nevirapine resistance mutations of human immunodeficiency virus type 1 selected during therapy. *J Virol*, 68:1660–1666
- [99] R Schuurman, M Nijhuis, R van Leeuwen, P Schipper, D de Jong, P Collis, SA Danner, J Mulder, C Loveday and C Christoperson. 1995. Rapid changes in human immunodeficiency virus type 1 RNA load and appearance of drug-resistant virus populations in persons treated with lamivudine (3TC). *J Infect Dis*, 171:1411–1419. doi: 10.1093/infdis/171.6.1411
- [100] JC Schmit, L Ruiz, B Clotet, A Raventos, J Tor, J Leonard, J Desmyter, E De Clercq and AM Vandamme. 1996. Resistance-related mutations in the HIV-1 protease gene

of patients treated for 1 year with the protease inhibitor ritonavir (ABT-538). *AIDS*, 10:995–999

- [101] T Creagh-Kirk, P Doi, E Andrews, S Nusinoff-Lehrman, H Tilson, D Hoth and DW Barry. 1988. Survival experience among patients with AIDS receiving zidovudine. Follow-up of patients in a compassionate plea program. *JAMA*, 260:3009–3015. doi: 10.1001/jama.1988.03410200065027
- [102] RD Moore, J Keruly, DD Richman, T Creagh-Kirk and RE Chaisson. 1992. Natural history of advanced HIV disease in patients treated with zidovudine. *AIDS*, 6:671–677
- [103] S Vella, B Schwartländer, SP Sow, SP Eholie and RL Murphy. 2012. The history of antiretroviral therapy and of its implementation in resource-limited areas of the world. *AIDS*, 26:1231–1241. doi: 10.1097/QAD.0b013e32835521a3
- [104] JO Kahn, SW Lagakos, DD Richman, A Cross, C Pettinelli, SH Liou, M Brown, PA Volberding, CS Crumpacker and G Beall. 1992. A controlled trial comparing continued zidovudine with didanosine in human immunodeficiency virus infection. *N Engl J Med*, 327:581–587. doi: 10.1056/NEJM199208273270901
- [105] G Skowron, SA Bozzette, L Lim, CB Pettinelli, HH Schaumburg, J Arezzo, MA Fischl, WG Powderly, DJ Gocke et al. 1993. Alternating and intermittent regimens of zidovudine and dideoxycytidine in patients with AIDS or AIDS-related complex. *Ann Intern Med*, 118:321–330
- [106] DI Abrams, AI Goldman, C Launer, JA Korvick, JD Neaton, LR Crane, M Grodesky, S Wakefield, K Muth and S Kornegay. 1994. A comparative trial of didanosine or zalcitabine after treatment with zidovudine in patients with human immunodeficiency virus infection. *N Engl J Med*, 330:657–662. doi: 10.1056/NEJM199403103301001
- [107] MD de Jong, M Loewenthal, CA Boucher, I van der Ende, D Hall, P Schipper, A Imrie, HM Weigel, RH Kauffmann and R Koster. 1994. Alternating nevirapine and zidovudine treatment of human immunodeficiency virus type 1-infected persons does not prolong nevirapine activity. *J Infect Dis*, 169:1346–1350. doi: 10.1093/infdis/169.6.1346
- [108] JC Schmit, J Cogniaux, P Hermans, C Van Vaeck, S Sprecher, B Van Remoortel, M Witvrouw, J Balzarini, J Desmyter et al. 1996. Multiple drug resistance to nucleoside analogues and nonnucleoside reverse transcriptase inhibitors in an efficiently replicating human immunodeficiency virus type 1 patient strain. *J Infect Dis*, 174:962–968. doi: 10.1093/infdis/174.5.962
- [109] AC Collier, RW Coombs, MA Fischl, PR Skolnik, D Northfelt, P Boutin, CJ Hooper, LD Kaplan, PA Volberding et al. 1993. Combination therapy with zidovudine and didanosine compared with zidovudine alone in HIV-1 infection. *Ann Intern Med*, 119: 786–793. doi: 10.7326/0003-4819-119-8-199310150-00003
- [110] SM Hammer, DA Katzenstein, MD Hughes, H Gundacker, RT Schooley, RH Haubrich,

- WK Henry, MM Lederman, JP Phair et al. 1996. A trial comparing nucleoside monotherapy with combination therapy in HIV-infected adults with CD4 cell counts from 200 to 500 per cubic millimeter. *N Engl J Med*, 335:1081–1090. doi: 10.1056/NEJM199610103351501
- [111] JJ Eron, SL Benoit, J Jemsek, RD MacArthur, J Santana, JB Quinn, DR Kuritzkes, MA Fallon and M Rubin. 1995. Treatment with lamivudine, zidovudine, or both in HIV-positive patients with 200 to 500 CD4+ cells per cubic millimeter. *N Engl J Med*, 333:1662–1669. doi: 10.1056/NEJM199512213332502
- [112] LD Saravolatz, DL Winslow, G Collins, JS Hodges, C Pettinelli, DS Stein, N Markowitz, R Reves, MO Loveless et al. 1996. Zidovudine alone or in combination with didanosine or zalcitabine in HIV-infected patients with the acquired immunodeficiency syndrome or fewer than 200 CD4 cells per cubic millimeter. *N Engl J Med*, 335:1099–1106. doi: 10.1056/NEJM199610103351503
- [113] J Darbyshire, Delta Coordinating Committee et al. 1996. Delta: a randomised double-blind controlled trial comparing combinations of zidovudine plus didanosine or zalcitabine with zidovudine alone in HIV-infected individuals. *Lancet*, 348:283–291. doi: 10.1016/S0140-6736(96)05387-1
- [114] RE Dornsife, MH St Clair, AT Huang, TJ Panella, GW Koszalka, CL Burns and DR Averett. 1991. Anti-human immunodeficiency virus synergism by zidovudine (3'-azidothymidine) and didanosine (dideoxyinosine) contrasts with their additive inhibition of normal human marrow progenitor cells. *Antimicrob Agents Chemother*, 35:322–328. doi: 10.1128/AAC.35.2.322
- [115] VA Johnson, DP Merrill, JA Videler, TC Chou, RE Byington, JJ Eron, RT D'Aquila and MS Hirsch. 1991. Two-drug combinations of zidovudine, didanosine, and recombinant interferon-alpha A inhibit replication of zidovudine-resistant human immunodeficiency virus type 1 synergistically in vitro. *J Infect Dis*, 164:646–655. doi: 10.1093/infdis/164.4.646
- [116] SW Cox, K Apéria, J Albert and B Wahren. 1994. Comparison of the sensitivities of primary isolates of HIV type 2 and HIV type 1 to antiviral drugs and drug combinations. *AIDS Res Hum Retroviruses*, 10:1725–1729. doi: 10.1177/095632029300400407
- [117] JY Feng, JK Ly, F Myrick, D Goodman, KL White, ES Svarovskaia, K Borroto-Esoda and MD Miller. 2009. The triple combination of tenofovir, emtricitabine and efavirenz shows synergistic anti-HIV-1 activity in vitro: a mechanism of action study. *Retrovirology*, 6:44. doi: 10.1186/1742-4690-6-44
- [118] BL Jilek, M Zarr, ME Sampah, SA Rabi, CK Bullen, J Lai, L Shen and RF Siliciano. 2012. A quantitative basis for antiretroviral therapy for HIV-1 infection. *Nat Med*, 18: 446–451. doi: 10.1038/nm.2649
- [119] R Kulkarni, R Hluhanich, DM McColl, MD Miller and KL White. 2014. The com-

- bined anti-HIV-1 activities of emtricitabine and tenofovir plus the integrase inhibitor elvitegravir or raltegravir show high levels of synergy in vitro. *Antimicrob Agents Chemother*, 58:6145–6150. doi: 10.1128/AAC.03591-14
- [120] YK Chow, MS Hirsch, DP Merrill, LJ Bechtel, JJ Eron, JC Kaplan and RT D'Aquila. 1993. Use of evolutionary limitations of HIV-1 multidrug resistance to optimize therapy. *Nature*, 361:650–654. doi: 10.1038/361650a0
- [121] BA Larder, SD Kemp and PR Harrigan. 1995. Potential mechanism for sustained antiretroviral efficacy of AZT-3TC combination therapy. *Science*, 269:696–699. doi: 10.1126/science.7542804
- [122] AC Collier, RW Coombs, DA Schoenfeld, RL Bassett, J Timpone, A Baruch, M Jones, K Facey, C Whitacre et al. 1996. Treatment of human immunodeficiency virus infection with saquinavir, zidovudine, and zalcitabine. *N Engl J Med*, 334:1011–1017. doi: 10.1056/NEJM199604183341602
- [123] SM Hammer, KE Squires, MD Hughes, JM Grimes, LM Demeter, JS Currier, J Eron, Jr, JE Feinberg, H Balfour, Jr et al. 1997. A controlled trial of two nucleoside analogues plus indinavir in persons with human immunodeficiency virus infection and CD4 cell counts of 200 per cubic millimeter or less. *N Engl J Med*, 337:725–733. doi: 10.1056/NEJM199709113371101
- [124] RM Gulick, JW Mellors, D Havlir, JJ Eron, C Gonzalez, D McMahon, DD Richman, FT Valentine, L Jonas et al. 1997. Treatment with indinavir, zidovudine, and lamivudine in adults with human immunodeficiency virus infection and prior antiretroviral therapy. *N Engl J Med*, 337:734–739. doi: 10.1056/NEJM199709113371102
- [125] JS Montaner, P Reiss, D Cooper, S Vella, M Harris, B Conway, MA Wainberg, D Smith, P Robinson et al. 1998. A randomized, double-blind trial comparing combinations of nevirapine, didanosine, and zidovudine for HIV-infected patients: the INCAS Trial. Italy, The Netherlands, Canada and Australia Study. *JAMA*, 279:930–937. doi: 10.1001/jama.279.12.930
- [126] RD Moore and RE Chaisson. 1999. Natural history of HIV infection in the era of combination antiretroviral therapy. *AIDS*, 13:1933–1942
- [127] Antiretroviral Therapy Cohort Collaboration, M Zwahlen, R Harris, M May, R Hogg, D Costagliola, F de Wolf, J Gill, G Fätkenheuer et al. 2009. Mortality of HIV-infected patients starting potent antiretroviral therapy: comparison with the general population in nine industrialized countries. *Int J Epidemiol*, 38:1624–1633. doi: 10.1093/ije/dyp306
- [128] AI van Sighem, LAJ Gras, P Reiss, K Brinkman, F de Wolf and ATHENAco . 2010. Life expectancy of recently diagnosed asymptomatic HIV-infected patients approaches that of uninfected individuals. *AIDS*, 24:1527–1535. doi: 10.1097/QAD.0b013e32833a3946

- [129] F Nakagawa, RK Lodwick, CJ Smith, R Smith, V Cambiano, JD Lundgren, V Delpech and AN Phillips. 2012. Projected life expectancy of people with HIV according to timing of diagnosis. *AIDS*, 26:335–343. doi: 10.1097/QAD.0b013e32834dcec9
- [130] F Nakagawa, M May and A Phillips. 2013. Life expectancy living with HIV: recent estimates and future implications. *Curr Opin Infect Dis*, 26:17–25. doi: 10.1097/QCO.0b013e32835ba6b1
- [131] LF Johnson, J Mossong, RE Dorrington, M Schomaker, CJ Hoffmann, O Keiser, MP Fox, R Wood, H Prozesky et al. 2013. Life expectancies of South African adults starting antiretroviral treatment: collaborative analysis of cohort studies. *PLoS Med*, 10:e1001418. doi: 10.1371/journal.pmed.1001418
- [132] G Hüttner, D Nowak, M Mossner, S Ganepola, A Müssig, K Allers, T Schneider, J Hoffmann, C Kücherer et al. 2009. Long-term control of HIV by CCR5 Delta32/Delta32 stem-cell transplantation. *N Engl J Med*, 360:692–698. doi: 10.1056/NEJMoa0802905
- [133] E Check Hayden. 2013. Hopes of HIV cure in 'Boston patients' dashed. *Nature*, 785: 6–8. doi: 10.1038/nature.2013.14324
- [134] RT Davey, N Bhat, C Yoder, TW Chun, JA Metcalf, R Dewar, V Natarajan, RA Lemppicki, JW Adelsberger et al. 1999. HIV-1 and T cell dynamics after interruption of highly active antiretroviral therapy (HAART) in patients with a history of sustained viral suppression. *Proc Natl Acad Sci U S A*, 96:15109–15114
- [135] E Hamlyn, FM Ewings, K Porter, DA Cooper, G Tambussi, M Schechter, C Pedersen, JF Okulicz, M McClure et al. 2012. Plasma HIV viral rebound following protocol-indicated cessation of ART commenced in primary and chronic HIV infection. *PLoS One*, 7:e43754. doi: 10.1371/journal.pone.0043754
- [136] W Stöhr, S Fidler, M McClure, J Weber, D Cooper, G Ramjee, P Kaleebu, G Tambussi, M Schechter et al. 2013. Duration of HIV-1 viral suppression on cessation of antiretroviral therapy in primary infection correlates with time on therapy. *PLoS One*, 8:e78287. doi: 10.1371/journal.pone.0078287
- [137] TW Chun, D Engel, MM Berrey, T Shea, L Corey and AS Fauci. 1998. Early establishment of a pool of latently infected, resting CD4(+) T cells during primary HIV-1 infection. *Proc Natl Acad Sci U S A*, 95:8869–8873
- [138] JB Whitney, AL Hill, S Sanisetty, P Penaloza-MacMaster, J Liu, M Shetty, L Parenteau, C Cabral, J Shields et al. 2014. Rapid seeding of the viral reservoir prior to SIV viraemia in rhesus monkeys. *Nature*, 512:74–77. doi: 10.1038/nature13594
- [139] D Finzi, M Hermankova, T Pierson, LM Carruth, C Buck, RE Chaisson, TC Quinn, K Chadwick, J Margolick et al. 1997. Identification of a reservoir for HIV-1 in patients on highly active antiretroviral therapy. *Science*, 278:1295–1300. doi: 10.1126/science.278.5341.1295

- [140] TW Chun, L Carruth, D Finzi, X Shen, JA DiGiuseppe, H Taylor, M Hermankova, K Chadwick, J Margolick et al. 1997. Quantification of latent tissue reservoirs and total body viral load in HIV-1 infection. *Nature*, 387:183–188. doi: 10.1038/387183a0
- [141] D Finzi, J Blankson, JD Siliciano, JB Margolick, K Chadwick, T Pierson, K Smith, J Lisziewicz, F Lori et al. 1999. Latent infection of CD4+ T cells provides a mechanism for lifelong persistence of HIV-1, even in patients on effective combination therapy. *Nat Med*, 5:512–517. doi: 10.1038/8394
- [142] JD Siliciano, J Kajdas, D Finzi, TC Quinn, K Chadwick, JB Margolick, C Kovacs, SJ Gange and RF Siliciano. 2003. Long-term follow-up studies confirm the stability of the latent reservoir for HIV-1 in resting CD4+ T cells. *Nat Med*, 9:727–728. doi: 10.1038/nm880
- [143] TW Chun, D Finzi, J Margolick, K Chadwick, D Schwartz and RF Siliciano. 1995. In vivo fate of HIV-1-infected T cells: quantitative analysis of the transition to stable latency. *Nat Med*, 1:1284–1290
- [144] JK Wong, M Hezareh, HF Günthard, DV Havlir, CC Ignacio, CA Spina and DD Richman. 1997. Recovery of replication-competent HIV despite prolonged suppression of plasma viremia. *Science*, 278:1291–1295. doi: 10.1126/science.278.5341.1291
- [145] DD Richman, DM Margolis, M Delaney, WC Greene, D Hazuda and RJ Pomerantz. 2009. The challenge of finding a cure for HIV infection. *Science*, 323:1304–1307. doi: 10.1126/science.1165706
- [146] NM Archin, A Espeseth, D Parker, M Cheema, D Hazuda and DM Margolis. 2009. Expression of latent HIV induced by the potent HDAC inhibitor suberoylanilide hydroxamic acid. *AIDS Res Hum Retroviruses*, 25:207–212. doi: 10.1089/aid.2008.0191
- [147] J Kulkosky, DM Culnan, J Roman, G Dornadula, M Schnell, MR Boyd and RJ Pomerantz. 2001. Prostratin: activation of latent HIV-1 expression suggests a potential inductive adjuvant therapy for HAART. *Blood*, 98:3006–3015. doi: 10.1182/blood.V98.10.3006
- [148] S Xing, CK Bullen, NS Shroff, L Shan, HC Yang, JL Manucci, S Bhat, H Zhang, JB Margolick et al. 2011. Disulfiram reactivates latent HIV-1 in a Bcl-2-transduced primary CD4+ T cell model without inducing global T cell activation. *J Virol*, 85: 6060–6064. doi: 10.1128/JVI.02033-10
- [149] DG Wei, V Chiang, E Fyne, M Balakrishnan, T Barnes, M Graupe, J Hesselgesser, A Irrinki, JP Murry et al. 2014. Histone deacetylase inhibitor romidepsin induces HIV expression in CD4 T cells from patients on suppressive antiretroviral therapy at concentrations achieved by clinical dosing. *PLoS Pathog*, 10:e1004071. doi: 10.1371/journal.ppat.1004071
- [150] MK Lewinski, D Bisgrove, P Shinn, H Chen, C Hoffmann, S Hannenhalli, E Verdin,

- CC Berry, JR Ecker and FD Bushman. 2005. Genome-wide analysis of chromosomal features repressing human immunodeficiency virus transcription. *J Virol*, 79:6610–6619. doi: 10.1128/JVI.79.11.6610-6619.2005
- [151] L Shan, HC Yang, SA Rabi, HC Bravo, NS Shroff, RA Irizarry, H Zhang, JB Margolick, JD Siliciano and RF Siliciano. 2011. Influence of host gene transcription level and orientation on HIV-1 latency in a primary-cell model. *J Virol*, 85:5384–5393. doi: 10.1128/JVI.02536-10
  - [152] MJ Pace, EH Graf, LM Agosto, AM Mexas, F Male, T Brady, FD Bushman and U O'Doherty. 2012. Directly infected resting CD4+ T cells can produce HIV Gag without spreading infection in a model of HIV latency. *PLoS Pathog*, 8:e1002818. doi: 10.1371/journal.ppat.1002818
  - [153] AG Dalgleish, PC Beverley, PR Clapham, DH Crawford, MF Greaves and RA Weiss. 1984. The CD4 (T4) antigen is an essential component of the receptor for the AIDS retrovirus. *Nature*, 312:763–767. doi: 10.1038/312763a0
  - [154] D Klatzmann, E Champagne, S Chamaret, J Gruest, D Guetard, T Hercend, JC Gluckman and L Montagnier. 1984. T-lymphocyte T4 molecule behaves as the receptor for human retrovirus LAV. *Nature*, 312:767–768. doi: 10.1038/312767a0
  - [155] JD Lifson, MB Feinberg, GR Reyes, L Rabin, B Banapour, S Chakrabarti, B Moss, F Wong-Staal, KS Steimer and EG Engleman. 1986. Induction of CD4-dependent cell fusion by the HTLV-III/LAV envelope glycoprotein. *Nature*, 323:725–728. doi: 10.1038/323725a0
  - [156] JD Lifson, GR Reyes, MS McGrath, BS Stein and EG Engleman. 1986. AIDS retrovirus induced cytopathology: giant cell formation and involvement of CD4 antigen. *Science*, 232:1123–1127. doi: 10.1126/science.3010463
  - [157] PJ Maddon, AG Dalgleish, JS McDougal, PR Clapham, RA Weiss and R Axel. 1986. The T4 gene encodes the AIDS virus receptor and is expressed in the immune system and the brain. *Cell*, 47:333–348. doi: 10.1016/0092-8674(86)90590-8
  - [158] Y Feng, CC Broder, PE Kennedy and EA Berger. 1996. HIV-1 entry cofactor: functional cDNA cloning of a seven-transmembrane, G protein-coupled receptor. *Science*, 272:872–877. doi: 10.1126/science.272.5263.872
  - [159] H Choe, M Farzan, Y Sun, N Sullivan, B Rollins, PD Ponath, L Wu, CR Mackay, G LaRosa et al. 1996. The beta-chemokine receptors CCR3 and CCR5 facilitate infection by primary HIV-1 isolates. *Cell*, 85:1135–1148. doi: 10.1016/S0092-8674(00)81313-6
  - [160] J He, Y Chen, M Farzan, H Choe, A Ohagen, S Gartner, J Busciglio, X Yang, W Hofmann et al. 1997. CCR3 and CCR5 are co-receptors for HIV-1 infection of microglia. *Nature*, 385:645–649. doi: 10.1038/385645a0

- [161] D Baltimore. 1970. RNA-dependent DNA polymerase in virions of RNA tumour viruses. *Nature*, 226:1209–1211. doi: 10.1038/2261209a0
- [162] HM Temin and S Mizutani. 1970. RNA-dependent DNA polymerase in virions of Rous sarcoma virus. *Nature*, 226:1211–1213. doi: 10.1038/2261211a0
- [163] DP Grandgenett, AC Vora and RD Schiff. 1978. A 32,000-dalton nucleic acid-binding protein from avian retravirus cores possesses DNA endonuclease activity. *Virology*, 89: 119–132. doi: 10.1016/0042-6822(78)90046-6
- [164] FD Bushman, T Fujiwara and R Craigie. 1990. Retroviral DNA integration directed by HIV integration protein in vitro. *Science*, 249:1555–1558. doi: 10.1126/science.2171144
- [165] CP Hill, D Worthy lake, DP Bancroft, AM Christensen and WI Sundquist. 1996. Crystal structures of the trimeric human immunodeficiency virus type 1 matrix protein: implications for membrane association and assembly. *Proc Natl Acad Sci U S A*, 93: 3099–3104
- [166] NK Heinzinger, MI Bukrinsky, SA Haggerty, AM Ragland, V Kewalramani, MA Lee, HE Gendelman, L Ratner, M Stevenson and M Emerman. 1994. The Vpr protein of human immunodeficiency virus type 1 influences nuclear localization of viral nucleic acids in nondividing host cells. *Proc Natl Acad Sci U S A*, 91:7311–7315
- [167] MI Bukrinsky, N Sharova, TL McDonald, T Pushkarskaya, WG Tarpley and M Stevenson. 1993. Association of integrase, matrix, and reverse transcriptase antigens of human immunodeficiency virus type 1 with viral nucleic acids following acute infection. *Proc Natl Acad Sci U S A*, 90:6125–6129
- [168] BK Ganser, S Li, VY Klishko, JT Finch and WI Sundquist. 1999. Assembly and analysis of conical models for the HIV-1 core. *Science*, 283:80–83. doi: 10.1126/science.283.5398.80
- [169] S Li, CP Hill, WI Sundquist and JT Finch. 2000. Image reconstructions of helical assemblies of the HIV-1 CA protein. *Nature*, 407:409–413. doi: 10.1038/35030177
- [170] IJL Byeon, X Meng, J Jung, G Zhao, R Yang, J Ahn, J Shi, J Concel, C Aiken et al. 2009. Structural convergence between Cryo-EM and NMR reveals intersubunit interactions critical for HIV-1 capsid function. *Cell*, 139:780–790. doi: 10.1016/j.cell.2009.10.010
- [171] G Zhao, JR Perilla, EL Yufenyuy, X Meng, B Chen, J Ning, J Ahn, AM Gronenborn, K Schulten et al. 2013. Mature HIV-1 capsid structure by cryo-electron microscopy and all-atom molecular dynamics. *Nature*, 497:643–646. doi: 10.1038/nature12162
- [172] K Lee, Z Ambrose, TD Martin, I Oztop, A Mulky, JG Julias, N Vandegraaff, JG Baumann, R Wang et al. 2010. Flexible use of nuclear import pathways by HIV-1. *Cell Host Microbe*, 7:221–233. doi: 10.1016/j.chom.2010.02.007

- [173] M Thali, A Bukovsky, E Kondo, B Rosenwirth, CT Walsh, J Sodroski and HG Göttlinger. 1994. Functional association of cyclophilin A with HIV-1 virions. *Nature*, 372:363–365. doi: 10.1038/372363a0
- [174] TR Gamble, FF Vajdos, S Yoo, DK Worthylake, M Houseweart, WI Sundquist and CP Hill. 1996. Crystal structure of human cyclophilin A bound to the amino-terminal domain of HIV-1 capsid. *Cell*, 87:1285–1294. doi: 10.1016/S0092-8674(00)81823-1
- [175] T Schaller, KE Ocwieja, J Rasaiyaah, AJ Price, TL Brady, SL Roth, S Hué, AJ Fletcher, K Lee et al. 2011. HIV-1 capsid-cyclophilin interactions determine nuclear import pathway, integration targeting and replication efficiency. *PLoS Pathog*, 7:e1002439. doi: 10.1371/journal.ppat.1002439
- [176] KE Ocwieja, TL Brady, K Ronen, A Huegel, SL Roth, T Schaller, LC James, GJ Towers, JAT Young et al. 2011. HIV integration targeting: a pathway involving Transportin-3 and the nuclear pore protein RanBP2. *PLoS Pathog*, 7:e1001313. doi: 10.1371/journal.ppat.1001313
- [177] J Rasaiyaah, CP Tan, AJ Fletcher, AJ Price, C Blondeau, L Hilditch, DA Jacques, DL Selwood, LC James et al. 2013. HIV-1 evades innate immune recognition through specific cofactor recruitment. *Nature*, 503:402–405. doi: 10.1038/nature12769
- [178] GP Harrison and AM Lever. 1992. The human immunodeficiency virus type 1 packaging signal and major splice donor region have a conserved stable secondary structure. *J Virol*, 66:4144–4153
- [179] J Dannull, A Surovoy, G Jung and K Moelling. 1994. Specific binding of HIV-1 nucleocapsid protein to Psi RNA in vitro requires N-terminal zinc finger and flanking basic amino acid residues. *EMBO J*, 13:1525–1533
- [180] FD Veronese, R Rahman, TD Copeland, S Oroszlan, RC Gallo and MG Sarngadharan. 1987. Immunological and chemical analysis of P6, the carboxyl-terminal fragment of HIV P15. *AIDS Res Hum Retroviruses*, 3:253–264. doi: 10.1089/aid.1987.3.253
- [181] HG Göttlinger, T Dorfman, JG Sodroski and WA Haseltine. 1991. Effect of mutations affecting the p6 gag protein on human immunodeficiency virus particle release. *Proc Natl Acad Sci U S A*, 88:3195–3199. doi: 10.1073/pnas.88.8.3195
- [182] B Strack, A Calistri, S Craig, E Popova and HG Göttlinger. 2003. AIP1/ALIX is a binding partner for HIV-1 p6 and EIAV p9 functioning in virus budding. *Cell*, 114: 689–699. doi: 10.1016/S0092-8674(03)00653-6
- [183] W Paxton, RI Connor and NR Landau. 1993. Incorporation of Vpr into human immunodeficiency virus type 1 virions: requirement for the p6 region of gag and mutational analysis. *J Virol*, 67:7229–7237
- [184] NT Parkin, M Chamorro and HE Varmus. 1992. Human immunodeficiency virus

- type 1 gag-pol frameshifting is dependent on downstream mRNA secondary structure: demonstration by expression in vivo. *J Virol*, 66:5147–5151
- [185] T Jacks, MD Power, FR Masiarz, PA Luciw, PJ Barr and HE Varmus. 1988. Characterization of ribosomal frameshifting in HIV-1 gag-pol expression. *Nature*, 331:280–283. doi: 10.1038/331280a0
- [186] H Reil and H Hauser. 1990. Test system for determination of HIV-1 frameshifting efficiency in animal cells. *Biochim Biophys Acta*, 1050:288–292. doi: 10.1016/0167-4781(90)90183-3
- [187] LA Kohlstaedt, J Wang, JM Friedman, PA Rice and TA Steitz. 1992. Crystal structure at 3.5 Å resolution of HIV-1 reverse transcriptase complexed with an inhibitor. *Science*, 256:1783–1790
- [188] AR Bellamy, SC Gillies and JD Harvey. 1974. Molecular weight of two oncornavirus genomes: derivation from particle molecular weights and RNA content. *J Virol*, 14: 1388–1393
- [189] HJ Kung, JM Bailey, N Davidson, MO Nicolson and RM McAllister. 1975. Structure, subunit composition, and molecular weight of RD-114 RNA. *J Virol*, 16:397–411
- [190] HJ Kung, S Hu, W Bender, JM Bailey, N Davidson, MO Nicolson and RM McAllister. 1976. RD-114, baboon, and woolly monkey viral RNA's compared in size and structure. *Cell*, 7:609–620. doi: 10.1016/0092-8674(76)90211-7
- [191] AT Panganiban and D Fiore. 1988. Ordered interstrand and intrastrand DNA transfer during reverse transcription. *Science*, 241:1064–1069. doi: 10.1126/science.2457948
- [192] WS Hu and HM Temin. 1990. Genetic consequences of packaging two RNA genomes in one retroviral particle: pseudodiploidy and high rate of genetic recombination. *Proc Natl Acad Sci U S A*, 87:1556–1560. doi: 10.1073/pnas.87.4.1556
- [193] WS Hu and HM Temin. 1990. Retroviral recombination and reverse transcription. *Science*, 250:1227–1233. doi: 10.1126/science.1700865
- [194] A Engelman, K Mizuuchi and R Craigie. 1991. HIV-1 DNA integration: mechanism of viral DNA cleavage and DNA strand transfer. *Cell*, 67:1211–1221. doi: 10.1016/0092-8674(91)90297-C
- [195] AT Panganiban and HM Temin. 1984. The retrovirus pol gene encodes a product required for DNA integration: identification of a retrovirus int locus. *Proc Natl Acad Sci U S A*, 81:7885–7889
- [196] GN Maertens, S Hare and P Cherepanov. 2010. The mechanism of retroviral integration from X-ray structures of its key intermediates. *Nature*, 468:326–329. doi: 10.1038/nature09517

- [197] S Hare, SS Gupta, E Valkov, A Engelman and P Cherepanov. 2010. Retroviral intasome assembly and inhibition of DNA strand transfer. *Nature*, 464:232–236. doi: 10.1038/nature08784
- [198] FD Bushman and R Craigie. 1991. Activities of human immunodeficiency virus (HIV) integration protein in vitro: specific cleavage and integration of HIV DNA. *Proc Natl Acad Sci U S A*, 88:1339–1343. doi: 10.1073/pnas.88.4.1339
- [199] A Wlodawer, M Miller, M Jaskólski, BK Sathyaranayana, E Baldwin, IT Weber, LM Selk, L Clawson, J Schneider and SB Kent. 1989. Conserved folding in retroviral proteases: crystal structure of a synthetic HIV-1 protease. *Science*, 245:616–621. doi: 10.1126/science.2548279
- [200] HG Kräusslich, RH Ingraham, MT Skoog, E Wimmer, PV Pallai and CA Carter. 1989. Activity of purified biosynthetic proteinase of human immunodeficiency virus on natural substrates and synthetic peptides. *Proc Natl Acad Sci U S A*, 86:807–811
- [201] NE Kohl, EA Emini, WA Schleif, LJ Davis, JC Heimbach, RA Dixon, EM Scolnick and IS Sigal. 1988. Active human immunodeficiency virus protease is required for viral infectivity. *Proc Natl Acad Sci U S A*, 85:4686–4690
- [202] FD Veronese, AL DeVico, TD Copeland, S Oroszlan, RC Gallo and MG Sarngadharan. 1985. Characterization of gp41 as the transmembrane protein coded by the HTLV-III/LAV envelope gene. *Science*, 229:1402–1405. doi: 10.1126/science.2994223
- [203] S Hallenberger, V Bosch, H Angliker, E Shaw, HD Klenk and W Garten. 1992. Inhibition of furin-mediated cleavage activation of HIV-1 glycoprotein gp160. *Nature*, 360:358–361. doi: 10.1038/360358a0
- [204] X Wei, JM Decker, S Wang, H Hui, JC Kappes, X Wu, JF Salazar-Gonzalez, MG Salazar, JM Kilby et al. 2003. Antibody neutralization and escape by HIV-1. *Nature*, 422:307–312. doi: 10.1038/nature01470
- [205] P Zhu, J Liu, J Bess, Jr, E Chertova, JD Lifson, H Grisé, GA Ofek, KA Taylor and KH Roux. 2006. Distribution and three-dimensional structure of AIDS virus envelope spikes. *Nature*, 441:847–852. doi: 10.1038/nature04817
- [206] EC Holmes, LQ Zhang, P Simmonds, CA Ludlam and AJ Brown. 1992. Convergent and divergent sequence evolution in the surface envelope glycoprotein of human immunodeficiency virus type 1 within a single infected patient. *Proc Natl Acad Sci U S A*, 89:4835–4839
- [207] R Shankarappa, JB Margolick, SJ Gange, AG Rodrigo, D Upchurch, H Farzadegan, P Gupta, CR Rinaldo, GH Learn et al. 1999. Consistent viral evolutionary changes associated with the progression of human immunodeficiency virus type 1 infection. *J Virol*, 73:10489–10502

- [208] S Bonhoeffer, EC Holmes and MA Nowak. 1995. Causes of HIV diversity. *Nature*, 376:125. doi: 10.1038/376125a0
- [209] SM Wolinsky, BT Korber, AU Neumann, M Daniels, KJ Kunstman, AJ Whetsell, MR Furtado, Y Cao, DD Ho and JT Safrit. 1996. Adaptive evolution of human immunodeficiency virus-type 1 during the natural course of infection. *Science*, 272: 537–542. doi: 10.1126/science.272.5261.537
- [210] HA Ross and AG Rodrigo. 2002. Immune-mediated positive selection drives human immunodeficiency virus type 1 molecular variation and predicts disease duration. *J Virol*, 76:11715–11720. doi: 10.1128/JVI.76.22.11715-11720.2002
- [211] J Sodroski, C Rosen, F Wong-Staal, SZ Salahuddin, M Popovic, S Arya, RC Gallo and WA Haseltine. 1985. Trans-acting transcriptional regulation of human T-cell leukemia virus type III long terminal repeat. *Science*, 227:171–173. doi: 10.1126/science.2981427
- [212] J Sodroski, R Patarca, C Rosen, F Wong-Staal and W Haseltine. 1985. Location of the trans-activating region on the genome of human T-cell lymphotropic virus type III. *Science*, 229:74–77. doi: 10.1126/science.2990041
- [213] BR Cullen. 1986. Trans-activation of human immunodeficiency virus occurs via a bimodal mechanism. *Cell*, 46:973–982. doi: 10.1016/0092-8674(86)90696-3
- [214] AI Dayton, JG Sodroski, CA Rosen, WC Goh and WA Haseltine. 1986. The trans-activator gene of the human T cell lymphotropic virus type III is required for replication. *Cell*, 44:941–947. doi: 10.1016/0092-8674(86)90017-6
- [215] TK Howcroft, K Strebel, MA Martin and DS Singer. 1993. Repression of MHC class I gene promoter activity by two-exon Tat of HIV. *Science*, 260:1320–1322. doi: 10.1126/science.8493575
- [216] Y Bennasser, SY Le, M Benkirane and KT Jeang. 2005. Evidence that HIV-1 encodes an siRNA and a suppressor of RNA silencing. *Immunity*, 22:607–619. doi: 10.1016/j.immuni.2005.03.010
- [217] R Triboulet, B Mari, YL Lin, C Chable-Bessia, Y Bennasser, K Lebrigand, B Cardinaud, T Maurin, P Barbry et al. 2007. Suppression of microRNA-silencing pathway by HIV-1 during virus replication. *Science*, 315:1579–1582. doi: 10.1126/science.1136319
- [218] S Qian, X Zhong, L Yu, B Ding, P de Haan and K Boris-Lawrie. 2009. HIV-1 Tat RNA silencing suppressor activity is conserved across kingdoms and counteracts translational repression of HIV-1. *Proc Natl Acad Sci U S A*, 106:605–610. doi: 10.1073/pnas.0806822106
- [219] J Lin and BR Cullen. 2007. Analysis of the interaction of primate retroviruses with the human RNA interference machinery. *J Virol*, 81:12218–12226. doi: 10.1128/JVI.01390-07

- [220] BE Meyer and MH Malim. 1994. The HIV-1 Rev trans-activator shuttles between the nucleus and the cytoplasm. *Genes Dev*, 8:1538–1547. doi: 10.1101/gad.8.13.1538
- [221] J Sodroski, WC Goh, C Rosen, A Dayton, E Terwilliger and W Haseltine. 1986. A second post-transcriptional trans-activator gene required for HTLV-III replication. *Nature*, 321:412–417. doi: 10.1038/321412a0
- [222] MB Feinberg, RF Jarrett, A Aldovini, RC Gallo and F Wong-Staal. 1986. HTLV-III expression and production involve complex regulation at the levels of splicing and translation of viral RNA. *Cell*, 46:807–817. doi: 10.1016/0092-8674(86)90062-0
- [223] DM Knight, FA Flomerfelt and J Ghrayeb. 1987. Expression of the art/trs protein of HIV and study of its role in viral envelope synthesis. *Science*, 236:837–840. doi: 10.1126/science.3033827
- [224] MH Malim, J Hauber, R Fenrick and BR Cullen. 1988. Immunodeficiency virus rev trans-activator modulates the expression of the viral regulatory genes. *Nature*, 335: 181–183. doi: 10.1038/335181a0
- [225] D Gutman and CJ Goldenberg. 1988. Virus-specific splicing inhibitor in extracts from cells infected with HIV-1. *Science*, 241:1492–1495. doi: 10.1126/science.3047873
- [226] MH Malim, J Hauber, SY Le, JV Maizel and BR Cullen. 1989. The HIV-1 rev trans-activator acts through a structured target sequence to activate nuclear export of unspliced viral mRNA. *Nature*, 338:254–257. doi: 10.1038/338254a0
- [227] MH Malim, S Bhnlein, J Hauber and BR Cullen. 1989. Functional dissection of the HIV-1 Rev trans-activator—derivation of a trans-dominant repressor of Rev function. *Cell*, 58:205–214. doi: 10.1016/0092-8674(89)90416-9
- [228] G Yu and RL Felsted. 1992. Effect of myristoylation on p27 nef subcellular distribution and suppression of HIV-LTR transcription. *Virology*, 187:46–55. doi: 10.1016/0042-6822(92)90293-X
- [229] JV Garcia and AD Miller. 1991. Serine phosphorylation-independent downregulation of cell-surface CD4 by nef. *Nature*, 350:508–511. doi: 10.1038/350508a0
- [230] RE Benson, A Sanfridson, JS Ottinger, C Doyle and BR Cullen. 1993. Downregulation of cell-surface CD4 expression by simian immunodeficiency virus Nef prevents viral super infection. *J Exp Med*, 177:1561–1566. doi: 10.1084/jem.177.6.1561
- [231] C Aiken, J Konner, NR Landau, ME Lenburg and D Trono. 1994. Nef induces CD4 endocytosis: requirement for a critical dileucine motif in the membrane-proximal CD4 cytoplasmic domain. *Cell*, 76:853–864. doi: 10.1016/0092-8674(94)90360-3
- [232] J Lama, A Mangasarian and D Trono. 1999. Cell-surface expression of CD4 reduces HIV-1 infectivity by blocking Env incorporation in a Nef- and Vpu-inhibitable manner. *Curr Biol*, 9:622–631. doi: 10.1016/S0960-9822(99)80284-X

- [233] TM Ross, AE Oran and BR Cullen. 1999. Inhibition of HIV-1 progeny virion release by cell-surface CD4 is relieved by expression of the viral Nef protein. *Curr Biol*, 9: 613–621. doi: 10.1016/S0960-9822(99)80283-8
- [234] N Michel, I Allespach, S Venzke, OT Fackler and OT Keppler. 2005. The Nef protein of human immunodeficiency virus establishes superinfection immunity by a dual strategy to downregulate cell-surface CCR5 and CD4. *Curr Biol*, 15:714–723. doi: 10.1016/j.cub.2005.02.058
- [235] O Schwartz, V Maréchal, S Le Gall, F Lemonnier and JM Heard. 1996. Endocytosis of major histocompatibility complex class I molecules is induced by the HIV-1 Nef protein. *Nat Med*, 2:338–342. doi: 10.1038/nm0396-338
- [236] KL Collins, BK Chen, SA Kalams, BD Walker and D Baltimore. 1998. HIV-1 Nef protein protects infected primary cells against killing by cytotoxic T lymphocytes. *Nature*, 391:397–401. doi: 10.1038/34929
- [237] P Stumptner-Cuvelette, S Morchoisne, M Dugast, S Le Gall, G Raposo, O Schwartz and P Benaroch. 2001. HIV-1 Nef impairs MHC class II antigen presentation and surface expression. *Proc Natl Acad Sci U S A*, 98:12144–12149. doi: 10.1073/pnas.221256498
- [238] AD Blagoveshchenskaya, L Thomas, SF Feliciangeli, CH Hung and G Thomas. 2002. HIV-1 Nef downregulates MHC-I by a PACS-1- and PI3K-regulated ARF6 endocytic pathway. *Cell*, 111:853–866. doi: 10.1016/S0092-8674(02)01162-5
- [239] XN Xu, B Laffert, GR Screaton, M Kraft, D Wolf, W Kolanus, J Mongkolsapay, AJ McMichael and AS Baur. 1999. Induction of Fas ligand expression by HIV involves the interaction of Nef with the T cell receptor zeta chain. *J Exp Med*, 189:1489–1496. doi: 10.1084/jem.189.9.1489
- [240] JA Schrager and JW Marsh. 1999. HIV-1 Nef increases T cell activation in a stimulus-dependent manner. *Proc Natl Acad Sci U S A*, 96:8167–8172. doi: 10.1073/pnas.96.14.8167
- [241] JK Wang, E Kiyokawa, E Verdin and D Trono. 2000. The Nef protein of HIV-1 associates with rafts and primes T cells for activation. *Proc Natl Acad Sci U S A*, 97: 394–399. doi: 10.1073/pnas.97.1.394
- [242] A Simmons, V Aluvihare and A McMichael. 2001. Nef triggers a transcriptional program in T cells imitating single-signal T cell activation and inducing HIV virulence mediators. *Immunity*, 14:763–777. doi: 10.1016/S1074-7613(01)00158-3
- [243] JA Schrager, V Der Minassian and JW Marsh. 2002. HIV Nef increases T cell ERK MAP kinase activity. *J Biol Chem*, 277:6137–6142. doi: 10.1074/jbc.M107322200
- [244] M Schindler, J Münch, O Kutsch, H Li, ML Santiago, F Bibollet-Ruche, MC Müller-Trutwin, FJ Novembre, M Peeters et al. 2006. Nef-mediated suppression of T cell

- activation was lost in a lentiviral lineage that gave rise to HIV-1. *Cell*, 125:1055–1067. doi: 10.1016/j.cell.2006.04.033
- [245] F Kirchhoff, M Schindler, A Specht, N Arhel and J Münch. 2008. Role of Nef in primate lentiviral immunopathogenesis. *Cell Mol Life Sci*, 65:2621–2636. doi: 10.1007/s00018-008-8094-2
- [246] F Kirchhoff. 2009. Is the high virulence of HIV-1 an unfortunate coincidence of primate lentiviral evolution? *Nat Rev Microbiol*, 7:467–476. doi: 10.1038/nrmicro2111
- [247] F Wong-Staal, PK Chanda and J Ghrayeb. 1987. Human immunodeficiency virus: the eighth gene. *AIDS Res Hum Retroviruses*, 3:33–39. doi: 10.1089/aid.1987.3.33
- [248] EA Cohen, EF Terwilliger, Y Jalinoos, J Proulx, JG Sodroski and WA Haseltine. 1990. Identification of HIV-1 vpr product and function. *J Acquir Immune Defic Syndr*, 3: 11–18
- [249] JB Jowett, V Planelles, B Poon, NP Shah, ML Chen and IS Chen. 1995. The human immunodeficiency virus type 1 vpr gene arrests infected T cells in the G2 + M phase of the cell cycle. *J Virol*, 69:6304–6313
- [250] F Re, D Braaten, EK Franke and J Luban. 1995. Human immunodeficiency virus type 1 Vpr arrests the cell cycle in G2 by inhibiting the activation of p34cdc2-cyclin B. *J Virol*, 69:6859–6864
- [251] J He, S Choe, R Walker, P Di Marzio, DO Morgan and NR Landau. 1995. Human immunodeficiency virus type 1 viral protein R (Vpr) arrests cells in the G2 phase of the cell cycle by inhibiting p34cdc2 activity. *J Virol*, 69:6705–6711
- [252] ME Rogel, LI Wu and M Emerman. 1995. The human immunodeficiency virus type 1 vpr gene prevents cell proliferation during chronic infection. *J Virol*, 69:882–888
- [253] CM de Noronha, MP Sherman, HW Lin, MV Cavrois, RD Moir, RD Goldman and WC Greene. 2001. Dynamic disruptions in nuclear envelope architecture and integrity induced by HIV-1 Vpr. *Science*, 294:1105–1108. doi: 10.1126/science.1063957
- [254] WC Goh, ME Rogel, CM Kinsey, SF Michael, PN Fultz, MA Nowak, BH Hahn and M Emerman. 1998. HIV-1 Vpr increases viral expression by manipulation of the cell cycle: a mechanism for selection of Vpr in vivo. *Nat Med*, 4:65–71. doi: 10.1038/nm0198-065
- [255] RA Subramanian, A Kessous-Elbaz, R Lodge, J Forget, XJ Yao, D Bergeron and EA Cohen. 1998. Human immunodeficiency virus type 1 Vpr is a positive regulator of viral transcription and infectivity in primary human macrophages. *J Exp Med*, 187: 1103–1111. doi: 10.1084/jem.187.7.1103
- [256] SA Stewart, B Poon, JB Jowett and IS Chen. 1997. Human immunodeficiency virus type 1 Vpr induces apoptosis following cell cycle arrest. *J Virol*, 71:5579–5592

- [257] LD Shostak, J Ludlow, J Fisk, S Pursell, BJ Rimel, D Nguyen, JD Rosenblatt and V Planelles. 1999. Roles of p53 and caspases in the induction of cell cycle arrest and apoptosis by HIV-1 vpr. *Exp Cell Res*, 251:156–165. doi: 10.1006/excr.1999.4568
- [258] EA Cohen, G Dehni, JG Sodroski and WA Haseltine. 1990. Human immunodeficiency virus vpr product is a virion-associated regulatory protein. *J Virol*, 64:3097–3099
- [259] X Yuan, Z Matsuda, M Matsuda, M Essex and TH Lee. 1990. Human immunodeficiency virus vpr gene encodes a virion-associated protein. *AIDS Res Hum Retroviruses*, 6: 1265–1271. doi: 10.1089/aid.1990.6.1265
- [260] AM Sheehy, NC Gaddis, JD Choi and MH Malim. 2002. Isolation of a human gene that inhibits HIV-1 infection and is suppressed by the viral Vif protein. *Nature*, 418: 646–650. doi: 10.1038/nature00939
- [261] R Mariani, D Chen, B Schröfelbauer, F Navarro, R König, B Bollman, C Münk, H Nymark-McMahon and NR Landau. 2003. Species-specific exclusion of APOBEC3G from HIV-1 virions by Vif. *Cell*, 114:21–31. doi: 10.1016/S0092-8674(03)00515-4
- [262] AM Sheehy, NC Gaddis and MH Malim. 2003. The antiretroviral enzyme APOBEC3G is degraded by the proteasome in response to HIV-1 Vif. *Nat Med*, 9:1404–1407. doi: 10.1038/nm945
- [263] M Marin, KM Rose, SL Kozak and D Kabat. 2003. HIV-1 Vif protein binds the editing enzyme APOBEC3G and induces its degradation. *Nat Med*, 9:1398–1403. doi: 10.1038/nm946
- [264] X Yu, Y Yu, B Liu, K Luo, W Kong, P Mao and XF Yu. 2003. Induction of APOBEC3G ubiquitination and degradation by an HIV-1 Vif-Cul5-SCF complex. *Science*, 302:1056–1060. doi: 10.1126/science.1089591
- [265] RS Harris, KN Bishop, AM Sheehy, HM Craig, SK Petersen-Mahrt, IN Watt, MS Neuberger and MH Malim. 2003. DNA deamination mediates innate immunity to retroviral infection. *Cell*, 113:803–809. doi: 10.1016/S0092-8674(03)00423-9
- [266] B Mangeat, P Turelli, G Caron, M Friedli, L Perrin and D Trono. 2003. Broad antiretroviral defence by human APOBEC3G through lethal editing of nascent reverse transcripts. *Nature*, 424:99–103. doi: 10.1038/nature01709
- [267] H Zhang, B Yang, RJ Pomerantz, C Zhang, SC Arunachalam and L Gao. 2003. The cytidine deaminase CEM15 induces hypermutation in newly synthesized HIV-1 DNA. *Nature*, 424:94–98. doi: 10.1038/nature01707
- [268] D Lecossier, F Bouchonnet, F Clavel and AJ Hance. 2003. Hypermutation of HIV-1 DNA in the absence of the Vif protein. *Science*, 300:1112. doi: 10.1126/science.1083338
- [269] EA Cohen, EF Terwilliger, JG Sodroski and WA Haseltine. 1988. Identification of a protein encoded by the vpu gene of HIV-1. *Nature*, 334:532–534. doi: 10.1038/334532a0

- [270] K Strebel, T Klimkait and MA Martin. 1988. A novel gene of HIV-1, vpu, and its 16-kilodalton product. *Science*, 241:1221–1223. doi: 10.1126/science.3261888
- [271] RL Willey, F Maldarelli, MA Martin and K Strebel. 1992. Human immunodeficiency virus type 1 Vpu protein induces rapid degradation of CD4. *J Virol*, 66:7193–7200
- [272] S Bour, U Schubert and K Strebel. 1995. The human immunodeficiency virus type 1 Vpu protein specifically binds to the cytoplasmic domain of CD4: implications for the mechanism of degradation. *J Virol*, 69:1510–1520
- [273] WL Marshall, DC Diamond, MM Kowalski and RW Finberg. 1992. High level of surface CD4 prevents stable human immunodeficiency virus infection of T-cell transfectants. *J Virol*, 66:5492–5499
- [274] MJ Cortés, F Wong-Staal and J Lama. 2002. Cell surface CD4 interferes with the infectivity of HIV-1 particles released from T cells. *J Biol Chem*, 277:1770–1779. doi: 10.1074/jbc.M109807200
- [275] B Crise, L Buonocore and JK Rose. 1990. CD4 is retained in the endoplasmic reticulum by the human immunodeficiency virus type 1 glycoprotein precursor. *J Virol*, 64: 5585–5593
- [276] S Bour, F Boulerice and MA Wainberg. 1991. Inhibition of gp160 and CD4 maturation in U937 cells after both defective and productive infections by human immunodeficiency virus type 1. *J Virol*, 65:6387–6396
- [277] SJD Neil, T Zang and PD Bieniasz. 2008. Tetherin inhibits retrovirus release and is antagonized by HIV-1 Vpu. *Nature*, 451:425–430. doi: 10.1038/nature06553
- [278] N Van Damme, D Goff, C Katsura, RL Jorgenson, R Mitchell, MC Johnson, EB Stephens and J Guatelli. 2008. The interferon-induced protein BST-2 restricts HIV-1 release and is downregulated from the cell surface by the viral Vpu protein. *Cell Host Microbe*, 3:245–252. doi: 10.1016/j.chom.2008.03.001
- [279] K Strebel, T Klimkait, F Maldarelli and MA Martin. 1989. Molecular and biochemical analyses of human immunodeficiency virus type 1 vpu protein. *J Virol*, 63:3784–3791
- [280] C Gélinas and HM Temin. 1986. Nondefective spleen necrosis virus-derived vectors define the upper size limit for packaging reticuloendotheliosis viruses. *Proc Natl Acad Sci USA*, 83:9211–9215
- [281] SA Herman and JM Coffin. 1987. Efficient packaging of readthrough RNA in ALV: implications for oncogene transduction. *Science*, 236:845–848. doi: 10.1126/science.3033828
- [282] NH Shin, D Hartigan-O'Connor, JK Pfeiffer and A Telesnitsky. 2000. Replication of lengthened Moloney murine leukemia virus genomes is impaired at multiple stages. *J Virol*, 74:2694–2702

- [283] S Kammler, M Otte, I Hauber, J Kjems, J Hauber and H Schaal. 2006. The strength of the HIV-1 3' splice sites affects Rev function. *Retrovirology*, 3:89. doi: 10.1186/1742-4690-3-89
- [284] CM Stoltzfus. 2009. Chapter 1. Regulation of HIV-1 alternative RNA splicing and its role in virus replication. *Adv Virus Res*, 74:1–40. doi: 10.1016/S0065-3527(09)74001-1
- [285] MM O'Reilly, MT McNally and KL Beemon. 1995. Two strong 5' splice sites and competing, suboptimal 3' splice sites involved in alternative splicing of human immunodeficiency virus type 1 RNA. *Virology*, 213:373–385. doi: 10.1006/viro.1995.0010
- [286] BA Amendt, D Hesslein, LJ Chang and CM Stoltzfus. 1994. Presence of negative and positive cis-acting RNA splicing elements within and flanking the first tat coding exon of human immunodeficiency virus type 1. *Mol Cell Biol*, 14:3960–3970. doi: 10.1128/MCB.14.6.3960
- [287] JD Levengood, C Rollins, CHJ Mishler, CA Johnson, G Miner, P Rajan, BM Znosko and BS Tolbert. 2012. Solution structure of the HIV-1 exon splicing silencer 3. *J Mol Biol*, 415:680–698. doi: 10.1016/j.jmb.2011.11.034
- [288] M Caputi, M Freund, S Kammler, C Asang and H Schaal. 2004. A bidirectional SF2/ASF- and SRp40-dependent splicing enhancer regulates human immunodeficiency virus type 1 rev, env, vpu, and nef gene expression. *J Virol*, 78:6517–6526. doi: 10.1128/JVI.78.12.6517-6526.2004
- [289] C Asang, I Hauber and H Schaal. 2008. Insights into the selective activation of alternatively used splice acceptors by the human immunodeficiency virus type-1 bidirectional splicing enhancer. *Nucleic Acids Res*, 36:1450–1463. doi: 10.1093/nar/gkm1147
- [290] TO Tange, CK Damgaard, S Guth, J Valcrcel and J Kjems. 2001. The hnRNP A1 protein regulates HIV-1 tat splicing via a novel intron silencer element. *EMBO J*, 20: 5748–5758. doi: 10.1093/emboj/20.20.5748
- [291] JA Jablonski, E Buratti, C Stuani and M Caputi. 2008. The secondary structure of the human immunodeficiency virus type 1 transcript modulates viral splicing and infectivity. *J Virol*, 82:8038–8050. doi: 10.1128/JVI.00721-08
- [292] A Tranell, EM Feny and S Schwartz. 2010. Serine- and arginine-rich proteins 55 and 75 (SRp55 and SRp75) induce production of HIV-1 vpr mRNA by inhibiting the 5'-splice site of exon 3. *J Biol Chem*, 285:31537–31547. doi: 10.1074/jbc.M109.077453
- [293] CM Stoltzfus and JM Madsen. 2006. Role of viral splicing elements and cellular RNA binding proteins in regulation of HIV-1 alternative RNA splicing. *Curr HIV Res*, 4: 43–55. doi: 10.2174/157016206775197655

- [294] E Buratti and FE Baralle. 2004. Influence of RNA secondary structure on the pre-mRNA splicing process. *Mol Cell Biol*, 24:10505–10514. doi: 10.1128/MCB.24.24.10505-10514.2004
- [295] PJ Shepard and KJ Hertel. 2008. Conserved RNA secondary structures promote alternative splicing. *RNA*, 14:1463–1469. doi: 10.1261/rna.1069408
- [296] M Alló, V Buggiano, JP Fededa, E Petrillo, I Schor, M de la Mata, E Agirre, M Plass, E Eyras et al. 2009. Control of alternative splicing through siRNA-mediated transcriptional gene silencing. *Nat Struct Mol Biol*, 16:717–724. doi: 10.1038/nsmb.1620
- [297] H Tilgner, C Nikolaou, S Althammer, M Sammeth, M Beato, J Valcrcel and R Guig. 2009. Nucleosome positioning as a determinant of exon recognition. *Nat Struct Mol Biol*, 16:996–1001. doi: 10.1038/nsmb.1658
- [298] S Schwartz, E Meshorer and G Ast. 2009. Chromatin organization marks exon-intron structure. *Nat Struct Mol Biol*, 16:990–995. doi: 10.1038/nsmb.1659
- [299] TL Crabb, BJ Lam and KJ Hertel. 2010. Retention of spliceosomal components along ligated exons ensures efficient removal of multiple introns. *RNA*, 16:1786–1796. doi: 10.1261/rna.2186510
- [300] K Takahara, U Schwarze, Y Imamura, GG Hoffman, H Toriello, LT Smith, PH Byers and DS Greenspan. 2002. Order of intron removal influences multiple splice outcomes, including a two-exon skip, in a COL5A1 acceptor-site mutation that results in abnormal pro-alpha1(V) N-propeptides and Ehlers-Danlos syndrome type I. *Am J Hum Genet*, 71:451–465. doi: 10.1086/342099
- [301] M de la Mata, C Lafaille and AR Kornblith. 2010. First come, first served revisited: factors affecting the same alternative splicing event have different effects on the relative rates of intron removal. *RNA*, 16:904–912. doi: 10.1261/rna.1993510
- [302] AM Zahler, KM Neugebauer, WS Lane and MB Roth. 1993. Distinct functions of SR proteins in alternative pre-mRNA splicing. *Science*, 260:219–222. doi: 10.1126/science.8385799
- [303] CW Smith and J Valcárcel. 2000. Alternative pre-mRNA splicing: the logic of combinatorial control. *Trends Biochem Sci*, 25:381–388. doi: 10.1016/S0968-0004(00)01604-2
- [304] J Ule, G Stefani, A Mele, M Ruggiu, X Wang, B Taneri, T Gaasterland, BJ Blencowe and RB Darnell. 2006. An RNA map predicting Nova-dependent splicing regulation. *Nature*, 444:580–586. doi: 10.1038/nature05304
- [305] Y Barash, JA Calarco, W Gao, Q Pan, X Wang, O Shai, BJ Blencowe and BJ Frey. 2010. Deciphering the splicing code. *Nature*, 465:53–59. doi: 10.1038/nature09000

- [306] HY Xiong, Y Barash and BJ Frey. 2011. Bayesian prediction of tissue-regulated splicing using RNA sequence and cellular context. *Bioinformatics*, 27:2554–2562. doi: 10.1093/bioinformatics/btr444
- [307] JT Witten and J Ule. 2011. Understanding splicing regulation through RNA splicing maps. *Trends Genet*, 27:89–97. doi: 10.1016/j.tig.2010.12.001
- [308] TO Tange, TH Jensen and J Kjems. 1996. In vitro interaction between human immunodeficiency virus type 1 Rev protein and splicing factor ASF/SF2-associated protein, p32. *J Biol Chem*, 271:10066–10072. doi: 10.1074/jbc.271.17.10066
- [309] R Berro, K Kehn, C de la Fuente, A Pumfery, R Adair, J Wade, AM Colberg-Poley, J Hiscott and F Kashanchi. 2006. Acetylated Tat regulates human immunodeficiency virus type 1 splicing through its interaction with the splicing regulator p32. *J Virol*, 80:3189–3204. doi: 10.1128/JVI.80.7.3189-3204.2006
- [310] S Jäger, P Cimermancic, N Gulbahce, JR Johnson, KE McGovern, SC Clarke, M Shales, G Mercenne, L Pache et al. 2012. Global landscape of HIV-human protein complexes. *Nature*, 481:365–370. doi: 10.1038/nature10719
- [311] J Bohne, A Schambach and D Zychlinski. 2007. New way of regulating alternative splicing in retroviruses: the promoter makes a difference. *J Virol*, 81:3652–3656. doi: 10.1128/JVI.02105-06
- [312] JA Jablonski, AL Amelio, M Giacca and M Caputi. 2010. The transcriptional transactivator Tat selectively regulates viral splicing. *Nucleic Acids Res*, 38:1249–1260. doi: 10.1093/nar/gkp1105
- [313] M Kuramitsu, C Hashizume, N Yamamoto, A Azuma, M Kamata, N Yamamoto, Y Tanaka and Y Aida. 2005. A novel role for Vpr of human immunodeficiency virus type 1 as a regulator of the splicing of cellular pre-mRNA. *Microbes Infect*, 7:1150–1160. doi: 10.1016/j.micinf.2005.03.022
- [314] C Hashizume, M Kuramitsu, X Zhang, T Kurosawa, M Kamata and Y Aida. 2007. Human immunodeficiency virus type 1 Vpr interacts with spliceosomal protein SAP145 to mediate cellular pre-mRNA splicing inhibition. *Microbes Infect*, 9:490–497. doi: 10.1016/j.micinf.2007.01.013
- [315] MT Vahey, ME Nau, LL Jagodzinski, J Valley-Ogunro, M Taubman, NL Michael and MG Lewis. 2002. Impact of viral infection on the gene expression profiles of proliferating normal human peripheral blood mononuclear cells infected with HIV type 1 RF. *AIDS Res Hum Retroviruses*, 18:179–192. doi: 10.1089/08892220252781239
- [316] AB van 't Wout, GK Lehrman, SA Mikheeva, GC O'Keeffe, MG Katze, RE Bumgarner, GK Geiss and JI Mullins. 2003. Cellular gene expression upon human immunodeficiency virus type 1 infection of CD4(+)T-cell lines. *J Virol*, 77:1392–1402. doi: 10.1128/JVI.77.2.1392-1402.2003

- [317] R Mitchell, CY Chiang, C Berry and F Bushman. 2003. Global analysis of cellular transcription following infection with an HIV-based vector. *Mol Ther*, 8:674–687. doi: 10.1016/S1525-0016(03)00215-6
- [318] M Rotger, KK Dang, J Fellay, EL Heinzen, S Feng, P Descombes, KV Shianna, D Ge, HF Gnathard et al. 2010. Genome-wide mRNA expression correlates of viral control in CD4+ T-cells from HIV-1-infected individuals. *PLoS Pathog*, 6:e1000781. doi: 10.1371/journal.ppat.1000781
- [319] ST Chang, P Sova, X Peng, J Weiss, GL Law, RE Palermo and MG Katze. 2011. Next-generation sequencing reveals HIV-1-mediated suppression of T cell activation and RNA processing and regulation of noncoding RNA expression in a CD4+ T cell line. *MBio*, 2. doi: 10.1128/mBio.00134-11
- [320] P Legrain and M Rosbash. 1989. Some cis- and trans-acting mutants for splicing target pre-mRNA to the cytoplasm. *Cell*, 57:573–583. doi: 10.1016/0092-8674(89)90127-X
- [321] U Fischer, S Meyer, M Teufel, C Heckel, R Lhrmann and G Rautmann. 1994. Evidence that HIV-1 Rev directly promotes the nuclear export of unspliced RNA. *EMBO J*, 13: 4105–4112
- [322] VW Pollard and MH Malim. 1998. The HIV-1 Rev protein. *Annu Rev Microbiol*, 52: 491–532. doi: 10.1146/annurev.micro.52.1.491
- [323] KA Jones and BM Peterlin. 1994. Control of RNA initiation and elongation at the HIV-1 promoter. *Annu Rev Biochem*, 63:717–743. doi: 10.1146/annurev.bi.63.070194.003441
- [324] TW McCloskey, M Ott, E Tribble, SA Khan, S Teichberg, MO Paul, S Pahwa, E Verdin and N Chirmule. 1997. Dual role of HIV Tat in regulation of apoptosis in T cells. *J Immunol*, 158:1014–1019
- [325] GR Campbell, E Pasquier, J Watkins, V Bourgarel-Rey, V Peyrot, D Esquieu, P Barbier, J de Mareuil, D Braguer et al. 2004. The glutamine-rich region of the HIV-1 Tat protein is involved in T-cell apoptosis. *J Biol Chem*, 279:48197–48204. doi: 10.1074/jbc.M406195200
- [326] HB Miller, TJ Robinson, R Gordn, AJ Hartemink and MA Garcia-Blanco. 2011. Identification of Tat-SF1 cellular targets by exon array analysis reveals dual roles in transcription and splicing. *RNA*, 17:665–674. doi: 10.1261/rna.2462011
- [327] AK Gubitz, W Feng and G Dreyfuss. 2004. The SMN complex. *Exp Cell Res*, 296: 51–56. doi: 10.1016/j.yexcr.2004.03.022
- [328] RS Yalow and SA Berson. 1960. Immunoassay of endogenous plasma insulin in man. *J Clin Invest*, 39:1157–1175. doi: 10.1172/JCI104130
- [329] E Engvall and P Perlmann. 1971. Enzyme-linked immunosorbent assay (ELISA).

- Quantitative assay of immunoglobulin G. *Immunochemistry*, 8:871–874. doi: 10.1016/0019-2791(71)90454-X
- [330] BK Van Weemen and AH Schuurs. 1971. Immunoassay using antigen-enzyme conjugates. *FEBS Lett.*, 15:232–236. doi: 10.1016/0014-5793(71)80319-8
- [331] JW Ward, AJ Grindon, PM Fecorino, C Schable, M Parvin and JR Allen. 1986. Laboratory and epidemiologic evaluation of an enzyme immunoassay for antibodies to HTLV-III. *JAMA*, 256:357–361. doi: 10.1001/jama.1986.03380030059028
- [332] H Towbin, T Staehelin and J Gordon. 1979. Electrophoretic transfer of proteins from polyacrylamide gels to nitrocellulose sheets: procedure and some applications. *Proc Natl Acad Sci U S A*, 76:4350–4354
- [333] Centers for Disease Control. 1985. Provisional Public Health Service inter-agency recommendations for screening donated blood and plasma for antibody to the virus causing acquired immunodeficiency syndrome. *MMWR Morb Mortal Wkly Rep*, 34:1–5
- [334] DS Burke and RR Redfield. 1986. False-positive Western blot tests for antibodies to HTLV-III. *JAMA*, 256:347. doi: 10.1001/jama.1986.03380030049013
- [335] DS Burke, JF Brundage, RR Redfield, JJ Damato, CA Schable, P Putman, R Visintine and HI Kim. 1988. Measurement of the false positive rate in a screening program for human immunodeficiency virus infections. *N Engl J Med*, 319:961–964. doi: 10.1056/NEJM198810133191501
- [336] RJ Chappel, KM Wilson and EM Dax. 2009. Immunoassays for the diagnosis of HIV: meeting future needs by enhancing the quality of testing. *Future Microbiol*, 4:963–982. doi: 10.2217/fmb.09.77
- [337] B Weber, EH Fall, A Berger and HW Doerr. 1998. Reduction of diagnostic window by new fourth-generation human immunodeficiency virus screening assays. *J Clin Microbiol*, 36:2235–2239
- [338] B Weber, L Görtler, R Thorstensson, U Michl, A Mühlbacher, P Bürgisser, R Villaescusa, A Eiras, C Gabriel et al. 2002. Multicenter evaluation of a new automated fourth-generation human immunodeficiency virus screening assay with a sensitive antigen detection module and high specificity. *J Clin Microbiol*, 40:1938–1946. doi: 10.1128/JCM.40.6.1938-1946.2002
- [339] WJ Kassler, C Haley, WK Jones, AR Gerber, EJ Kennedy and JR George. 1995. Performance of a rapid, on-site human immunodeficiency virus antibody assay in a public health setting. *J Clin Microbiol*, 33:2899–2902
- [340] Centers for Disease Control and Prevention. 1998. Update: HIV counseling and testing using rapid tests—United States, 1995. *MMWR Morb Mortal Wkly Rep*, 47:211–215

- [341] Centers for Disease Control and Prevention. 2002. Approval of a new rapid test for HIV antibody. *MMWR Morb Mortal Wkly Rep*, 51:1051–1052
- [342] D Gallo, JR George, JH Fitchen, AS Goldstein and MS Hindahl. 1997. Evaluation of a system using oral mucosal transudate for HIV-1 antibody screening and confirmatory testing. OraSure HIV Clinical Trials Group. *JAMA*, 277:254–258. doi: 10.1001/jama.1997.03540270080030
- [343] KP Delaney, BM Branson, A Uniyal, PR Kerndt, PA Keenan, K Jafa, AD Gardner, DJ Jamieson and M Bulterys. 2006. Performance of an oral fluid rapid HIV-1/2 test: experience from four CDC studies. *AIDS*, 20:1655–1660. doi: 10.1097/01.aids.0000238412.75324.82
- [344] C Semá Baltazar, C Raposo, IV Jani, D Shodell, D Correia, C Gonçalves da Silva, M Kalou, H Patel and B Parekh. 2014. Evaluation of performance and acceptability of two rapid oral fluid tests for HIV detection in Mozambique. *J Clin Microbiol*, 52: 3544–3548. doi: 10.1128/JCM.01098-14
- [345] TC Granade, BS Parekh, SK Phillips and JS McDougal. 2004. Performance of the OraQuick and Hema-Strip rapid HIV antibody detection assays by non-laboratorians. *J Clin Virol*, 30:229–232. doi: 10.1016/j.jcv.2003.12.006
- [346] N Pant Pai, J Sharma, S Shrivkumar, S Pillay, C Vadnais, L Joseph, K Dheda and RW Peeling. 2013. Supervised and unsupervised self-testing for HIV in high- and low-risk populations: a systematic review. *PLoS Med*, 10:e1001414. doi: 10.1371/journal.pmed.1001414
- [347] M Usdin, M Guillerm and A Calmy. 2010. Patient needs and point-of-care requirements for HIV load testing in resource-limited settings. *J Infect Dis*, 201 Suppl 1:S73–S77. doi: 10.1086/650384
- [348] SA Fiscus, B Cheng, SM Crowe, L Demeter, C Jennings, V Miller, R Respess, W Stevens and FfCHIVRAVLAWG . 2006. HIV-1 viral load assays for resource-limited settings. *PLoS Med*, 3:e417. doi: 10.1371/journal.pmed.0030417
- [349] S Wang, F Xu and U Demirci. 2010. Advances in developing HIV-1 viral load assays for resource-limited settings. *Biotechnol Adv*, 28:770–781. doi: 10.1016/j.biotechadv.2010.06.004
- [350] P Mee, KL Fielding, S Charalambous, GJ Churchyard and AD Grant. 2008. Evaluation of the WHO criteria for antiretroviral treatment failure among adults in South Africa. *AIDS*, 22:1971–1977. doi: 10.1097/QAD.0b013e32830e4cd8
- [351] JJG van Oosterhout, L Brown, R Weigel, JJ Kumwenda, D Mzinganjira, N Saukila, B Mhango, T Hartung, S Phiri and MC Hosseinipour. 2009. Diagnosis of antiretroviral therapy failure in Malawi: poor performance of clinical and immunological WHO criteria. *Trop Med Int Health*, 14:856–861. doi: 10.1111/j.1365-3156.2009.02309.x

- [352] MC Hosseinpour, JJG van Oosterhout, R Weigel, S Phiri, D Kamwendo, N Parkin, SA Fiscus, JAE Nelson, JJ Eron and J Kumwenda. 2009. The public health approach to identify antiretroviral therapy failure: high-level nucleoside reverse transcriptase inhibitor resistance among Malawians failing first-line antiretroviral therapy. *AIDS*, 23:1127–1134. doi: 10.1097/QAD.0b013e32832ac34e
- [353] S Sherrill-Mix, MK Lewinski, M Famiglietti, A Bosque, N Malani, KE Ocwieja, CC Berry, D Looney, L Shan et al. 2013. HIV latency and integration site placement in five cell-based models. *Retrovirology*, 10:90. doi: 10.1186/1742-4690-10-90
- [354] LS Weinberger, RD Dar and ML Simpson. 2008. Transient-mediated fate determination in a transcriptional circuit of HIV. *Nat Genet*, 40:466–470. doi: 10.1038/ng.116
- [355] A Singh, B Razooky, CD Cox, ML Simpson and LS Weinberger. 2010. Transcriptional bursting from the HIV-1 promoter is a significant source of stochastic noise in HIV-1 gene expression. *Biophys J*, 98:L32–L34. doi: 10.1016/j.bpj.2010.03.001
- [356] BS Razooky and LS Weinberger. 2011. Mapping the architecture of the HIV-1 Tat circuit: A decision-making circuit that lacks bistability and exploits stochastic noise. *Methods*, 53:68–77. doi: 10.1016/j.ymeth.2010.12.006
- [357] HJ Muller. 1930. Types of visible variations induced by X-rays in *Drosophila*. *J Genet*, 22:299–334
- [358] M Gaszner and G Felsenfeld. 2006. Insulators: exploiting transcriptional and epigenetic mechanisms. *Nat Rev Genet*, 7:703–713. doi: 10.1038/nrg1925
- [359] A Jordan, P Defechereux and E Verdin. 2001. The site of HIV-1 integration in the human genome determines basal transcriptional activity and response to Tat transactivation. *EMBO J*, 20:1726–1738. doi: 10.1093/emboj/20.7.1726
- [360] A Jordan, D Bisgrove and E Verdin. 2003. HIV reproducibly establishes a latent infection after acute infection of T cells in vitro. *EMBO J*, 22:1868–1877. doi: 10.1093/emboj/cdg188
- [361] R Pearson, YK Kim, J Hokello, K Lassen, J Friedman, M Tyagi and J Karn. 2008. Epigenetic silencing of human immunodeficiency virus (HIV) transcription by formation of restrictive chromatin structures at the viral long terminal repeat drives the progressive entry of HIV into latency. *J Virol*, 82:12291–12303. doi: 10.1128/JVI.01383-08
- [362] F Romerio, MN Gabriel and DM Margolis. 1997. Repression of human immunodeficiency virus type 1 through the novel cooperation of human factors YY1 and LSF. *J Virol*, 71:9375–9382
- [363] JJ Coull, F Romerio, JM Sun, JL Volker, KM Galvin, JR Davie, Y Shi, U Hansen and DM Margolis. 2000. The human factors YY1 and LSF repress the human immun-

odeficiency virus type 1 long terminal repeat via recruitment of histone deacetylase 1. *J Virol*, 74:6790–6799. doi: 10.1128/JVI.74.15.6790-6799.2000

- [364] G He and DM Margolis. 2002. Counterregulation of chromatin deacetylation and histone deacetylase occupancy at the integrated promoter of human immunodeficiency virus type 1 (HIV-1) by the HIV-1 repressor YY1 and HIV-1 activator Tat. *Mol Cell Biol*, 22:2965–2973. doi: 10.1128/MCB.22.9.2965-2973.2002
- [365] T Lenasi, X Contreras and BM Peterlin. 2008. Transcriptional interference antagonizes proviral gene expression to promote HIV latency. *Cell Host Microbe*, 4:123–133. doi: 10.1016/j.chom.2008.05.016
- [366] Y Han, YB Lin, W An, J Xu, HC Yang, K O'Connell, D Dordai, JD Boeke, JD Siliciano and RF Siliciano. 2008. Orientation-dependent regulation of integrated HIV-1 expression by host gene transcriptional readthrough. *Cell Host Microbe*, 4:134–146. doi: 10.1016/j.chom.2008.06.008
- [367] L Shan, K Deng, NS Shroff, CM Durand, SA Rabi, HC Yang, H Zhang, JB Margolick, JN Blankson and RF Siliciano. 2012. Stimulation of HIV-1-specific cytolytic T lymphocytes facilitates elimination of latent viral reservoir after virus reactivation. *Immunity*, 36:491–501. doi: 10.1016/j.jimmuni.2012.01.014
- [368] D Boehm, V Calvanese, RD Dar, S Xing, S Schroeder, L Martins, K Aull, PC Li, V Planelles et al. 2013. BET bromodomain-targeting compounds reactivate HIV from latency via a Tat-independent mechanism. *Cell Cycle*, 12:452–462. doi: 10.4161/cc.23309
- [369] A Savarino, A Mai, S Norelli, SE Daker, S Valente, D Rotili, L Altucci, AT Palamarra and E Garaci. 2009. “Shock and kill” effects of class I-selective histone deacetylase inhibitors in combination with the glutathione synthesis inhibitor buthionine sulfoximine in cell line models for HIV-1 quiescence. *Retrovirology*, 6:52. doi: 10.1186/1742-4690-6-52
- [370] NM Archin, AL Liberty, AD Kashuba, SK Choudhary, JD Kuruc, AM Crooks, DC Parker, EM Anderson, MF Kearney et al. 2012. Administration of vorinostat disrupts HIV-1 latency in patients on antiretroviral therapy. *Nature*, 487:482–485. doi: 10.1038/nature11286
- [371] A Bosque and V Planelles. 2009. Induction of HIV-1 latency and reactivation in primary memory CD4+ T cells. *Blood*, 113:58–65. doi: 10.1182/blood-2008-07-168393
- [372] A Bosque and V Planelles. 2011. Studies of HIV-1 latency in an ex vivo model that uses primary central memory T cells. *Methods*, 53:54–61. doi: 10.1016/jymeth.2010.10.002
- [373] X Wu, Y Li, B Crise and SM Burgess. 2003. Transcription start regions in the human genome are favored targets for MLV integration. *Science*, 300:1749–1751. doi: 10.1126/science.1083413

- [374] RS Mitchell, BF Beitzel, ARW Schroder, P Shinn, H Chen, CC Berry, JR Ecker and FD Bushman. 2004. Retroviral DNA integration: ASLV, HIV, and MLV show distinct target site preferences. *PLoS Biol*, 2:e234. doi: 10.1371/journal.pbio.0020234
- [375] R Core Team. *R: A Language and Environment for Statistical Computing*. R Foundation for Statistical Computing, Vienna, Austria, 2012
- [376] C Berry, S Hannenhalli, J Leipzig and FD Bushman. 2006. Selection of target sites for mobile DNA integration in the human genome. *PLoS Comput Biol*, 2:e157. doi: 10.1371/journal.pcbi.0020157
- [377] GP Wang, A Ciuffi, J Leipzig, CC Berry and FD Bushman. 2007. HIV integration site selection: analysis by massively parallel pyrosequencing reveals association with epigenetic modifications. *Genome Res*, 17:1186–1194. doi: 10.1101/gr.6286907
- [378] H Mochizuki, JP Schwartz, K Tanaka, RO Brady and J Reiser. 1998. High-titer human immunodeficiency virus type 1-based vector systems for gene delivery into nondividing cells. *J Virol*, 72:8873–8883
- [379] Y Han, K Lassen, D Monie, AR Sedaghat, S Shimoji, X Liu, TC Pierson, JB Margolick, RF Siliciano and JD Siliciano. 2004. Resting CD4+ T cells from human immunodeficiency virus type 1 (HIV-1)-infected individuals carry integrated HIV-1 genomes within actively transcribed host genes. *J Virol*, 78:6122–6133. doi: 10.1128/JVI.78.12.6122-6133.2004
- [380] G Plesa, J Dai, C Baytop, JL Riley, CH June and U O'Doherty. 2007. Addition of deoxynucleosides enhances human immunodeficiency virus type 1 integration and 2LTR formation in resting CD4+ T cells. *J Virol*, 81:13938–13942. doi: 10.1128/JVI.01745-07
- [381] N Malani. hiReadsProcessor R package. URL <http://github.com/malnirav/hiReadsProcessor>
- [382] WJ Kent. 2002. BLAT—the BLAST-like alignment tool. *Genome Res*, 12:656–664. doi: 10.1101/gr.229202
- [383] CC Berry, K Ocwieja, N Malani and FD Bushman. 2014. Comparing DNA integration site clusters with Scan Statistics. *Bioinformatics*, 30:1493–1500. doi: 10.1093/bioinformatics/btu035
- [384] C Trapnell, BA Williams, G Pertea, A Mortazavi, G Kwan, MJ van Baren, SL Salzberg, BJ Wold and L Pachter. 2010. Transcript assembly and quantification by RNA-Seq reveals unannotated transcripts and isoform switching during cell differentiation. *Nat Biotechnol*, 28:511–515. doi: 10.1038/nbt.1621
- [385] J Ernst and M Kellis. 2010. Discovery and characterization of chromatin states for systematic annotation of the human genome. *Nat Biotechnol*, 28:817–825. doi: 10.1038/nbt.1662

- [386] AS Hinrichs, D Karolchik, R Baertsch, GP Barber, G Bejerano, H Clawson, M Diekhans, TS Furey, RA Harte et al. 2006. The UCSC Genome Browser Database: update 2006. *Nucleic Acids Res*, 34:D590–D598. doi: 10.1093/nar/gkj144
- [387] KR Rosenbloom, CA Sloan, VS Malladi, TR Dreszer, K Learned, VM Kirkup, MC Wong, M Maddren, R Fang et al. 2013. ENCODE data in the UCSC Genome Browser: year 5 update. *Nucleic Acids Res*, 41:D56–D63. doi: 10.1093/nar/gks1172
- [388] J Han, SG Park, JB Bae, J Choi, JM Lyu, SH Park, HS Kim, YJ Kim, S Kim and TY Kim. 2012. The characteristics of genome-wide DNA methylation in naïve CD4+ T cells of patients with psoriasis or atopic dermatitis. *Biochem Biophys Res Commun*, 422:157–163. doi: 10.1016/j.bbrc.2012.04.128
- [389] LR Meyer, AS Zweig, AS Hinrichs, D Karolchik, RM Kuhn, M Wong, CA Sloan, KR Rosenbloom, G Roe et al. 2013. The UCSC Genome Browser database: extensions and updates 2013. *Nucleic Acids Res*, 41:D64–D69. doi: 10.1093/nar/gks1048
- [390] Z Wang, C Zang, JA Rosenfeld, DE Schones, A Barski, S Cuddapah, K Cui, TY Roh, W Peng et al. 2008. Combinatorial patterns of histone acetylations and methylations in the human genome. *Nat Genet*, 40:897–903. doi: 10.1038/ng.154
- [391] A Barski, S Cuddapah, K Cui, TY Roh, DE Schones, Z Wang, G Wei, I Chepelev and K Zhao. 2007. High-resolution profiling of histone methylations in the human genome. *Cell*, 129:823–837. doi: 10.1016/j.cell.2007.05.009
- [392] Z Wang, C Zang, K Cui, DE Schones, A Barski, W Peng and K Zhao. 2009. Genome-wide mapping of HATs and HDACs reveals distinct functions in active and inactive genes. *Cell*, 138:1019–1031. doi: 10.1016/j.cell.2009.06.049
- [393] DE Schones, K Cui, S Cuddapah, TY Roh, A Barski, Z Wang, G Wei and K Zhao. 2008. Dynamic regulation of nucleosome positioning in the human genome. *Cell*, 132: 887–898. doi: 10.1016/j.cell.2008.02.022
- [394] F Hsu, WJ Kent, H Clawson, RM Kuhn, M Diekhans and D Haussler. 2006. The UCSC Known Genes. *Bioinformatics*, 22:1036–1046. doi: 10.1093/bioinformatics/btl048
- [395] J Friedman, T Hastie and R Tibshirani. 2010. Regularization paths for generalized linear models via coordinate descent. *J Stat Softw*, 33:1–22
- [396] IH Greger, F Demarchi, M Giacca and NJ Proudfoot. 1998. Transcriptional interference perturbs the binding of Sp1 to the HIV-1 promoter. *Nucleic Acids Res*, 26:1294–1301
- [397] A De Marco, C Biancotto, A Knezevich, P Maiuri, C Vardabasso and A Marcello. 2008. Intragenic transcriptional cis-activation of the human immunodeficiency virus 1 does not result in allele-specific inhibition of the endogenous gene. *Retrovirology*, 5:98. doi: 10.1186/1742-4690-5-98

- [398] JS Waye and HF Willard. 1987. Nucleotide sequence heterogeneity of alpha satellite repetitive DNA: a survey of alphoid sequences from different human chromosomes. *Nucleic Acids Res*, 15:7549–7569. doi: 10.1093/nar/15.18.7549
- [399] J Jurka, VV Kapitonov, A Pavlicek, P Klonowski, O Kohany and J Walichiewicz. 2005. Repbase Update, a database of eukaryotic repetitive elements. *Cytogenet Genome Res*, 110:462–467. doi: 10.1159/000084979
- [400] E Verdin, P Paras and C Van Lint. 1993. Chromatin disruption in the promoter of human immunodeficiency virus type 1 during transcriptional activation. *EMBO J*, 12: 3249–3259
- [401] C Van Lint, S Emiliani, M Ott and E Verdin. 1996. Transcriptional activation and chromatin remodeling of the HIV-1 promoter in response to histone acetylation. *EMBO J*, 15:1112–1120
- [402] KG Lassen, KX Ramyar, JR Bailey, Y Zhou and RF Siliciano. 2006. Nuclear retention of multiply spliced HIV-1 RNA in resting CD4+ T cells. *PLoS Pathog*, 2:e68. doi: 10.1371/journal.ppat.0020068
- [403] M Dieudonné, P Maiuri, C Biancotto, A Knezevich, A Kula, M Lusic and A Marcello. 2009. Transcriptional competence of the integrated HIV-1 provirus at the nuclear periphery. *EMBO J*, 28:2231–2243. doi: 10.1038/emboj.2009.141
- [404] RF Siliciano and WC Greene. 2011. HIV Latency. *Cold Spring Harb Perspect Med*, 1: a007096. doi: 10.1101/cshperspect.a007096
- [405] M Lusic, B Marini, H Ali, B Lucic, R Luzzati and M Giacca. 2013. Proximity to PML nuclear bodies regulates HIV-1 latency in CD4+ T cells. *Cell Host Microbe*, 13: 665–677. doi: 10.1016/j.chom.2013.05.006
- [406] KE Ocwieja, S Sherrill-Mix, R Mukherjee, R Custers-Allen, P David, M Brown, S Wang, DR Link, J Olson et al. 2012. Dynamic regulation of HIV-1 mRNA populations analyzed by single-molecule enrichment and long-read sequencing. *Nucleic Acids Res*, 40:10345–10355. doi: 10.1093/nar/gks753
- [407] Q Pan, O Shai, LJ Lee, BJ Frey and BJ Blencowe. 2008. Deep surveying of alternative splicing complexity in the human transcriptome by high-throughput sequencing. *Nature Genetics*, 40:1413–1415. doi: 10.1038/ng.259
- [408] ET Wang, R Sandberg, S Luo, I Khrebtukova, L Zhang, C Mayr, SF Kingsmore, GP Schroth and CB Burge. 2008. Alternative isoform regulation in human tissue transcriptomes. *Nature*, 456:470–476. doi: 10.1038/nature07509
- [409] F Pagani, M Raponi and FE Baralle. 2005. Synonymous mutations in CFTR exon 12 affect splicing and are not neutral in evolution. *Proc Natl Acad Sci U S A*, 102: 6368–6372. doi: 10.1073/pnas.0502288102

- [410] C Wang, Y Mitsuya, B Gharizadeh, M Ronaghi and SR W. 2007. Characterization of mutation spectra with ultra-deep pyrosequencing: Application to HIV-1 drug resistance. *Genome Research*, 17:1195–1201. doi: 10.1101/gr.6468307
- [411] K Wang, R Wernersson and S Brunak. 2011. The strength of intron donor splice sites in human genes displays a bell-shaped pattern. *Bioinformatics*, 27:3079–3084. doi: 10.1093/bioinformatics/btr532
- [412] DF Purcell and MA Martin. 1993. Alternative splicing of human immunodeficiency virus type 1 mRNA modulates viral protein expression, replication, and infectivity. *J Virol*, 67:6365–6378
- [413] DM Benko, S Schwartz, GN Pavlakis and BK Felber. 1990. A novel human immunodeficiency virus type 1 protein, tev, shares sequences with tat, env, and rev proteins. *J Virol*, 64:2505–2518
- [414] C Carrera, M Pinilla, L Pérez-Alvarez and MM Thomson. 2010. Identification of unusual and novel HIV type 1 spliced transcripts generated in vivo. *AIDS Res Hum Retroviruses*, 26:815–820. doi: 10.1089/aid.2010.0011
- [415] M Lützelberger, LS Reinert, AT Das, B Berkhout and J Kjems. 2006. A novel splice donor site in the gag-pol gene is required for HIV-1 RNA stability. *J Biol Chem*, 281: 18644–18651. doi: 10.1074/jbc.M513698200
- [416] J Salfeld, HG Gttlinger, RA Sia, RE Park, JG Sodroski and WA Haseltine. 1990. A tripartite HIV-1 tat-env-rev fusion protein. *EMBO J*, 9:965–970
- [417] S Schwartz, BK Felber, DM Benko, EM Fenyö and GN Pavlakis. 1990. Cloning and functional analysis of multiply spliced mRNA species of human immunodeficiency virus type 1. *J Virol*, 64:2519–2529
- [418] J Smith, A Azad and N Deacon. 1992. Identification of two novel human immunodeficiency virus type 1 splice acceptor sites in infected T cell lines. *J Gen Virol*, 73 ( Pt 7):1825–1828
- [419] N Bakkour, YL Lin, S Maire, L Ayadi, F Mahuteau-Betzer, CH Nguyen, C Mettling, P Portales, D Grierson et al. 2007. Small-molecule inhibition of HIV pre-mRNA splicing as a novel antiretroviral therapy to overcome drug resistance. *PLoS Pathog*, 3: 1530–1539. doi: 10.1371/journal.ppat.0030159
- [420] AL Brass, DM Dykxhoorn, Y Benita, N Yan, A Engelman, RJ Xavier, J Lieberman and SJ Elledge. 2008. Identification of host proteins required for HIV infection through a functional genomic screen. *Science*, 319:921–926. doi: 10.1126/science.1152725
- [421] JA Jablonski and M Caputi. 2009. Role of cellular RNA processing factors in human immunodeficiency virus type 1 mRNA metabolism, replication, and infectivity. *J Virol*, 83:981–992. doi: 10.1128/JVI.01801-08

- [422] R König, Y Zhou, D Elleder, TL Diamond, GMC Bonamy, JT Irelan, CY Chiang, BP Tu, PDD Jesus et al. 2008. Global analysis of host-pathogen interactions that regulate early-stage HIV-1 replication. *Cell*, 135:49–60. doi: 10.1016/j.cell.2008.07.032
- [423] A Tranell, S Tingsborg, EM Feny and S Schwartz. 2011. Inhibition of splicing by serine-arginine rich protein 55 (SRp55) causes the appearance of partially spliced HIV-1 mRNAs in the cytoplasm. *Virus Res*, 157:82–91. doi: 10.1016/j.virusres.2011.02.010
- [424] H Zhou, M Xu, Q Huang, AT Gates, XD Zhang, JC Castle, E Stec, M Ferrer, B Strulovici et al. 2008. Genome-scale RNAi screen for host factors required for HIV replication. *Cell Host Microbe*, 4:495–504. doi: 10.1016/j.chom.2008.10.004
- [425] Y Zhu, G Chen, F Lv, X Wang, X Ji, Y Xu, J Sun, L Wu, YT Zheng and G Gao. 2011. Zinc-finger antiviral protein inhibits HIV-1 infection by selectively targeting multiply spliced viral mRNAs for degradation. *Proc Natl Acad Sci U S A*, 108:15834–15839. doi: 10.1073/pnas.1101676108
- [426] MJ Saltarelli, E Hadziyannis, CE Hart, JV Harrison, BK Felber, TJ Spira and GN Pavlakis. 1996. Analysis of human immunodeficiency virus type 1 mRNA splicing patterns during disease progression in peripheral blood mononuclear cells from infected individuals. *AIDS Res Hum Retroviruses*, 12:1443–1456. doi: 10.1089/aid.1996.12.1443
- [427] E Delgado, C Carrera, P Nebreda, A Fernndez-Garca, M Pinilla, V Garca, L Prelvarez and MM Thomson. 2012. Identification of new splice sites used for generation of rev transcripts in human immunodeficiency virus type 1 subtype C primary isolates. *PLoS One*, 7:e30574. doi: 10.1371/journal.pone.0030574
- [428] P Grabowski. 2011. Alternative splicing takes shape during neuronal development. *Curr Opin Genet Dev*, 21:388–394. doi: 10.1016/j.gde.2011.03.005
- [429] M Llorian and CWJ Smith. 2011. Decoding muscle alternative splicing. *Curr Opin Genet Dev*, 21:380–387. doi: 10.1016/j.gde.2011.03.006
- [430] JY Ip, A Tong, Q Pan, JD Topp, BJ Blencowe and KW Lynch. 2007. Global analysis of alternative splicing during T-cell activation. *RNA*, 13:563–572. doi: 10.1261/rna.457207
- [431] JD Topp, J Jackson, AA Melton and KW Lynch. 2008. A cell-based screen for splicing regulators identifies hnRNP LL as a distinct signal-induced repressor of CD45 variable exon 4. *RNA*, 14:2038–2049. doi: 10.1261/rna.1212008
- [432] S Sonza, HP Mutimer, K O'Brien, P Ellery, JL Howard, JH Axelrod, NJ Deacon, SM Crowe and DFJ Purcell. 2002. Selectively reduced tat mRNA heralds the decline in productive human immunodeficiency virus type 1 infection in monocyte-derived macrophages. *J Virol*, 76:12611–12621
- [433] D Dowling, S Nasr-Esfahani, CH Tan, K O'Brien, JL Howard, DA Jans, DF j Purcell, CM Stoltzfus and S Sonza. 2008. HIV-1 infection induces changes in expression of

- cellular splicing factors that regulate alternative viral splicing and virus production in macrophages. *Retrovirology*, 5:18. doi: 10.1186/1742-4690-5-18
- [434] J Hull, S Campino, K Rowlands, MS Chan, RR Copley, MS Taylor, K Rockett, G Elvidge, B Keating et al. 2007. Identification of common genetic variation that modulates alternative splicing. *PLoS Genet*, 3:e99. doi: 10.1371/journal.pgen.0030099
- [435] T Kwan, D Benovoy, C Dias, S Gurd, D Serre, H Zuzan, TA Clark, A Schweitzer, MK Staples et al. 2007. Heritability of alternative splicing in the human genome. *Genome Res*, 17:1210–1218. doi: 10.1101/gr.6281007
- [436] R Collman, JW Balliet, SA Gregory, H Friedman, DL Kolson, N Nathanson and A Srinivasan. 1992. An infectious molecular clone of an unusual macrophage-tropic and highly cytopathic strain of human immunodeficiency virus type 1. *J Virol*, 66: 7517–7521
- [437] J Eid, A Fehr, J Gray, K Luong, J Lyle, G Otto, P Peluso, D Rank, P Baybayan et al. 2009. Real-time DNA sequencing from single polymerase molecules. *Science*, 323:133–138. doi: 10.1126/science.1162986
- [438] H Deng, R Liu, W Ellmeier, S Choe, D Unutmaz, M Burkhart, P Di Marzio, S Marmon, RE Sutton et al. 1996. Identification of a major co-receptor for primary isolates of HIV-1. *Nature*, 381:661–666. doi: 10.1038/381661a0
- [439] NR Landau and DR Littman. 1992. Packaging system for rapid production of murine leukemia virus vectors with variable tropism. *J Virol*, 66:5110–5113
- [440] N Srinivasakumar, N Chazal, C Helga-Maria, S Prasad, ML Hammarskjöld and D Rekosh. 1997. The effect of viral regulatory protein expression on gene delivery by human immunodeficiency virus type 1 vectors produced in stable packaging cell lines. *J Virol*, 71:5841–5848
- [441] DC Shugars, MS Smith, DH Glueck, PV Nantermet, F Seillier-Moiseiwitsch and R Swanstrom. 1993. Analysis of human immunodeficiency virus type 1 nef gene sequences present in vivo. *J Virol*, 67:4639–4650
- [442] R Tewhey, JB Warner, M Nakano, B Libby, M Medkova, PH David, SK Kotsopoulos, ML Samuels, JB Hutchison et al. 2009. Microdroplet-based PCR enrichment for large-scale targeted sequencing. *Nat Biotechnol*, 27:1025–1031. doi: 10.1038/nbt.1583
- [443] KJ Travers, CS Chin, DR Rank, JS Eid and SW Turner. 2010. A flexible and efficient template format for circular consensus sequencing and SNP detection. *Nucleic Acids Res*, 38:e159. doi: 10.1093/nar/gkq543
- [444] TA Thanaraj and F Clark. 2001. Human GC-AG alternative intron isoforms with weak donor sites show enhanced consensus at acceptor exon positions. *Nucleic Acids Res*, 29:2581–2593. doi: 10.1093/nar/29.12.2581

- [445] M Aebi, H Hornig, RA Padgett, J Reiser and C Weissmann. 1986. Sequence requirements for splicing of higher eukaryotic nuclear pre-mRNA. *Cell*, 47:555–565
- [446] M Burset, IA Seledtsov and VV Solovyev. 2000. Analysis of canonical and non-canonical splice sites in mammalian genomes. *Nucleic Acids Res*, 28:4364–4375. doi: 10.1093/nar/28.21.4364
- [447] M Burset, IA Seledtsov and VV Solovyev. 2001. SpliceDB: database of canonical and non-canonical mammalian splice sites. *Nucleic Acids Res*, 29:255–259. doi: 10.1093/nar/29.1.255
- [448] N Sheth, X Roca, ML Hastings, T Roeder, AR Krainer and R Sachidanandam. 2006. Comprehensive splice-site analysis using comparative genomics. *Nucleic Acids Res*, 34: 3955–3967. doi: 10.1093/nar/gkl556
- [449] JC Guatelli, TR Gingras and DD Richman. 1990. Alternative splice acceptor utilization during human immunodeficiency virus type 1 infection of cultured cells. *J Virol*, 64:4093–4098
- [450] C Kuiken, B Foley, T Leitner, C Apetrei, B Hahn, I Mizrahi, J Mullins, A Rambaut, S Wolinsky and B Korber. 2010. HIV Sequence Compendium 2010. Theoretical Biology and Biophysics Group, Los Alamos National Laboratory, New Mexico. URL <http://www.hiv.lanl.gov/content/sequence/HIV/COMPENDIUM/2010compendium.html>
- [451] C Burge, T Tuschl and P Sharp. 1999. Splicing of precursors to mRNAs by the spliceosomes. *Cold Spring Harbor Monograph Archive*, 37. doi: 10.1101/087969589.37. 525
- [452] TEM Abbink and B Berkhout. 2008. RNA structure modulates splicing efficiency at the human immunodeficiency virus type 1 major splice donor. *J Virol*, 82:3090–3098. doi: 10.1128/JVI.01479-07
- [453] K Verhoef, PS Bilodeau, JL van Wamel, J Kjems, CM Stoltzfus and B Berkhout. 2001. Repair of a Rev-minus human immunodeficiency virus type 1 mutant by activation of a cryptic splice site. *J Virol*, 75:3495–3500. doi: 10.1128/JVI.75.7.3495-3500.2001
- [454] AM Zahler, CK Damgaard, J Kjems and M Caputi. 2004. SC35 and heterogeneous nuclear ribonucleoprotein A/B proteins bind to a juxtaposed exonic splicing enhancer/exonic splicing silencer element to regulate HIV-1 tat exon 2 splicing. *J Biol Chem*, 279:10077–10084. doi: 10.1074/jbc.M312743200
- [455] S Sherrill-Mix, K Ocieja and F Bushman. Under Review. Gene activity in primary T cells infected with HIV89.6: intron retention and induction of distinctive genomic repeats. *Retrovirology*
- [456] S Wain-Hobson, P Sonigo, O Danos, S Cole and M Alizon. 1985. Nucleotide sequence of the AIDS virus, LAV. *Cell*, 40:9–17. doi: 10.1016/0092-8674(85)90303-4

- [457] SK Arya, C Guo, SF Josephs and F Wong-Staal. 1985. Trans-activator gene of human T-lymphotropic virus type III (HTLV-III). *Science*, 229:69–73
- [458] RA Marciniak and PA Sharp. 1991. HIV-1 Tat protein promotes formation of more-processive elongation complexes. *EMBO J*, 10:4189–4196
- [459] P Wei, ME Garber, SM Fang, WH Fischer and KA Jones. 1998. A novel CDK9-associated C-type cyclin interacts directly with HIV-1 Tat and mediates its high-affinity, loop-specific binding to TAR RNA. *Cell*, 92:451–462. doi: 10.1016/S0092-8674(00)80939-3
- [460] S Kanazawa, T Okamoto and BM Peterlin. 2000. Tat competes with CIITA for the binding to P-TEFb and blocks the expression of MHC class II genes in HIV infection. *Immunity*, 12:61–70. doi: 10.1016/S1074-7613(00)80159-4
- [461] M Barboric, JHN Yik, N Czudnochowski, Z Yang, R Chen, X Contreras, M Geyer, B Matija Peterlin and Q Zhou. 2007. Tat competes with HEXIM1 to increase the active pool of P-TEFb for HIV-1 transcription. *Nucleic Acids Res*, 35:2003–2012. doi: 10.1093/nar/gkm063
- [462] SK O'Brien, H Cao, R Nathans, A Ali and TM Rana. 2010. P-TEFb kinase complex phosphorylates histone H1 to regulate expression of cellular and HIV-1 genes. *J Biol Chem*, 285:29713–29720. doi: 10.1074/jbc.M110.125997
- [463] L Muniz, S Egloff, B Ughy, BE Jády and T Kiss. 2010. Controlling cellular P-TEFb activity by the HIV-1 transcriptional transactivator Tat. *PLoS Pathog*, 6:e1001152. doi: 10.1371/journal.ppat.1001152
- [464] J Corbeil, D Sheeter, D Genini, S Rought, L Leoni, P Du, M Ferguson, DR Masys, JB Welsh et al. 2001. Temporal gene regulation during HIV-1 infection of human CD4+ T cells. *Genome Res*, 11:1198–1204. doi: 10.1101/gr.180201
- [465] CH Woelk, F Ottones, CR Plotkin, P Du, CD Royer, SE Rought, J Lozach, R Sasik, RS Kornbluth et al. 2004. Interferon gene expression following HIV type 1 infection of monocyte-derived macrophages. *AIDS Res Hum Retroviruses*, 20:1210–1222. doi: 10.1089/0889222042545009
- [466] MD Hyrcza, C Kovacs, M Loutfy, R Halpenny, L Heisler, S Yang, O Wilkins, M Ostrowski and SD Der. 2007. Distinct transcriptional profiles in ex vivo CD4+ and CD8+ T cells are established early in human immunodeficiency virus type 1 infection and are characterized by a chronic interferon response as well as extensive transcriptional changes in CD8+ T cells. *J Virol*, 81:3477–3486. doi: 10.1128/JVI.01552-06
- [467] JQ Wu, DE Dwyer, WB Dyer, YH Yang, B Wang and NK Saksena. 2008. Transcriptional profiles in CD8+ T cells from HIV+ progressors on HAART are characterized by coordinated up-regulation of oxidative phosphorylation enzymes and interferon responses. *Virology*, 380:124–135. doi: 10.1016/j.virol.2008.06.039

- [468] AJ Smith, Q Li, SW Wietgrefe, TW Schacker, CS Reilly and AT Haase. 2010. Host genes associated with HIV-1 replication in lymphatic tissue. *J Immunol*, 185:5417–5424. doi: 10.4049/jimmunol.1002197
- [469] M Imbeault, K Giguère, M Ouellet and MJ Tremblay. 2012. Exon level transcriptomic profiling of HIV-1-infected CD4(+) T cells reveals virus-induced genes and host environment favorable for viral replication. *PLoS Pathog*, 8:e1002861. doi: 10.1371/journal.ppat.1002861
- [470] P Mohammadi, S Desfarges, I Bartha, B Joos, N Zangger, M Muoz, HF Gnethard, N Beerenwinkel, A Telenti and A Ciuffi. 2013. 24 hours in the life of HIV-1 in a T cell line. *PLoS Pathog*, 9:e1003161. doi: 10.1371/journal.ppat.1003161
- [471] X Peng, P Sova, RR Green, MJ Thomas, MJ Korth, S Proll, J Xu, Y Cheng, K Yi et al. 2014. Deep sequencing of HIV-infected cells: insights into nascent transcription and host-directed therapy. *J Virol*, 88:8768–8782. doi: 10.1128/JVI.00768-14
- [472] C de la Fuente, F Santiago, L Deng, C Eadie, I Zilberman, K Kehn, A Maddukuri, S Baylor, K Wu et al. 2002. Gene expression profile of HIV-1 Tat expressing cells: a close interplay between proliferative and differentiation signals. *BMC Biochem*, 3:14. doi: 10.1186/1471-2091-3-14
- [473] G Lefebvre, S Desfarges, F Uyttebroeck, M Muoz, N Beerenwinkel, J Rougemont, A Telenti and A Ciuffi. 2011. Analysis of HIV-1 expression level and sense of transcription by high-throughput sequencing of the infected cell. *J Virol*, 85:6205–6211. doi: 10.1128/JVI.00252-11
- [474] B Langmead, C Trapnell, M Pop and SL Salzberg. 2009. Ultrafast and memory-efficient alignment of short DNA sequences to the human genome. *Genome Biology*, 10:R25. doi: 10.1186/gb-2009-10-3-r25
- [475] GR Grant, MH Farkas, AD Pizarro, NF Lahens, J Schug, BP Brunk, CJ Stoeckert, JB Hogenesch and EA Pierce. 2011. Comparative analysis of RNA-Seq alignment algorithms and the RNA-Seq unified mapper (RUM). *Bioinformatics*, 27:2518–2528. doi: 10.1093/bioinformatics/btr427
- [476] Q Li, AJ Smith, TW Schacker, JV Carlis, L Duan, CS Reilly and AT Haase. 2009. Microarray analysis of lymphatic tissue reveals stage-specific, gene expression signatures in HIV-1 infection. *J Immunol*, 183:1975–1982. doi: 10.4049/jimmunol.0803222
- [477] A Subramanian, P Tamayo, VK Mootha, S Mukherjee, BL Ebert, MA Gillette, A Paulovich, SL Pomeroy, TR Golub et al. 2005. Gene set enrichment analysis: a knowledge-based approach for interpreting genome-wide expression profiles. *Proc Natl Acad Sci U S A*, 102:15545–15550. doi: 10.1073/pnas.0506580102
- [478] WJ Kent, CW Sugnet, TS Furey, KM Roskin, TH Pringle, AM Zahler and D Haussler.

2002. The human genome browser at UCSC. *Genome Res*, 12:996–1006. doi: 10.1101/gr.229102
- [479] H Li, B Handsaker, A Wysoker, T Fennell, J Ruan, N Homer, G Marth, G Abecasis, R Durbin and GPDPS . 2009. The Sequence Alignment/Map format and SAMtools. *Bioinformatics*, 25:2078–2079. doi: 10.1093/bioinformatics/btp352
- [480] RP Subramanian, JH Wildschutte, C Russo and JM Coffin. 2011. Identification, characterization, and comparative genomic distribution of the HERV-K (HML-2) group of human endogenous retroviruses. *Retrovirology*, 8:90. doi: 10.1186/1742-4690-8-90
- [481] G La Mantia, D Maglione, G Pengue, A Di Cristofano, A Simeone, L Lanfrancone and L Lania. 1991. Identification and characterization of novel human endogenous retroviral sequences preferentially expressed in undifferentiated embryonal carcinoma cells. *Nucleic Acids Res*, 19:1513–1520
- [482] G La Mantia, B Majello, A Di Cristofano, M Strazzullo, G Minchietti and L Lania. 1992. Identification of regulatory elements within the minimal promoter region of the human endogenous ERV9 proviruses: accurate transcription initiation is controlled by an Inr-like element. *Nucleic Acids Res*, 20:4129–4136. doi: 10.1093/nar/20.16.4129
- [483] KE Plant, SJ Routledge and NJ Proudfoot. 2001. Intergenic transcription in the human beta-globin gene cluster. *Mol Cell Biol*, 21:6507–6514. doi: 10.1128/MCB.21.19.6507-6514.2001
- [484] J Ling, W Pi, R Bollag, S Zeng, M Keskintepe, H Saliman, S Krantz, B Whitney and D Tuan. 2002. The solitary long terminal repeats of ERV-9 endogenous retrovirus are conserved during primate evolution and possess enhancer activities in embryonic and hematopoietic cells. *J Virol*, 76:2410–2423. doi: 10.1128/jvi.76.5.2410-2423.2002
- [485] X Yu, X Zhu, W Pi, J Ling, L Ko, Y Takeda and D Tuan. 2005. The long terminal repeat (LTR) of ERV-9 human endogenous retrovirus binds to NF-Y in the assembly of an active LTR enhancer complex NF-Y/MZF1/GATA-2. *J Biol Chem*, 280:35184–35194. doi: 10.1074/jbc.M508138200
- [486] RC Edgar. 2004. MUSCLE: a multiple sequence alignment method with reduced time and space complexity. *BMC Bioinformatics*, 5:113. doi: 10.1186/1471-2105-5-113
- [487] M Rotger, J Dalmau, A Rauch, P McLaren, SE Bosinger, R Martinez, NG Sandler, A Roque, J Liebner et al. 2011. Comparative transcriptomics of extreme phenotypes of human HIV-1 infection and SIV infection in sooty mangabey and rhesus macaque. *J Clin Invest*, 121:2391–2400. doi: 10.1172/JCI45235
- [488] K Breuer, AK Foroushani, MR Laird, C Chen, A Sribnaia, R Lo, GL Winsor, REW Hancock, FSL Brinkman and DJ Lynn. 2013. InnateDB: systems biology of innate immunity and beyond—recent updates and continuing curation. *Nucleic Acids Res*, 41: D1228–D1233. doi: 10.1093/nar/gks1147

- [489] I Rusinova, S Forster, S Yu, A Kannan, M Masse, H Cumming, R Chapman and PJ Hertzog. 2013. Interferome v2.0: an updated database of annotated interferon-regulated genes. *Nucleic Acids Res*, 41:D1040–D1046. doi: 10.1093/nar/gks1215
- [490] ST Chang, MJ Thomas, P Sova, RR Green, RE Palermo and MG Katze. 2013. Next-generation sequencing of small RNAs from HIV-infected cells identifies phased microRNA expression patterns and candidate novel microRNAs differentially expressed upon infection. *MBio*, 4:e00549–e00512. doi: 10.1128/mBio.00549-12
- [491] Z Kalender Atak, K De Keersmaecker, V Gianfelici, E Geerdens, R Vandepoel, D Pauwels, M Porcu, I Lahortiga, V Brys et al. 2012. High accuracy mutation detection in leukemia on a selected panel of cancer genes. *PLoS One*, 7:e38463. doi: 10.1371/journal.pone.0038463
- [492] ES Patel and LJ Chang. 2012. Synergistic effects of interleukin-7 and pre-T cell receptor signaling in human T cell development. *J Biol Chem*, 287:33826–33835. doi: 10.1074/jbc.M112.380113
- [493] M Imbeault, M Ouellet and MJ Tremblay. 2009. Microarray study reveals that HIV-1 induces rapid type-I interferon-dependent p53 mRNA up-regulation in human primary CD4+ T cells. *Retrovirology*, 6:5. doi: 10.1186/1742-4690-6-5
- [494] S Iwase, Y Furukawa, J Kikuchi, M Nagai, Y Terui, M Nakamura and H Yamada. 1997. Modulation of E2F activity is linked to interferon-induced growth suppression of hematopoietic cells. *J Biol Chem*, 272:12406–12414. doi: 10.1074/jbc.272.19.12406
- [495] RW Johnstone, JA Kerry and JA Trapani. 1998. The human interferon-inducible protein, IFI 16, is a repressor of transcription. *J Biol Chem*, 273:17172–17177. doi: 10.1074/jbc.273.27.17172
- [496] BR Williams. 1999. PKR; a sentinel kinase for cellular stress. *Oncogene*, 18:6112–6120. doi: 10.1038/sj.onc.1203127
- [497] CV Ramana, N Grammatikakis, M Chernov, H Nguyen, KC Goh, BR Williams and GR Stark. 2000. Regulation of c-myc expression by IFN-gamma through Stat1-dependent and -independent pathways. *EMBO J*, 19:263–272. doi: 10.1093/emboj/19.2.263
- [498] SL Liang, D Quirk and A Zhou. 2006. RNase L: its biological roles and regulation. *IUBMB Life*, 58:508–514. doi: 10.1080/15216540600838232
- [499] F Maldarelli, C Xiang, G Chamoun and SL Zeichner. 1998. The expression of the essential nuclear splicing factor SC35 is altered by human immunodeficiency virus infection. *Virus Res*, 53:39–51
- [500] A Monette, L Ajamian, M López-Lastra and AJ Mouland. 2009. Human immunodeficiency virus type 1 (HIV-1) induces the cytoplasmic retention of heterogeneous

- nuclear ribonucleoprotein A1 by disrupting nuclear import: implications for HIV-1 gene expression. *J Biol Chem*, 284:31350–31362. doi: 10.1074/jbc.M109.048736
- [501] R Contreras-Galindo, P López, R Vélez and Y Yamamura. 2007. HIV-1 infection increases the expression of human endogenous retroviruses type K (HERV-K) in vitro. *AIDS Res Hum Retroviruses*, 23:116–122. doi: 10.1089/aid.2006.0117
- [502] R Contreras-Galindo, MH Kaplan, S He, AC Contreras-Galindo, MJ Gonzalez-Hernandez, F Kappes, D Dube, SM Chan, D Robinson et al. 2013. HIV infection reveals widespread expansion of novel centromeric human endogenous retroviruses. *Genome Res*, 23:1505–1513. doi: 10.1101/gr.144303.112
- [503] N Bhardwaj, F Maldarelli, J Mellors and JM Coffin. 2014. HIV-1 infection leads to increased transcription of human endogenous retrovirus HERV-K (HML-2) proviruses in vivo but not to increased virion production. *J Virol*, 88:11108–11120. doi: 10.1128/JVI.01623-14
- [504] RB Jones, H Song, Y Xu, KE Garrison, AA Buzdin, N Anwar, DV Hunter, S Mujib, V Mihajlovic et al. 2013. LINE-1 retrotransposable element DNA accumulates in HIV-1-infected cells. *J Virol*, 87:13307–13320. doi: 10.1128/JVI.02257-13
- [505] P Medstrand and DL Mager. 1998. Human-specific integrations of the HERV-K endogenous retrovirus family. *J Virol*, 72:9782–9787
- [506] C Macfarlane and P Simmonds. 2004. Allelic variation of HERV-K(HML-2) endogenous retroviral elements in human populations. *J Mol Evol*, 59:642–656. doi: 10.1007/s00239-004-2656-1
- [507] K Büscher, U Trefzer, M Hofmann, W Sterry, R Kurth and J Denner. 2005. Expression of human endogenous retrovirus K in melanomas and melanoma cell lines. *Cancer Res*, 65:4172–4180. doi: 10.1158/0008-5472.CAN-04-2983
- [508] G Howard, R Eiges, F Gaudet, R Jaenisch and A Eden. 2008. Activation and transposition of endogenous retroviral elements in hypomethylation induced tumors in mice. *Oncogene*, 27:404–408. doi: 10.1038/sj.onc.1210631
- [509] RC Iskow, MT McCabe, RE Mills, S Torene, WS Pittard, AF Neuwald, EG Van Meir, PM Vertino and SE Devine. 2010. Natural mutagenesis of human genomes by endogenous retrotransposons. *Cell*, 141:1253–1261. doi: 10.1016/j.cell.2010.05.020
- [510] E Lee, R Iskow, L Yang, O Gokcumen, P Haseley, LJ Luquette, 3rd, JG Lohr, CC Harris, L Ding et al. 2012. Landscape of somatic retrotransposition in human cancers. *Science*, 337:967–971. doi: 10.1126/science.1222077
- [511] SW Criscione, Y Zhang, W Thompson, JM Sedivy and N Neretti. 2014. Transcriptional landscape of repetitive elements in normal and cancer human cells. *BMC Genomics*, 15:583. doi: 10.1186/1471-2164-15-583

- [512] AW Whisnant, HP Bogerd, O Flores, P Ho, JG Powers, N Sharova, M Stevenson, CH Chen and BR Cullen. 2013. In-depth analysis of the interaction of HIV-1 with cellular microRNA biogenesis and effector mechanisms. *MBio*, 4:e000193. doi: 10.1128/mBio.00193-13
- [513] NF Lahens, IH Kavakli, R Zhang, K Hayer, MB Black, H Dueck, A Pizarro, J Kim, R Irizarry et al. 2014. IVT-seq reveals extreme bias in RNA sequencing. *Genome Biol*, 15:R86. doi: 10.1186/gb-2014-15-6-r86
- [514] RD Hockett, JM Kilby, CA Derdeyn, MS Saag, M Sillers, K Squires, S Chiz, MA Nowak, GM Shaw and RP Bucy. 1999. Constant mean viral copy number per infected cell in tissues regardless of high, low, or undetectable plasma HIV RNA. *J Exp Med*, 189: 1545–1554. doi: 10.1084/jem.189.10.1545
- [515] RJ De Boer, RM Ribeiro and AS Perelson. 2010. Current estimates for HIV-1 production imply rapid viral clearance in lymphoid tissues. *PLoS Comput Biol*, 6: e1000906. doi: 10.1371/journal.pcbi.1000906
- [516] T Ikeda, J Shibata, K Yoshimura, A Koito and S Matsushita. 2007. Recurrent HIV-1 integration at the BACH2 locus in resting CD4+ T cell populations during effective highly active antiretroviral therapy. *J Infect Dis*, 195:716–725. doi: 10.1086/510915
- [517] TA Wagner, S McLaughlin, K Garg, CYK Cheung, BB Larsen, S Styrcak, HC Huang, PT Edlefsen, JI Mullins and LM Frenkel. 2014. Proliferation of cells with HIV integrated into cancer genes contributes to persistent infection. *Science*, 345:570–573. doi: 10.1126/science.1256304
- [518] F Maldarelli, X Wu, L Su, FR Simonetti, W Shao, S Hill, J Spindler, AL Ferris, JW Mellors et al. 2014. Specific HIV integration sites are linked to clonal expansion and persistence of infected cells. *Science*, 345:179–183. doi: 10.1126/science.1254194
- [519] LB Cohn, IT Silva, TY Oliveira, RA Rosales, EH Parrish, GH Learn, BH Hahn, JL Czartoski, MJ McElrath et al. 2015. HIV-1 integration landscape during latent and active infection. *Cell*, 160:420–432. doi: 10.1016/j.cell.2015.01.020
- [520] ARW Schröder, P Shinn, H Chen, C Berry, JR Ecker and F Bushman. 2002. HIV-1 integration in the human genome favors active genes and local hotspots. *Cell*, 110: 521–529. doi: 10.1016/S0092-8674(02)00864-4
- [521] T Brady, YN Lee, K Ronen, N Malani, CC Berry, PD Bieniasz and FD Bushman. 2009. Integration target site selection by a resurrected human endogenous retrovirus. *Genes Dev*, 23:633–642. doi: 10.1101/gad.1762309
- [522] B Marini, A Kertesz-Farkas, H Ali, B Lucic, K Lisek, L Manganaro, S Pongor, R Luzzati, A Recchia et al. 2015. Nuclear architecture dictates HIV-1 integration site selection. *Nature*. doi: 10.1038/nature14226

- [523] M Cavazzana-Calvo, E Payen, O Negre, G Wang, K Hehir, F Fusil, J Down, M Denaro, T Brady et al. 2010. Transfusion independence and HMGA2 activation after gene therapy of human  $\beta$ -thalassaemia. *Nature*, 467:318–322. doi: 10.1038/nature09328
- [524] S Hacein-Bey-Abina, A Garrigue, GP Wang, J Soulier, A Lim, E Morillon, E Clappier, L Caccavelli, E Delabesse et al. 2008. Insertional oncogenesis in 4 patients after retrovirus-mediated gene therapy of SCID-X1. *J Clin Invest*, 118:3132–3142. doi: 10.1172/JCI35700
- [525] A Moiani, Y Paleari, D Sartori, R Mezzadra, A Miccio, C Cattoglio, F Cocchiarella, MR Lidonnici, G Ferrari and F Mavilio. 2012. Lentiviral vector integration in the human genome induces alternative splicing and generates aberrant transcripts. *J Clin Invest*, 122:1653–1666. doi: 10.1172/JCI61852
- [526] D Cesana, J Sgualdino, L Rudiloso, S Merella, L Naldini and E Montini. 2012. Whole transcriptome characterization of aberrant splicing events induced by lentiviral vector integrations. *J Clin Invest*, 122:1667–1676. doi: 10.1172/JCI62189
- [527] S Pääbo, DM Irwin and AC Wilson. 1990. DNA damage promotes jumping between templates during enzymatic amplification. *J Biol Chem*, 265:4718–4721
- [528] SJ Odelberg, RB Weiss, A Hata and R White. 1995. Template-switching during DNA synthesis by *Thermus aquaticus* DNA polymerase I. *Nucleic Acids Res*, 23:2049–2057. doi: 10.1093/nar/23.11.2049
- [529] XC Zeng and SX Wang. 2002. Evidence that BmTXK beta-BmKCT cDNA from Chinese scorpion *Buthus martensii* Karsch is an artifact generated in the reverse transcription process. *FEBS Lett*, 520:183–4; author reply 185
- [530] B Tasic, CE Nabholz, KK Baldwin, Y Kim, EH Rueckert, SA Ribich, P Cramer, Q Wu, R Axel and T Maniatis. 2002. Promoter choice determines splice site selection in protocadherin alpha and gamma pre-mRNA splicing. *Mol Cell*, 10:21–33
- [531] M Geiszt, K Lekstrom and TL Leto. 2004. Analysis of mRNA transcripts from the NAD(P)H oxidase 1 (Nox1) gene. Evidence against production of the NADPH oxidase homolog-1 short (NOH-1S) transcript variant. *J Biol Chem*, 279:51661–51668. doi: 10.1074/jbc.M409325200
- [532] J Cocquet, A Chong, G Zhang and RA Veitia. 2006. Reverse transcriptase template switching and false alternative transcripts. *Genomics*, 88:127–131. doi: 10.1016/j.ygeno.2005.12.013
- [533] CJ McManus, JD Coolon, MO Duff, J Eipper-Mains, BR Graveley and PJ Wittkopp. 2010. Regulatory divergence in *Drosophila* revealed by mRNA-seq. *Genome Res*, 20: 816–825. doi: 10.1101/gr.102491.109
- [534] B Cogné, R Snyder, P Lindenbaum, JB Dupont, R Redon, P Moullier and A Leger.

2014. NGS library preparation may generate artifactual integration sites of AAV vectors. *Nat Med*, 20:577–578. doi: 10.1038/nm.3578
- [535] E Gilboa, SW Mitra, S Goff and D Baltimore. 1979. A detailed model of reverse transcription and tests of crucial aspects. *Cell*, 18:93–100. doi: 10.1016/0092-8674(79)90357-X
- [536] GX Luo and J Taylor. 1990. Template switching by reverse transcriptase during DNA synthesis. *J Virol*, 64:4321–4328
- [537] J Houseley and D Tollervey. 2010. Apparent non-canonical trans-splicing is generated by reverse transcriptase in vitro. *PLoS One*, 5:e12271. doi: 10.1371/journal.pone.0012271
- [538] A Meyerhans, JP Vartanian and S Wain-Hobson. 1990. DNA recombination during PCR. *Nucleic Acids Res*, 18:1687–1691
- [539] DJG Lahr and LA Katz. 2009. Reducing the impact of PCR-mediated recombination in molecular evolution and environmental studies using a new-generation high-fidelity DNA polymerase. *Biotechniques*, 47:857–866. doi: 10.2144/000113219
- [540] W Al-Ahmadi, L Al-Haj, FA Al-Mohanna, RH Silverman and KSA Khabar. 2009. RNase L downmodulation of the RNA-binding protein, HuR, and cellular growth. *Oncogene*, 28:1782–1791. doi: 10.1038/onc.2009.16
- [541] RB Jones, KE Garrison, S Mujib, V Mihaiovic, N Aidarus, DV Hunter, E Martin, VM John, W Zhan et al. 2012. HERV-K-specific T cells eliminate diverse HIV-1/2 and SIV primary isolates. *J Clin Invest*, 122:4473–4489. doi: 10.1172/JCI64560
- [542] K Boller, O Janssen, H Schuldes, RR Tönjes and R Kurth. 1997. Characterization of the antibody response specific for the human endogenous retrovirus HTDV/HERV-K. *J Virol*, 71:4581–4588
- [543] KE Garrison, RB Jones, DA Meiklejohn, N Anwar, LC Ndhlovu, JM Chapman, AL Erickson, A Agrawal, G Spotts et al. 2007. T cell responses to human endogenous retroviruses in HIV-1 infection. *PLoS Pathog*, 3:e165. doi: 10.1371/journal.ppat.0030165
- [544] R Tandon, D SenGupta, LC Ndhlovu, RGS Vieira, RB Jones, VA York, VA Vieira, ER Sharp, AA Wiznia et al. 2011. Identification of human endogenous retrovirus-specific T cell responses in vertically HIV-1-infected subjects. *J Virol*, 85:11526–11531. doi: 10.1128/JVI.05418-11
- [545] D SenGupta, R Tandon, RGS Vieira, LC Ndhlovu, R Lown-Hecht, CE Ormsby, L Loh, RB Jones, KE Garrison et al. 2011. Strong human endogenous retrovirus-specific T cell responses are associated with control of HIV-1 in chronic infection. *J Virol*, 85: 6977–6985. doi: 10.1128/JVI.00179-11

- [546] W Pi, Z Yang, J Wang, L Ruan, X Yu, J Ling, S Krantz, C Isales, SJ Conway et al. 2004. The LTR enhancer of ERV-9 human endogenous retrovirus is active in oocytes and progenitor cells in transgenic zebrafish and humans. *Proc Natl Acad Sci U S A*, 101:805–810. doi: 10.1073/pnas.0307698100
- [547] XHF Zhang and LA Chasin. 2006. Comparison of multiple vertebrate genomes reveals the birth and evolution of human exons. *Proc Natl Acad Sci USA*, 103:13427–13432. doi: 10.1073/pnas.0603042103
- [548] FA Santoni, J Guerra and J Luban. 2012. HERV-H RNA is abundant in human embryonic stem cells and a precise marker for pluripotency. *Retrovirology*, 9:111. doi: 10.1186/1742-4690-9-111
- [549] NV Fuchs, S Loewer, GQ Daley, Z Izsvák, J Löwer and R Löwer. 2013. Human endogenous retrovirus K (HML-2) RNA and protein expression is a marker for human embryonic and induced pluripotent stem cells. *Retrovirology*, 10:115. doi: 10.1186/1742-4690-10-115
- [550] A Fort, K Hashimoto, D Yamada, M Salimullah, CA Keya, A Saxena, A Bonetti, I Voineagu, N Bertin et al. 2014. Deep transcriptome profiling of mammalian stem cells supports a regulatory role for retrotransposons in pluripotency maintenance. *Nat Genet*, 46:558–566. doi: 10.1038/ng.2965
- [551] J Wang, G Xie, M Singh, AT Ghanbarian, T Raskó, A Szvetnik, H Cai, D Besser, A Prigione et al. 2014. Primate-specific endogenous retrovirus-driven transcription defines naive-like stem cells. *Nature*, 516:405–409. doi: 10.1038/nature13804
- [552] B Joos, M Fischer, H Kuster, SK Pillai, JK Wong, J Böni, B Hirscher, R Weber, A Trkola et al. 2008. HIV rebounds from latently infected cells, rather than from continuing low-level replication. *Proc Natl Acad Sci U S A*, 105:16725–16730. doi: 10.1073/pnas.0804192105
- [553] TP Brennan, JO Woods, AR Sedaghat, JD Siliciano, RF Siliciano and CO Wilke. 2009. Analysis of human immunodeficiency virus type 1 viremia and provirus in resting CD4+ T cells reveals a novel source of residual viremia in patients on antiretroviral therapy. *J Virol*, 83:8470–8481. doi: 10.1128/JVI.02568-08
- [554] TA Wagner, JL McKernan, NH Tobin, KA Tapia, JI Mullins and LM Frenkel. 2013. An increasing proportion of monotypic HIV-1 DNA sequences during antiretroviral treatment suggests proliferation of HIV-infected cells. *J Virol*, 87:1770–1778. doi: 10.1128/JVI.01985-12
- [555] MF Kearney, J Spindler, W Shao, S Yu, EM Anderson, A O’Shea, C Rehm, C Poethke, N Kovacs et al. 2014. Lack of detectable HIV-1 molecular evolution during suppressive antiretroviral therapy. *PLoS Pathog*, 10:e1004010. doi: 10.1371/journal.ppat.1004010
- [556] KE Ocwieja\*, S Sherrill-Mix\*, C Liu, J Song, H Bau and FD Bushman. 2015. A

- reverse transcription loop-mediated isothermal amplification assay optimized to detect multiple HIV subtypes. *PLoS One*, 10:e0117852. doi: 10.1371/journal.pone.0117852
- [557] CJL Murray, KF Ortblad, C Guinovart, SS Lim, TM Wolock, DA Roberts, EA Dansereau, N Graetz, RM Barber et al. 2014. Global, regional, and national incidence and mortality for HIV, tuberculosis, and malaria during 1990–2013: a systematic analysis for the Global Burden of Disease Study 2013. *Lancet*, 384:1005–1070. doi: 10.1016/S0140-6736(14)60844-8
- [558] KA Sollis, PW Smit, S Fiscus, N Ford, M Vitoria, S Essajee, D Barnett, B Cheng, SM Crowe et al. 2014. Systematic review of the performance of HIV viral load technologies on plasma samples. *PLoS One*, 9:e85869. doi: 10.1371/journal.pone.0085869
- [559] C Liu, M Mauk, R Gross, FD Bushman, PH Edelstein, RG Collman and HH Bau. 2013. Membrane-based, sedimentation-assisted plasma separator for point-of-care applications. *Anal Chem*, 85:10463–10470. doi: 10.1021/ac402459h
- [560] KA Curtis, DL Rudolph, I Nejad, J Singleton, A Beddoe, B Weigl, P LaBarre and SM Owen. 2012. Isothermal amplification using a chemical heating device for point-of-care detection of HIV-1. *PLoS One*, 7:e31432. doi: 10.1371/journal.pone.0031432
- [561] T Notomi, H Okayama, H Masubuchi, T Yonekawa, K Watanabe, N Amino and T Hase. 2000. Loop-mediated isothermal amplification of DNA. *Nucleic Acids Res*, 28:E63
- [562] KA Curtis, DL Rudolph and SM Owen. 2008. Rapid detection of HIV-1 by reverse-transcription, loop-mediated isothermal amplification (RT-LAMP). *J Virol Methods*, 151:264–270. doi: 10.1016/j.jviromet.2008.04.011
- [563] KA Curtis, DL Rudolph and SM Owen. 2009. Sequence-specific detection method for reverse transcription, loop-mediated isothermal amplification of HIV-1. *J Med Virol*, 81:966–972. doi: 10.1002/jmv.21490
- [564] Y Zeng, X Zhang, K Nie, X Ding, BZ Ring, L Xu, L Dai, X Li, W Ren et al. 2014. Rapid quantitative detection of Human immunodeficiency virus type 1 by a reverse transcription-loop-mediated isothermal amplification assay. *Gene*, 541:123–128. doi: 10.1016/j.gene.2014.03.015
- [565] N Hosaka, N Ndembí, A Ishizaki, S Kageyama, K Numazaki and H Ichimura. 2009. Rapid detection of human immunodeficiency virus type 1 group M by a reverse transcription-loop-mediated isothermal amplification assay. *J Virol Methods*, 157: 195–199. doi: 10.1016/j.jviromet.2009.01.004
- [566] KA Curtis, PL Niedzwiedz, AS Youngpairoj, DL Rudolph and SM Owen. 2014. Real-time detection of HIV-2 by reverse transcription-loop-mediated isothermal amplification. *J Clin Microbiol*, 52:2674–2676. doi: 10.1128/JCM.00935-14

- [567] C Kuiken, H Yoon, W Abfalterer, B Gaschen, C Lo and B Korber. 2013. Viral genome analysis and knowledge management. *Methods Mol Biol*, 939:253–261. doi: 10.1007/978-1-62703-107-3\_16
- [568] M Manak, S Sina, B Anekella, I Hewlett, E Sanders-Buell, V Ragupathy, J Kim, M Vermeulen, SL Stramer et al. 2012. Pilot studies for development of an HIV subtype panel for surveillance of global diversity. *AIDS Res Hum Retroviruses*, 28:594–606. doi: 10.1089/AID.2011.0271
- [569] J Louwagie, FE McCutchan, M Peeters, TP Brennan, E Sanders-Buell, GA Eddy, G van der Groen, K Fransen, GM Gershay-Damet and R Deleye. 1993. Phylogenetic analysis of gag genes from 70 international HIV-1 isolates provides evidence for multiple genotypes. *AIDS*, 7:769–780
- [570] L Buonaguro, ML Tornesello and FM Buonaguro. 2007. Human immunodeficiency virus type 1 subtype distribution in the worldwide epidemic: pathogenetic and therapeutic implications. *J Virol*, 81:10209–10219. doi: 10.1128/JVI.00872-07
- [571] NF Parrish, F Gao, H Li, EE Giorgi, HJ Barbian, EH Parrish, L Zajic, SS Iyer, JM Decker et al. 2013. Phenotypic properties of transmitted founder HIV-1. *Proc Natl Acad Sci U S A*, 110:6626–6633. doi: 10.1073/pnas.1304288110
- [572] AG Abimiku, TL Stern, A Zwandor, PD Markham, C Calef, S Kyari, WC Saxinger, RC Gallo, M Robert-Guroff and MS Reitz. 1994. Subgroup G HIV type 1 isolates from Nigeria. *AIDS Res Hum Retroviruses*, 10:1581–1583
- [573] Zhang, Chung and Oldenburg. 1999. A simple statistical parameter for use in evaluation and validation of high throughput screening assays. *J Biomol Screen*, 4:67–73. doi: 10.1177/108705719900400206
- [574] C Liu, E Geva, M Mauk, X Qiu, WR Abrams, D Malamud, K Curtis, SM Owen and HH Bau. 2011. An isothermal amplification reactor with an integrated isolation membrane for point-of-care detection of infectious diseases. *Analyst*, 136:2069–2076. doi: 10.1039/c1an00007a
- [575] CA Spina, J Anderson, NM Archin, A Bosque, J Chan, M Famiglietti, WC Greene, A Kashuba, SR Lewin et al. 2013. An in-depth comparison of latent HIV-1 reactivation in multiple cell model systems and resting CD4+ T cells from aviremic patients. *PLoS Pathog*, 9:e1003834. doi: 10.1371/journal.ppat.1003834
- [576] G Lehrman, IB Hogue, S Palmer, C Jennings, CA Spina, A Wiegand, AL Landay, RW Coombs, DD Richman et al. 2005. Depletion of latent HIV-1 infection in vivo: a proof-of-concept study. *Lancet*, 366:549–555. doi: 10.1016/S0140-6736(05)67098-5
- [577] NM Archin, M Cheema, D Parker, A Wiegand, RJ Bosch, JM Coffin, J Eron, M Cohen and DM Margolis. 2010. Antiretroviral intensification and valproic acid lack sustained

- effect on residual HIV-1 viremia or resting CD4+ cell infection. *PLoS One*, 5:e9390. doi: 10.1371/journal.pone.0009390
- [578] AM Spivak, A Andrade, E Eisele, R Hoh, P Bacchetti, NN Bumpus, F Emad, R Buckheit, 3rd, EF McCance-Katz et al. 2014. A pilot study assessing the safety and latency-reversing activity of disulfiram in HIV-1-infected adults on antiretroviral therapy. *Clin Infect Dis*, 58:883–890. doi: 10.1093/cid/cit813
- [579] AR Cillo, MD Sobolewski, RJ Bosch, E Fyne, M Piatak, Jr, JM Coffin and JW Mellors. 2014. Quantification of HIV-1 latency reversal in resting CD4+ T cells from patients on suppressive antiretroviral therapy. *Proc Natl Acad Sci U S A*, 111:7078–7083. doi: 10.1073/pnas.1402873111
- [580] AL Hill, DIS Rosenbloom, F Fu, MA Nowak and RF Siliciano. 2014. Predicting the outcomes of treatment to eradicate the latent reservoir for HIV-1. *Proc Natl Acad Sci U S A*, 111:13475–13480. doi: 10.1073/pnas.1406663111
- [581] ENCODE Project Consortium. 2012. An integrated encyclopedia of DNA elements in the human genome. *Nature*, 489:57–74. doi: 10.1038/nature11247
- [582] T Barrett, SE Wilhite, P Ledoux, C Evangelista, IF Kim, M Tomashevsky, KA Marshall, KH Phillippy, PM Sherman et al. 2013. NCBI GEO: archive for functional genomics data sets—update. *Nucleic Acids Res*, 41:D991–D995. doi: 10.1093/nar/gks1193
- [583] D Karolchik, GP Barber, J Casper, H Clawson, MS Cline, M Diekhans, TR Dreszer, PA Fujita, L Guruvadoo et al. 2014. The UCSC Genome Browser database: 2014 update. *Nucleic Acids Res*, 42:D764–D770. doi: 10.1093/nar/gkt1168
- [584] M Goldman, B Craft, T Swatloski, M Cline, O Morozova, M Diekhans, D Haussler and J Zhu. 2015. The UCSC Cancer Genomics Browser: update 2015. *Nucleic Acids Res*, 43:D812–D817. doi: 10.1093/nar/gku1073
- [585] F Cunningham, MR Amode, D Barrell, K Beal, K Billis, S Brent, D Carvalho-Silva, P Clapham, G Coates et al. 2015. Ensembl 2015. *Nucleic Acids Res*, 43:D662–D669. doi: 10.1093/nar/gku1010
- [586] ML Metzker. 2010. Sequencing technologies - the next generation. *Nat Rev Genet*, 11: 31–46. doi: 10.1038/nrg2626
- [587] ER Mardis. 2011. A decade's perspective on DNA sequencing technology. *Nature*, 470: 198–203. doi: 10.1038/nature09796
- [588] K Wetterstrand. 2015. DNA Sequencing Costs: Data from the NHGRI Genome Sequencing Program (GSP). URL [www.genome.gov/sequencingcosts](http://www.genome.gov/sequencingcosts)
- [589] DP Depledge, AL Palser, SJ Watson, IYC Lai, ER Gray, P Grant, RK Kanda, E Leproust, P Kellam and J Breuer. 2011. Specific capture and whole-genome

- sequencing of viruses from clinical samples. *PLoS One*, 6:e27805. doi: 10.1371/journal.pone.0027805
- [590] TR Mercer, MB Clark, J Crawford, ME Brunck, DJ Gerhardt, RJ Taft, LK Nielsen, ME Dinger and JS Mattick. 2014. Targeted sequencing for gene discovery and quantification using RNA CaptureSeq. *Nat Protoc*, 9:989–1009. doi: 10.1038/nprot.2014.058
- [591] JJ Mosher, B Bowman, EL Bernberg, O Shevchenko, J Kan, J Korlach and LA Kaplan. 2014. Improved performance of the PacBio SMRT technology for 16S rDNA sequencing. *J Microbiol Methods*, 104:59–60. doi: 10.1016/j.mimet.2014.06.012
- [592] AS Mikheyev and MMY Tin. 2014. A first look at the Oxford Nanopore MinION sequencer. *Mol Ecol Resour*, 14:1097–1102. doi: 10.1111/1755-0998.12324
- [593] M Jain, IT Fiddes, KH Miga, HE Olsen, B Paten and M Akeson. 2015. Improved data analysis for the MinION nanopore sequencer. *Nat Methods*, 12:351–356. doi: 10.1038/nmeth.3290
- [594] A Kilianski, JL Haas, EJ Corriveau, AT Liem, KL Willis, DR Kadavy, CN Rosenzweig and SS Minot. 2015. Bacterial and viral identification and differentiation by amplicon sequencing on the MinION nanopore sequencer. *Gigascience*, 4:12. doi: 10.1186/s13742-015-0051-z
- [595] S Jünemann, FJ Sedlazeck, K Prior, A Albersmeier, U John, J Kalinowski, A Mellmann, A Goesmann, A von Haeseler et al. 2013. Updating benchtop sequencing performance comparison. *Nat Biotechnol*, 31:294–296. doi: 10.1038/nbt.2522
- [596] Illumina, Inc. 2015. System specification sheet: MiSeq system. URL <http://www.illumina.com/products/miseq-reagent-kit-v3.html>
- [597] D Rossell, C Stephan-Otto Attolini, M Kroiss and A Stöcker. 2014. Quantifying alternative splicing from paired-end RNA-sequencing data. *Ann Appl Stat*, 8:309–330. doi: 10.1214/13-AOAS687
- [598] N Bray, H Pimentel, P Melsted and L Pachter. 2015. Near-optimal RNA-Seq quantification. *arXiv preprint*, page 1505.02710
- [599] NL Michael, MT Vahey, L d'Arcy, PK Ehrenberg, JD Mosca, J Rappaport and RR Redfield. 1994. Negative-strand RNA transcripts are produced in human immunodeficiency virus type 1-infected cells and patients by a novel promoter downregulated by Tat. *J Virol*, 68:979–987
- [600] S Landry, M Halin, S Lefort, B Audet, C Vaquero, JM Mesnard and B Barbeau. 2007. Detection, characterization and regulation of antisense transcripts in HIV-1. *Retrovirology*, 4:71. doi: 10.1186/1742-4690-4-71

- [601] NCT Schopman, M Willemsen, YP Liu, T Bradley, A van Kampen, F Baas, B Berkhout and J Haasnoot. 2012. Deep sequencing of virus-infected cells reveals HIV-encoded small RNAs. *Nucleic Acids Res*, 40:414–427. doi: 10.1093/nar/gkr719
- [602] M Kobayashi-Ishihara, M Yamagishi, T Hara, Y Matsuda, R Takahashi, A Miyake, K Nakano, T Yamochi, T Ishida and T Watanabe. 2012. HIV-1-encoded antisense RNA suppresses viral replication for a prolonged period. *Retrovirology*, 9:38. doi: 10.1186/1742-4690-9-38
- [603] S Saayman, A Ackley, AMW Turner, M Famiglietti, A Bosque, M Clemson, V Planelles and KV Morris. 2014. An HIV-encoded antisense long noncoding RNA epigenetically regulates viral transcription. *Mol Ther*, 22:1164–1175. doi: 10.1038/mt.2014.29
- [604] CT Berger, A Llano, JM Carlson, ZL Brumme, MA Brockman, S Cedeño, PR Harrigan, DE Kaufmann, D Heckerman et al. 2015. Immune screening identifies novel T cell targets encoded by antisense reading frames of HIV-1. *J Virol*, 89:4015–4019. doi: 10.1128/JVI.03435-14
- [605] LB Ludwig, JL Ambrus, KA Krawczyk, S Sharma, S Brooks, CB Hsiao and SA Schwartz. 2006. Human Immunodeficiency Virus-Type 1 LTR DNA contains an intrinsic gene producing antisense RNA and protein products. *Retrovirology*, 3:80. doi: 10.1186/1742-4690-3-80
- [606] C Torresilla, É Larocque, S Landry, M Halin, Y Coulombe, JY Masson, JM Mesnard and B Barbeau. 2013. Detection of the HIV-1 minus-strand-encoded antisense protein and its association with autophagy. *J Virol*, 87:5089–5105. doi: 10.1128/JVI.00225-13
- [607] A Bansal, J Carlson, J Yan, OT Akinsiku, M Schaefer, S Sabbaj, A Bet, DN Levy, S Heath et al. 2010. CD8 T cell response and evolutionary pressure to HIV-1 cryptic epitopes derived from antisense transcription. *J Exp Med*, 207:51–59. doi: 10.1084/jem.20092060
- [608] JZ Levin, M Yassour, X Adiconis, C Nusbaum, DA Thompson, N Friedman, A Gnrke and A Regev. 2010. Comprehensive comparative analysis of strand-specific RNA sequencing methods. *Nat Methods*, 7:709–715. doi: 10.1038/nmeth.1491
- [609] J Podnar, H Deiderick, G Huerta and S Hunicke-Smith. 2014. Next-generation sequencing RNA-Seq library construction. *Curr Protoc Mol Biol*, 106:4.21.1–4.21.19. doi: 10.1002/0471142727.mb0421s106
- [610] S Cardinaud, A Moris, M Février, PS Rohrlich, L Weiss, P Langlade-Demoyen, FA Lemonnier, O Schwartz and A Habel. 2004. Identification of cryptic MHC I-restricted epitopes encoded by HIV-1 alternative reading frames. *J Exp Med*, 199: 1053–1063. doi: 10.1084/jem.20031869
- [611] CT Berger, JM Carlson, CJ Brumme, KL Hartman, ZL Brumme, LM Henry, PC Rosato, A Piechocka-Trocha, MA Brockman et al. 2010. Viral adaptation to

- immune selection pressure by HLA class I-restricted CTL responses targeting epitopes in HIV frameshift sequences. *J Exp Med*, 207:61–75. doi: 10.1084/jem.20091808
- [612] NT Ingolia, S Ghaemmaghami, JRS Newman and JS Weissman. 2009. Genome-wide analysis in vivo of translation with nucleotide resolution using ribosome profiling. *Science*, 324:218–223. doi: 10.1126/science.1168978
- [613] NT Ingolia, LF Lareau and JS Weissman. 2011. Ribosome profiling of mouse embryonic stem cells reveals the complexity and dynamics of mammalian proteomes. *Cell*, 147: 789–802. doi: 10.1016/j.cell.2011.10.002
- [614] NT Ingolia. 2014. Ribosome profiling: new views of translation, from single codons to genome scale. *Nat Rev Genet*, 15:205–213. doi: 10.1038/nrg3645
- [615] NJ Maness, AD Walsh, SM Piaskowski, J Furlott, HL Kolar, AT Bean, NA Wilson and DI Watkins. 2010. CD8+ T cell recognition of cryptic epitopes is a ubiquitous feature of AIDS virus infection. *J Virol*, 84:11569–11574. doi: 10.1128/JVI.01419-10
- [616] A Bet, EA Maze, A Bansal, S Sterrett, A Gross, S Graff-Dubois, A Samri, A Guihot, C Katlama et al. 2015. The HIV-1 antisense protein (ASP) induces CD8 T cell responses during chronic infection. *Retrovirology*, 12:15. doi: 10.1186/s12977-015-0135-y
- [617] S Koenig, HE Gendelman, JM Orenstein, MC Dal Canto, GH Pezeshkpour, M Yungbluth, F Janotta, A Aksamit, MA Martin and AS Fauci. 1986. Detection of AIDS virus in macrophages in brain tissue from AIDS patients with encephalopathy. *Science*, 233:1089–1093. doi: 10.1126/science.3016903
- [618] S Sonza, HP Mutimer, R Oelrichs, D Jardine, K Harvey, A Dunne, DF Purcell, C Birch and SM Crowe. 2001. Monocytes harbour replication-competent, non-latent HIV-1 in patients on highly active antiretroviral therapy. *AIDS*, 15:17–22
- [619] M Hermankova, JD Siliciano, Y Zhou, D Monie, K Chadwick, JB Margolick, TC Quinn and RF Siliciano. 2003. Analysis of human immunodeficiency virus type 1 gene expression in latently infected resting CD4+ T lymphocytes in vivo. *J Virol*, 77: 7383–7392. doi: 10.1128/JVI.77.13.7383-7392.2003
- [620] N Soriano-Sarabia, RE Bateson, NP Dahl, AM Crooks, JD Kuruc, DM Margolis and NM Archin. 2014. Quantitation of replication-competent HIV-1 in populations of resting CD4+ T cells. *J Virol*, 88:14070–14077. doi: 10.1128/JVI.01900-14
- [621] BF Keele, EE Giorgi, JF Salazar-Gonzalez, JM Decker, KT Pham, MG Salazar, C Sun, T Grayson, S Wang et al. 2008. Identification and characterization of transmitted and early founder virus envelopes in primary HIV-1 infection. *Proc Natl Acad Sci USA*, 105:7552–7557. doi: 10.1073/pnas.0802203105
- [622] JF Salazar-Gonzalez, MG Salazar, BF Keele, GH Learn, EE Giorgi, H Li, JM Decker, S Wang, J Baalwa et al. 2009. Genetic identity, biological phenotype, and evolutionary

- pathways of transmitted/founder viruses in acute and early HIV-1 infection. *J Exp Med*, 206:1273–1289. doi: 10.1084/jem.20090378
- [623] MP Wentz, BE Moore, MW Cloyd, SM Berget and LA Donehower. 1997. A naturally arising mutation of a potential silencer of exon splicing in human immunodeficiency virus type 1 induces dominant aberrant splicing and arrests virus production. *J Virol*, 71:8542–8551
- [624] JM Madsen and CM Stoltzfus. 2005. An exonic splicing silencer downstream of the 3' splice site A2 is required for efficient human immunodeficiency virus type 1 replication. *J Virol*, 79:10478–10486. doi: 10.1128/JVI.79.16.10478-10486.2005
- [625] S Paca-Uccaralertkun, CK Damgaard, P Auewarakul, A Thitithanyanont, P Suphaphiphat, M Essex, J Kjems and TH Lee. 2006. The effect of a single nucleotide substitution in the splicing silencer in the tat/rev intron on HIV type 1 envelope expression. *AIDS Research & Human Retroviruses*, 22:76–82. doi: 10.1089/aid.2006.22.76
- [626] D Mandal, Z Feng and CM Stoltzfus. 2008. Gag-processing defect of human immunodeficiency virus type 1 integrase E246 and G247 mutants is caused by activation of an overlapping 5' splice site. *J Virol*, 82:1600–1604. doi: 10.1128/JVI.02295-07
- [627] FD Bushman, N Malani, J Fernandes, I D'Orso, G Cagney, TL Diamond, H Zhou, DJ Hazuda, AS Espeseth et al. 2009. Host cell factors in HIV replication: meta-analysis of genome-wide studies. *PLoS Pathog*, 5:e1000437. doi: 10.1371/journal.ppat.1000437
- [628] T Fukuwara, T Hosoya, S Shimizu, K Sumi, T Oshiro, Y Yoshinaka, M Suzuki, N Yamamoto, LA Herzenberg et al. 2006. Utilization of host SR protein kinases and RNA-splicing machinery during viral replication. *Proc Natl Acad Sci USA*, 103: 11329–11333. doi: 10.1073/pnas.0604616103
- [629] R Wong, A Balachandran, AY Mao, W Dobson, S Gray-Owen and A Cochrane. 2011. Differential effect of CLK SR Kinases on HIV-1 gene expression: potential novel targets for therapy. *Retrovirology*, 8:47. doi: 10.1186/1742-4690-8-47
- [630] RW Wong, A Balachandran, MA Ostrowski and A Cochrane. 2013. Digoxin suppresses HIV-1 replication by altering viral RNA processing. *PLoS Pathog*, 9:e1003241. doi: 10.1371/journal.ppat.1003241
- [631] TH Finkel, G Tudor-Williams, NK Banda, MF Cotton, T Curiel, C Monks, TW Baba, RM Ruprecht and A Kupfer. 1995. Apoptosis occurs predominantly in bystander cells and not in productively infected cells of HIV- and SIV-infected lymph nodes. *Nat Med*, 1:129–134. doi: 10.1038/nm0295-129
- [632] G Doitsh, NLK Galloway, X Geng, Z Yang, KM Monroe, O Zepeda, PW Hunt, H Hatano, S Sowinski et al. 2014. Cell death by pyroptosis drives CD4 T-cell depletion in HIV-1 infection. *Nature*, 505:509–514. doi: 10.1038/nature12940

- [633] B Bahbouhi and L al Harthi. 2004. Enriching for HIV-infected cells using anti-gp41 antibodies indirectly conjugated to magnetic microbeads. *Biotechniques*, 36:139–147
- [634] S Hrvatin, F Deng, CW O'Donnell, DK Gifford and DA Melton. 2014. MARIS: method for analyzing RNA following intracellular sorting. *PLoS One*, 9:e89459. doi: 10.1371/journal.pone.0089459
- [635] KM Monroe, Z Yang, JR Johnson, X Geng, G Doitsh, NJ Krogan and WC Greene. 2014. IFI16 DNA sensor is required for death of lymphoid CD4 T cells abortively infected with HIV. *Science*, 343:428–432. doi: 10.1126/science.1243640
- [636] M Wilkinson. 1988. A rapid and convenient method for isolation of nuclear, cytoplasmic and total cellular RNA. *Nucleic Acids Res*, 16:10934. doi: 10.1093/nar/16.22.1093
- [637] HW Trask, R Cowper-Sal-lari, MA Sartor, J Gui, CV Heath, J Renuka, AJ Higgins, P Andrews, M Korc et al. 2009. Microarray analysis of cytoplasmic versus whole cell RNA reveals a considerable number of missed and false positive mRNAs. *RNA*, 15: 1917–1928. doi: 10.1261/rna.1677409
- [638] BW Solnestam, H Stranneheim, J Hällman, M Käller, E Lundberg, J Lundeberg and P Akan. 2012. Comparison of total and cytoplasmic mRNA reveals global regulation by nuclear retention and miRNAs. *BMC Genomics*, 13:574. doi: 10.1186/1471-2164-13-574
- [639] M Lagos-Quintana, R Rauhut, W Lendeckel and T Tuschl. 2001. Identification of novel genes coding for small expressed RNAs. *Science*, 294:853–858. doi: 10.1126/science.1064921
- [640] V Ambros. 2004. The functions of animal microRNAs. *Nature*, 431:350–355. doi: 10.1038/nature02871
- [641] P Landgraf, M Rusu, R Sheridan, A Sewer, N Iovino, A Aravin, S Pfeffer, A Rice, AO Kamphorst et al. 2007. A mammalian microRNA expression atlas based on small RNA library sequencing. *Cell*, 129:1401–1414. doi: 10.1016/j.cell.2007.04.040
- [642] Z Klase, P Kale, R Winograd, MV Gupta, M Heydarian, R Berro, T McCaffrey and F Kashanchi. 2007. HIV-1 TAR element is processed by Dicer to yield a viral micro-RNA involved in chromatin remodeling of the viral LTR. *BMC Mol Biol*, 8:63. doi: 10.1186/1471-2199-8-63
- [643] DL Ouellet, I Plante, P Landry, C Barat, ME Janelle, L Flamand, MJ Tremblay and P Provost. 2008. Identification of functional microRNAs released through asymmetrical processing of HIV-1 TAR element. *Nucleic Acids Res*, 36:2353–2365. doi: 10.1093/nar/gkn076
- [644] Z Klase, R Winograd, J Davis, L Carpio, R Hildreth, M Heydarian, S Fu, T McCaffrey, E Meiri et al. 2009. HIV-1 TAR miRNA protects against apoptosis by altering cellular gene expression. *Retrovirology*, 6:18. doi: 10.1186/1742-4690-6-18

- [645] S Omoto, M Ito, Y Tsutsumi, Y Ichikawa, H Okuyama, EA Brisibe, NK Saksena and YR Fujii. 2004. HIV-1 nef suppression by virally encoded microRNA. *Retrovirology*, 1: 44. doi: 10.1186/1742-4690-1-44
- [646] C Chable-Bessia, O Meziane, D Latreille, R Triboulet, A Zamborlini, A Wagschal, JM Jacquet, J Reynes, Y Levy et al. 2009. Suppression of HIV-1 replication by microRNA effectors. *Retrovirology*, 6:26. doi: 10.1186/1742-4690-6-26
- [647] S Pfeffer, A Sewer, M Lagos-Quintana, R Sheridan, C Sander, FA Grässer, LF van Dyk, CK Ho, S Shuman et al. 2005. Identification of microRNAs of the herpesvirus family. *Nat Methods*, 2:269–276. doi: 10.1038/nmeth746
- [648] TL Sung and AP Rice. 2009. miR-198 inhibits HIV-1 gene expression and replication in monocytes and its mechanism of action appears to involve repression of cyclin T1. *PLoS Pathog*, 5:e1000263. doi: 10.1371/journal.ppat.1000263
- [649] G Swaminathan, F Rossi, LJ Sierra, A Gupta, S Navas-Martín and J Martín-García. 2012. A role for microRNA-155 modulation in the anti-HIV-1 effects of Toll-like receptor 3 stimulation in macrophages. *PLoS Pathog*, 8:e1002937. doi: 10.1371/journal.ppat.1002937
- [650] HS Zhang, TC Wu, WW Sang and Z Ruan. 2012. MiR-217 is involved in Tat-induced HIV-1 long terminal repeat (LTR) transactivation by down-regulation of SIRT1. *Biochim Biophys Acta*, 1823:1017–1023. doi: 10.1016/j.bbamcr.2012.02.014
- [651] HS Zhang, XY Chen, TC Wu, WW Sang and Z Ruan. 2012. MiR-34a is involved in Tat-induced HIV-1 long terminal repeat (LTR) transactivation through the SIRT1/NF $\kappa$ B pathway. *FEBS Lett*, 586:4203–4207. doi: 10.1016/j.febslet.2012.10.023
- [652] K Chiang, H Liu and AP Rice. 2013. miR-132 enhances HIV-1 replication. *Virology*, 438:1–4. doi: 10.1016/j.virol.2012.12.016
- [653] E Orecchini, M Doria, A Michienzi, E Giuliani, L Vassena, SA Ciafrè, MG Farace and S Galardi. 2014. The HIV-1 Tat protein modulates CD4 expression in human T cells through the induction of miR-222. *RNA Biol*, 11:334–338. doi: 10.4161/rna.28372
- [654] L Farberov, E Herzig, S Modai, O Isakov, A Hizi and N Shomron. 2015. MicroRNA-mediated regulation of p21 and TASK1 cellular restriction factors enhances HIV-1 infection. *J Cell Sci*, 128:1607–1616. doi: 10.1242/jcs.167817
- [655] J Huang, F Wang, E Argyris, K Chen, Z Liang, H Tian, W Huang, K Squires, G Verlinghieri and H Zhang. 2007. Cellular microRNAs contribute to HIV-1 latency in resting primary CD4+ T lymphocytes. *Nat Med*, 13:1241–1247. doi: 10.1038/nm1639
- [656] K Chiang, TL Sung and AP Rice. 2012. Regulation of cyclin T1 and HIV-1 Replication by microRNAs in resting CD4+ T lymphocytes. *J Virol*, 86:3244–3252. doi: 10.1128/JVI.05065-11

- [657] K Chiang and AP Rice. 2012. MicroRNA-mediated restriction of HIV-1 in resting CD4+ T cells and monocytes. *Viruses*, 4:1390–1409. doi: 10.3390/v4091390
- [658] PJ Kanki, DJ Hamel, JL Sankalé, C Hsieh, I Thior, F Barin, SA Woodcock, A Guèye-Ndiaye, E Zhang et al. 1999. Human immunodeficiency virus type 1 subtypes differ in disease progression. *J Infect Dis*, 179:68–73. doi: 10.1086/314557
- [659] P Kaleebu, N French, C Mahe, D Yirrell, C Watera, F Lyagoba, J Nakiyangi, A Rutebeemberwa, D Morgan et al. 2002. Effect of human immunodeficiency virus (HIV) type 1 envelope subtypes A and D on disease progression in a large cohort of HIV-1-positive persons in Uganda. *J Infect Dis*, 185:1244–1250. doi: 10.1086/340130
- [660] JM Baeten, B Chohan, L Lavreys, V Chohan, RS McClelland, L Certain, K Mandaliya, W Jaoko and J Overbaugh. 2007. HIV-1 subtype D infection is associated with faster disease progression than subtype A in spite of similar plasma HIV-1 loads. *J Infect Dis*, 195:1177–1180. doi: 10.1086/512682
- [661] N Kiwanuka, O Laeyendecker, M Robb, G Kigozi, M Arroyo, F McCutchan, LA Eller, M Eller, F Makumbi et al. 2008. Effect of human immunodeficiency virus Type 1 (HIV-1) subtype on disease progression in persons from Rakai, Uganda, with incident HIV-1 infection. *J Infect Dis*, 197:707–713. doi: 10.1086/527416
- [662] B Renjifo, P Gilbert, B Chaplin, G Msamanga, D Mwakagile, W Fawzi, M Essex, TV and HIVS Group. 2004. Preferential in-utero transmission of HIV-1 subtype C as compared to HIV-1 subtype A or D. *AIDS*, 18:1629–1636
- [663] GC John-Stewart, RW Nduati, CM Rousseau, DA Mbori-Ngacha, BA Richardson, S Rainwater, DD Panteleeff and J Overbaugh. 2005. Subtype C Is associated with increased vaginal shedding of HIV-1. *J Infect Dis*, 192:492–496. doi: 10.1086/431514
- [664] W Huang, SH Eshleman, J Toma, S Fransen, E Stawiski, EE Paxinos, JM Whitcomb, AM Young, D Donnell et al. 2007. Coreceptor tropism in human immunodeficiency virus type 1 subtype D: high prevalence of CXCR4 tropism and heterogeneous composition of viral populations. *J Virol*, 81:7885–7893. doi: 10.1128/JVI.00218-07
- [665] J Snoeck, R Kantor, RW Shafer, K Van Laethem, K Deforche, AP Carvalho, B Wynhoven, MA Soares, P Cane et al. 2006. Discordances between interpretation algorithms for genotypic resistance to protease and reverse transcriptase inhibitors of human immunodeficiency virus are subtype dependent. *Antimicrob Agents Chemother*, 50: 694–701. doi: 10.1128/AAC.50.2.694-701.2006
- [666] PJ Easterbrook, M Smith, J Mullen, S O'Shea, I Chrystie, A de Ruiter, ID Tatt, AM Geretti and M Zuckerman. 2010. Impact of HIV-1 viral subtype on disease progression and response to antiretroviral therapy. *J Int AIDS Soc*, 13:4. doi: 10.1186/1758-2652-13-4
- [667] AU Scherrer, B Ledergerber, V von Wyl, J Böni, S Yerly, T Klimkait, P Bürgisser,

- A Rauch, B Hirschel et al. 2011. Improved virological outcome in White patients infected with HIV-1 non-B subtypes compared to subtype B. *Clin Infect Dis*, 53: 1143–1152. doi: 10.1093/cid/cir669
- [668] C Liu, MM Sadik, MG Mauk, PH Edelstein, FD Bushman, R Gross and HH Bau. 2014. Nuclemeter: a reaction-diffusion based method for quantifying nucleic acids undergoing enzymatic amplification. *Sci Rep*, 4:7335. doi: 10.1038/srep07335
- [669] MG Mauk, C Liu, M Sadik and HH Bau. 2015. Microfluidic devices for nucleic acid (NA) isolation, isothermal NA amplification, and real-time detection. *Methods Mol Biol*, 1256:15–40. doi: 10.1007/978-1-4939-2172-0\_2
- [670] A Piantadosi, B Chohan, V Chohan, RS McClelland and J Overbaugh. 2007. Chronic HIV-1 infection frequently fails to protect against superinfection. *PLoS Pathog*, 3:e177. doi: 10.1371/journal.ppat.0030177
- [671] RLR Powell, MM Urbanski, S Burda, T Kinge and PN Nyambi. 2009. High frequency of HIV-1 dual infections among HIV-positive individuals in Cameroon, West Central Africa. *J Acquir Immune Defic Syndr*, 50:84–92. doi: 10.1097/QAI.0b013e31818d5a40
- [672] K Ronen, CO McCoy, FA Matsen, DF Boyd, S Emery, K Odem-Davis, W Jaoko, K Mandaliya, RS McClelland et al. 2013. HIV-1 superinfection occurs less frequently than initial infection in a cohort of high-risk Kenyan women. *PLoS Pathog*, 9:e1003593. doi: 10.1371/journal.ppat.1003593
- [673] AD Redd, D Ssemwanga, J Vandepitte, SK Wendel, N Ndembí, J Bukenya, S Nakubulwa, H Grosskurth, CM Parry et al. 2014. Rates of HIV-1 superinfection and primary HIV-1 infection are similar in female sex workers in Uganda. *AIDS*, 28:2147–2152. doi: 10.1097/QAD.0000000000000365
- [674] AD Redd, CE Mullis, D Serwadda, X Kong, C Martens, SM Ricklefs, AAR Tobian, C Xiao, MK Grabowski et al. 2012. The rates of HIV superinfection and primary HIV incidence in a general population in Rakai, Uganda. *J Infect Dis*, 206:267–274. doi: 10.1093/infdis/jis325
- [675] S Jost, MC Bernard, L Kaiser, S Yerly, B Hirschel, A Samri, B Autran, LE Goh and L Perrin. 2002. A patient with HIV-1 superinfection. *N Engl J Med*, 347:731–736. doi: 10.1056/NEJMoa020263
- [676] G Fang, B Weiser, C Kuiken, SM Philpott, S Rowland-Jones, F Plummer, J Kimani, B Shi, R Kaul et al. 2004. Recombination following superinfection by HIV-1. *AIDS*, 18:153–159
- [677] G Blick, RM Kagan, E Coakley, C Petropoulos, L Maroldo, P Greiger-Zanlungo, S Gretz and T Garton. 2007. The probable source of both the primary multidrug-resistant (MDR) HIV-1 strain found in a patient with rapid progression to AIDS and

- a second recombinant MDR strain found in a chronically HIV-1-infected patient. *J Infect Dis*, 195:1250–1259. doi: 10.1086/512240
- [678] GS Gottlieb, DC Nickle, MA Jensen, KG Wong, RA Kaslow, JC Shepherd, JB Margolick and JI Mullins. 2007. HIV type 1 superinfection with a dual-tropic virus and rapid progression to AIDS: a case report. *Clin Infect Dis*, 45:501–509. doi: 10.1086/520024
- [679] H Streeck, B Li, AFY Poon, A Schneidewind, AD Gladden, KA Power, D Daskalakis, S Bazner, R Zuniga et al. 2008. Immune-driven recombination and loss of control after HIV superinfection. *J Exp Med*, 205:1789–1796. doi: 10.1084/jem.20080281
- [680] O Clerc, S Colombo, S Yerly, A Telenti and M Cavassini. 2010. HIV-1 elite controllers: beware of super-infections. *J Clin Virol*, 47:376–378. doi: 10.1016/j.jcv.2010.01.013
- [681] DM Smith, JK Wong, GK Hightower, CC Ignacio, KK Koelsch, CJ Petropoulos, DD Richman and SJ Little. 2005. HIV drug resistance acquired through superinfection. *AIDS*, 19:1251–1256
- [682] M Pernas, C Casado, R Fuentes, MJ Pérez-Elías and C López-Galíndez. 2006. A dual superinfection and recombination within HIV-1 subtype B 12 years after primo-infection. *J Acquir Immune Defic Syndr*, 42:12–18. doi: 10.1097/01.qai.0000214810.65292.73
- [683] DL Robertson, PM Sharp, FE McCutchan and BH Hahn. 1995. Recombination in HIV-1. *Nature*, 374:124–126. doi: 10.1038/374124b0
- [684] MH Malim and M Emerman. 2001. HIV-1 sequence variation: drift, shift, and attenuation. *Cell*, 104:469–472. doi: 10.1016/S0092-8674(01)00234-3
- [685] SK Gire, A Goba, KG Andersen, RSG Sealton, DJ Park, L Kanneh, S Jalloh, M Momoh, M Fullah et al. 2014. Genomic surveillance elucidates Ebola virus origin and transmission during the 2014 outbreak. *Science*, 345:1369–1372. doi: 10.1126/science.1259657
- [686] WHO Ebola Response Team. 2014. Ebola virus disease in West Africa—the first 9 months of the epidemic and forward projections. *N Engl J Med*, 371:1481–1495. doi: 10.1056/NEJMoa1411100
- [687] World Health Organization. 2015. Ebola situation report: 13 May 2014. URL <http://apps.who.int/ebola/en/current-situation/ebola-situation-report-13-may-2015>
- [688] G Chowell and H Nishiura. 2014. Transmission dynamics and control of Ebola virus disease (EVD): a review. *BMC Med*, 12:196. doi: 10.1186/s12916-014-0196-0
- [689] AS Fauci. 2014. Ebola—underscoring the global disparities in health care resources. *N Engl J Med*, 371:1084–1086. doi: 10.1056/NEJMmp1409494

- [690] World Health Organization. 2015. Interim guidance on the use of rapid Ebola antigen detection tests. URL <http://www.who.int/csr/resources/publications/ebola/ebola-antigen-detection/en/>
- [691] Y Kurosaki, A Takada, H Ebihara, A Grolla, N Kamo, H Feldmann, Y Kawaoka and J Yasuda. 2007. Rapid and simple detection of Ebola virus by reverse transcription-loop-mediated isothermal amplification. *J Virol Methods*, 141:78–83. doi: 10.1016/j.jviromet.2006.11.031
- [692] T Hoenen, D Safronetz, A Groseth, KR Wollenberg, OA Koita, B Diarra, IS Fall, FC Haidara, F Diallo et al. 2015. Mutation rate and genotype variation of Ebola virus from Mali case sequences. *Science*, 348:117–119. doi: 10.1126/science.aaa5646